Materials Chemistry Principal Investigators' Meeting

Virtual Meeting, July 18–20 and 25–26, 2023

Program and Abstracts

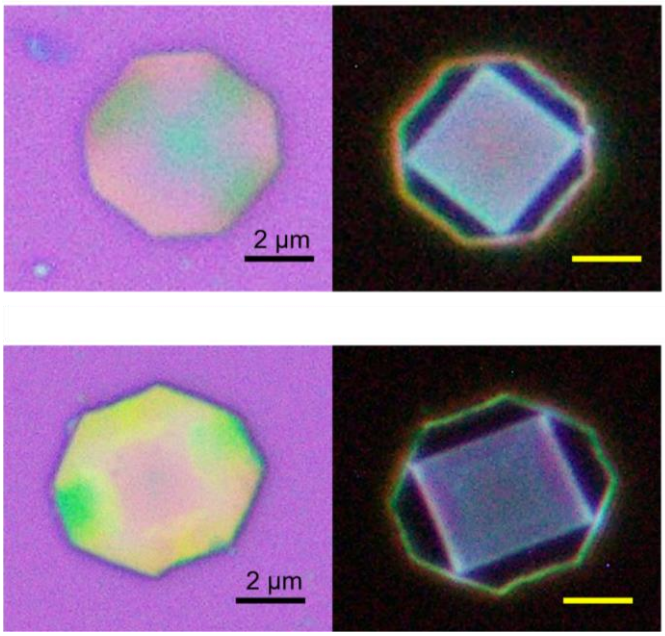

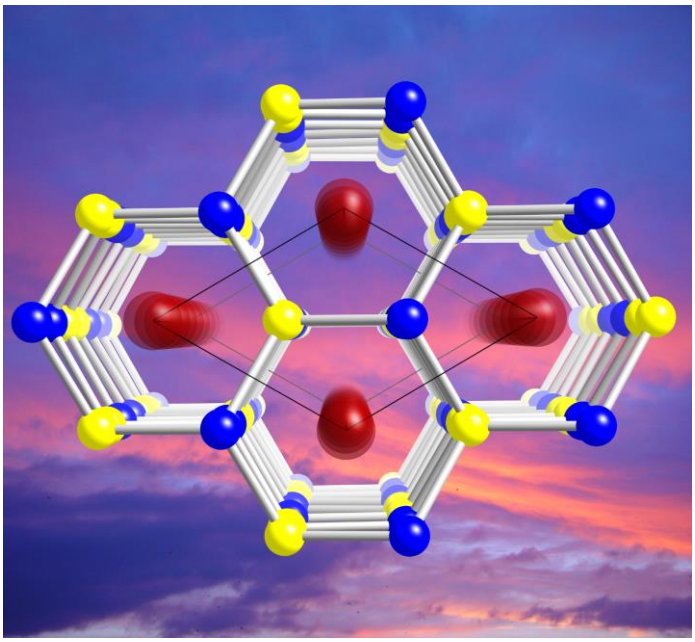

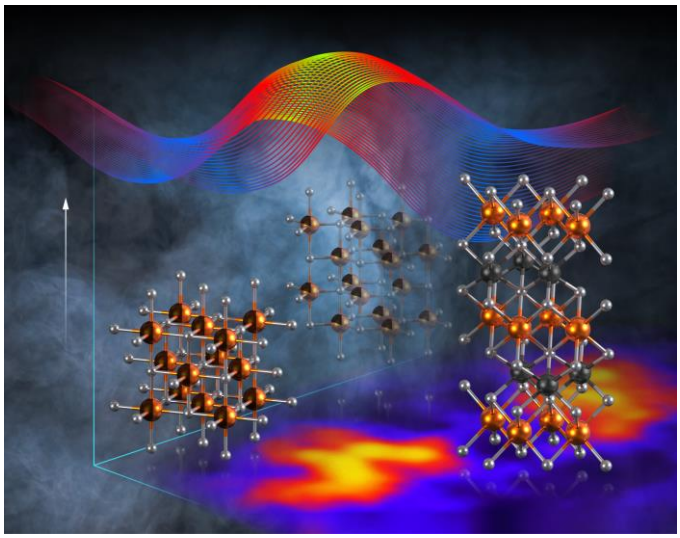

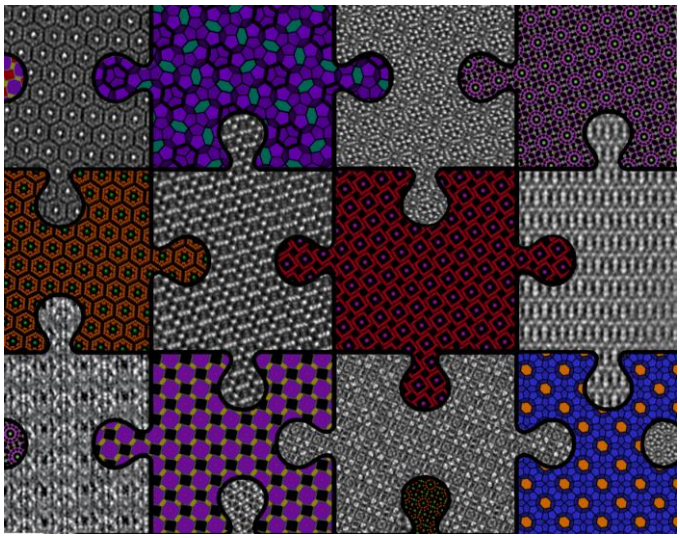

U.S. DEPARTMENT OF ENERGY | Office of Science

Office of Basic Energy Sciences
Materials Sciences and Engineering Division

On the Cover

Top Left: First demonstration of solution phase grown lead perovskite (Pb) – lead-free double perovskite (Na-Sb and Na-In) epitaxial lateral heterostructures. **Left**: optical microscope images; **Right**: photoluminescent images (under 375 nm UV excitation). Unique crystal growth mechanism of lead-free double perovskites was unveiled in this work.
Letian Dou, Purdue University

Top Right: Projection of the hexagonal crystal structure of the ternary bismuthide BaLiBi, established from single-crystal X-ray diffraction methods. In the structure of this compound, the Bi atoms (blue spheres) and Li atoms (yellow spheres) each form a hexagonal close packing array, with the Ba atoms (red spheres) occupying the available octahedral voids. In the absence of direct Bi–Bi bonding, the BaLiBi formula can be partitioned according to the fully-ionic approximation as $[Ba^{2+}][Li^{+}][Bi^{3-}]$, suggesting an electron-balanced composition. If the covalent character of the Bi–Li interactions is emphasized, as in the picture with the white cylinders connecting the two types of atoms, the chemical bonding can be rationalized as $Ba^{2+}(LiBi)^{2-}$, i.e., as layered Zintl phase.
Svilen Bobev, University of Delaware

Bottom Left: Artistic illustration of energy landscape for controlled synthesis of ternary magnesium tungsten nitrides. Thermodynamically stable layered 'rocksaline' structure, and two metastable cubic rocksalt and hexagonal BN-like structures have been synthesized at $MgWN_2$ composition using bulk and film methods. Polymorphic transformation between the rocksalt and 'rocksaline' polymorphs has been demonstrated using rapid thermal annealing.
Andriy Zakutayev, National Renewable Energy Laboratory

Bottom Right: Jigsaw puzzle of transmission electron microscopy TEM images and crystal structure models of predicted and discovered unconventional inorganic clathrates with T-Pn tetrahedral frameworks and A guest atoms, where A = Rb, Cs, Ba; T = Zn, Cd, Cu, Au; Pn = P, As, Sb, and related sodalite-type structures. Image credit: Frank Cerasoli (UC Davis), Oleg Lebedev (CNRS, France).
Davide Donadio, University of California, Davis

Foreword

This document is a collection of abstracts of the presentations made at the Principal Investigators' Meeting of the Materials Chemistry program, sponsored by the Materials Sciences and Engineering (MSE) division in the Office of Basic Energy Sciences (BES) of the U.S. Department of Energy (DOE). The meeting took place July 18-20 and July 25-26, 2023 as a virtual event conducted entirely over the internet. The 2023 virtual meeting was arranged as a miniseries of short talks to serve as a bridge back to in-person PI meetings which will return in 2024 and occur every two years thereafter (in the even years).

This meeting is one of a series of Principal Investigators' Meetings organized by BES. The purpose of the meeting is to bring together all the Principal Investigators with currently active projects in the Materials Chemistry program for the multiple purposes of raising awareness among PIs of the overall program content and of each other's research, encouraging exchange of ideas, promoting collaboration, and stimulating innovation. The meeting also provides an opportunity for the Program Managers and MSE/BES management to get a comprehensive overview of the program on a periodic basis, which provides opportunities to identify program needs and potential new research directions. The meeting agenda is organized in twelve technical sessions around topical areas in materials research that encompass many of the projects in the current Materials Chemistry portfolio. These topics include: New Materials for Energy Storage; Ion and Mass Transport in Energy Materials; Electrochemical Mechanisms in Energy Materials; Chemistry of Polymer Upcycling; Transport Phenomena in Polymers; Emergence of Functionality in Polymers; Solid State Synthesis of Functional Materials; Hierarchical Solid State Materials; Emergence of Functionality in Solid State Materials; Emergence of 2D/3D Material Properties; Chemistry at the Interface of Materials; and Chemistry of Clusters, Complexes, & Low-Dimensional Materials

The Materials Chemistry program supports hypothesis-driven research on materials with a focus on the role of chemical reactivity, chemical transformation, and chemical dynamics on the material composition, structure, function, and lifetime across the range of length scales from atomic to mesoscopic. Discovery of the mechanistic detail for chemical synthesis, transformations and dynamics of materials, fundamental understanding of structure-property relationships of functional materials, and utilization of chemistry to control interfacial properties and interactions between materials are common themes.

We would like to thank all the meeting attendees for their active participation and for sharing their ideas and new research results. Sincere thanks also go to Teresa Crockett of BES/MSE and Tia Moua and her colleagues at the Oak Ridge Institute of Science and Education (ORISE) for their excellent work providing all the logistical support for the meeting.

Chris Chervin
Craig Henderson
Program Managers, Materials Chemistry
Materials Sciences and Engineering Division
Office of Basic Energy Sciences
U.S. Department of Energy

Table of Contents

Agenda

U.S. DEPARTMENT OF ENERGY | Office of Science

BES Materials Chemistry Topical Sessions – 2023 PI Meeting
Virtual Format
July 18-20, 2023 and July 25-26, 2023
12:00 PM – 5:00 PM Eastern (each day)

Event contacts	Dr. Craig Henderson; craig.henderson@science.doe.gov Dr. Chris Chervin; christopher.chervin@science.doe.gov Website:

Registration Open June 20 – July 7, 2023		
Requested	**Date/Deadline**	**Comment**
Long Abstract	Submit by June 30, 2023	Requesting a long abstract (2-page format) from each research project in the current Materials Chemistry program
Virtual Session	Register by July 7, 2023	Requesting each Materials Chemistry PI to participate in at least one virtual session (see schedule below for presenters)

Tuesday, July 18, 2023		
12:00 – 12:05 p.m.	Opening Remarks	BES Program Managers
Technical Session A: New Materials for Energy Storage		
12:05 – 12:20 p.m.	**A1** – Materials and Interfacial Chemistry for Next-Generation Electric Energy Storage	Manthiram UT-Austin
12:20 – 12:35 p.m.	**A2** – Porous, Lightweight, and Semiconducting Chalcogel as High Energy Density Electrode for Lithium-ion and Sodium-ion Batteries	Islam Jackson State
12:35 – 12:50 p.m.	**A3** – Liquid-Metal Electrodes for Low-Cost and Low Temperature Solid State Batteries for Long Duration Energy Storage	Hatzell Princeton
12:50 – 1:05 p.m.	**A4** – Understanding the interfaces for high energy batteries using anions as charge carriers	Ji Oregon State
1:05 – 1:15 p.m.	BREAK	

Tuesday, July 18, 2023 (continued)		
Technical Session A (continued)		
1:15 – 1:30 p.m.	**A5** – Materials and Interfacial Chemistry for Next-Generation Electric Energy Storage	Dai ORNL
1:30 – 1:45 p.m.	**A6** – Two-Dimensional Chalcogenide Nanomaterials	Cui SLAC/Stanford
1:45 – 1:50 p.m.	**BREAK to move to Parallel Sessions for *Technical Session B: Ion and Mass Transport in Energy Materials* and *Technical Session C: Electrochemical Mechanisms in Energy Materials***	
1:50 – 2:05 p.m.	**B1** – Elucidating the Link Between Alkali Metal Ions and Reaction-Transport Mechanisms in Cathode Electrodes **C1** – Using Nanoporous Materials to Understand Kinetic Constraints in Pseudocapacitive Energy Storage	Capraz, Oklahoma St. Tolbert, UCLA
2:05 – 2:20 p.m.	**B2** – Thin Film Platforms to Advance Scientific Frontiers in Solid State Energy Storage **C2** – Understanding Interfacial Chemistry and Cation Order-Disorder in Mixed-Phased Complex Sodium Metal Oxide Cathodes for Sodium Ion Batteries	Rubloff, Maryland Xiong, Boise State
2:20 – 2:35 p.m.	**B3** – Understanding Flow Cell Porous Electrodes as Active Materials for Electrochemical Transformations **C3** – Enabling Energy-Dense Grid Scale Batteries with Earth Abundant Materials	Aziz, Harvard Amanchukwu, UChicago
2:35 – 2:45 p.m.	BREAK	
2:45 – 3:00 p.m.	**B4** – Designing Efficient Nanostructured Polymer Electrolytes Using Tapered Block Polymers - Joint Experiment and Theory Effort in Controlled Interface Design **C4** – Direct Reduction of Metal Oxides to Metals for Electrowinning and Energy Storage	Epps, Delaware Kempler, Oregon
3:00 – 3:15 p.m.	**B5** – Designing Chemical Disorder in Solid-State Superionic Conductors **C5** – Elucidating the Electrochemically Enhanced Surface Diffusion Mechanism in Materials for Clean Energy	Kim, Stevens Institute Papa Lopes, ANL
3:15 – 3:30 p.m.	**B6** – Polyelectrolyte-Grafted Nanochannels for Enhanced Electromechanical Energy Conversion **C6** – A New Paradigm for Water Splitting in Layered Materials by Modulation of Catalyst Oxidation State	Das, Maryland Zdilla, Temple

3:30 – 3:40 p.m.	BREAK
3:40 – 4:10 p.m. Parallel Discussion Sessions	**Small Group Discussions** – assigned by Technical Session for Q&A and discussion
4:10 – 4:50 p.m. Parallel Discussion Sessions	**Small Group Discussions** – open format for further Q&A, discussion, collaboration, etc (freely move between Discussion Rooms to mingle with the other Materials Chemistry PIs)
4:50 – 5:00 p.m.	**BES Program Manager Comments and Closeout of Meeting**

Wednesday, July 19, 2023		
12:00 – 12:05 p.m.	Opening Remarks	BES Program Managers
Technical Session D: Chemistry of Polymer Upcycling		
12:05 – 12:20 p.m.	**D1** – The Role of Local Structure and Dynamics on Proton and Hydroxide Transport in Ion-Conducting Polymers	Winey, UPenn
12:20 – 12:35 p.m.	**D2** – Development of Recyclable Thermosets for Additive Manufacturing	Chowdhury, NM Tech
12:35 – 12:50 p.m.	**D3** – Autooxidation Mechanisms and Methods for Plastics Upcycling	Hermans, Wisconsin
12:50 – 1:05 p.m.	**D4** – Unlocking Chemical Circularity in Recycling by Controlling Polymer Reactivity Across Scales	Helms, LBNL
1:05 – 1:15 p.m.	BREAK	

Wednesday, July 19, 2023 (continued)		
Technical Session D (continued)		
1:15 – 1:30 p.m.	**D5** – Precision Deconstruction of Polymers by Tailored Ionic Liquids	Saito, ORNL
1:30 – 1:45 p.m.	**D6** – Understanding Structure, Phase Behavior, and Physical Properties of Polysulfamides and Polysulfamates using Simulations, Experiments, and Machine Learning	Jayaraman, Delaware
1:45 – 1:50 p.m.	**BREAK to move to Parallel Sessions for *Technical Session E: Transport Phenomena in Polymers* and *Technical Session F: Emergence of Functionality in Polymers***	
1:50 – 2:05 p.m.	**E1** – Facilitating Ionic and Electronic Conduction in Radical Polymers through Controlled Assembly **F1** – Precision Synthesis and Assembly of Ionic and Liquid Crystal Polymers	Boudouris, Purdue Nealey, ANL
2:05 – 2:20 p.m.	**E2** – Exploration of Radial Conjucation Pathways in Pi-Electron Materials **F2**– Charging and Polarization of Organic Semiconductors in Energy Efficient Circuits and Energy Capture Models	Tovar, Johns Hopkins Katz, Johns Hopkins
2:20 – 2:35 p.m.	**E3** – Multi-Metalloporphyrin Synthetic Polymers for Long-Range Charge Transport **F3** – Inorganic/Organic Nanocomposites	Moore, UIUC Xu, LBNL
2:35 – 2:45 p.m.	BREAK	
2:45 – 3:00 p.m.	**E4** – High Electron Affinity Conjugated Polymers: Synthesis, Electron Transport and Discovery of New Class of Two-Dimensional Organic Solid-State Materials **F4** – Shaping Symmetry and Molding Morphology of Triply-Periodic Assemblies via Molecular Design and Processing of Block Copolymers	Jenehke, Washington Grason, UMass
3:00 – 3:15 p.m.	**E5** – Energy Flow in Polymers with Mixed Conduction Pathways **F5** – Molecular and Network Design of Liquid Crystal Elastomer Elastocalorics	Segalman, UCSB Davidson, Princeton
3:15 – 3:30 p.m.	**E6** – New Synthetic Approaches Towards Atomically Precise π–d Conjugated Materials **F6** – Polyolefin Upcycling Through Dehydrogenation and Functionalization	Xiao, Washington Winey, UPenn
3:30 – 3:40 p.m.	BREAK	
3:40 – 4:10 p.m.	**Small Group Discussions** – assigned by Technical Session for Q&A and discussion	

Parallel Discussion Sessions	
4:10 – 4:50 p.m. Parallel Discussion Sessions	**Small Group Discussions** – open format for further Q&A, discussion, collaboration, etc (freely move between Discussion Rooms to mingle with the other Materials Chemistry PIs)
4:50 – 5:00 p.m.	**BES Program Manager Comments and Closeout of Meeting**

Thursday, July 20, 2023		
12:00 – 12:05 p.m.	Opening Remarks	BES Program Managers
Technical Session G: Solid State Synthesis of Functional Materials		
12:05 – 12:20 p.m.	**G1** – New Superconducting Materials	Cava, Princeton
12:20 – 12:35 p.m.	**G2** – Directed Synthesis of New Actinide Containing Oxides, Fluorides and Chalcogenides	Zur Loye, South Carolina
12:35 – 12:50 p.m.	**G3** – The Synthesis of Metal Superhydrides through Extreme Temperature/Pressure Conditions: Towards RT Superconductivity	Salamat, UNLV
12:50 – 1:05 p.m.	**G4** – Solid State Chemistry of Novel Pnictides with Complex Structures	Bobev, Delaware
1:05 – 1:15 p.m.	BREAK	

Thursday, July 20, 2023 (continued)		
Technical Session G (continued)		
1:15 – 1:30 p.m.	**G5** – Kinetic Synthesis of Metastable Nitrides	Zakutayev, NREL
1:30 – 1:45 p.m.	**G6** – Carbon-Based Clathrates as a New Class of sp3-Bonded Framework Materials	Strobel, Carnegie Inst.
1:45 – 1:50 p.m.	**BREAK to move to Parallel Sessions for *Technical Session H: Hierarchical Solid State Materials* and *Technical Session I: Emergence of Functionality in Solid State Materials***	
1:50 – 2:05 p.m.	**H1** – Chemo-Mechanically Driven In Situ Hierarchical Structure Formation in Mixed Conductors **I1** – Design and Validation of Defect-Resistant Multinary Chalcogenide Semiconductors for Energy Conversion	Perry, UIUC Mitzi, Duke
2:05 – 2:20 p.m.	**H2** – Hierarchical Hybrid Multifunctional Materials through Interface Engineering **I2** – Unraveling the Mysteries of the Platinum Group Elements	Poudeu, Michigan Schurko, Florida
2:20 – 2:35 p.m.	**H3** – Intermetallic Reactivity: From Frustrated Bonding to Mechanisms for Intergrowth and Modular Functionality in Metals and Alloys **I3** – Solid State NMR Spectroscopy for Advanced Energy Materials	Fredrickson, Wisconsin Rossini, Ames Lab
2:35 – 2:45 p.m.	BREAK	
2:45 – 3:00 p.m.	**H4** – Hybrid Halide Perovskites: Novel Materials with Contraindicated Properties **I4** – Additive-Assisted Preparation of Multinary Halides	Seshadri, UCSB Saparov, Oklahoma
3:00 – 3:15 p.m.	**H5** – Design Exciton and Spin Functionalities in Halide Perovskite Epitaxial Heterostructures **I5** – New Cooperative Adsorbents and Regeneration Methods for the Efficient Removal of Carbon Dioxide from Air	Dou, Purdue Long, LBNL
3:15 – 3:30 p.m.	**H6** – Fundamental Studies of Charge Transfer in Quantum Confined Nanostructure Heterojunctions and Applications to Solar Energy Conversion **I6** – Fundamental Mechanisms Driving Efficiency of CO2 Capture Using Mineral Looping	Jin, Wisconsin Weber, ORNL
3:30 – 3:40 p.m.	BREAK	

3:40 – 4:10 p.m. Parallel Discussion Sessions	**Small Group Discussions** – assigned by Technical Session for Q&A and discussion
4:10 – 4:50 p.m. Parallel Discussion Sessions	**Small Group Discussions** – open format for further Q&A, discussion, collaboration, etc (freely move between Discussion Rooms to mingle with the other Materials Chemistry PIs)
4:50 – 5:00 p.m.	**BES Program Manager Comments and Closeout of Meeting**

U.S. DEPARTMENT OF ENERGY | Office of Science

BES Materials Chemistry Topical Sessions – 2023 PI Meeting
Virtual Format
July 25-26, 2023
12:00 PM – 5:00 PM Eastern (each day)

Event contacts	Dr. Craig Henderson; craig.henderson@science.doe.gov Dr. Chris Chervin; christopher.chervin@science.doe.gov Website: 2023 Materials Chemistry Virtual PI Meeting

Registration Open June 20 – July 7, 2023		
Requested	**Date/Deadline**	**Comment**
Long Abstract	Submit by June 30, 2023	Requesting a long abstract (2-page format) from each research project in the current Materials Chemistry program
Virtual Session	Register by July 7, 2023	Requesting each Materials Chemistry PI to participate in at least one virtual session (see schedule below for presenters)

Tuesday, July 25, 2023		
12:00 – 12:05 p.m.	Opening Remarks	BES Program Managers
Technical Session J: Emergence of 2D/3D Material Properties		
12:05 – 12:20 p.m.	**J1** – Compositional Control of Fundamental Electronic and Magnetic Properties of Ordered Layered Multi-element MXenes	Gogotsi, Drexel
12:20 – 12:35 p.m.	**J2** – Novel 2D Materials and Structures via Janus Manipulation	Kong, MIT
12:35 – 12:50 p.m.	**J3** – Building Artificial Layered Solids from the Bottom-up: Materials by Design to Enable New Energy	Yu, UT-Austin
12:50 – 1:05 p.m.	**J4** – Rational Synthesis of Superconductors	Kanatzidis, ANL
1:05 – 1:15 p.m.	BREAK	

Tuesday, July 25, 2023 (continued)		
Technical Session J (continued)		
1:15 – 1:30 p.m.	**J5** – Permanent Magnets Featuring Heavy Main Group Elements for Magnetic Anisotropy	Freedman, MIT
1:30 – 1:45 p.m.	**J6** – Discovering Dopable, Next Generation Defect Tolerant Hybrid Semiconductors	Neilson, Colorado State
1:45 – 1:50 p.m.	**BREAK to move to Parallel Sessions for *Technical Session K: Chemistry at the Interface of Materials* and *Technical Session L: Chemistry of Clusters, Complexes, & Low-Dimensional Materials***	
1:50 – 2:05 p.m.	**K1** – Understanding Degradation Mechanisms of Aminopolymers **L1**– Transforming Critical Materials Separation using Precision Control	Pang, LLNL Jansone-Popova, ORNL
2:05 – 2:20 p.m.	**K2**– Reversible Electrochemical Capture/Release of Carbon Dioxide Mediated by Electrostatically-Enhanced Charge Transfer **L2** – Molecular Mo Sulifide Clusters for H2-Evolution: Surface Immobilization and Water Solubility, Composition-Function Relationships, and Probes of Mechanisms	Rodríguez-López, UIUC Donahue, Tulane
2:20 – 2:35 p.m.	**K3** – Modulating Complex Chemical Conversion with Multi-site Electrocatalyst for Energy Dense Liquids **L3** – Largely pi-Extended Molecular Systems: Porphryins Fused with PAHs	Cheng, Northern Illinois Wang, North Texas
2:35 – 2:45 p.m.	BREAK	
2:45 – 3:00 p.m.	**K4** – Making an Inorganic Analogue of a Cell for Direct Air Capture of CO2 **L4** – High Efficiency Biomimetic Organic Solar Cells	Heldebrandt, PNNL Baldo, MIT
3:00 – 3:15 p.m.	**K5** – Passive and Enhanced Capture and Conversion of CO2 by d/f0 Molecules and Materials **L5** – Probing the Hydrogen Bonded Networks and Ion Interactions in Deep Eutectic Solvents (DESs) through Solute Molecules.	Nyman, Oregon State Suarez, CUNY
3:15 – 3:30 p.m.	**K6** – Kinetics and Thermodynamics of Gaseous Mixtures in Nano-Confined Environments **L6**– Li-ion Battery Critical Metal Recycling Using Sugars	Tan, UT-Dallas Amarasekara, PVSU
3:30 – 3:45 p.m.	**K7** – Novel Strategies for Direct Air Capture and Conversion of CO2 Using Dual-Function Materials **L7**– Fundamental Understanding of Electrochemical – Mechanical Driven Instability of Sodium Metal	Kuila, NCAT Mukherjee, Purdue

3:45 – 3:55 p.m.	BREAK
3:55 – 4:20 p.m. Parallel Discussion Sessions	**Small Group Discussions** – assigned by Technical Session for Q&A and discussion
4:20 – 4:50 p.m. Parallel Discussion Sessions	**Small Group Discussions** – open format for further Q&A, discussion, collaboration, etc (freely move between Discussion Rooms to mingle with the other Materials Chemistry PIs)
4:50 – 5:00 p.m.	**BES Program Manager Comments and Closeout of Meeting**

Wednesday, July 26, 2023		
12:00 – 12:05 p.m.	Opening Remarks	BES Program Managers
Technical Session M		
12:05 – 12:20 p.m.	**M1** – Impacts of Dynamic Bonding on the Properties of Porous Materials	Brozek, Oregon
12:20 – 12:35 p.m.	**M2** – Uncovering Intrinsic Transport and Magnetic Properties of Two-Dimensional Electrically Conducting Metal-Organic Frameworks	Dincă, MIT
12:35 – 12:50 p.m.	**M3** – Spatio-Temporal Dynamics of CO2 Capture by Sorbents: Multimodal, In-Situ and Operando Measurements	Farha, Northwestern
12:50 – 1:05 p.m.	**M4** – Molecular Mechanisms of Moisture-Driven DAC within Charged Polymers	Wade, Northern Arizona
1:05 – 1:15 p.m.	BREAK	

Wednesday, July 26, 2023 (continued)		
Technical Session M (continued)		
1:15 – 1:30 p.m.	**M5** – Controlling Solid-State Packing and Properties of Conjugated Materials with Discrete Aromatic Interactions of Side Chains	Thomas, Tufts
1:30 – 1:45 p.m.	**M6** – New Paradigms for Controlling Molecular and Ion Transport in Precise, Tight and Reconfigurable Polymer Networks	Braun, UIUC
1:45 – 1:50 p.m.	**BREAK to move to Parallel Sessions for *Technical Session N: Precision Synthesis and Characterization of Network Materials* and *Technical Session O: Bonding in Network Materials***	
1:50 – 2:05 p.m.	**N1** – Metal Organic Frameworks: Structure, Function and Design via Hyperpolarized NMR Spectroscopy: Collaborative Proposal **O1** – Elastomeric Miktoarm Star Polymers: Theory and Experiment	Reimer, UC-Berkeley Fredrickson, UCSB
2:05 – 2:20 p.m.	**N2** – MOF-Polymer Hybrides for Energy Science **O2** – A synergistic computational ans experimental approach for unprecedented III-IV and II-VI clathrates	Cohen – UCSD Donadio, UC-Davis
2:20 – 2:35 p.m.	**N3** – Pore Space Engineering and Functionalization in Porous Metal-Organic Framework Materials **O3** – Multi-Length Scale Synthesis of Silicon Materials	Feng, UC-Irvine Klausen, Johns Hopkins
2:35 – 2:45 p.m.	BREAK	
2:45 – 3:00 p.m.	**N4** – Symmetry Breaking for the Synthesis of Nanostructured Porous Materials **O4** – Expanding iClick to Link Metal Ions in Multidimensional Metallopolymers and Materials Synthesis	Matzger, Michigan Veige, Florida
3:00 – 3:15 p.m.	**N5** – Multi-scale Study of Self-Healing Polymers to Enhance Carbon Dioxie Removal **O5** – Converting Metal–Organic Liquids into Microporous Glasses via Non-Equilibrium Syntheses	Ma, Vermont Mason, Harvard
3:15 – 3:30 p.m.	**N6** – When Covalent Organic Frameworks Meet Cross-coupling Reactions: Directed Synthesis, Mechanistic Investigation, and Energy Application **O6** – Kinetically trapped Poly(pseudo)rotaxane Networks	Li, Clark Atlanta Ke, Dartmouth
3:30 – 3:40 p.m.	BREAK	
3:40 – 4:10 p.m. Parallel Discussion Sessions	**Small Group Discussions** – assigned by Technical Session for Q&A and discussion	

4:10 – 4:50 p.m. Parallel Discussion Sessions	**Small Group Discussions** – open format for further Q&A, discussion, collaboration, etc (freely move between Discussion Rooms to mingle with the other Materials Chemistry PIs)
4:50 – 5:00 p.m.	**BES Program Manager Comments and Closeout of Meeting**

Laboratory Abstracts

Synthesis and Interfacial Control of Electrode Architectures

Sheng Dai, Albina Y. Borisevich, Craig A. Bridges, M. Parans Paranthaman, and Xiao-Guang Sun

Oak Ridge National Laboratory

Keywords: Architectures, Interfaces, Transport

Research Scope

The advancement of electrochemical energy storage relies on the creation of tailored nanotextures through precise control of the compositions and structures of electrode materials. This research focuses on investigating the complex interplay between solvent and solute structures and dynamics at the charged interface, as well as the transport of ions into and out of the electrodes. The solvation/desolvation processes taking place and the formation of interfaces through chemical reactions are all crucial factors to be explored. This study has addressed several synthesis methods for designing inorganic and polymer electrodes specifically tailored for energy storage applications. The primary objective is to demonstrate the effectiveness of our synthesis strategies in producing nanostructured polymers and oxides that exhibit not only high storage capacity but, more importantly, significantly enhanced electronic and ionic conductivities. By enhancing the transport properties within electrode architectures, such as improved electronic and ionic conductivities, we can enable high-rate capabilities for the corresponding energy storage systems. The key focus will be on developing materials with enhanced transport properties, which are vital for achieving high-performance electrochemical energy storage.

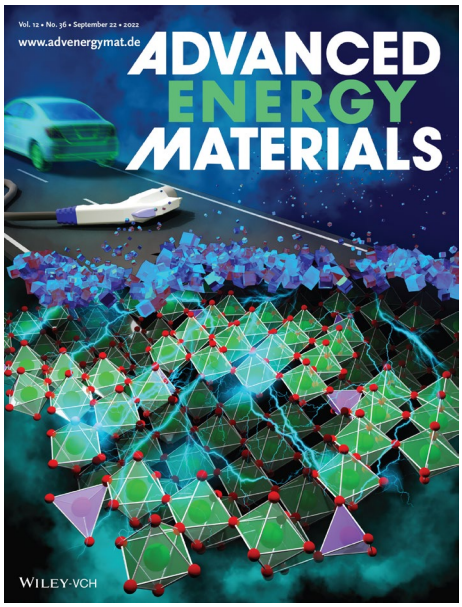

Fig. 1. Schematic structure motifs of $Mo_{1.5}W_{1.5}Nb_{14}O_{44}$ (MWNO) through an ionothermal-synthesis-assisted doping strategy.[1]

Recent Progress

Wadsley-Roth phased niobates, characterized by open and interconnected crystallographic shear structures, show promise as anode materials for lithium-ion batteries. However, their inherent low electrical conductivity limits their rate-capability. We have recently successfully prepared a doped material called $Mo_{1.5}W_{1.5}Nb_{14}O_{44}$ (MWNO) through an ionothermal-synthesis-assisted doping strategy (Fig. 1).[1] The crystal structure of MWNO was thoroughly examined using neutron powder diffraction and aberration-corrected

scanning transmission electron microscopy, which revealed the complete occupancy of Mo^{6+}-dopant at the t1 tetrahedral site. This MWNO demonstrated exceptional fast-rechargeability, achieving a capacity of 92.1 mAh g^{-1} at 100°C and retaining 81.7% of its capacity over 2000 cycles at 10°C. The remarkable performance of MWNO was further investigated through ultraviolet-visible diffuse reflectance spectroscopy, density functional theory (DFT) computations, and electrochemical impedance spectroscopy. These analyses revealed that the improved electrical conductivity of MWNO is attributed to bandgap narrowing.

Future Plans

The purpose of our future research plan is to further investigate the potential of composition doping as a strategy to enhance the electronic conductivity of Wadsley-Roth phased niobates through band narrowing. By modifying the composition of the niobates, we aim to understand the structural dependence of their rate-capability on electronic structures for lithium-ion insertion reactions. Wadsley-Roth phased niobates with controlled compositions will be synthesized using established methods, incorporating dopant elements known to influence electronic properties. Various doping concentrations and combinations including high entropy phases will be explored to achieve optimal band narrowing effects. The synthesized materials will be characterized using a combination of techniques, including neutron and X-ray diffractions, scanning electron microscopy (SEM), transmission electron microscopy (TEM), and energy-dispersive X-ray spectroscopy (EDX). These analyses will provide insights into the crystal structure, elemental composition, and morphology of the doped niobates. Density functional theory (DFT) calculations will be employed to investigate the electronic band structure of the doped niobates. These calculations will provide valuable insights into the impact of composition doping on the band structure, bandgap narrowing, and charge carrier mobility. Theoretical predictions will be compared with experimental results to validate the band narrowing strategy. A mechanistic understanding of the role of composition doping in enhancing electronic conductivity will be established through a comprehensive analysis of the experimental and theoretical results. The relationships between the dopant concentration, band structure, electronic conductivity, and electrochemical performance will be elucidated, providing valuable insights into the underlying mechanisms driving the observed enhancements.

References

1. Tao, R. M.; Zhang, T. Y.; Tan, S. S.; Jafta, C. J.; Li, C.; Liang, J. Y.; Sun, X. G.; Wang, T.; Fan, J. T.; Lu, Z. Y.; Bridges, C. A.; Suo, X.; Do-Thanh, C. L.; Dai, S. Insight into the Fast-Rechargeability of a Novel Mo1.5W1.5Nb14O44 Anode Material for High-Performance Lithium-Ion Batteries. Adv. Energy Mater., 16, 2200519 (2022).

Publications

1. Juntian Fan, Tao Wang, Bishnu P. Thapaliya, Meijia Li, Chi-Linh Do-Thanh, Takeshi Kobayashi, Ilja Popovs, Zhenzhen Yang, Sheng Dai, Construction of Nitrogen-abundant Graphyne Scaffolds via Mechanochemistry-Promoted Cross-Linking of Aromatic Nitriles with Carbide Toward Enhanced Energy Storage*., Small* **19**, 2205533 (2023), DOI: 10.1002/smll.202205533
2. R. M. Tao, S. S. Tan, C. J. Jafta, T. Y. Zhang, C. Li, X. G. Sun, T. Wang, J. T. Fan, C. A. Bridges, X. Suo, and S. Dai, Insight into the high-performance $Mo_{1.5}W_{1.5}Nb_{14}O_{44}$ anode materials in fast-rechargeable lithium-ion batteries, *Adv. Energy Mater.* 202200519 (2022). DOI: 10.1002/aenm.202200519
3. B. P. Thapaliya, S. Misra, S.-Z. Yang, C. J. Jafta, H. M. Meyer III, P. Bagri, R. R. Unocic, C. A. Bridges, and S. Dai, Enhancing cycling stability and capacity retention of NMC811 cathodes by reengineering interfaces via electrochemical fluorination, *Adv. Mater. Interfaces* **9**, 2200035 (2022). DOI: 0.1002/admi.202200035
4. B. P. Thapaliya, A. Y. Borisevich, H. M. Meyer III, X.-G. Sun, C. A. Bridges, and S. Dai, Conformal LiF stabilized interfaces via electrochemical fluorination on high voltage spinel cathodes (~4.9 V) for lithium-ion batteries, *Adv. Mater. Interfaces* 2201600 (2022). DOI: 10.1002/admi.202201600
5. T. Wang, J. A. Gaugler, M. Li, B. P. Thapaliya, J. Fan, L. Qui, D. Moitra, T. Kobayashi, I. Popovs, Z. Z. Yang, and S. Dai, Construction of fluorine- and piperazine-engineered covalent triazine framework towards dual-ion positive electrode performances, *ChemSusChem*, e202201219 (2022). DOI: 10.1002/cssc.202201219
6. J. Fan, T. Wang, B. P. Thapaliya, L. Qiu, M. Li, Z. Wang, T. Kobayashi, I. Popovs, Z. Yang, and S. Dai, Fully conjugated Poly(phthalocyanine) scaffolds derived from a mechanochemical approach towards enhanced energy storage, *Angew. Chemie.* **61**, e202207607 (2022). DOI: 10.1002/anie.202207607
7. J. Fan, T. Wang, H. Chen, Z. Wang, B. P. Thapaliya, T. Kobayashi, Y. Yuan, I, Popovs, Z. Yang, and S. Dai, Mechanochemistry-driven construction of aza-fused π-conjugated networks toward enhanced energy storage, *Adv. Funct. Mater*. **32**, 2202669 (2022). DOI: 0.1002/adfm.202202669
8. R. M. Tao, T. Wang, J. T. Fan, H. M. Meyer, A. Y. Borisevich, C. L. Do-Thanh, and S. Dai, Ionothermal synthesis of carbon/TiO_2 nanocomposite for supercapacitors, *ChemNanoMat* **8**, e202200075 (2022). DOI: 10.1002/cnma.202200075
9. C. J. Jafta, X.-G. Sun, H. Lyu, H. Chen, B. P. Thapalia, W. T. Heller, M. J. Cuneo, R. T. Mayes, M. P. Paranthaman, S. Dai, and C. A. Bridges, Insight into the solid electrolyte Interphase formation in Bis(fluorosulfonyl)Imide Based Ionic Liquid Electrolytes, *Adv. Func. Mater*. 2008708 (2021). DOI: 10.1002/adfm.202008708
10. Z. Z. Yang, T. Wang, H. Chen, X. Suo, P. Halstenberg, H. Lyu, W. Jiang, S. M. Mahurin, I. Popovs, and S. Dai, Surpassing the organic cathode performance for lithium-ion batteries with robust fluorinated covalent quinazoline networks, *ACS Energy Lett.* **6**, 41 (2021). DOI: 10.1021/acsenergylett.0c01750

Elucidating the Electrochemically Enhanced Surface Diffusion Mechanism in Materials for Clean Energy

Pietro Papa Lopes, Materials Science Division, Argonne National Laboratory

Keywords: electrochemistry, durability, dissolution, redeposition, surface diffusion

Research Scope

This project aims to understand the mechanism of surface diffusion in electrochemical media, which can become orders of magnitude faster than observed in gas-phase conditions. The key hypothesis of this project is that fast surface diffusion in electrochemical environments occurs as concerted dissolution and redeposition events occur at the nanoscale. Thus, by understanding and controlling the rates and locus of dissolution and redeposition as a function of electrode polarization, surface adsorption, and electrolyte complexation effects we can establish the relationships between dissolution/redeposition events at atomic levels to changes in surface defect distribution and overall morphological evolution. As the early stages of surface dissolution may involve less than 0.1% of the surface area, and different surface sites (e.g. terrace, step edges, kinks, etc), this project will rely on precision electrochemical approaches leveraging well-defined materials and interfaces such as single crystal surfaces with different surface orientation and composition to properly establish the relationships between dissolution/re-deposition and surface diffusion. The insights on the driving force behind surface dissolution, site-selective electrodeposition, and overall surface diffusion have a direct impact on materials degradation effects that lead to a loss in reactivity on materials that are relevant for electrochemical conversion and storage reactions part of clean energy systems such as fuel cells, electrolyzers, and batteries. As such, precise control of the process behind surface diffusion will allow us to devise strategies for guiding surface atom mobility targeting specific surface site arrangements.

Recent Progress

The loss of functional properties that occur in materials used in electrochemical energy storage and conversion systems poses a challenge in the design of materials that must be simultaneously stable and functional. In this portion of this project, we present a framework by which changes to material properties such as its structure and composition have a direct impact on its ability to sustain the desired reactivity during operation and long periods of time[1]. This framework emphasizes the distinction between reaction durability and materials stability, two concepts that separate the loss in current density or capacity (e.g. reaction durability) from the changes in the material structure and/or composition (e.g. material stability). Thus, the focus on material stability allows us to classify the changes to the material properties arising from additive and subtractive processes (Figure 1), as they are related to redeposition events that may lead to

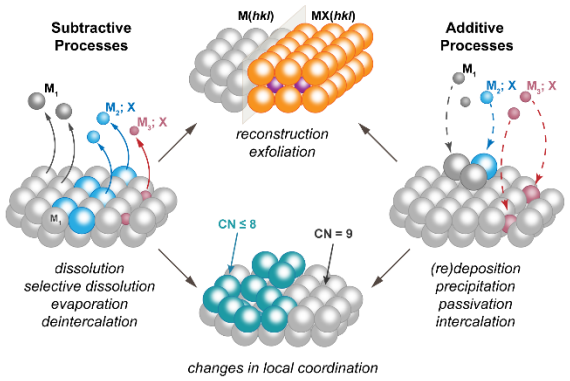

Figure 1. Schematic representation of subtractive and additive mechanisms behind trends in material stability and possible changes to coordination environments, reconstruction, passivation, and material loss.

changes in surface sites or the formation of passive films (e.g. additive) and dissolution which lead to changes in local coordination environments and changes to the initial crystal structure (e.g. subtractive). Therefore, the focus on additive and subtractive events that inherently change the nature of the material active center can explain when degradation occurs[2] or when material evolution ensues with superior properties than the initial material[3]. It also implies that controlling surface diffusion through dissolution and redeposition may open new pathways toward the design of functional and stable materials and ways to regenerate them.

To uncover the relationships between dissolution and surface diffusion on Ir surfaces, we have begun our investigation by exploring the dissolution trends over Ir single-crystal surfaces as a function of pH and electrochemical conditions. The results obtained thus far indicate that dissolution events related to the transition between metal and metal oxides are far more intricate and distinct from deep oxidation conditions that are often explored in the context of the O_2 evolution reaction[4]. Upon first immersion of a clean, pristine Ir(111) surface we can observe an immediate dissolution transient that equates to the removal of 0.65 mML of the surface atoms (Figure 2a), about 6 times greater than observed on Pt(111)[5]. Dissolution transients are also observed during electrode voltage sweeps but only when H_{upd} adsorption/OH desorption occurs below 0.2V vs. RHE, indicating that dissolution upon oxide reduction process might be more universal than the need for redox transitions involving higher oxidation states (e.g., +4)[4]. The formation of defect sites becomes much more prominent upon high voltage excursions (Figure 2b), which also follows the increase in dissolution rates. Lastly, differences in dissolution rates and changes to adsorption profiles for various surface orientations provide new insights about the

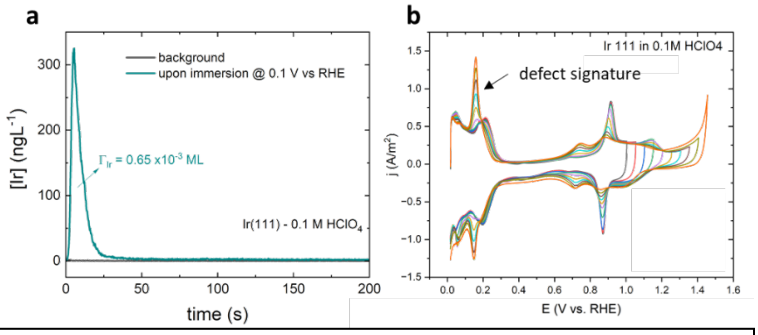

Figure 2. a) Recorded Ir dissolution transient during immersion of clean Ir(111) surface in 0.1M $HClO_4$ electrolyte at 0.1V vs. RHE. b) Evolution of surface adsorption features upon varying electrode voltage excursions up to 1.45V, and corresponding formation of defect sites indicated by the pronounced Hupd desorption/OH adsorption around 0.15V.

surface species and locus of dissolution as it relates to changes in surface morphology.

References

1. P. P. Lopes, *A Framework for the Relationships between Stability and Functional Properties of Electrochemical Energy Materials*, ACS Materials Au **3, 1**, 8-17 (2023).
2. P. P. Lopes, D. Li, H. Lv, C. Wang, D. Tripkovic, Y. Zhu, R. Schimmenti, H. Daimon, Y. Kang, J. Snyder, N. Becknell, K. L. More, D. Strmcnik, N. M. Markovic, M. Mavrikakis, V. R. Stamenkovic, *Eliminating dissolution of platinum-based electrocatalysts at the atomic scale*, Nature Materials **19**, 1207-1214 (2020).
3. P. P. Lopes, D. Y. Chung, X. Rui, H. Zheng, H. He, P. F. B.D. Martins, D. Strmcnik, V. R. Stamenkovic, P. Zapol, J. F. Mitchell, R. F. Klie, N. M. Markovic, *Dynamically Stable Active Sites from Surface Evolution of Perovskite Materials during the Oxygen Evolution Reaction*, Journal of the American Chemical Society **143, 7**, 2741-2750 (2021).
4. S. Cherevko, A. R. Zeradjanin, A. A. Topalov, N. Kulyk, I. Katsounaros, K. J. J. Mayrhofer, *Dissolution of noble metals during oxygen evolution in acidic media*, ChemCatChem **6**, 2219-2223 (2014).
5. P. P. Lopes, D. Strmcnik, D. Tripkovic, J. G. Connell, V. R. Stamenkovic, N. M. Markovic, *Relationships between atomic level surface structure and stability/activity of platinum surface atoms in aqueous environments*, ACS Catalysis **6, 4**, 2536-2544 (2016).

Publications

1. P. P. Lopes, *A Framework for the Relationships between Stability and Functional Properties of Electrochemical Energy Materials*, ACS Materials Au **3, 1**, 8-17 (2023).

Precision Deconstruction of Polymers by Tailored Ionic Liquids

Tomonori Saito, Jeffrey Foster, Ilja Popovs, Sheng Dai, Bobby Sumpter, Changwoo Do, Oak Ridge National Laboratory, Robert Davis, The University of Virginia

Keywords: Polymer Upcycling, Polymer Deconstruction, Organocatalyst, Mixed Plastics, Condensation Polymers

Research Scope

Condensation polymers comprise ~30% of global plastics production. Although there has been some progress on chemically recycling condensation polymers, most condensation polymers are not recycled because of the difficulty in depolymerization to pure building blocks in an energy efficient manner. New processes and catalysts are needed to lower the energy requirements and temperature for deconstruction of condensation polymers. Ionic liquids hold great potential to address these challenges due to their unique physical and chemical properties, including good miscibility with polymers, high thermal stability, low vapor pressure, tailorable functionality and catalytic activity. Thus, *the overarching goal of this project is to unravel the fundamental principles for precise deconstruction of condensation polymers using ionic liquids as both solvent and organocatalyst while establishing approaches for their reconstruction* (Figure 1). To achieve the overarching goal, the following three specific aims will be pursued. **Aim 1**: Develop low energy depolymerization pathways for condensation polymers by tailoring functionality, structure, and composition of ionic liquids as solvents and catalysts. **Aim 2**: Develop design principles for ionic liquid organocatalysts that generate well-defined deconstructed intermediates. **Aim 3**: Understand and control the product selectivity in the deconstruction of mixed streams of condensation polymers using designed ionic liquids and unravel the pathways for reconstruction. Successful implementation of this project will deliver the fundamental knowledge to establish the design principles for energy efficient polymer deconstruction and lay a versatile platform for polymer reconstruction with tailored composition, topology and functionality. These upcycled polymers can be recycled to establish an energy efficient closed-loop recycling pathway for condensation polymers.

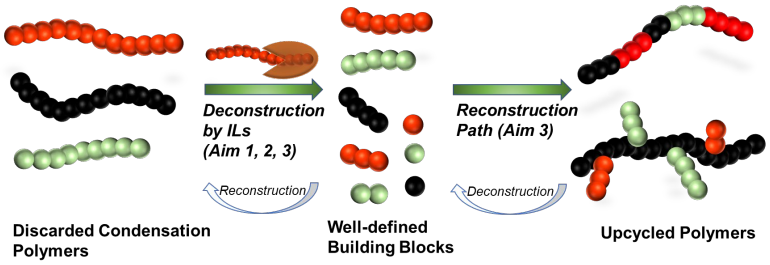

Figure 1. Deconstruction and reconstruction of condensation polymers by tailored ionic liquids

Recent Progress

A highly efficient and versatile protic ionic salt organocatalyst is unveiled for selective glycolysis of diverse condensation polymers (**Aim 1**) and their mixed waste streams into corresponding monomers (**Aim 3**).[1] It allows for quantitative conversion of multiple condensation polymers to small molecules, including poly(ethylene terephthalate) (PET), poly(carbonate) (PC), poly(urethane) (PU), and poly(amide) (PA) within 2h, where no other reported catalysts can deconstruct such broad range of condensation polymers (Figure 2). All electron density functional theory (DFT) calculations combined with molecular dynamics (MD) simulations revealed a deep mechanistic understanding on the high catalytic activity of the organocatalyst in glycolysis. The catalyst exhibited lower barrier of intermolecular dissociation and minimized unnecessary interaction to the host polymers compared with those of the-state-of-the-art organocatalyst, allowing exceptionally efficient polymer deconstruction by high activation of carbonyl on the polymer and deprotonation of ethylene glycol. The establishment of DFT and MD simulation methods sets critical foundation for predictive understanding of new polymer deconstruction mechanisms. We further unraveled selective and sequential deconstruction of different condensation polymers at specific temperatures depending on the bond strength of condensation polymers (carbonate, ester, urethane and amid), while additives or other plastics such as polyolefin and cellulose were kept intact and readily separated (Figure 2). The ability of sequential deconstruction coupled with facile separation of the mixed inert components at specific temperatures provides a new recycling pathway for a variety of currently unrecyclable mixed plastics. We have also established the methods to determine deconstruction kinetics by various catalyst systems using small model compounds. The establishment of experimental methods to precisely determine the kinetics of the polymer deconstruction is an important foundation for understanding mechanistic pathways. The polymer/oligomer conformation and solvation are currently being investigated using small-angle neutron scattering, coupled with computation. The protocol is established to correlate polymer solvation and conformation upon deconstruction or reconstruction of polymers, which is critical not only for this project but also various other polymer science projects. We also described a guide to understand the gap between industry and academia in plastic recycling,

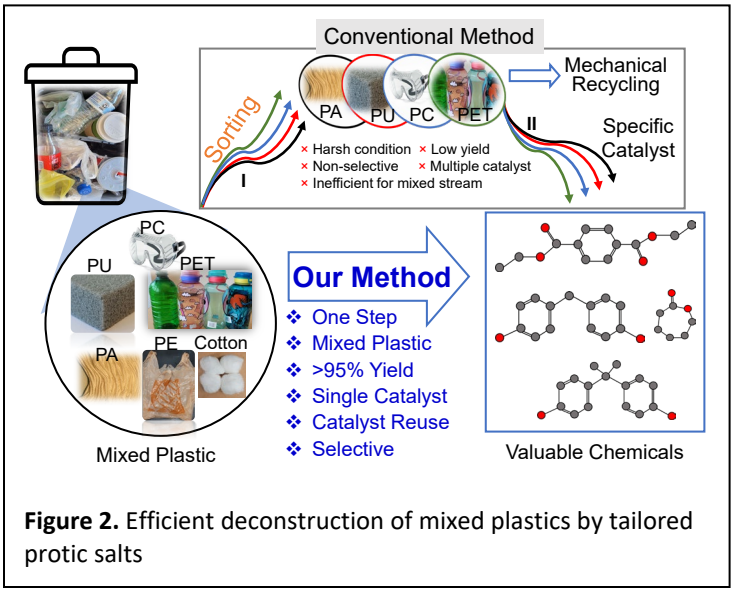

Figure 2. Efficient deconstruction of mixed plastics by tailored protic salts

aiming to help creating a path for new discovery in academic research to be integrated into industrial practices.[2]

References

1. Md. Arifuzzaman, Bobby Sumpter, Zoriana Demchuk, Changwoo Do, Mark Arnould, Md Anisur Rahman, Peng-Fei Cao, Ilja Popovs, Robert Davis, Sheng Dai, Tomonori Saito, Selective Deconstruction of Mixed Plastics by a Tailored Organocatalyst, *Mater. Horiz.*, under revision
2. Jackie Zheng, Md Arifuzzaman, Xiaomin Tang, Xi Chelsea Chen, Tomonori Saito, Recent Development of End-of-Life Strategies for Plastic in Industry and Academia: Bridging Their Gap for Future Deployment, *Mater. Horiz.*, 2023, 10, 1608–1624

Publications

1. Jackie Zheng, Md Arifuzzaman, Xiaomin Tang, Xi Chelsea Chen, Tomonori Saito, Recent Development of End-of-Life Strategies for Plastic in Industry and Academia: Bridging Their Gap for Future Deployment, *Mater. Horiz.*, 2023, 10, 1608–1624 Journal Cover
2. Sungjin Kim, Md Anisur Rahman, Md Arifuzzaman, Dustin B. Gilmer, Bingrui Li, Jackson K. Wilt, Edgar Lara-Curzio, Tomonori Saito*, Closed-loop Additive Manufacturing of Upcycled Commodity Plastic through Dynamic Crosslinking, *Sci. Adv. 2022,* 8, eabn6006

Kinetically Controlled Synthesis of Metastable Nitride Materials

Andriy Zakutayev, National Renewable Energy Laboratory

Keywords: ion exchanged, thin film, ternary, perovskite, ferroelectric, phosphide

Research Scope

The objective of this program is to understand selective synthesis of new metastable nitride materials with desired structure and useful properties. This program aims to answer the following scientific question: "*how to synthesize metastable materials by surpassing kinetic energy barriers under non-equilibrium conditions*?". The hypothesis is that metastable ternary nitrides can be obtained by a kinetically controlled synthesis approach through intermediate energy states that are structurally or compositionally related to the metastable product. The approach consists of two kinetically controlled synthesis methods: 1) cation-exchange reactions controlled by composition; and 2) crystallographic transformation from precursor to product controlled by structure. Examples of nitride materials classes studied in the past two years include multivalent ternary nitrides (e.g. cation-ordered Zn_3WN_4, layered $MgMoN_2$), wurtzite nitride ferroelectrics (i.e. $Al_{1-x}Sc_xN$), perovskites-structured nitrides ($LaWN_3$, $CeMoN_3$), with an extension of pnictides to phosphide chemistry (e.g. CuP_2, CaCuP), as discussed in more details below. The two expected outcomes of this program are a fundamental understanding of non-equilibrium kinetically controlled synthesis pathways for nitrides and other inorganic materials chemistries, and the discovery of new nitride materials that could impact energy applications.

Recent Progress

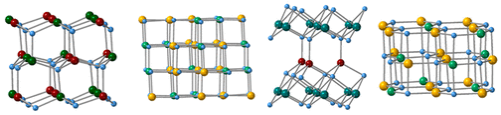

(1) ***Multivalent ternary nitrides:*** We focused the efforts on synthesis of multivalent ternary nitride materials (**Fig.1**), which combine two metal cations with a nitrogen anion in equal amounts and charge balanced stoichiometry, as defined in our invited perspective in *Chemistry of Materials*. This class of materials tends to have relatively simple crystal structures with hexagonal close packing of nitrogen atoms, metals in 4-fold or 6-fold coordination, and promising properties for a broad range of applications [1]. For example, we synthesized (a) cation-ordered Zn_3WN_4 in bulk powder form by cation exchange with halide precursors at conditions determined from in-situ synchrotron XRD measurements, (b) $MgMoN_2$ in metastable rocksalt polymorph vs. stable rocksaline (layers rocksalt and nickeline) structure controlled by annealing, with energy barrier quantified by nanocalorimetry measurements in thin film form, as well as (c) $MgWN_2$ in rocksalt, rocksaline, h-BN type crystal structures by thin film and bulk solid state synthesis methods. These multivalent ternary nitride syntheses provide

insight into kinetically controlled reaction pathways and suggest stabilization mechanisms of other metastable materials predicted by theory [2].

(2) Nitride wurtzite ferroelectrics: One potential application of multivalent ternary nitrides is as ferroelectric layers for CMOS-compatible energy-efficient nonvolatile memories [3]. A recently discovered prototypical nitride wurtzite ferroelectric is a metastable heterostructural alloy $Al_{1-x}Sc_xN$ [4]. (a) We experimentally showed that ferroelectric behavior in wurtzite nitrides has local chemical origin from the displacement of Al atoms caused by Sc substitution, rather than extended structural origin of the unit cell distortion. (b) We also observed anomalously abrupt switching dynamics $Al_{0.7}Sc_{0.3}N$ ferroelectrics using a unique custom-built ultrafast measured instrument, and explained it by a simultaneous nucleation and growth model described in our *Materials Horizons* article. (c) Despite the highly metastable character, the $Al_{0.7}Sc_{0.3}N$ ferroelectric alloys can be operated up to >400 °C, much higher than Si limited to <200 °C. These results provide guidance to reduce the coercive field in other wurtzite ferroelectrics [5], and show long-term reliable applications of metastable nitride materials.

(3) Perovskite-structured nitrides: Our demonstration of synthesis of one of the first nitride with perovskite crystal structure $LaWN_3$ has been published in *Science*. (a) A large piezoelectric response measured with scanning probe microscopy together with synchrotron diffraction confirm polar symmetry of the perovskite $LaWN_3$. (b) Properties of $LaWN_3$ films, such as optical band gap and electrical conductivity, are highly sensitive to cation stoichiometry, calling for more precise composition control. (c) We also synthesized two new Ce-based nitride perovskites $CeMoN_3$ and $CeWN_3$, showing how processing routes can overcome the competing fluorite phase, and measured their antiferromagnetic properties. This pioneering work already inspired synthesis of other predicted nitride perovskites [6][7], and property measurements for the integration with nitride semiconductors in microelectromechanical devices [8].

(4) Phosphide materials chemistry: The lessons learned from metastable nitride synthesis in this program have been applied to related pnictide materials chemistry of the phosphides. (a) Kinetic stabilization of phosphorus-rich CuP_2 thin-film semiconductor has been demonstrated in a *JACS* article, with the metastable phase achieved by stoichiometric atomic dispersion of the Cu and P precursors, followed by rapid thermal annealing which crystalizes short-range bonds but avoids long-range diffusion. (b) A related stoichiometric binary Cu_3P material has been conclusively demonstrated to be a semimetal resolving a long-standing controversy if it was a metal or a semiconductor. (c) The ternary CaCuP predicted by theory [9] has been realized in the thin film form, showing degenerate p-type conductivity with high hole mobility, which ispromising for transparent conductor applications [10]. These results show how kinetically controlled synthesis approach developed in this program transcends materials chemistries from nitrides to phosphides, and potential applications from ferroelectric to optoelectronic.

References

1. Jena, D., Page, R., Casamento, J., Dang, P., Singhal, J., Zhang, Z., Wright, J., Khalsa, G., Cho, Y. and Xing, H.G. The new nitrides: Layered, ferroelectric, magnetic, metallic and superconducting nitrides to boost the GaN photonics and electronics eco-system. *Japanese Journal of Applied Physics*, *58*(SC), p.SC0801 (2019)
2. Sun, W., Bartel, C.J., Arca, E., Bauers, S.R., Matthews, B., Orvañanos, B., Chen, B.R., Toney, M.F., Schelhas, L.T., Tumas, W. and Tate, J., A map of the inorganic ternary metal nitrides. *Nature materials*, *18*(7), pp.732-739 (2019)
3. Kim, K.H., Karpov, I., Olsson III, R.H. and Jariwala, D. Wurtzite and fluorite ferroelectric materials for electronic memory. *Nature Nanotechnology*, pp.1-20. (2023)
4. Fichtner, S., Wolff, N., Lofink, F., Kienle, L. and Wagner, B. AlScN: A III-V semiconductor based ferroelectric. *Journal of Applied Physics*, *125*(11), p.114103 (2019)
5. Moriwake, H., Yokoi, R., Taguchi, A., Ogawa, T., Fisher, C.A., Kuwabara, A., Sato, Y., Shimizu, T., Hamasaki, Y., Takashima, H. and Itoh, M., A computational search for wurtzite-structured ferroelectrics with low coercive voltages. *APL Materials*, *8*(12), p.121102 (2020)
6. Kloß, S.D., Weidemann, M.L. and Attfield, J.P., Preparation of Bulk-Phase Nitride Perovskite $LaReN_3$ and Topotactic Reduction to $LaNiO_2$-Type $LaReN_2$. *Angewandte Chemie International Edition*, *60*(41), pp.22260-22264 (2021)
7. Hanzawa, K. and Hiramatsu, H., Heteroepitaxial Growth, Degenerate State, and Superconductivity of Perovskite-Type $LaWN_3$ Thin Films. *ACS Applied Electronic Materials*, *5*(5), pp.2793-2798 (2023)
8. Yan, R., Khalsa, G., Vishwanath, S., Han, Y., Wright, J., Rouvimov, S., Katzer, D.S., Nepal, N., Downey, B.P., Muller, D.A. and Xing, H.G., GaN/NbN epitaxial semiconductor/superconductor heterostructures. *Nature*, *555*(7695), pp.183-189 (2018)
9. Williamson, B.A., Buckeridge, J., Brown, J., Ansbro, S., Palgrave, R.G. and Scanlon, D.O. Engineering valence band dispersion for high mobility p-type semiconductors. *Chemistry of Materials*, *29*(6), pp.2402-2413 (2017)
10. Woods-Robinson, R., Han, Y., Zhang, H., Ablekim, T., Khan, I., Persson, K.A. and Zakutayev, A., Wide band gap chalcogenide semiconductors. *Chemical reviews*, *120*(9), pp.4007-4055. (2020)

Publications (10 most relevant)

1. Zakutayev, A., Bauers, S.R. and Lany, S. Experimental synthesis of theoretically predicted multivalent ternary nitride materials. *Chemistry of Materials*, *34*(4), pp.1418-1438 (2022)
2. Rom, C.L., Smaha, R.W., Knebel, C.A., Heinselman, K.N., Neilson, J.R., Bauers, S.R. and Zakutayev, A., Bulk and film synthesis pathways to ternary magnesium tungsten nitrides. *arXiv:2306.02233*. (2023)
3. Yazawa, K., Mangum, J.S., Gorai, P., Brennecka, G.L. and Zakutayev, A. Local chemical origin of ferroelectric behavior in wurtzite nitrides. *Journal of Materials Chemistry C*, *10*(46), pp.17557-17566 (2022)
4. Yazawa, K., Hayden, J., Maria, J.P., Zhu, W., Trolier-McKinstry, S., Zakutayev, A. and Brennecka, G.L.,. Anomalously abrupt switching of wurtzite-structured ferroelectrics: simultaneous non-linear nucleation and growth model. *Materials horizons* (2023) DOI: 10.1039/D3MH00365E
5. Talley, K.R., Perkins, C.L., Diercks, D.R., Brennecka, G.L. and Zakutayev, A., Synthesis of $LaWN_3$ nitride perovskite with polar symmetry. *Science*, *374*(6574), pp.1488-1491 (2021)
6. Smaha, R.W., Mangum, J.S., Leahy, I.A., Calder, J., Hautzinger, M.P., Muzzillo, C.P., Perkins, C.L., Talley, K.R., Eley, S., Gorai, P. and Bauers, S.R., 2023. Structural and Optoelectronic Properties of Thin Film $LaWN_3$ *arXiv:2305.00098*. (2023)

7. Sherbondy, R., Smaha, R.W., Bartel, C.J., Holtz, M.E., Talley, K.R., Levy-Wendt, B., Perkins, C.L., Eley, S., Zakutayev, A. and Brennecka, G.L., High-Throughput Selection and Experimental Realization of Two New Ce-Based Nitride Perovskites: $CeMoN_3$ and $CeWN_3$. *Chemistry of Materials*, *34*(15), pp.6883-6893 (2022)
8. Crovetto, A., Kojda, D., Yi, F., Heinselman, K.N., LaVan, D.A., Habicht, K., Unold, T. and Zakutayev, A. Crystallize it before it diffuses: Kinetic stabilization of thin-film phosphorus-rich semiconductor CuP_2. *Journal of the American Chemical Society*, *144*(29), pp.13334-13343 (2022)
9. Crovetto, A., Unold, T. and Zakutayev, A., Is $Cu_{3-x}P$ a Semiconductor, a Metal, or a Semimetal?. *Chemistry of Materials*, *35*(3), pp.1259-1272 (2023)
10. Willis, J., Bravić, I., Schnepf, R.R., Heinselman, K.N., Monserrat, B., Unold, T., Zakutayev, A., Scanlon, D.O. and Crovetto, A., Prediction and realisation of high mobility and degenerate p-type conductivity in CaCuP thin films. *Chemical Science*, *13*(20), pp.5872-5883 (2022)

University Abstracts

Li-Ion Battery Critical Metal Recycling Using Sugars

Ananda Amarasekara, Prairie View A&M University, TX

Keywords: Recycling; Critical metals; Glycolic acid; Lactic acid; Pyrolysis

Research Scope

The primary objective of the project is the development of a new energy efficient method for the recovery of Li, Ni, Mn and Co critical metals from spent Li-ion batteries (LiBs) using inexpensive sugars and oxygen or air. The proposed work is based on the hypothesis that: *Ni, Mn and Co complexes in the spent Li-ion battery cathode material can act as a catalyst to oxidize sugars to hydroxy acids and these carboxylic acids can selectively chelate and extract Li, Ni, Mn and Co critical metals from cathode material under mild hydrothermal conditions.* We are aiming to achieve the following specific objectives under this project (1). Uncover the catalytic potential of Ni, Mn and Co in Li-ion battery materials to oxidize carbohydrates to degradation products with multiple carboxylic acid and hydroxyl functions, using oxygen or air as the oxidant (2). Study the recovery of critical metals by two approaches: (i) isolation of pure Li, Ni, Mn and Co compounds from Li-ion battery black material (LiBBM) leachate (ii) re-synthesis of LiB cathode material from leachate.

Recent Progress

In the first year of the project we have partially completed the following tasks:

Task 1. Separation of LiBBM from batteries and composition analysis

Six different types common Li-ion batteries were identified at the initial step. The batteries were discharged by immersing in 10% aq. sodium chloride at room temperature for 5 days. Then cathode and anode coatings were collected. For example, DELL 1525 laptop battery (87Wh, 11.1V) casing was opened to collect nine 18650 Li-ion cells and these cells were dismantled and black anode coatings on copper foil and black cathode coating on aluminum foil were collected, combined and air dried for 2 days to give 45.67 g of combined Li-ion battery black material as shown in figure 1. Categorized battery groups were disassembled separately and LiBBM from each group of batteries were separately collected. The powders collected were separately pulverized in a ball mill and sieved through a mesh of size 25, air dried and stored in air-tight glass bottles till they are extracted.

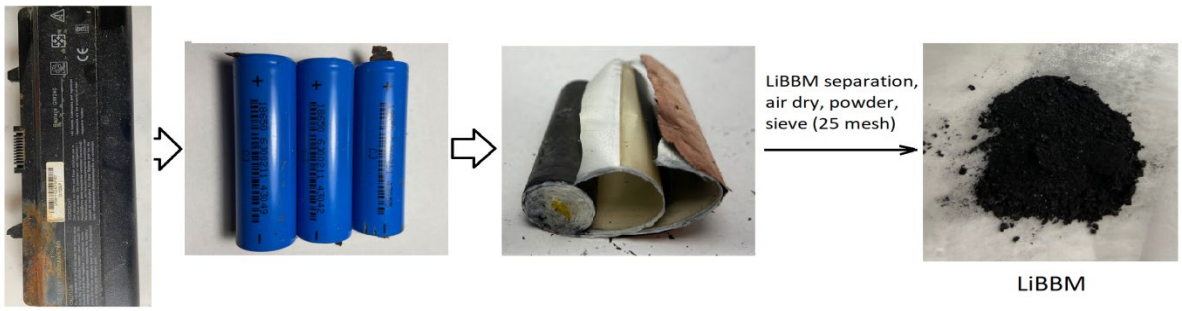

Figure 1. Collection of Li-ion battery black material (LiBBM) from a spent DELL 1525 laptop battery (87Wh, 11.1 V)

We have found that representative LiBBM from a spent DELL 1525 laptop battery contain lithium nickel manganese cobalt oxide ($Li_aNi_bMn_cCo_dO_e$) impregnated on graphite carbon, by SEM, EDX and X-ray crystallography analysis. Furthermore, the most likely active material has an empirical composition of Ni : Mn : Co 4.12 : 2.10 : 1.50 as indicated by the EDX data.

Task 2a. Catalytic activity of $Li_aNi_bMn_cCo_dO_e$ /C in oxidation of sugars

The LiBBM collected was tested for oxidation of D-glucose and D-Fructose under an oxygen atmosphere (1.0-3.4 Atm.), at 100-150 °C, in water and aq. NaOH or LiOH mediums. The highest glucose conversion and a 94% yield of glycolic acid was obtained for an experiment carried out at 120 °C, 2 h, under 3.4 Atm. O_2 in 0.50 M aq. NaOH. Tartaric, malic, succinic and 2-hydroxybutaric acids were identified as minor products in D-glucose oxidation reactions.

Task 2b. Catalytic activity of $Li_aNi_bMn_cCo_dO_e$ /C in oxidation of glycerol

Next LiBBM was tested for the oxidation of glycerol under an oxygen atmosphere (1.0-3.4 Atm), at 100-250 °C, in water and aq. NaOH or LiOH mediums. The highest lactic and glycolic acid yields of 54 and 41% respectively with 100% glycerol conversion was achieved in an experiment carried out under 3.4 Atm. O_2 at 230 °C, 4 h.

Task 3. Leaching of Li, Ni, Mn and Co from LiBBMs using lactic and glycolic acids

In this task, different LiBBM powders were hydrothermally extracted with aq. lactic and glycolic acid solutions. Our preliminary experiments using pure 0.50 M aq. lactic and glycolic acid solutions resulted only 50-65% leachings of Li, Ni, Mn and Co from LiBBM. However, the use of lactic and glycolic acid mixtures of 0.50 M in each resulted high leaching efficiencies of 90-98% for Li, Ni, Mn and Co from LiBBM collected from a spent laptop battery. Currently we are working on optimization of leaching efficiencies using factorial experimental design method.

Task 4. Re-synthesis of the original cathode material from leaching solution

The re-synthesis approach was studied as a batch process for use with the same type of LiBs and with well-defined cathode materials. The leachate solution collected under Task 3 from 0.50 M lactic and glycolic acid mixtures were analyzed for Li, Ni, Mn, and Co contents and only a selected set of solutions with favorable Li, Ni, Mn, and Co ratios were used in re-synthesis

experiments. These leachate solutions were evaporated to dryness at 90 °C and then sintered in air at 800 °C in alumina crucibles for 10-15 h to obtain the re-synthesized cathode material. Currently we are characterizing the regenerated LiNMC materials by using chemical, X-ray and surface area analysis methods.

Publications

[1] Oxidation of Glucose to Glycolic Acid Using Oxygen and Pyrolyzed Spent Li-Ion Battery Electrode Material as Catalyst. Ananda S. Amarasekara, Hashini N. K. Herath, Tony L. Grady, Cristian D. Gutierrez Reyes. *Applied Catalysis A: General*, 648, 118920, **2022**. https://doi.org/10.1016/j.apcata.2022.118920

[2] Two step Synthesis of poly(Lactic-co-Glycolic acid) from Glycerol by Spent Li-Ion Battery Electrode $LiNi_xMn_yCo_zO_2$/C Catalyzed Oxidation to Lactic, Glycolic Acid Mixture and *p*-TsOH - $SnCl_2$ Catalyzed Polymerization. Ananda S. Amarasekara, Hashini N. K. Herath,Deping Wang. *Under Review*: *Industrial Crops and Products*. 05-**2023**.

Enabling energy-dense grid scale batteries with earth abundant materials

Chibueze Amanchukwu
Neubauer Family Assistant Professor of Molecular Engineering
Pritzker School of Molecular Engineering
The University of Chicago

Keywords: molten salts, dual-ion batteries, solvent-free electrolytes, lithium intercalation, anion intercalation

Research Scope

The need for energy dense and cheap long duration grid scale batteries requires new battery chemistries. Dual ion batteries are a class of batteries that eschew the use of transition metals and can use earth abundant carbons as both anode and cathode. This battery chemistry operates through cation intercalation at the anode and anion intercalation at the cathode [1,2]. Furthermore, the active species are hosted in the electrolyte (instead of the cathode in Li-ion) [3]. Current electrolytes use high salt concentration (to increase capacity) or ionic liquids (to increase the electrochemical working window). However, high salt concentration electrolytes still contain organic solvents which are vulnerable thermally and detract from the energy density [4]. Unfortunately, ionic liquid organic cations suffer from undesired co-intercalation [5,6]. Here, we focus on the discovery of novel low melting solvent-less alkali-based molten salt electrolytes for next generation batteries. First, we study their physicochemical properties especially the influence of anion identity on melting transition and ionic conductivity. Secondly, we explore their influence on fundamental electrochemical reactions such as electrodeposition, cation, and anion intercalation. Our focus on fundamental understanding of molten salt properties and subsequent electrochemical behavior is of great interest for the development of next generation battery chemistries and electrochemical processes such as electrocatalysis and beyond.

Recent Progress

We have made progress in the study of alkali-based molten salts and the understanding of their physicochemical properties. To make them 'low melting,' we have pursued two strategies. (1) the synthesis of novel salts with bulky anions and (2) the formation of eutectics to decrease the salt melting transition. These strategies have yielded high ionic conductivities (> 1mS/cm) (Figure 1a), low melting transitions (~45C), and high oxidative stability (6V) (Figure 1b). As a first step, we have shown that these electrolytes can support battery chemistries such as lithium batteries with facile electrodeposition and electro-dissolution (manuscript submitted). More importantly, the electrode/electrolyte interface is enriched with inorganic decomposition products that limit

further electrochemical degradation [7]. Future work will focus on probing the influence of these electrolytes on reversible cation and anion (de)intercalation. Many mechanisms of intercalation indicate that solvent intercalation and decomposition occurs to form the anodic solid electrolyte interface (SEI) [7]. The lack of solvents change the intercalation and passivation processes for both cation and anions and is poorly understood. Insights garnered from our fundamental study of the intercalation behavior will then lead to novel electrolytes of interest in batteries and electrochemistry.

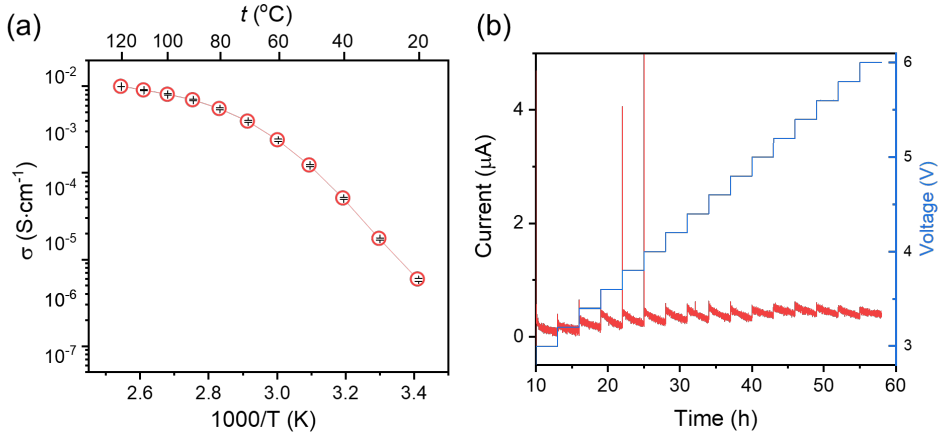

Figure 1. (a) Ionic conductivity and (b) oxidative stability in a Li|Al cell using molten salt electrolyte from 3-6V, voltage ramp step of 0.2V at 80 °C. These data show high ionic conductivities and a wide electrochemical stability window.

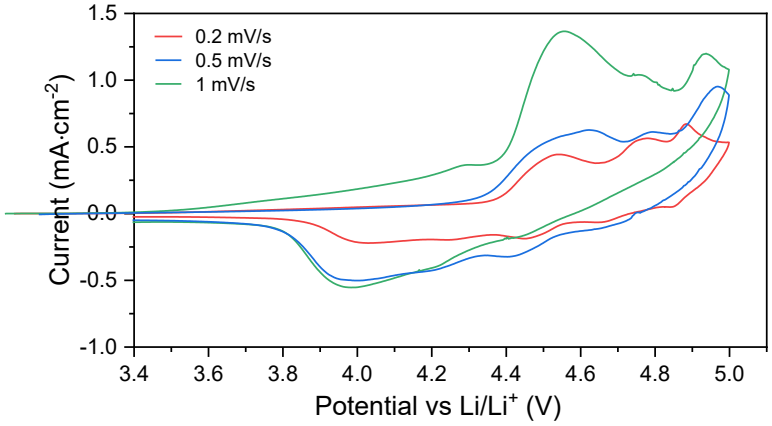

Figure 2. CV of Li|Graphite cell of molten salt electrolyte enabling reversible anion intercalation within a graphitic electrode.

References

1. K. V Kravchyk, M. V Kovalenko, *Rechargeable Dual-Ion Batteries with Graphite as a Cathode: Key Challenges and Opportunities*, Adv Energy Mater. **9** 1901749 (2019).
2. L. Zhang, H. Wang, X. Zhang, Y. Tang, *A Review of Emerging Dual-Ion Batteries: Fundamentals and Recent Advances*, Adv Funct Mater. **31** (2021).

3. A. Kotronia, H.D. Asfaw, C.W. Tai, M. Hahlin, D. Brandell, K. Edström, *Nature of the Cathode-Electrolyte Interface in Highly Concentrated Electrolytes Used in Graphite Dual-Ion Batteries*, ACS Appl Mater Interfaces. **13** 3867–3880 (2021).
4. L. Xiang, X. Ou, X. Wang, Z. Zhou, X. Li, Y. Tang, *Highly Concentrated Electrolyte towards Enhanced Energy Density and Cycling Life of Dual-Ion Batter*y, Angewandte Chemie International Edition. **59** 17924–17930 (2020).
5. S. Rothermel, P. Meister, G. Schmuelling, O. Fromm, H.W. Meyer, S. Nowak, M. Winter, T. Placke, *Dual-graphite cells based on the reversible intercalation of bis(trifluoromethanesulfonyl)imide anions from an ionic liquid electrolyte*, Energy Environ Sci. **7** 3412–3423 (2014).
6. X. Tong, X. Ou, N. Wu, H. Wang, J. Li, Y. Tang, X.Y. Tong, X.W. Ou, N.Z. Wu, H.Y. Wang, J. Li, Y.B. Tang, *High Oxidation Potential ≈6.0 V of Concentrated Electrolyte toward High-Performance Dual-Ion Battery*, Adv Energy Mater. **11** 2100151 (2021).
7. H. Adenusi, G.A. Chass, S. Passerini, K. V Tian, G. Chen, H. Adenusi, G. Chen, G.A. Chass, K. V Tian, S. Passerini, *Lithium Batteries and the Solid Electrolyte Interphase (SEI)—Progress and Outlook*, Adv Energy Mater. **13** 2203307 (2023).

Publications

1. Minh Canh Vu, Priyadarshini Mirmira, Reginaldo J. Gomes, Peiyuan Ma, Emily S. Doyle, Hrishikesh S. Srinivasan, and Chibueze V. Amanchukwu, *Solvent-free low melting alkali-based molten salt electrolytes for lithium metal batteries*, **submitted**.

Biomolecular Interactions in Organic Semiconductors

M. A. Baldo, ***Research Laboratory of Electronics, MIT***
T. Van Voorhis, ***Dept. of Chemistry, MIT***

Keywords: Excitons, Organic Semiconductors, Triplet-triplet Annihilation

Research Scope

Light emitting devices, photocatalysis, sensing, and bioimaging are examples of important technologies that upconvert (UC) long-wavelength photons or excitons to higher energies. But interactions between photons are weak, and traditional nonlinear optical approaches cannot be used with low intensity sources. To solve this challenge, there has been much recent research on using molecular excited states to mediate interactions between photons. Triplet-triplet annihilation (TTA) is particularly promising approach. Here, two spin 1 triplet excited states combine to form a high energy spin 0 singlet state that can re-emit light. TTA, however, does not always generate the desired high-energy singlet state. Sometimes, it generates other higher energy triplet states that waste energy, potentially limiting the overall efficiency to 40%, or less. In recent work, we have addressed this crucial and fundamental efficiency limit for TTA.

Recent Progress

A major source of loss in TTA originates from triplet-triplet (TT) pairs with triplet rather than singlet spin multiplicity. Assuming that the other steps are 100% efficient, the spin statistics imply that the theoretical limit on the TTA efficiency is 20% per triplet or 40% per TT pair [1]. Interestingly, experimental studies have reported annihilators with efficiencies that appear to exceed this limit, such as 9,10-diphenylanthracene (DPA)18 and 5,6,11,12-tetraphenyltetracene (rubrene) [2]. A number of explanations have been proposed to solve this paradox. First, T2 might be higher in energy than twice T1 [1]. Then, a triplet TT pair would be unable to produce a unimolecular T2 state. For example, the efficiency of perylene derivatives have been shown to depend on the T2 energy [3,4]. Second, T2 might undergo ISC to S1 [1]. Indeed, experimental studies found evidence of T2 -> S1 ISC in rubrene [5].

To determine whether T2 is higher in energy than twice T1, we calculated the excited states of DPA, rubrene, and their parent molecules using time-dependent density functional theory (TDDFT). We find that T2 is not higher than twice T1 in these molecules. Besides, T2 is so close in energy to S1 that T1 + T1 -> T2 should be allowed as long as T1 + T1 -> S1

Next, to determine whether the T2 -> S1 ISC could be facile, we examined the SOC between the TDDFT states. We find that the T2 - S1 SOC is 7 and 60 times stronger in DPA and rubrene than anthracene and tetracene, respectively. In an effort to produce other systems with strong T2 - S1 SOC, we substituted electron withdrawing amide and electron-donating amine

groups at the 4', 4"-positions of DPA (DPA-diamine). Another popular way to increase the SOC in organic molecules is using heavy atoms. In this approach, the heavy atom should be near the core of the molecule to ensure excitation densities on the heavy atom. To demonstrate this effect, we compare the oxygen-containing 1,3-diphenylisobenzofuran (DPBF) to the sulfur-containing 1,3-diphenylisobenzothiophene (DPBT). DPBT exhibits a 6-fold enhancement in the T2 - S1 SOC and a 30-fold enhancement in the T2 -> S1 ISC rate with respect to DPBF. In particular, the T2 -> S1 ISC rate is predicted to enter the picosecond timescales.

To study the impact of ISC rates on the efficiency of TTA, we fabricated films and measured optical upconversion using a sensitizer platinum tetraphenyltetrabenzyl-porphyrin (PtTPTBP). The results are shown in Fig. 1.

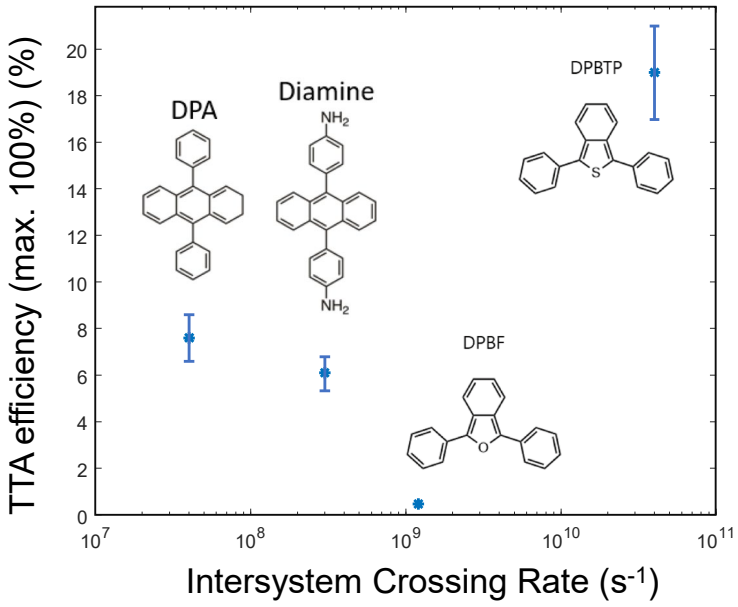

Fig. 1. The efficiency of TTA versus predicted ISC rate.

As shown in Fig. 1, increasing the T2 - S1 ISC rate does not necessarily increase the efficiency. TTA competes with the non-radiative decay of T1. Modifications to increase the desirable T2 - S1 SOC also increase the undesirable T1 - S0 SOC. Whereas the T1 - S0 ISC rate is only 3 times higher in DPA than anthracene, it is 300 times higher in Diamine than DPA. In addition, the T2 -> S1 ISC competes with the decay of T2. Though *ab initio* calculation of IC rates is challenging [6], experimental values in related systems range from picosecond [7] to nanosecond [8] timescales. On the other hand, the T2 -> S1 ISC on the order of tens to hundreds of picoseconds might be one of the fastest photophysical transitions in DPBT, and responsible for its very high efficiency.

Our results demonstrate the potential importance of T2 -> S1 ISC in TTA. The energies of S1, T1, and T2 do not explain the limit-breaking efficiency in DPA and rubrene. Instead, T2 -> S1 ISC enhances TTA in these molecules. But the comparison between DPA and DPA-diamine demonstrates the importance of also considering the associated loss pathways, especially T1->S0. Through simultaneous design of T2->S1 and T1->S0, engineering intersystem crossing promises to increase the efficiency of TTA from its current limit of 40% per TT pair to 100%.

References

1. Cheng, Y.Y., Khoury, T., Clady, R.G.C.R., Tayebjee, M.J.Y., Ekins-Daukes, N.J., Crossley, M.J., Schmidt, T.W., "On the efficiency limit of triplet-triplet annihilation for photochemical upconversion", Phys. Chem. Chem. Phys. 12, 66-71 (2010).
2. Di, D., Yang, L., Richter, J.M., Meraldi, L., Altamimi, R.M., Alyamani, A.Y., Credgington, D., Musselman, K.P., MacManus-Driscoll, J.L., Friend, R.H., "Efficient Triplet Exciton Fusion in Molecularly Doped Polymer Light-Emitting Diodes", Adv. Mater. 29, 1605987 (2017).
3. Sun, W., Ronchi, A., Zhao, T., Han, J., Monguzzi, A., Duan, P. "Highly efficient photon upconversion based on triplet-triplet annihilation from bichromophoric annihilators", J. Mater. Chem. C, 9, 14201-14208 (2021).
4. Carrod, A. J., Cravcenco, A., Ye, C., Börjesson, K. "Modulating TTA efficiency through control of high energy triplet states", J. Mater. Chem. C, 10, 4923-4928 (2022).
5. Bossanyi, D. G., Sasaki, Y., Wang, S., Chekulaev, D., Kimizuka, N., Yanai, N., Clark, J., "Spin Statistics for Triplet-Triplet Annihilation Upconversion: Exchange Coupling, Intermolecular Orientation, and Reverse Intersystem Crossing" JACS Au, 1, 2188-2201 (2021).
6. Rashev, S. "Calculation of internal conversion rate constants of single vibronic levels in S1 benzene". J. Chem. Phys. 101, 6632-6639 (1994).
7. Bohne, C., Kennedy, S. R., Boch, R., Negri, F., Orlandi, G., Siebrand, W., Scaiano, J. C. Determination of the Lifetime of the Second Excited Triplet State of Anthracenes. J. Phys. Chem. 95, 10300-10306 (1991).
8. Yang, W., Zhao, J., Tang, G., Li, X., Gurzadyan, G. G. Direct Observation of Long-Lived Upper Excited Triplet States and Intersystem Crossing in Anthracene-Containing Pt^{II} Complexes. J. Phys. Chem. Lett., 10, 7767-7773 (2019).

Publications

1. Dong-Gwang Ha, Ruomeng Wan, Changhae Andrew Kim, Ting-An Lin, Luming Yang, Troy Van Voorhis, Marc Baldo & Mircea Dinca, "Exchange controlled triplet fusion in metal–organic frameworks", Nature Materials, Volume 21, 1275, (2022), DOI: https://doi.org/10.1038/s41563-022-01368-
2. Collin F. Perkinson, Markus Einzinger, Joseph Finley, Moungi G. Bawendi, Marc A. Baldo, "Magnetic-field switchable laser via optical pumping of rubrene", Advanced Materials, 2103870, (2021), DOI: https://doi.org/10.1002/adma.202103870.
3. Changhae Andrew Kim and Troy Van Voorhis, "Maximizing TADF via Conformational Optimization", The Journal of Physical Chemistry, Volume 125, 7644, (2021), DOI: https://doi.org/10.1021/acs.jpca.1c05104.
4. Wang, Lili Yoo, Jason J. Lin, Ting-An Perkinson, Collin F. Lu, Yongli Baldo, Marc A. Bawendi, Moungi G., "Interfacial Trap- Assisted Triplet Generation in Lead Halide Perovskite Sensitized Solid-State Upconversion", Advanced Materials, Volume 33, 2100854, (2021), DOI: https://doi.org/10.1002/adma.202100854

Solid-State Chemistry of Novel Pnictides with Complex Structures

Svilen Bobev

Department of Chemistry and Biochemistry, University of Delaware, Newark DE 19716

Keywords: New Materials, Synthesis, Thermoelectrics, Topological Behavior, Zintl Phases

Research Scope

Our program is focuses on synthetic and structural work of novel materials, stepping up the research efforts in the creation of new crystalline forms of matter for energy production and conversion. Specifically, we work on Zintl phases, which in recent years, have established themselves as promising candidates for thermoelectric applications. Owing to their narrow bandgaps, Zintl phases exhibit high electrical conductivity, while their complex crystal structures and/or presence of heavy elements yield low thermal conductivity. All of the above provide for a favorable combination of transport properties, beneficial for high thermoelectric performance. From a more fundamental point of view, the structure-property relationships derived from our work can be further used for developing a rationale for the synthesis of other new compounds, as well as for tuning of properties of existing ones.

Recent Progress

More recently, the peculiar band structures of Zintl phases, featuring narrow bandgaps or pseudogaps, have evoked renewed interest in this class of compounds as potential candidates for topological materials.[1] In an idealized charge-balanced Zintl phase, the valence and conduction bands are expected to be separated by a well-defined bandgap. In reality, the incomplete electron transfer between the cationic and anionic parts of a crystal structure may result in a gapless state where only a small number of bands cross or "touch" the Fermi level.[2] Such an electronic situation is characteristic of semimetals. In certain instances, non-trivial electronic band topology is realized, as in the case of Na_3Bi – a structurally simple Zintl phase ($[Na^+]_3Bi^{3-}$), which was found to be one of the first three-dimensional topological Dirac semimetals.[3] Non-trivial electronic band topologies have been proposed in some equiatomic Zintl phases with the general composition *AEAPn* (*AE* = alkaline-earth metal, *A* = alkali metal, *Pn* = pnictogen, i.e., a group 15 element).[4,5] These materials are derivatives of the afore-mentioned Na_3Bi, where one of the Na^+ cations is removed and another one is replaced by a divalent alkaline-earth metal. *AEAPn* crystallize in several different structure types and although many of the possible *AEAPn* compositions have been experimentally realized, more than half of the theoretically possible elemental combinations have not been reported. In this report, we present the crystal and electronic structure of the bismuthide BaLiBi, which to date, has not been properly characterized.

BaLiBi crystallizes hexagonally (Figure 1). However, considering the low atomic scattering power of Li, unambiguous discrimination between the ZrBeSi type and the structurally related LiGaGe type is challenging. It is worth noting that recent investigations of the ZrBeSi-type SrAgBi provide hints for possible buckling of the [AgBi] layers, which would indicate breaking of the corresponding mirror symmetry.[6] Therefore, we conducted an accurate single-crystal X-ray diffraction analysis, which confirms the ZrBeSi structure type for this material with the space group $P6_3/mmc$, a = 4.9917(6) Å, c = 9.079(2) Å, V = 195.92(7) Å^3. Attempts to refine the structure of BaLiBi in the non-centrosymmetric space group $P6_3mc$ resulted in a model with the same atomic coordinates as in the centrosymmetric ZrBeSi type (within one e.s.d.).

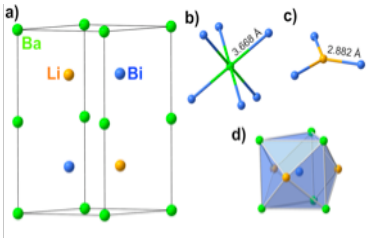

Fig. 1 Crystal structure of BaLiBi (a) and coordination environments of the Ba, Li, and Bi atoms (b–d).

The ZrBeSi type can be regarded as a "colored" variant of another common structure, that of AlB_2, with two distinct atomis replacing the singular B in the honeycomb network of the original AlB_2 structure.[7] In BaLiBi, these atoms are Li and Bi, while the positions of Ba correspond to the Al positions in AlB_2. The Bi atoms adopt trigonal-prismatic coordination by Ba and trigonal-planar coordination by Li, so that the Ba+Li coordination polyhedron around Bi can be described as a trigonal prism with capped rectangular faces. The crystal structure of BaLiBi can be alternatively viewed as a "stuffed" variant of the NiAs structure, where the Bi atoms form a hexagonal close packing, the Ba atoms occupy the octahedral voids in this packing, and the Li atoms are located between adjacent tetrahedral voids on their common triangular faces.

Since the shortest Bi–Bi distance in the BaLiBi crystal structure measures 4.99 Å, no Bi–Bi bonding can be expected, and the formal charges can be assigned according to the notation $[Ba^{2+}][Li^{+}][Bi^{3-}]$, suggesting an electron-balanced composition. In line with this notation, first-principle calculations with the LMTO code reveal a semiconducting ground state, with a bandgap of about 0.64 eV. It is worth noting that this sizeable bandgap is observed already without considering spin-orbit coupling (SOC) in our calculations. This is different from the cases of transition-metal-containing bismuthides *AETM*Bi (*AE* = Sr, Ba; *TM* = Cu, Ag, Au), which exhibit a semimetallic ground state. The occurrence of a bandgap in BaLiBi can be explained by the higher polarity of the chemical bonding in this compound, evidenced by the states just below the Fermi level, which have a prevalent contribution from Bi(6p), pointing toward electron transfer onto the Bi atoms. However, purely ionic bonding is not the case, since contributions from Ba and Li states exist in the same energy region. In the narrow energy region -10.2 eV $< E - E_F < -9.5$ eV, a sharp peak consisting mainly of the Bi(6s) states is located, corresponding to the electron lone pairs on the Bi atoms. Integration of the all-electron density from the LMTO calculations in the

atomic basins defined by the Quantum Theory of Atoms in Molecules (QTAIM) yielded the following Bader charges: Ba +1.01, Li +0.81, Bi –1.82.

References

1. M. O. Ogunbunmi, and S. Bobev, *Exploiting the Fraternal Twin Nature of Thermoelectrics and Topological Insulators in Zintl Phases as a Tool for Engineering New Efficient Thermoelectric Generators,* J. Mater. Chem. C **in print** (2023), DOI 10.1039/D3TC00556A
2. A. Ovchinnikov, and S. Bobev, *Zintl Phases with Group 15 Elements and the Transition Metals: A Brief Overview of Pnictides with Diverse and Complex Structures,* J. Solid State Chem. **270**, 346 (2019).
3. Z. K. Liu, B. Zhou, Y. Zhang, Z. J. Wang, H. M. Weng, D. Prabhakaran, S.-K. Mo, Z. X. Shen, Z. Fang, X. Dai, Z. Hussain, and Y. L. Chen, *Discovery of a three-dimensional topological Dirac semimetal, Na_3Bi,* Science **343**, 864 (2014).
4. C. Mondal, C. K. Barman, S. Kumar, A. Alam, and B. Pathak, *Emergence of Topological insulator and Nodal line semi-metal states in XX'Bi (X = Na, K, Rb, Cs; X' = Ca, Sr)*, Sci. Rep. **9**, 527 (2019).
5. D. Shao, Z. Guo, X. Wu, S. Nie, J. Sun, H. Weng, and Z. Wang, *Topological insulators in the NaCaBi family with large spin-orbit coupling gaps,* Phys. Rev. Res **3**, 013278 (2021).
6. Z. Hu, J. Deng, H. Li, M. O. Ogunbunmi, X. Tong, Q. Wang, D. Graf, W. R. Pudełko, Y. Liu, H. Lei, S. Bobev, M. Radovic, Z. Wang, and C. Petrovic, *Robust Three-dimensional Type-II Dirac Semimetal State in SrAgBi,* npj Quantum Mater. **8**, 1 (2023).
7. S. F. Matar, and R. Pöttgen, *Coloring in the ZrBeSi-type structure*, Z. Naturforsch. B **74**, 307 (2019).

Publications

1. M. O. Ogunbunmi, S. Baranets, and S. Bobev, *Materials Design, Synthesis, and Transport Properties of Disordered Rare-earth Metal Zintl Bismuthides with the anti-Th_3P_4 Structure Type,* Dalton Trans. **51**, 5227 (2022).
2. S. Baranets, A. Balvanz, G. M. Darone, and S. Bobev, *On the Effects of Aliovalent Substitutions in Thermoelectric Zintl Pnictides. Varied Polyanionic Dimensionality and Complex Structural Transformations—the Case of Sr_3ZnP_3 vs $Sr_3Al_xZn_{1-x}P_3$,* Chem. Mater. **34**, 4172 (2022).
3. M. O. Ogunbunmi, and S. Bobev, *The Highly Disordered Zintl Phase $Ca_{10}GdCdSb_9$ – New Example of a p-type Semiconductor with Remarkable Thermoelectric Properties,* Mater. Today Phys. **26**, 100725 (2022).
4. M. O. Ogunbunmi, S. Baranets, and S. Bobev, *Structural Complexity and Tuned Thermoelectric Properties of a New Polymorph of the Zintl Phase Ca_2CdSb_2 with a non-centrosymmetric Monoclinic Structure,* Inorg. Chem. **61**, 10888 (2022).
5. R. Janzen, S. Baranets, and S. Bobev, *Synthesis, Structural Characterization, and Properties of the New Zintl phases $Eu_{10}Mn_6Bi_{12}$ and $Yb_{10}Zn_6Sb_{12}$,* Dalton Trans. **51**, 13470 (2022).
6. M. O. Ogunbunmi, and S. Bobev, *Observation of Anomalously High Seebeck Coefficients in the Family of Zintl Phase Semiconductors $Ca_{10}RECdSb_9$ (RE = Rare-Earth Metal),* Chem. Mater. **34**, 8808 (2022).
7. M. O. Ogunbunmi, and S. Bobev, *Enhanced Thermoelectric Performance in the Zintl Antimonides $(Ca,RE)_9Cd_4Sb_9$ (RE = rare-earth metal). Synergy Between Increased Structural Complexity and Drive Towards Optimized Chemical Bonding,* Mater. Today Adv. **16**, 100310 (2022).
8. B. Saparov, and S. Bobev, *Synthesis and Crystal Structure of the Zintl Phases $Na_2CaCdSb_2$, $Na_2SrCdSb_2$ and $Na_2EuCdSb_2$,* Inorganics **10**, 265 (2022).
9. Y. Wang, and S. Bobev, *Synthesis and Crystal structure of the Zintl phases NaSrSb, NaBaSb and NaEuSb,* Materials **16**, 1428 (2023).

10. M. O. Ogunbunmi, and S. Bobev, *The Electronic and Thermoelectric Transport Properties of Zintl Pnictides,* Encycl. Inorg. Bioinorg. Chem. **in print** (2023).

Facilitating Ionic and Electronic Conduction in Radical Polymers through Controlled Assembly

Bryan W. Boudouris and Brett M. Savoie, Purdue University

Keywords: Open-shell molecules; Radical polymers; Mixed ion-electron conduction; Tailored nanostructure; Radical-radical coupling

Research Scope

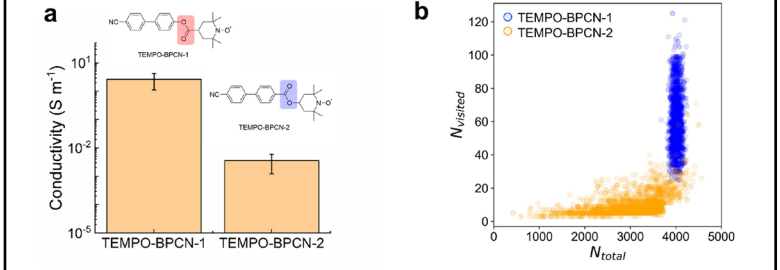

Figure 1. (a) Room temperature electrical conductivity values of TEMPO-BPCN-1 and TEMPO-BPCN-2 single crystals. The chemical structures of the open-shell molecules are inset. (b) The count of distinctly visited hopping sites and the total hopping sites in TEMPO-BPCN-1 (blue) and TEMPO-BPCN-2 (orange) single crystals. The computation includes 200 Kinetic Monte Carlo (kMC) runs.

The scope of this work centers on addressing the still-lingering, overarching question of how the local structural order of open-shell small molecules and radical polymers impacts their mass and charge transport.[1-3] The overarching hypothesis is that partially percolating radical networks govern transport in these materials.[4-6] It is put forward that designing radical materials with tailored chemical designs that allow for spatially close radical-radical packing will produce systems with faster rates of charge and mass transport.[7,8] This idea is directly interrogated through coupled computational and experimental aims with the primary objective of enabling the assembly of radical moieties to precisely control radical-radical couplings and macromolecular backbone interactions such that order can be introduced in a rational manner at different scales. To address this point, the project has the Specific Aims of: (1) Design and Syntheses of Open-Shell Chemistries; (2) Control of Open-Shell Assembly; (3) Determining the Mechanics of Coupled Transport at Multiple Scales; and (4) Experimental Evaluation of Transport Properties in Testbed Devices. In the first two years of the project, these aims have been addressed using a combination of physics-based computation and machine learning to characterize these materials and through the experimental design, synthesis, and evaluation of open-shell small molecule crystals; liquid crystalline open-shell molecules; and nonconjugated radical polymers. By coupling these key parameters, clear structure-property relationships have been developed. Importantly, this has led to the development of new radical-containing chemistries that have close radical-radical interactions that have the highest electrical conductivity values for any nonconjugated radical-based system.

Recent Progress

While progress has been made on multiple fronts, here we highlight three specific efforts that are representative of our approach and how coupling experiment and computation lead to

rapid and impactful results. In the first example, we quantified the electrical conductivity in two organic radical single crystals and showed that a subtle change in atomic connectivity drastically altered the macroscopic electronic properties of the materials. That is, one radical crystal has an electrical conductivity of ~3 S m^{-1}, which is the highest value for nonconjugated radical conductors over a 1 µm-scale reported to date (Figure 1). However, the other radical crystal has a 1,000-fold lower conductivity despite their extremely similar molecular structures. The temperature-dependent conductivity follows the variable range hopping (VRH) mechanism for both radical crystals, and the difference in effective charge mobility is the reason for the conductivity difference. This mechanism is also backed by the fact that the magnetic field-dependent electrical resistance in the radical crystals follows the magnetoresistance model under the VRH mechanism. This effort specifically highlights how radical-radical interactions, and the manner in which the radical groups in single crystals of open-shell small molecules pack is critical to charge transport. In the second effort, we provide an example of how computational design informs the synthesis of high-performance materials. Quantum chemical studies on a large group of radical polymers were performed, and these computations explicitly included the coupling between polymer constraints and radical-mediated intramolecular charge transfer. A chemical space of 64 radical polymer chemistries were constructed based on varying backbone units, open-shell chemistries, and spacer units between the backbone and the radical groups. A comprehensive conformational sampling was used to calculate the expected values of intrachain transport using several complementary metrics. In brief, this work highlights that transport in radical polymers is primarily driven by the choice of radical chemistry, which in turn, influences the optimal choice of backbone and spacer chemistries. From these data, we synthesized a specific verdazyl-based radical polymer that demonstrated high electrical conductivity and reasonable lithium-ion conductivity as well. In the third portion, we explain how the design of radical-bearing monomer units that are capable of undergoing topochemical polymerization lead to intriguing results. First, single crystals of these monomers display electrical conductivity values approaching 100 S m^{-1} across macroscopic scales, and these (currently unpublished) values break our own record described above. Second, this is the first example of topochemical polymerization of the open-shell monomers, and it yields highly ordered radical polymer as well. By sharing these stories, we

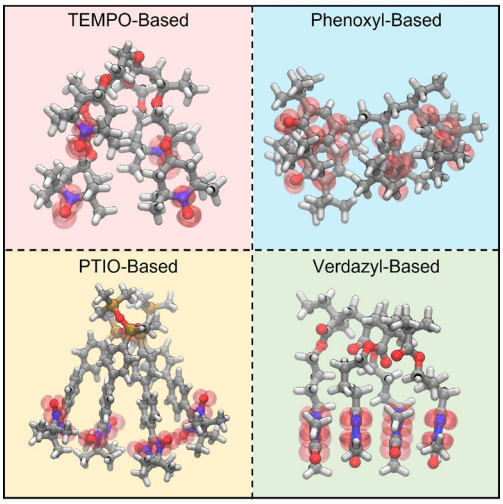

Figure 2. Representative lowest energy conformers for radical polymers based on four distinct open-shell designs. The panels highlight how the radical chemistry can promote (or disincentivize) radical-radical coupling when the open-shell groups are attached to the macromolecular backbones.

aim to highlight how the team is addressing the original research hypotheses and answering our key scientific questions.

References

1. K. Oyaizu and H. Nishide, *Radical Polymers for Organic Electronic Devices: A Radical Departure from Conjugated Polymers?*, Advanced Materials **21**, 2339-2344 (2009).
2. S. Wang, F. Li, A. D. Easley, and J. L. Lutkenhaus, *Real-time Insight into the Doping Mechanism of Redox-active Organic Radical Polymers*, Nature Materials **18**, 69-75 (2019).
3. T. Ma, C.-H. Li, R. M. Thakur, D. P. Tabor, and J. L. Lutkenhaus, *The Role of the Electrolyte in Non-Conjugated Radical Polymers for Metal-free Aqueous Energy Storage Electrodes*, Nature Materials **22**, 495-502 (2023).
4. Y. Joo, V. Agarkar, S. H. Sung, B. M. Savoie, and B. W. Boudouris, *A Nonconjugated Radical Polymer Glass with High Electrical Conductivity*, Science **359**, 1391-1395 (2018).
5. C.-H. Li and D. P. Tabor, *Reorganization Energy Predictions with Graph Neural Networks Informed by Low-Cost Conformers*, Journal of Physical Chemistry A **2023**, 3484-3489 (2023).
6. S. S. S. V., J. N. Law, C. E. Tripp, D. Duplyakin, E. Skordilis, D. Biagioni, R. S. Paton, and P. C. St. John. *Multi-Objective Goal-Directed Optimization of de Novo Stable Organic Radicals for Aqueous Redox Flow Batteries*, Nature Machine Intelligence 4, 720-730 (2022).
7. S. Moro, N. Siemons, O. Drury, D. A. Warr, T. A., Moriarty, L. M. A. Perdigão, D. Pearce, M. Moser, R. K. Hallani, J. Parker, I. McCulloch, J. M. Frost, J. Nelson, and G. Costantini. *The Effect of Glycol Side Chains on the Assembly and Microstructure of Conjugated Polymers*, ACS Nano **16**, 21303-21314 (2022).
8. N. Siemons, D. Pearce, C. Cendra, H. Yu, S. M. Tuladhar, R. K. Hallani, R. Sheelamanthula, G. S. LeCroy, L. Siemons, A. J. P. White, I. McCulloch, A. Salleo, J. M. Frost, A. Giovannitti, and J. Nelson. *Impact of Side-Chain Hydrophilicity on Packing, Swelling, and Ion Interactions in Oxy-Bithiophene Semiconductors*, Advanced Materials **34**, 2204258 (2022).

Publications

1. Y. Tan, B. W. Boudouris, and B. M. Savoie. *Bridging the Monomer to Polymer Gap in Radical Polymer Design*, ACS Macro Letters **12**, 801-807 (2023).
2. B. Seo and B. M. Savoie. *Evidence That Less Can Be More for Transferable Force Fields,* Journal of Chemical Information and Modeling ***63****, 1188-1195 (2023).*
3. Z. Liang, S.-N. Hsu, Y. Tan, H. Tahir, H. J. Kim, K. Liu, J. F. Stoehr, M. Zeller, L. Dou, B. M. Savoie, and B. W. Boudouris. *Significant Charge Transport Effects due to Subtle Molecular Changes in Nitroxide Radical Single Crystals*, Cell Reports Physical Sciences **4**, 101409 (2023).
4. Z. Liang, Y. Tan, S.-N. Hsu, J. F. Stoehr, H. Tahir, A. B. Woeppel, S. Debnath, M. Zeller, L. Dou, B. M. Savoie, and B. W. Boudouris. *Charge Transport and Antiferromagnetic Ordering in Nitroxide Radical Crystals*, Molecular Systems Design and Engineering **8**, 464-472 (2023).
5. H. J. Kim, K. Perera, Z. Liang, B. Bowen, J. Mei, and B. W. Boudouris. *Radical Polymer-based Organic Electrochemical Transistors*, ACS Macro Letters **11**, 243-250 (2022).
6. Y. Tan, S.-N. Hus, H. Tahir, L. Dou, B. M. Savoie, and B. W. Boudouris. *Electronic and Spintronic Open-Shell Macromolecules, Quo Vadis?*, Journal of the American Chemical Society **144**, 626-647 (2022).
7. J. Zhang, K. Kim, H. J. Kim, D. M. Schneider, W. Park, S. A. Lee, Y. Dai, B. Kim, H. Moon, J. V. Shah, K. E. Harris, B. Collar, K. Liu, P. Irazoqui, H. Lee, S. A. Park, P. S. Kollbaum, B. W. Boudouris, and C. H. Lee. *Smart Soft Contact Lenses for Continuous 24-hour Monitoring of Intraocular Pressure in Glaucoma Care*, Nature Communications **13**, 5518 (2022).

8. H. Yeo, S. Akkirau, Y. Tan, H. Tahir, N. R. Dilley, B. M. Savoie, and B. W. Boudouris. *Electronic and Magnetic Properties of a 3-Arm Nonconjugated Open-Shell Macromolecule*, ACS Polymers Au **2**, 59-68 (2022).

Charging and Polarization of Organic Semiconductors in Energy-Efficient Circuits and Energy Capture

Arthur E. Bragg, Howard E. Katz, and Daniel H. Reich, Johns Hopkins University

Keywords: polymer electronics, organic microcrystals, organic photophysics, charge storage, morphology

Research Scope

Synthesis, growth, and investigation of phase-separated donors and acceptors as charged sites in polarizable media. Diblock polymer and molecular surfactants are designed with segments interacting with electroactive molecules and polymer matrix moieties to promote formation of nanoscale crystallites in polymer matrices. Spectroscopic signatures for charged crystallites are being determined, and charge stored by the crystallites is being quantified. **Testing the hypothesis that charge storage in aggregates is stabilized by the combined contributions of intermolecular interactions and local polarizable surroundings.** We hypothesize that charges injected into crystallites will be additionally stabilized by the surrounding polarizable segments separately from any contribution from mixing of frontier orbitals of multiple molecules. If correct, this would further allow testing the hypothesis that counter-charging can be used to enhance emission from molecular aggregates and crystallites by *compensating* charges accrued during material processing. **New phenomena in <10-nm crystallites.** With increased control of crystallite size and structure, we can address previously untested hypotheses about the relationship between aggregate size and charge interactions and energetics.

Recent Progress

Recent work has focused on modifying charge storage in dielectrics with added crystallites of small-molecule charge acceptors, using diblock copolymers to manipulate the aggregation of acceptors within dielectric layers,[1] and determining permittivity and conductivity thresholds for maintaining charge separation in insulating dielectrics. Literature precedents for polymer-templated crystallites are mostly with inorganics.

The effects of inserting α-quaterthiophene (α4T) crystallites in polystyrene (PS) multilayer transistor gates and capacitor dielectrics were investigated. X-ray diffraction (XRD), scanning electron microscopy with energy dispersive x-ray spectroscopy (SEM/EDS), and confocal microscopy showed α4T crystallites in the PS. (These techniques developed under this project also contributed separately to our understanding of doped conducting polymers.) A modified saturation-regime current voltage relationship[2] was used to estimate transistor threshold voltage (V_{TH}) shifting and quantities

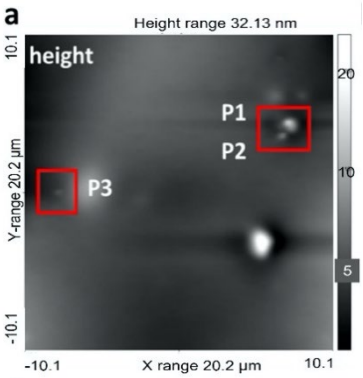

Figure 1. Height profile measurement of bilayer with 4T crystallites using KPFM with three observed crystallites (P1, P2, P3).

of charge stored by dielectric charging. Crystallites increased the maximum charge-storage capacity. Kelvin probe force microscopy (KPFM, Figure 1) showed localized charges near crystallites, nearly unprecedented.[3] Trilayer experiments showed improved charge retention via α4T crystallites. Crystallites improved breakdown characteristics in PS capacitors, suggesting their potential for energy storage in addition to OFET logic.

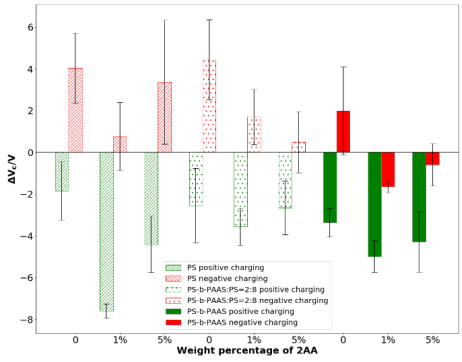

Figure 2. ΔV_c of 2-aminoanthracene blends after positive or negative charging. Note that the initial V_c are negative so a positive (negative) ΔV_c actually means that the magnitude of V_c decreased (increased).

In order to manipulate crystallite formation, we synthesized polystyrene-block-poly(anthrylamino-methylstyrene) (PS-b-PAAS), where the PAAS block is 50% of the repeat units. The co-aggregation of 2-aminoanthracene (2AA) within thin films of PS and PS-b-PAAS was observed by optical microscopy and x-ray diffraction, with clear morphological differences observed between polymers. Excited-state lifetimes of 2AA were measured by transient absorption, confirming differences in 2AA crystallite morphologies that impact aggregation-caused quenching. Blends were used as gate dielectrics in pentacene transistors. We compared a characteristic voltage (V_c, related to V_{th}) before and after charging of PS-b-PAAS blended with unsubstituted PS and both polymers individually blended with 2AA (Figure 2). For blended PS-b-PAAS and PS, as the concentration of PS-b-PAAS increased, a decreased V_c especially with negative charging of the pentacene indicated a larger concentration of charge carriers induced by the dielectric film. The charging experiments also revealed that the unique structure formed by the 2AA/PS-b-PAAS blend significantly affected the charge storage capability of the OFET.

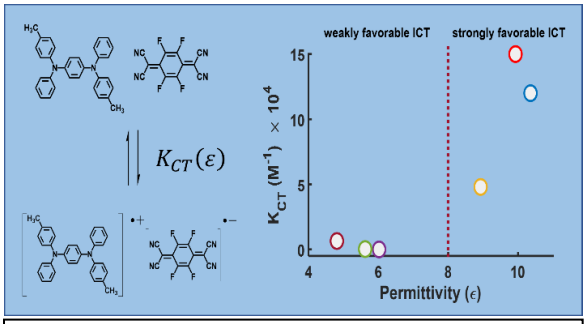

Figure 3. Permittivity threshold for strongly-favored integer charge transfer, ICT, via K_{CT}.

We have also investigated the limits for stabilizing charge-separated species in dielectric media, focusing on molecular charge doping interactions that form integer charge-transfer (ICT) complexes[4] of the p-dopant 2,3,5,6-tetrafluoro-7,7,8,8-tetracyanoquinodimethane (F_4TCNQ) complexed with the electron donor and hole transport material *N,N'*-Diphenyl-*N*-*N'*-di-p-tolylbenzene-1,4-diamine (MPDA). Equilibrium formation constants (K_{CT})[5] were determined for donor-acceptor pairs in solvents covering a range of values of relative permittivity (ε_r). A threshold for strongly favorable complex formation was observed to occur at ε_r~8-9, with large (>10^4) K_{CT} obtained at greater ε_r (Figure 3). Anomalously favorable complexation in chloroform (ε_r=4.81) was found to be both exothermic and entropically disfavored, indicating that inner-shell solvent-solute interactions likely stabilize the complex in this solvent. Our results indicate that modifications to chemical or material environment that induce modest changes in local ε_r could be used to support stable charge separation for doping applications.

Future Plans

In future work under this award, we will consider which advanced diffraction techniques would give us the most information about the distribution of crystallites in polystyrene matrices. We will investigate whether chargeability of crystallites is influenced more by interactions with matrix polymer side chains or the general dielectric environment. We will attempt to add greater precision to models for the localization of countercharges to the injected static charges. We will evaluate the applicability of the critical dielectric constant observed in the solution studies to solid systems.

References

1. P. Kumari, K. Khawas, M. K. Bera, S. Hazra, S. Malik, and B. K. Kuila, *Enhanced Charge Carrier Mobility and Tailored Luminescence of n-Type Organic Semiconductor through Block Copolymer Supramolecular Assembly*, Macromolecular Chemistry and Physics **218,** 1600508 (2017).
2. C. Reese and Z. Bao, *Overestimation of the Field-Effect Mobility via Transconductance Measurements and the Origin of the Output/Transfer Characteristic Discrepancy in Organic Field-Effect Transistors*, Journal of Applied Physics **105**, 024506 (2009).
3. Y. Park, K. J. Baeg, and C. Kim, *Solution-Processed Nonvolatile Organic Transistor Memory Based on Semiconductor Blends*, ACS Applied Materials & Interfaces **11**, 8327-8336 (2019).
4. K. P. Goetz, D. Vermeulen, M. E. Payne, C. Kloc, L. E. McNeil, and O. D. Jurchescu, *Charge-Transfer Complexes: New Perspectives on an Old Class of Compounds*, Journal of Materials Chemistry C **2**, 3065-3076 (2014).
5. W. D. McKim, J. Ray, and B. R. Arnold, *Analysis of the Association Constants for Charge-Transfer Complex Formation*, Journal of Molecular Structure **1033**, 131-136 (2013).

Publications

1. T. Lee, Y. Luo, C. Wang, A. Park, E. Zapata-Mercado, K. Hristova, T. Mueller, W.L. Wilson, D.H. Reich, and H.E. Katz, *Effect of Organic Electroactive Crystallites in a Dielectric Matrix on the Electrical Properties of a Polymer Dielectric,* Physical Review Materials, in press (2023).
2. B. J. Barrett, H.E. Katz, and A.E. Bragg, *Permittivity Threshold and Thermodynamics of Integer Charge-Transfer Complexation for an Organic Donor–Acceptor Pair*, Journal of Physical Chemistry B, **127**, 2792-2800 (2023).
3. T. Mukhopadhyaya, T. Lee, C. Ganley, S. Tanwar, P. Raj, L. Li, Y. Song, P. Clancy, I. Barman, S. M. Thon, and H. E. Katz, *Stable High-Conductivity Ethylenedioxythiophene Polymers via Borane-Adduct Doping,* Advanced Functional Materials **32**, 202208541 (2022)
4. C. Chi, Y. Song, T. Lee, A.E. Bragg, D.H. Reich, and H.E. Katz, *2-Aminoanthracene Crystallization in Its Compatible Polystyrene Block: RAFT Synthesis and Enhanced Charge Retention in Pentacene Transistor Gate Dielectrics, submitted for publication* (2023)

Impacts of Dynamic Bonding on the Properties of Porous Materials

Assist. Prof. Carl K. Brozek, Department of Chemistry and Biochemistry, University of Oregon

Keywords: dynamic bonding, metal-organic frameworks, soft modes, phase change

Research Scope

This project identifies signatures of dynamic bonding in porous materials and studies its influence on electronic, photophysical, catalytic, and magnetic properties.[1] With these insights, previously unexplained behavior in porous materials can be understood in terms of fundamental microscopic principles developed in our lab that will also provide design guidelines for leveraging dynamic bonding to access new energy materials.

We study metal-ligand bonding in porous materials, which we have shown[2] to be in dynamic equilibrium between bound and unbound states (**Fig. 1**). Dynamic bonding in conventional semiconductors with comparatively rigid bonding have been extensively studied in the form of vibronic and polaronic interactions,[3] which have wide-ranging consequences for semiconductor fundamental physics and technology.[4] Because the metal-carboxylate and metal-azolate bonds typical of porous materials are far more labile[5] than the bonds in conventional semiconductors, we anticipate their dynamic bonding to cause unprecedented changes to material behavior.

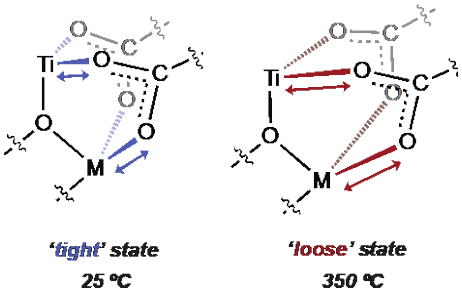

Fig. 1. Illustration of the bound and unbound metal-linker states.

Specifically, the major goals of this proposal are to: 1) Develop spectroscopic methodology as evidence of dynamic bonding in porous metal-organic materials. 2) Elucidate the impact of dynamic bonding on conductivity mechanisms of porous frameworks. 3) Leverage dynamic bonding for porous metal-organic phase-change materials (PCM).

Recent Progress

In the last year we have made substantial progress in developing spectroscopic methods to identify dynamic bonding in porous materials, prepare porous semiconductor materials to study the impact of dynamic bonding on conductivity mechanisms, and develop new classes of porous materials with phase change properties leveraging dynamic bonding.

Toward spectroscopic signatures of dynamic bonding, we pioneered the use of variable-temperature UV-vis electronic absorption to identify signatures of dynamic bonding.

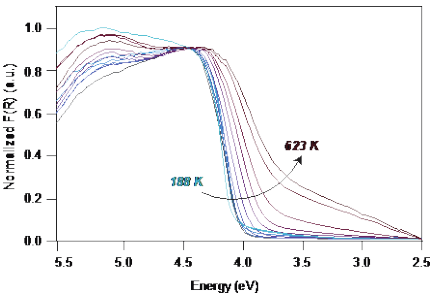

Fig. 2. Variable-temperature diffuse reflectance UV-vis-near IR spectra of 80-nm Ti8O8(OH)4(terephthalate)6 particles.

Conventional semiconductor nanocrystals exhibit wide-ranging optical behavior, whereas the size-dependent photophysical properties of metal-organic framework (MOF) nanocrystals remains an open research frontier. In the previous year, we uncovered size- and temperature-dependent optical absorption spectra of common MOFs with particle sizes ranging from tens of nanometers to several microns. All materials exhibited optical gaps that decrease at elevated temperatures, which we attributed to the dynamic nature of MOF metal-linker bonds (**Fig. 2**). Accordingly, whereas the labile titanium-carboxylate bonds of MIL-125 gave rise to bandgaps that redshift by ~600 meV over 300 K, the more rigid zinc-imidazolate bonds of ZIF-8 produce a redshift of only ~10 meV. Furthermore, smaller particles induce far larger decreases to optical gaps. Taken together, these results suggested MOF bonding becomes more flexible with smaller nanocrystal sizes, offering a powerful tool for manipulating optical behavior through composition, temperature, and dimensionality.

Additionally, we demonstrated that guest molecules impact the metal-linker bond dynamics in porous materials. Metal-ligand stability constants provide a metric for relating bond lability to the reactivity and physical behavior of molecules and materials. While stability constants have been studied for molecular and polymeric materials, the stability constants of MOFs remain scarcely reported. In the previous year, we reported stability constants of UiO-66 ($Zr_6O_4(OH_4)$(1,4-benzenedicarboxylate)$_{12}$), the prototypical "stable" MOF, across a wide temperature range in both vacuum and in the presence of typical guest solvents. With these data, we extract key thermodynamic parameters governing the bond equilibrium and demonstrate that guest molecules strongly favor the reversible dissociation of MOF metal-linker bonds.

Toward understanding the impact of dynamic bonding on charge transport, we prepared framework materials based on iron-sulfur cubane clusters and multitopic N-heterocyclic carbene (NHC) linkers. Designing electrically conductive coordination materials, *e.g.* MOFs, has relied on single-metal nodes because the metal-oxo clusters present in the vast majority of MOFs are not suitable for electrical conduction due to their localized electron orbitals. Therefore, the development of metal-cluster nodes with delocalized bonding would greatly expand the structural and electrochemical tunability of conductive materials. Whereas the cuboidal [Fe_4S_4] cluster is a ubiquitous cofactor for electron transport in biological systems, few electrically conductive artificial materials employ the [Fe_4S_4] cluster as a building unit due to the lack of suitable bridging linkers.[6] In the previous year, we bridged the [Fe_4S_4] clusters with ditopic NHC linkers through charge-delocalized Fe-C bonds that enhance electronic communication between

the clusters. [$Fe_4S_4Cl_2$(ditopic NHC)] exhibits a high electrical conductivity of 1 mS cm^{-1} at 25 ºC, surpassing the conductivity of related but less covalent materials.

References

1. Grzywa, M. *et al. Cooperative Large-Hysteresis Spin-Crossover Transition in the Iron(II) Triazolate [Fe(ta)$_2$] Metal-Organic Framework*. Inorg. Chem. **6**, 10501-10511 (2020).
2. Andreeva, A. B. *et al. Soft Mode Metal-Linker Dynamics in Carboxylate MOFs Evidenced by Variable-Temperature Infrared Spectroscopy.* J. Am. Chem. Soc. **142**, 19291–19299 (2020).
3. Varshni, Y. P. T*emperature dependence of the energy gap in semiconductors.* Physica **34**, 149–154 (1967).
4. Bersuker, I. B. & Polinger, V. Z. *Vibronic Interactions in Molecules and Crystals*. (Springer, Berlin, Heidelberg, 1989).
5. Bunting, J. W. & Thong, K. M. *Stability constants for some 1:1 metal–carboxylate complexes.* Can. J. Chem. **48**, 1654–1656 (1970).
6. Horwitz, N. E. *et al. Redox-Active 1D Coordination Polymers of Iron–Sulfur Clusters.* J. Am. Chem. Soc. **141**, 3940–3951 (2019).

Publications

1. K. Fabrizio, C. K. Brozek, *Size-Dependent Thermal Shifts to MOF Nanocrystal Optical Gaps Induced by Dynamic Bonding*. Nano Lett. **23**, 925–930 (2023).
2. K. Fabrizio, A. B. Andreeva, K. Kadota, A. J. Morris, C. K. Brozek, *Guest-dependent bond flexibility in UiO-66, a "stable" MOF.* Chem. Commun. **59**, 1309–1312 (2023).
3. J. McKenzie, P. A. Kempler, C. K. Brozek, *Solvent-controlled ion-coupled charge transport in microporous metal chalcogenides.* Chem. Sci. **13**, 12747–12759 (2022).
4. B. Andreeva, K. N. Le, K. Kadota, S. Horike, C. H. Hendon, C. K.; Brozek, *Cooperativity and Metal–Linker Dynamics in Spin Crossover Framework Fe(1,2,3-triazolate)$_2$*. Chem. Mater. **33**, 8534–8545 (2021).
5. J. McKenzie, K. N. Le, D. J. Bardgett, K. Collins, T. Ericson, M. E. Wojnar, J. Chouinard, S. Golledge, A. F. Cozzolino, D. C. Johnson, C. H. Hendon, C. K. Brozek, *Conductivity in Open-Framework Chalcogenides Tuned via Band Engineering and Redox Chemistry.* Chem. Mater. **34**, 1905-1920. (2022)
6. K. Fabrizio, K. N. Le, A. B. Andreeva, C. H. Hendon, C. K. Brozek, *Determining Optical Band Gaps of MOFs.* ACS Materials Lett. **4**, 457–463 (2022).

Unravelling the Mechanisms of Phase Determination in Metastable Multinary Chalcogenides

Richard L. Brutchey

Department of Chemistry, University of Southern California, Los Angeles, CA 90089, USA

Keywords: synthesis science; far from equilibrium; data driven; chalcogenides

Research Scope

The "materials by design" approach has identified vast numbers of materials with a wide range of properties; however, a significant bottleneck now exists at the next step of the process, which is the Edisonian nature of materials synthesis. We are addressing this challenge within the framework of solution-phase materials chemistry, using *chimie douce* (or soft chemistry) methods. By combining *chimie douce* methods with multivariate analyses via data-driven learning techniques, we can accelerate predictive materials synthesis by charting multidimensional "phase maps" that incorporate the effects of statistically significant experimental variables with a focus on (i) improving the synthesis of thermodynamic phases in complex phase diagrams and (ii) gaining new insights into accessing metastable phases.

Recent Progress

Binary copper selenides are an important family of materials with applications in plasmonics, photovoltaics, and thermoelectrics; these wide-ranging functional properties are a direct result of the rich and complex Cu–Se phase diagram that encompasses compositions from Cu_2Se to $CuSe_2$.[1] In addition to their unique physicochemical properties, copper selenides function as essential binary intermediates in the synthesis of multinary structures that adopt topologically related anion sublattices.[2] Umangite Cu_3Se_2, which has a nearly hexagonal Se^{2-} sublattice, is a necessary intermediate in the synthesis of the metastable, wurtzite-like phases of $CuInSe_2$, $Cu_2ZnSnSe_4$, and $Cu_2FeSnSe_4$ that do not exist on thermodynamic phase diagrams.[3-5]

C*himie douce* materials syntheses are developed *via* fragmented empirical knowledge of the underlying experimental variables.[6,7] For this reason, achieving phase control in such syntheses is tedious and laborious. One solution is to utilize data-driven learning to rationally target materials within the high-dimensional variable space. Convolutional neural networks can map the multidimensional variable space, but they require large datasets that are not feasible when novel chemistry is being employed and/or done in a low-throughput manner.[8] On the other hand, a trained classification algorithm can handle both smaller data sets and categorical variables, making it a tractable solution to this problem.[9]

Our solution-phase synthesis of copper selenides is based on the low-temperature reaction of $Cu(oleate)_2$ with diorganyl diselenide precursors in oleylamine and 1-octadecene (ODE). Diselenides (R-Se-Se-R, where R = alkyl, allyl, benzyl, or phenyl) have emerged as versatile

precursors for the kinetically controlled synthesis of metal selenides.[10] Our previously experience with this synthetic system resulted in the isolation of only two phase-pure copper selenides; that is, berzelianite $Cu_{2-x}Se$ and umangite Cu_3Se_2.[3] We have now trained and tested a classification algorithm on sparse reaction data that was assembled using design of experiments, which provides an orthogonally balanced experimental sampling of the design space.[11] This prevents the over- and under-sampling of any one region in the *n*-dimensional domain. The experimental variables chosen for this training set were: (1) C–Se precursor bond strength, (2) volumetric ratio of oleylamine to ODE, (3) temperature, and (4) time.

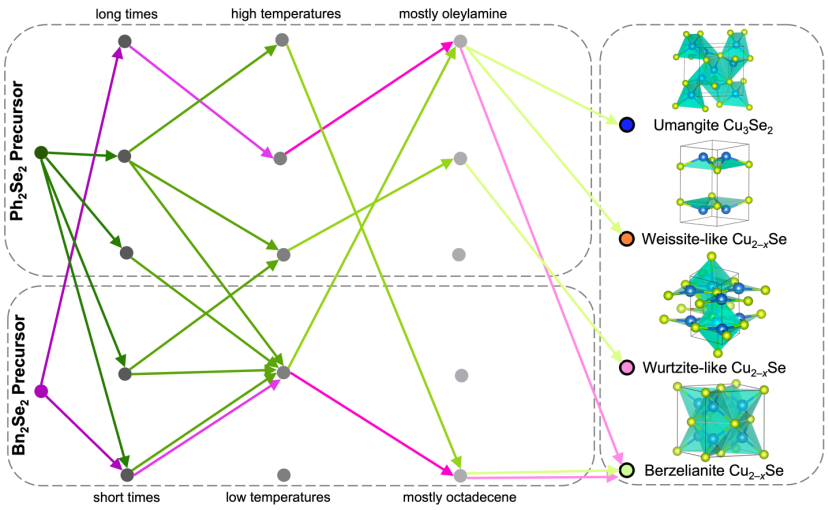

Fig. 1. Simplified decision tree for the Cu–Se phase map predicted by the classification algorithm, with Bn_2Se_2 precursor pathways to phase-pure products indicated by purple arrows and Ph_2Se_2 precursor pathways to phase-pure products indicated by green arrows.

After assembling the surrogate model, calculation of variable importance scores and multivariate, high-dimensional phase maps enabled detailed conclusions to be drawn about the relationships between experimental variables and phase outcome (**Fig. 1**). The type of diselenide precursor was shown to be the most important factor for phase determination, followed by temperature, with certain phases lying in very narrow temperature ranges within the phase map. The importance of the volumetric ratio of oleylamine to ODE depends on the precursor type, suggesting that the resulting phase is dictated by different precursor conversion mechanisms with amines. The precursor with a higher C–Se bond strength (Ph_2Se_2) led to a richer phase map with more unique phase combinations, including two metastable wurtzite-like $Cu_{2-x}Se$ and weissite-like $Cu_{2-x}Se$ phases. The resulting multidimensional phase map allows an outcome to be predicted for a given set of experimental variables. We show that the phase map guided the accelerated isolation of klockmannite CuSe in just six additional experiments. The ability of these phase maps to capture both thermodynamic and kinetic complexity in a way that typical phase diagrams do not is incredibly valuable for experimentalists trying to isolate new materials, including *terra incognita* metastable phases not found on the thermodynamic Cu–Se phase diagram.

References

1. Glazov, V. M.; Pashinkin, A. S.; Fedorov, V. A. Phase Equilibria in the Cu-Se System. *Inorg. Mater.* **2000**, *36*, 641-652.
2. Tappan, B. A.; Brutchey, R. L. Polymorphic Metastability in Colloidal Semiconductor Nanocrystals. *ChemNanoMat* **2020**, *6*, 1567-1588.
3. Tappan, B. A.; Barim, G.; Kwok, J. C.; Brutchey, R. L. Utilizing Diselenide Precursors toward Rationally Controlled Synthesis of Metastable $CuInSe_2$ Nanocrystals. *Chem. Mater.* **2018**, *30*, 5704-5713.
4. Tappan, B. A.; Chu, W.; Mecklenburg, M.; Prezhdo, O. V.; Brutchey, R. L. Discovery of a Wurtzite-like $Cu_2FeSnSe_4$ Semiconductor Nanocrystal Polymorph and Implications for Related $CuFeSe_2$ Materials. *ACS Nano* **2021**, *15*, 13463-13474.
5. Tappan, B. A.; Crans, K. D.; Brutchey, R. L. Formation Pathway of Wurtzite-like $Cu_2ZnSnSe_4$ Nanocrystals. *Inorg. Chem.* **2021**, *60*, 17178-17185.
6. Braham, E. J.; Davidson, R. D.; Al-Hashimi, M.; Arróyave, R.; Banerjee, S. Navigating the Design Space of Inorganic Materials Synthesis Using Statistical Methods and Machine Learning. *Dalton Trans.* **2020**, *49*, 11480-11488.
7. Koziel, A. C.; Goldfarb, R. B.; Endres, E. J.; Macdonald, J. E. Molecular Decomposition Routes of Diaryl Diselenide Precursors in Relation to the Phase Determination of Copper Selenides. *Inorg. Chem.* **2022**, *61*, 14673-14683.
8. Dimiduk, D. M.; Holm, E. A.; Niezgoda, S. R. Perspectives on the Impact of Machine Learning, Deep Learning, and Artificial Intelligence on Materials, Processes, and Structures Engineering. *Integrating Mater. Manuf. Innov.* **2018**, *7*, 157-172.
9. Wong, T.-T. Performance Evaluation of Classification Algorithms by K-Fold and Leave-One-out Cross Validation. *Pattern Recognit.* **2015**, *48*, 2839-2846.
10. Brutchey, R. L. Diorganyl Dichalcogenides as Useful Synthons for Colloidal Semiconductor Nanocrystals. *Acc. Chem. Res.* **2015**, *48*, 2918-2926.
11. Box, G. E. P.; Hunter, J. S.; Hunter, W. G. *Statistics for Experimenters. Design, Innovation, and Discovery*, 2nd ed.; Wiley-Interscience, 2005.

Publications

1. Tappan, B. A.; Chu, W.; Mecklenburg, M.; Prezhdo, O. V.; Brutchey, R. L. Discovery of a Wurtzite-like $Cu_2FeSnSe_4$ Semiconductor Nanocrystal Polymorph and Implications for Related $CuFeSe_2$ Materials. *ACS Nano* **2021**, *15*, 13463-13474.
2. Tappan, B. A.; Crans, K. D.; Brutchey, R. L. Formation Pathway of Wurtzite-like $Cu_2ZnSnSe_4$ Nanocrystals. *Inorganic Chemistry* **2021**, *60*, 17178-17185.
3. Williamson, E. M.; Sun, Z.; Mora-Tamez, L.; Brutchey, R. L. Design of Experiments for Nanocrystal Syntheses: A How-To Guide for Proper Implementation. *Chemistry of Materials* **2022**, *34*, 9823-9835.
4. Williamson, E. M.; Ghrist, A.; Karadaghi, L. R.; Smock, S. R.; Barim, G.; Brutchey, R. L. Creating Ground Truth for Nanocrystal Morphology: A Fully Automated Pipeline for Unbiased Transmission Electron Microscopy Image Analysis. *Nanoscale* **2022**, *14*, 15327-15339.
5. Cottingham, P.; Brutchey, R. L. Temperature-Dependent Behavior in the Local Structure of $BaTiO_3$ Nanocrystals. *CrystEngComm* **2022**, *24*, 5400-5404.
6. Tappan, B. A.; Zhu, B.; Cottingham, P.; Mecklenburg, M.; Scanlon, D. O.; Brutchey, R. L. Crystal Structure of Colloidally Prepared Metastable Ag_2Se Nanocrystals. *Nano Letters* **2021**, *21*, 5881-5887.

Elucidating the Link Between Alkali Metal Ions and Reaction-Transport Mechanisms in Cathode Electrodes for Alkali-ion Batteries

Assistant Prof. Ö. Özgür Çapraz, The School of Chemical Engineering, Oklahoma State University, Stillwater, Oklahoma

Keywords: Alkali Metal-Ion Batteries, Cathode, Stress, Strain, Instabilities

Program Scope

The main objective of our study is to identify the intrinsic relationship between the role of alkali metal ions and electrochemically driven mechanical stability and kinetic properties of battery materials. The overall question is "What is the role of alkali metal ions on the electrochemical and mechanical behavior of cathode electrodes? Our guiding hypothesis is that intercalation of larger alkali metal ions (Na and K) inevitably alters the coupled transport-reaction processes during battery operation in organic electrolytes, leading to intensive chemo-mechanical instabilities in cathode electrodes, resulting in rapid capacity fade. To validate the hypothesis, we experimentally characterize the reaction-transport processes and driving governing forces on the instability of electrode materials in different alkali metal-ion environments by employing operando mechanical measurements coupled with electrochemical and chemical analysis. Here, we report our recent progress with structural, interfacial, and rate-dependent instabilities in alkali-metal ion cathodes.

Recent Progress

Probing Crystalline to Amorphous Phase Transformation in Iron Phosphate Cathodes: The Intercalation of large alkali metal ions can lead to the partial or complete loss of crystalline structure in electrode materials[1-2]. The lack of understanding regarding the evolving amorphous nanostructure during battery operation hinders further advancements. In-operando XRD revealed that the electrode's nanostructure underwent amorphization during K-ion intercalation into the $FePO_4$ structure. Additionally, high-resolution transmission electron microscopy (HR-TEM) analysis confirmed the amorphization in the electrode. The operando strain analysis identified reversible deformations linked to redox reactions in the amorphous phases. K-ion intercalation results in a non-linear strain generation based on the state of charge/discharge. Our study indicated that the strain rate, rather than the absolute value of strain, plays a critical role in the

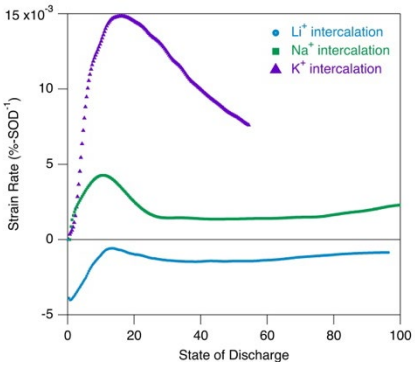

Figure 1: Strain rates in cobalt oxide upon intercalation of Li, Na and K-ions.

amorphization of the crystalline electrode. The study was published in ACS Nano Letters and Electrochem. Sci. Advances.

Impact of Alkali-ion Intercalation into Cobalt Oxide Cathode: First, we investigated chemo-mechanical instabilities in $LiCoO_2$ cathodes by employing operando curvature interferometry and digital image correlation (DIC), supported by structural and morphological characterizations. Synchronization of operando stress and strain measurements indicated governing forces behind the structural and interfacial instabilities in $LiCoO_2$ at different state-of-charge. By building on it, we investigated the impact of alkali metal ion intercalation on the instabilities in cobalt oxide cathodes. Significant contrast in the mechanical deformations was detected upon intercalation of Li, Na, and K-ions into cobalt oxide structure (Figure 1). We are currently preparing manuscripts for publication.

The Role of Transition Metals on Chemo-Mechanical Instabilities in Prussian Blue Analogues (PBAs) For K-ion Batteries: PBA cathodes suffer from poor cycle life associated with chemo-mechanical instabilities[3]. This study investigated the driving forces behind chemo-mechanical instabilities in Ni- and Mn-based PBAs cathodes for K-ion batteries by combining electrochemical analysis, digital image correlation, and spectroscopy techniques. Overall, both cathodes underwent similar reversible electrochemical strains in each charge-discharge cycle. XPS studies indicated richer organic layer compounds in the CEI layer formed on KMHCF cathodes compared to the KNHCF ones. Faster capacity fade in Mn-based PBA, compared to Ni-based ones, was attributed to the formation of richer organic compounds in CEI layers, rather than mechanical deformations. This study is currently under review for publication.

Probing the Formation of Cathode-Electrolyte Interphase on Lithium Iron Phosphate Cathodes: While the formation of the solid-electrolyte interphase (SEI) on anodes has received much attention, there is still a lack of understanding about the formation of the cathode-electrolyte interphase (CEI) on the cathodes[4]. We reported on dynamic deformations on $LiFePO_4$ cathode cycled in either $LiPF_6$, $LiClO_4$, or LiTFSI- containing organic liquid electrolytes. Unexpected mechanical deformations were detected when cycled in $LiPF_6$-based electrolytes. The formation of fluorinated compounds on the surface of the electrode was captured by Cryo XPS on the onset of an increase in impedance and positive strain generation during the first charge in $LiPF_6$-electrolytes. This study was posted on ChemRxiv and is currently under review for publication.

Mechanistic Elucidation of Electronically Conductive PEDOT: PSS Binder for K-ion Batteries: A larger ion size reduces rate capabilities and exacerbates capacity fading from volumetric expansion in K-ion batteries[5]. Herein, we investigated the chemo-mechanical properties of the conductive PEDOT: PSS binder. Strain generation in the composite graphite electrode during the first potassiation was associated with intercalation-induced structural changes and the formation

of the solid-electrolyte interphase. DIC measurements showed that PEDOT: PSS/CB binder provides good mechanical integrity during potassium intercalation into graphite electrodes, even when the electrode expands 23%. This study was published in Advanced Energy Materials.

Rate-Dependent Mechanical Deformations in Iron Phosphate Cathodes: The performance of battery electrodes is significantly impacted by chemo-mechanical instabilities at faster charge/discharge rates[6]. In this study, we investigated the rate-dependent mechanical response of $LiFePO_4$ and $NaFePO_4$ cathodes. The combination of strain measurements with the analytical model provided information about diffusion-induced mechanical deformations in $NaFePO_4$ cathodes at faster rates. The study also compared the irreversible strains in $LiFePO_4$ for Li-ion batteries with its analogous $NaFePO_4$ cathodes for Na-ion batteries. $LiFePO_4$ electrode experienced larger strains per capacity at faster rates, and it was associated with a delay in the phase transformations at faster rates. This study was published in J. Power Sources and J. Materials Research.

References

1. Hosaka, T.; Shimamura, T.; Kubota, K.; Komaba, S. Polyanionic Compounds for Potassium-Ion Batteries. Chem. Rec., **19** (4), 735–745 (2019)
2. Xiang, K.; Xing, W.; Ravnsbæk, D. B.; Hong, L.; Tang, M.; Li, Z.; Wiaderek, K. M.; Borkiewicz, O. J.; Chapman, K. W.; Chupas, P. J.; et al. Accommodating High Transformation Strains in Battery Electrodes via the Formation of Nanoscale Intermediate Phases: Operando Investigation of Olivine NaFePO4. Nano Lett., **17**, 1696–1702 (2017)
3. Zhou, A. J., Cheng, W. J., Wang, W., Zhao, Q., Xie, J., Zhang, W. X., Gao, H. C., Xue, L. G., Li, J. Z., Hexacyanoferrate-Type Prussian Blue Analogs: Principles and Advances Toward High-Performance Sodium and Potassium Ion Batteries. Adv. Energy Mater., **11**, 2000943 (2021)
4. Fu, W.; Kim, D.; Wang, F.; Yushin, G. Stabilizing Cathodes and Interphases for Next-Generation Li-Ion Batteries. J Power Sources, **561**, 232738 (2023)
5. Hosaka, T.; Kubota, K.; Hameed, A. S.; Komaba, S. Research Development on K-Ion Batteries. Chemical Reviews, **120**, 14, 6358–6466 (2020).
6. Mukhopadhyay, A. & Sheldon, B. W. Deformation and stress in electrode materials for Li-ion batteries. Prog. Mater. Sci. **63**, 58–116 (2014).

Publications supported by this Project.

1. B. Ozdogru, Y. Cha, B. Gwalani, V. Murugesan, M. Song, and Ö. Ö. Çapraz, In Situ Probing Potassium-ion Intercalation-induced Amorphization in Crystalline Iron Phosphate Cathode Materials, Nano Letters, **21**, 7579–7586 (2021).
2. B. Ozdogru, B. Koohbor and Ö. Ö. Çapraz, The Impact of Alkali-ion Intercalation on Redox Chemistry and Mechanical Deformations: Case Study on Intercalation of Li, Na and K Ions into FePO4 Cathode, Electrochemical Science Advances, **2**, e2100106 (2021).
3. B. Ozdogru, V. Murugesan, and Ö. Ö. Çapraz, Rate-Dependent Electrochemical Strain Generation in Composite Iron Phosphate Cathodes in Li-ion Batteries, Journal of Materials Research, **37**, 3237–3248 (2022).

4. B. Özdogru, H. Dykes, D. Gregory, D. Saurel, V. Murugesan, M. Casas Cabanas and Ö. Ö. Çapraz, Elucidating Cycling Rate-Dependent Electrochemical Strains in Sodium Iron Phosphate Cathode for Na-ion Batteries, Journal of Power Sources, **507**, 230297 (2021)
5. D. A. Gribble, Z. Li, B. Ozdogru, E. McCulfor, Ö. Ö. Çapraz and V. Pol, Mechanistic Elucidation of Electronically Conductive PEDOT:PSS Binder for a Potassium-ion Battery Graphite Anode: Electrochemical, Mechanical, and Thermal Safety Aspects, Advanced Energy Materials, **12**, 2103439 (2022).
6. B. Bal, B. Ozdogru, D. Nguyen, Z. Li, V. Murugesan and Ö. Ö. Çapraz, Probing the Formation of Cathode-Electrolyte Interface on Lithium Iron Phosphate Cathodes via In Operando Mechanical Measurements, pre-print on Chemrxiv (2023)

Energy Flow in Polymers with Mixed Conduction Pathways

Rachel Segalman and Michael Chabinyc - University of California, Santa Barbara

Keywords: Organic Electronics, Ion Transport, Electron Transport, Conducting Polymers

Research Scope

The simultaneous transport of ions and electrons is essential for a broad range of applications in electrochemical energy conversion and storage, organic electronics, and bioelectronics. Polymers with mixed conduction are of interest due to the possibility to control mechanical properties and microstructure in tandem with ionic and electronic transport. Controlling the morphologies that optimize the different types of transport is critical, i.e. ordered structures to maximize electronic transport versus amorphous structure to maximize ionic transport. This project addresses overarching questions including: 1) What molecular designs allow for increased salt solubility within a mixed conductor and how do dielectric environment and local structure affect mixed conduction? 2) How do the electrostatic interactions within a mixed conductor affect the mesostructure and how can these be leveraged for processing and self-assembly? 3) What role does the identity of the ion and counterion coupling play in the overall behavior of the system and how does the method and timescale of processing affect the non-equilibrium structure of this microenvironment?

Recent Progress

Polyelectrolyte complexation offers unique opportunities to compatibilize polymers with very different backbone chemistries and to control the morphology of the resulting blend via electrostatic manipulation.[1–5] We have examined how the electrostatic complexation strength between conjugated polyelectrolytes and polymeric ionic liquids can be used to control microstructure.[2] We used a model system that varies the frequency of charged repeat units from 50% to 100% on an anionic polythiophene-based CPE and a complimentary cationic PIL to control

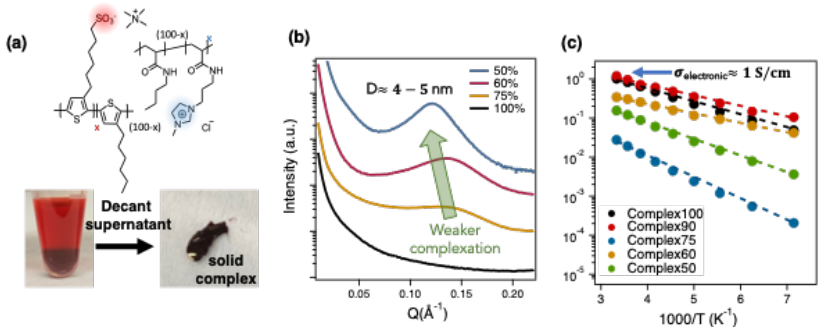

Figure 1. (a) Complexes of blends of a conjugated polyelectrolyte (CPE) with a polymerized ionic liquid (PIL) can be controlled by the charge fraction (number of charged pendants per repeat unit). (b) Small angle X-ray scattering shows that microphase separation of the two polymers increases as the charge fraction decreases. (c) These complexes have high electronic conductivity (1 S/cm) when electrically doped with the most homogeneous blends having the highest performance.

the complexation strength. Variation of electrostatic parameters, such as counterion concentration or charge fraction, tuned the morphology of these functional polymer complexes from homogeneously disordered blend to weakly structured microemulsions (Fig. 1b). Here the local ordering arises from backbone-immiscibility-induced microphase segregation in agreement with predictions from theory. Our findings show that ionic interactions are an effective pathway to compatibilize polymers at macroscopic length scales while achieving controlled nanostructures in these ionic blends.

The high polymer loading in complexes of conjugated and insulating polyelectrolytes offers unique opportunities for fabrication of conductive thick films and bulk structures.[3] We examined the connection between the microstructure defined by electrostatic interactions and the resulting electronic properties in the solid state. In highly charged complexes, the intimate mixing between the CPE and the PIL is found to reduce the structural disorder along the CPE backbone, enhancing its intrachain conjugation and interchain stacking (Figure 1X). In weakly charged complexes (<90%), these chain planarization effects are absent and microphase separation occurs. At all charge fractions examined, the electrical conductivity of a doped complex is higher than that of the unblended constituent CPE. The highest electrical conductivity near 1 S cm^{-1} is found for a charge fraction of 100% (Fig. 1c) and is comparable to state-of-the-art conductive polymers.

These new electrostatically mediated complexes are mixed conductors relevant for conducting battery binders.[6] Polymer binders add structural integrity to lithium ion battery composite cathodes, but standard binders, such as polyvinylidene fluoride (PVDF), are insulating to ions and electrons, detrimentally adding resistance to the overall system. We found that a blend of a charged conjugated polymer with an oppositely charged polyelectrolyte provides a processable, stable binder with effective ionic and electronic conduction. Using $LiFePO_4$ cathodes as a model system, we found significant improvement in rate capability and stability of model batteries, with the conducting binder enabling a 39% utilization at 6C compared to 1.6% when PVDF is the binder (Fig. 2). These results show that electrostatically

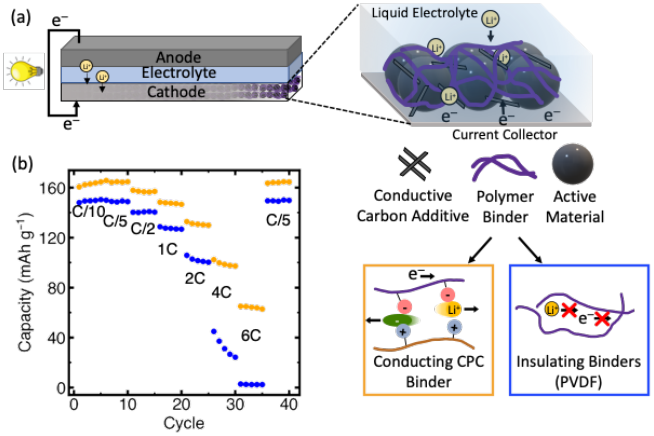

Figure 2. (a) Polymer binders are a critical, but traditionally insulating component of battery cathodes. (b) Complexation enables a processable, mixed-conducting polymer binder (orange) that dramatically improves cathode rate capability over traditional binders (PVDF, blue).

stabilized complexation is a promising strategy to integrate both electronic and ionic conductivity into a binder, while simultaneously maintaining stability and processability.

References

1. G.H. Fredrickson, S. Xie, J. Edmund, M.L. Le, D. Sun, G.J. Grzetic, D.L. Virgil, K.T. Delaney, M.L. Chabinyc, R.A. Segalman, *Ionic Compatibilization of Polymers*, ACS Polymers Au **2,** 299–312 (2022).
2. M.L. Le, D.J. Grzetic, K.T. Delaney, K.-C. Yang, S. Xie, G.H Fredrickson, M.L. Chabinyc, R.A. Segalman, *Electrostatic Interactions Control the Nanostructure of Conjugated Polyelectrolyte–Polymeric Ionic Liquid Blends*, Macromolecules **55(18),** 8321–8331 (2022).
3. M.L. Le, C. Warner, R.A. Segalman, M.L. Chabinyc, *The Role of Complexation Strength on the Photophysical and Transport Properties of Semiconducting Charged Polymer Complexes* Chemistry of Materials **35**, 4449-4460 (2023).
4. M.L. Le, D. Rawlings, S.P.O. Danielsen, R.M. Kennard, M.L. Chabinyc, R.A. Segalman, *Aqueous Formulation of Concentrated Semiconductive Fluid Using Polyelectrolyte Coacervation*, ACS Macro Letters **10(8),** 1008–1014 (2021).
5. S.P.O Danielsen, T.Q. Nguyen, G.H. Fredrickson, R.A. Segalman, *Complexation of a Conjugated Polyelectrolyte and Impact on Optoelectronic Properties*, ACS Macro Letters **8**, 88–94 (2019).
6. G.T. Pace, M.L. Le, R.J. Clément, & R.A. Segalman, *A Coacervate-based Mixed Conducting Binder for High Power, High Energy Batteries*, ACS Energy Letters **8,** 2781-2788 (2023).

Publications

1. G.T. Pace, M.L. Le, R.J. Clément, & R.A. Segalman, *A Coacervate-based Mixed Conducting Binder for High Power, High Energy Batteries*, ACS Energy Letters **8,** 2781-2788 (2023).
2. M.L. Le, C. Warner, R.A. Segalman, M.L. Chabinyc, *The Role of Complexation Strength on the Photophysical and Transport Properties of Semiconducting Charged Polymer Complexes* Chemistry of Materials **35**, 4449-4460 (2023).
3. D. Yuan, E. Plunkett, P.H. Nguyen, D. Rawlings, M.L. Le, R. Kroon, C. Müller, R.A Segalman, & M.L. Chabinyc, *Double Doping of Semiconducting Polymers Using Ion-Exchange with a Dianion*, Advanced Functional Materials, 2300934 (2023).
4. Agee, T.M. Gill, G. Pace, R.A. Segalman, & A. Furst, *Electrochemical Characterization of Biomolecular Electron Transfer at Conductive Polymer Interfaces*, Journal of the Electrochemical Society **170(1),** 016509 (2023).
5. M.L. Le, D.J. Grzetic, K.T. Delaney, K.-C. Yang, S. Xie, G.H Fredrickson, M.L. Chabinyc, & R.A. Segalman, *Electrostatic Interactions Control the Nanostructure of Conjugated Polyelectrolyte–Polymeric Ionic Liquid Blends*, Macromolecules **55(18),** 8321–8331 (2022).
6. G.H. Fredrickson, S. Xie, J. Edmund, M.L. Le, D. Sun, D.J. Grzetic, D.L. Vigil, D. L., Delaney, K. T., Chabinyc, M. L., & Segalman, R. A*. Ionic Compatibilization of Polymers*, ACS Polymers Au **2(5),** 299–312 (2022).
7. G. Pace, O. Nordness, K. Asham, R.J. Clément, & R.A. Segalman, *Impact of Side Chain Chemistry on Lithium Transport in Mixed Ion–Electron-Conducting Polymers*, Chemistry of Materials **34(10),** 4672–4681 (2022).
8. E.M. Thomas, P.H. Nguyen, S.D. Jones, M.L. Chabinyc, R.A. Segalman, *Electronic, Ionic, and Mixed Conduction in Polymeric Systems*, Annual Review of Materials Research **51,** 1-20 (2021).
9. M.L. Le, D. Rawlings, S.P.O. Danielsen, R.M. Kennard, M.L. Chabinyc, R.A. Segalman, *Aqueous Formulation of Concentrated Semiconductive Fluid Using Polyelectrolyte Coacervation*, ACS Macro Letters **10(8),** 1008–1014 (2021).

Modulating Complex Chemical Conversion with Multi-site Electrocatalyst for Energy Dense Liquids

Yingwen Cheng (Principal Investigator), Department of Chemistry and Biochemistry, Northern Illinois University.

Keywords: electrocatalysis, energy storage, transformative manufacturing, chemical conversion

Research Scope

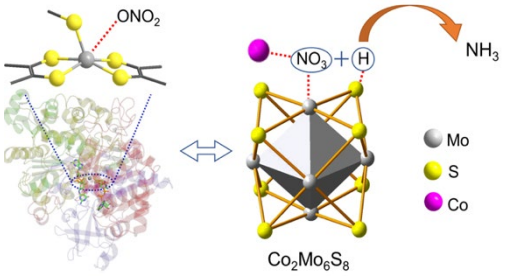

The goal of this project is to employ Chevrel phase chalcogenides with the general formula $M_xMo_6T_8$ as model catalysts to examine and hopefully establish a new, multi-site mechanism for selective hydrogenation of CO_2 and NO_x to value added chemicals. This project has several synergistic objectives that start with synthesis of a library of well-defined solid catalysts where the metal binding site (M = Fe, Li, Na, Mn, Ti, Co, Ni, Cu and Zn) and non-metal binding site T=S, Se and Te, are systematically tuned without major changes in crystal structure. This will be followed by systematic structural, spectroscopic and electrochemical characterizations to establish the chemistry of active motifs as a function of M and T combinations. We will then employ the CO_2 and nitrate reductions as model electrochemical hydrogenation reactions to correlate active motifs with activity and product selectivity. Representative catalysts will be further studied using *ex situ* and *operando* ^{57}Fe Mossbauer spectroscopy to identify dynamics of Fe sites and density functional theory calculations to quantify how the synergy of multi-site binding reduces the free energy landscape and modulates the transit catalysis species.

Recent Progress

This is the first project year and we primary focused on: 1) synthesis of catalysts with complex but essential compositions; 2) electrochemical evaluations of simple catalysts that were previously synthesized; 3) develop and optimize *in situ* and *ex situ* spectroscopic characterization tools to rationalize dynamics of active sites.

Catalyst synthesis: we successfully synthesized a series of new catalyst with the general composition $Fe_xM_{2-x}Mo_6T_8$, with M= first row transition metals, and T= a combination of S, Se and Te. Some potentially significant examples include $FeCoMo_6S_8$, $Fe_2Mo_6Te_8$, $Fe_2Mo_6Se_8$, $Fe_2Mo_6S_6Te_2$, and $Fe_2Mo_6S_6Se_2$. Phase-purity of these catalysts have been verified with X-ray diffractometry, scanning and transmission electron microscopy, Raman and energy-dispersive X-ray spectroscopy. Selected high performance compositions are being evaluated using X-ray photoelectron spectroscopy and synchrotron X-ray absorption spectroscopy.

$Co_2Mo_6S_8$ for nitrate-to-ammonia conversion: we discovered that $Co_2Mo_6S_8$ exhibits intrinsic activities for ambient electrochemical conversion of nitrate to ammonia. Despite of having a low surface area due to large particle size, this catalyst delivered a high Faradaic efficiency of 97% in a wide voltage range in neutral electrolytes, outperforming many prevailing nanocluster and single atom catalysts. We rationalize the high activities as the unique composition and atomic coordination of active motifs in $Co_2Mo_6S_8$, which provide synergistic multi-sites for activating and selectively associating key reaction intermediates. Specifically, the Co/Mo sites assist NO_3^- adsorption and activation whereas the S sites stabilize hydrogen intermediates H_{ad}^*. In addition, the ligand effect of Co enhances binding strength of S with H_{ad}^* and effectively inhibits the otherwise competing hydrogen evolution reaction. The unique spatial geometry of the Co, Mo and S sites promotes fast association of reaction intermediates for selective ammonia production, reaching to an enzyme-like high turnover frequency of 91 s^{-1}.

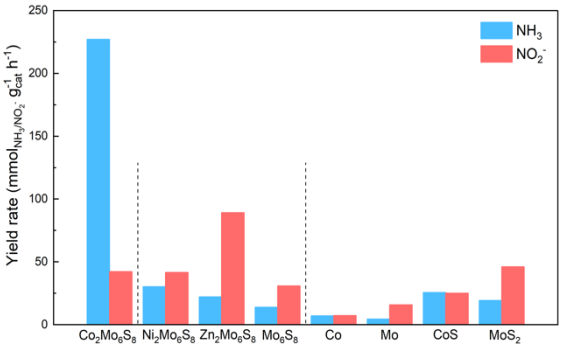

Role of chalcogenide sites on catalyst durability: understanding and controlling degradation of solid electrocatalysts have been challenging due to difficulties in defining the true active sites on complicated surfaces. Catalysts being studied here are advantageous in this regard due to the flexibility in controlling and defining the active site. As such, also using the nitrate-to-ammonia conversion as a model, we evaluated a series of $Ni_2Mo_6T_8$ catalysts where the chalcogenide site was systematically changed (T=S, Se and Te). Our results uncover critical roles of anions on the long-term durability and activity. The best performing catalyst was determined as the $Ni_2Mo_6Te_8$, with Faradaic efficiencies up to 99.9% and ammonia yielding rate more than 5 times higher compared with the $Ni_2Mo_6S_8$ catalysts. More importantly, this catalyst exhibited significantly improved durability with ~10% degradation after 50 hours of operation in strong alkaline electrolytes, much better than ~ 65% degradation for the $Ni_2Mo_6S_8$ catalysts.

^{57}Fe Mössbauer spectroscopy characterizations on dynamics of active sites: we employ model $Fe_2Mo_6S_8$ and $Fe_2Mo_6S_8/Fe_3C$ catalysts and study dynamics of Fe sites as a function of electrochemical potentials and electrolysis duration for nitrate reduction. We previously reported activities of these catalysts for nitrogen reduction, and discovered here that these catalysts also exhibited outstanding activities for nitrate reduction, with good stability and >90% Faradic efficiencies for a wide range of voltages. We verified their catalytic activities with our comprehensive testing protocols and are currently performing ex situ and in situ Mössbauer spectroscopy analysis. The results we have thus far suggest outstanding stability, as no new Fe phases were observed even after 40 hours of electrolysis.

References

1. K. Lu, F. Xia, B. Li, Y. Liu, I. Abdul Razak, S. Gao, J. Kaelin, D.E. Brown, Y. Cheng, *Synergistic Multisites $Fe_2Mo_6S_8$ Electrocatalysts for Ambient Nitrogen Conversion to Ammonia,* ACS Nano, **15**, 16887 (2021).
2. F. Xia, B. Li, Y. Liu, Y. Liu, S. Gao; K. Lu, J. Kaelin, R. Wang, T. Marks, Y. Cheng, *Carbon Free and Noble Metal Free $Ni_2Mo_6S_8$ Electrocatalyst for Selective Electrosynthesis of H_2O_2*, Advanced Functional Materials, **31**, 2104716 (2021).
3. J. Strachan, A. F. Masters, T. Maschmeyer, *The Catalytic Nature of Chevrel Phases ($M_xMo_6S_8$) in Review*. Materials Research Bulletin, **139**, 111286 (2021).
4. H. T. Zhang, C. Liu, P. Liu, Y. H. Hu, *Mo_6S_8-based Single-Metal-Atom Catalysts for Direct Methane to Methanol Conversion*, The Journal of Chemical Physics, **151**, 024304 (2019).
5. M. Liu, M. S. Hybertsen, Q. Wu, *A Physical Model for Understanding the Activation of MoS_2 Basal- Plane Sulfur Atoms for the Hydrogen Evolution Reaction*, Angew. Chem. Int. Ed., **59**, 14835 (2020).
6. X. Hong, K. Chan, C. Tsai, J. K. Nørskov, *How Doped MoS_2 Breaks Transition-Metal Scaling Relations for CO_2 Electrochemical Reduction*, ACS Catalysis, **6**, 4428 (2016).
7. N. R. Singstock, C. B. Musgrave, *How the bio-inspired $Fe_2Mo_6S_8$ chevrel breaks electrocatalytic nitrogen reduction scaling relationship,* J. Am. Chem. Soc., **144**, 12800 (2022).

Publications (since 09/01/2022)

1. B. Li, F. Xia, Y. Liu, H. Tan, S. Gao, J. Kaelin, Y. Liu, K. Lu, T. J. Marks, Y. Cheng, *$Co_2Mo_6S_8$ Catalyzes Nearly Exclusive Electrochemical Nitrate Conversion to Ammonia with Enzyme-like Activity*, Nano Letters, **23**, 1459 (2023).

Thermodynamics, Electroosmosis, and Electrokinetic Energy Generation in Nanochannels Functionalized with Anionic and Cationic Polyelectrolyte Brushes in Presence of Multivalent Counterions

Siddhartha Das (**Department of Mechanical Engineering, University of Maryland, Email: sidd@umd.edu**)

Keywords: Polyelectrolyte brushes; nanochannels; multivalent counterions; electroosmosis; electrokinetic energy

Research Scope

The overall scope of this project is to perform extensive atomistic molecular dynamics (MD) simulations [1-5] to understand the effect of multivalent counterions in the conformation and thermodynamics of anionic and cationic polyelectrolyte (PE) brushes and in electroosmotic transport and electrokinetic energy generation in nanochannels grafted with such PE brushes. This project scope is divided into five major objectives. The **first** and **second** objectives are to understand the effect of multivalent counterions in the conformation of anionic and cationic PE brushes and brush supported water molecules and counterions with the PE brushes being grafted to a single surface (1st objective) or to the inner walls of a nanochannel (2nd objective). The **third objective** is to study the electroosmotic (EOS) transport in anionic and cationic PE brush grafted nanochannels where the brushes are screened by multivalent counterions. The **fourth objective** is to study the pressure-driven transport and the resulting electrokinetic energy generation in nanochannels grafted with anionic and cationic PE brushes (with different types of screening counterions and corresponding added salts). The **fifth and the final objective** is to conduct a continuum analysis to model the equilibrium behavior of such brushes and the associated EOS and pressure-driven transport and the resulting electrokinetic energy generation in nanochannels grafted with such multivalent-counterion-screened cationic and anionic brushes.

Recent Progress

We had previously studied the configuration of anionic poly (acrylic acid) (PAA) brushes screened by multivalent counterions (namely, Li^+, Na^+, Cs^+, Mg^{2+}, Ca^{2+}, Ba^{2+}, Y^{3+}, and La^{3+} ions) [6]. Recently, we employed all-atom MD simulations to study the behavior of such anionic brushes [PAA, and poly-styrene sulfonate or PSS] in presence of an applied electric field [7]. It was revealed that depending on the charge density of the brushes, the electric field reduced the brush height by enforcing a bending effect (PAA brushes) or a tilting effect (PSS brushes) [**Fig. 1(a)**]. In another study [8], we probed the EOS transport in nanochannels grafted with PAA brushes that are screened by different multivalent counterions (namely, Na^+, Cs^+, Ca^{2+}, Ba^{2+}, and Y^{3+}). In a previous study probing EOS transport in nanochannels grafted with Na^+-ion-screened PAA brushes [9], we had identified the most remarkable overscreening (OS) effect (i.e., the presence of a greater number of counterions within the brush layer than needed to screen the brush charges), coion driven EOS transport for low to moderate electric fields, and reversal in the EOS flow directions with an increase in the strength of the electric field. In this study [8], we revealed the presence

of OS for weak to moderate electric field strengths for the cases of all the different counterions except for the case of Cs^+ ion [**Fig. 1(b)**]; however, at larger electric fields, OS effect ceases to exist for the cases of all the different types of counterions (except for the cases of the PAA brushes screened with the Ca^{2+} and Y^{3+} ions, as these ions remain strongly condensed on the PAA brushes) [**Fig. 1(b)**]. As a result, for all the cases (except for the cases of brushes screened with the Cs^+, Ca^{2+} and Y^{3+} ions), there occurs coion-driven EOS transport for low to moderate electric fields and the reversal in the direction of the EOS transport with an increase in the electric field strength [**Figs. 1(c,d)**]. In a recent submission [10], we have probed in details the equilibrium configuration of the Cl^- ion screened *cationic PE* brushes (namely, PMETAC brushes) and the properties of brush-supported water molecules and counterions. We reveal, most strikingly, anionic and hydrophobic nature of these cationic brushes in terms of the manner in which the water molecules respond [see the water dipole orientation around the PMETAC brush; **Fig. 1(e)**]; furthermore, these water molecules form separate domains around the charged $\{N(CH_3)_3\}^+$ group and the C=O group of the PMETAC chain. We have also started to probe the effect of the presence of multivalent screening anions and the nanoconfinement on the behavior of PMETAC brush and brush-supported counterions and water molecules. Finally, we have employed clustering-based machine learning approach [11] to quantify the water-water hydrogen bonds (HBs) inside the densely grafted PAA [12] [**Figs. 1(f-h)**] and PMETAC brush layers [13]. The results confirm that the

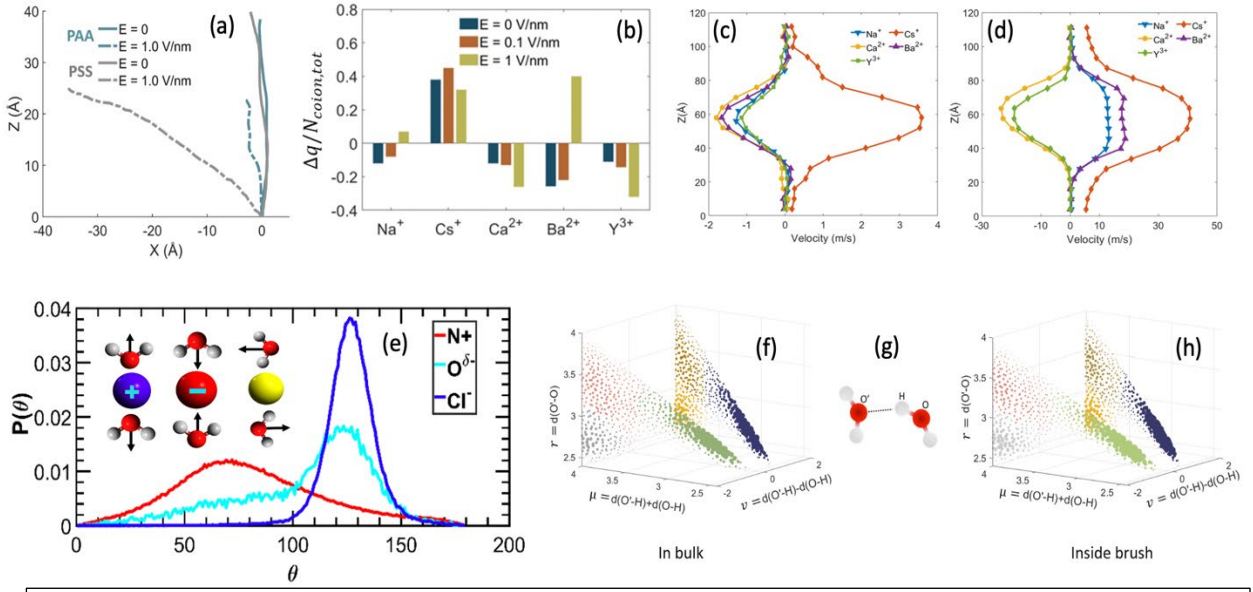

Figure 1: (a) Response of the PAA and PSS brushes to applied axial electric field (E) [7]. **(b)** Presence ($\Delta q<0$) and absence ($\Delta q>0$) of OS inside brush layer (for different E) for nanochannels grafted with PAA brushes and screened with multivalent counterions [8] (here Δq is the difference between the negative and positive charges inside the PAA brush layer). **(c,d)** EOS flow profile for **(c)** E=0.1 V/nm and **(d)** E=1 V/nm [8] for the case considered in (b). **(e)** Probability distribution of the orientation angle of the water dipole around N^+ ion, C=O group, and Cl^- ion of the Cl^--ion-screened PMETAC brushes. The inset shows the expected water dipole orientation in the vicinity of a cation, an anion, and a hydrophobe [10]. **(f-h)** Distribution of (v,μ,r) for water, characterizing the water-water HBs [**(g)**] in **(f)** bulk and **(h)** inside the brush layer [12].

large confinement effect afforded by the densely grafted brush layer enforces a change in the governing conditions that dictate the formation of water-water HBs inside the brush layers.

References

1. H. S. Sachar, T. H. Pial, P. R. Desai, S. A. Etha, Y. Wang, P. W. Chung, and S. Das, *Densely Grafted Polyelectrolyte Brushes Trigger "Water-in-Salt" like Scenarios and Ultraconfinement Effect*, Matter, **2**, 1509-1521 (2020).
2. H. S. Sachar, T. H. Pial, B. S. Chava, and **S. Das**, *All-atom Molecular Dynamics Simulations of Weak Polyionic Brushes: Influence of Charge Density on the Properties of Polyelectrolyte Chains, Brush-Supported Counterions, and Water Molecules*, Soft Matter, **16**, 7808-7822 (2020).
3. H. S. Sachar, B. S. Chava, T. H. Pial, and S. Das, *All-Atom Molecular Dynamics Simulations of the Temperature Response of Densely Grafted Polyelectrolyte Brushes*, Macromolecules, **54**, 6342-6354 (2021).
4. H. S. Sachar, B. S. Chava, T. H. Pial, and S. Das, *Hydrogen Bonding and its Effect on the Orientational Dynamics of Water Molecules inside Polyelectrolyte Brush-Induced Soft and Active Nanoconfinement*, Macromolecules, **54**, 2011-2021 (2021).
5. H. S. Sachar, T. H. Pial, V. S. Sivasankar, and S. Das, *Simultaneous Energy Generation and Flow Enhancement (Electroslippage Effect) in Polyelectrolyte Brush Functionalized Nanochannels*, ACS Nano, **15**, 17337-17347 (2021).
6. T. H. Pial, H. S. Sachar, and **S. Das**, *Quantification of Mono- and Multivalent Counterion-mediated Bridging in Polyelectrolyte Brushes*, Macromolecules, **54**, 4154-4163 (2021).
7. T. H. Pial, M. Prajapati, B. S. Chava, H. S. Sachar, and **S. Das**, *Charge-Density-Specific Response of Grafted Polyelectrolytes to Electric Fields: Bending or Tilting?* Macromolecules, **55**, 2413-2423 (2022).
8. T. H. Pial and S. Das, *Specific Ion and Electric Field Controlled Diverse Ion Distributions and Electroosmotic Transport in a Polyelectrolyte Brush Grafted Nanochannel*, The Journal of Physical Chemistry B, **126**, 10543-10553 (2022).
9. T. H. Pial, H. S. Sachar, P. R. Desai, and S. Das, *Overscreening, Coion-Dominated Electroosmosis, and Electric Field Strength Mediated Flow Reversal in Polyelectrolyte Brush Functionalized Nanochannels*, ACS Nano, **15**, 6507-6516 (2021).
10. R. Ishraaq, T. S. Akash, A. Bera, and S. Das, *Anionic and Hydrophobic Nature of Densely Grafted Cationic Brushes Trigger Multiple Water Domains with Diverse Properties and Counterions with Large Mobilities*, Macromolecules (**Under Revision**).
11. P. Gasparotto and M. Ceriotti, *Recognizing Molecular Patterns by Machine Learning: An Agnostic Structural Definition of the Hydrogen Bond*, Journal of Chemical Physics, **141**, 174110 (2014).
12. T. H. Pial and S. Das, *Machine Learning Enabled Quantification of the Hydrogen Bonds Inside the Polyelectrolyte Brush Layer Probed Using All-Atom Molecular Dynamics Simulations*, Soft Matter, **18**, 8945-8951 (2022).

A. Bera, T. S. Akash, R. Ishraaq, T. H. Pial, and S. Das, *Hydrogen Bonding Inside Anionic Polymeric Brush Layer: Machine Learning Driven Exploration of the Relative Roles of the Polymer Steric Effect and Charging*, Macromolecules (**Under Revision**).

Publications (in the past 2 years from the work supported by this BES funding)

1. T. H. Pial and S. Das, *Specific Ion and Electric Field Controlled Diverse Ion Distributions and Electroosmotic Transport in a Polyelectrolyte Brush Grafted Nanochannel*, The Journal of Physical Chemistry B, **126**, 10543-10553 (2022).

2. T. H. Pial and S. Das, *Machine Learning Enabled Quantification of the Hydrogen Bonds Inside the Polyelectrolyte Brush Layer Probed Using All-Atom Molecular Dynamics Simulations*, Soft Matter, **18**, 8945-8951 (2022).
3. T. H. Pial, M. Prajapati, B. S. Chava, H. S. Sachar, and **S. Das**, *Charge-Density-Specific Response of Grafted Polyelectrolytes to Electric Fields: Bending or Tilting?* Macromolecules, **55**, 2413-2423 (2022).
4. H. S. Sachar, T. H. Pial, V. S. Sivasankar, and S. Das, *Simultaneous Energy Generation and Flow Enhancement (Electroslippage Effect) in Polyelectrolyte Brush Functionalized Nanochannels*, ACS Nano, **15**, 17337-17347 (2021).
5. H. S. Sachar, B. S. Chava, T. H. Pial, and S. Das, *All-Atom Molecular Dynamics Simulations of the Temperature Response of Densely Grafted Polyelectrolyte Brushes*, Macromolecules, **54**, 6342-6354 (2021).
6. T. H. Pial, H. S. Sachar, and **S. Das**, *Quantification of Mono- and Multivalent Counterion-mediated Bridging in Polyelectrolyte Brushes*, Macromolecules, **54**, 4154-4163 (2021).
7. T. H. Pial, H. S. Sachar, P. R. Desai, and S. Das, *Overscreening, Coion-Dominated Electroosmosis, and Electric Field Strength Mediated Flow Reversal in Polyelectrolyte Brush Functionalized Nanochannels*, ACS Nano, **15**, 6507-6516 (2021).
8. V. S. Sivasankar, S. A. Etha, H. S. Sachar, and **S. Das**, *Thermoosmotic Transport in Nanochannels Grafted with pH-responsive Polyelectrolyte Brushes Modelled Using Augmented Strong Stretching Theory*, Journal of Fluid Mechanics, **917**, A31 (2021).
9. H. S. Sachar, B. S. Chava, T. H. Pial, and S. Das, *Hydrogen Bonding and its Effect on the Orientational Dynamics of Water Molecules inside Polyelectrolyte Brush-Induced Soft and Active Nanoconfinement*, Macromolecules, **54**, 2011-2021 (2021).

Discovery of New Inorganic Clathrates from Computational Predictions and Directed Synthesis

Davide Donadio, University of California, Davis. Kirill Kovnir, Iowa State University

Keywords: Clathrate, Transport properties, Density Functional Theory, Synthesis.

Research Scope

Clathrates are crystal structures that consist of nanometer-size polyhedral cages encapsulating guest atoms or molecules that are not directionally bonded to the framework. These materials have a high potential for energy storage and energy conversion technologies, including batteries and thermoelectrics. The overarching goal of this project is to discover and synthesize new unconventional inorganic clathrates, exploring the chemical space of transition-metal-stabilized III-V and II-VI compounds to form the clathrate framework, encapsulating alkali and alkaline-earth elements as guest ions. This scope is pursued through the development of a synergistic theoretical and experimental approach that combine electronic structure calculations at the level of density functional theory (DFT), artificial intelligence (AI), and directed synthesis. The objectives of the first two years of the project consist of (i) the development of an infrastructure to perform high-throughput screening of ternary or quaternary compounds based on DFT; (ii) the development of fast AI-based algorithms to predict the stability of thousands of potential inorganic clathrates; (iii) synthesis of new clathrates guided by theoretical predictions.

Recent Progress

Zintl electron counting provides a simple yet powerful rule to synthesize electron balanced materials. Following this principle and the former discovery of two alkali metal clathrates to date, $Cs_8Zn_{18}Sb_{28}$ and $K_{58}Zn_{122}Sb_{207}$,[1,2] we explored the rich Ba-Zn-*Pn* (*Pn* = As, Sb) compositional space, proximal to the expected composition of the type-I clathrate $Ba_8Zn_{20.67}Pn_{25.33}$. *In-situ* powder X-ray diffraction studies revealed two "hidden" compounds which can only be synthesized in a relatively narrow temperature range. Instead of the type I clathrate, compositionally close but structurally different new pseudoclathrates formed, $Ba_2Zn_5As_6$ and $Ba_2Zn_5Sb_6$ (Figure 1). These materials crystallize in a unique structure, in the orthorhombic space group *Pmna* with Wyckoff sequence i^2h^6gfe. DFT calculations and characterization, enabled by single-phase synthesis, revealed that these crystals have high Seebeck coefficients

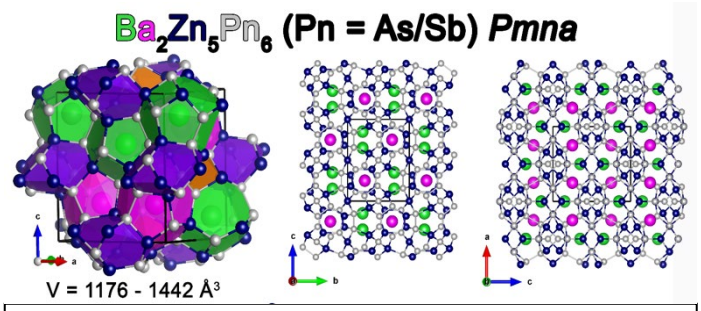

Figure 1. Structure of the newly discovered pseudo-clathrates $Ba_2Zn_5Pn_6$.

and low thermal conductivity, originated by the rattling dynamics of the Ba cations in oversized cages. These properties concur to make $Ba_2Zn_5As_6$ and $Ba_2Zn_5Sb_6$ promising thermoelectric materials, and calculations suggest that further optimization of the TE performance may be achieved by aliovalent doping.[3]

While the discovery of the $Ba_2Zn_5As_6$ pseudo-clathrates may be considered serendipitous, in this project we aim at providing systematic theoretical guidance to synthesis, identifying energetically favorable ternary and quaternary clathrates from a chemical palette that comprises elements from groups I and II as guests and IIb, III, V and VI for the framework, possibly stabilized by noble metals (Cu, Ag, Au). To this purpose, we have developed an automatic tool that exploits the Materials Project API[4,5] to identify the vertexes of the convex hull and compute the formation energy of a given ternary or quaternary compositions by DFT. We used this tool to predict the stability (decomposition energy) and electronic properties of the electron-balanced $A_8T_{27}Pn_{19}$ clathrate family (A=Na, K, Rb, Cs; T=Al, Ga, In; Pn=P, As, Sb, Bi, which consists of 48 unique clathrate compounds, three of which have been synthesized.[6] Following the prediction that compounds containing Bi with either Ga or In are particularly stable, we attempted to synthesize them. However, no synthesis route yielded ternary compounds, suggesting that a higher-level computational approach may be necessary. In fact, spin-polarized calculations including relativistic spin-orbit coupling and non collinear magnetization[7] revealed that these effects stabilize elemental Bi and Bismuth-containing binary compounds at the expense of the stability of ternary clathrates. The synthetic exploration of the compositional diagram of Ga-Sb and Ga-As compounds is currently in progress.

Considering noble metal stabilization, the families of clathrates blow up to several thousand possible compositions. High-throughput DFT calculations of so many compounds are not viable, especially when one needs to figure out superstructural order. Different ordered bonding patterns are possible by assigning atomic species to the crystalline sites of the type-I clathrate lattice. To this purpose we have developed a site permutation Monte Carlo (SPMC) algorithm that leverages energies predicted very rapidly by the crystal graph convolutional neural network MEGNet (MatErials Graph Network).[8,9] This approach, verified on known compounds, allows us to rapidly identify groups of potentially stable compounds, whose decomposition energy and structural stability can be refined by DFT, and they may be eventually

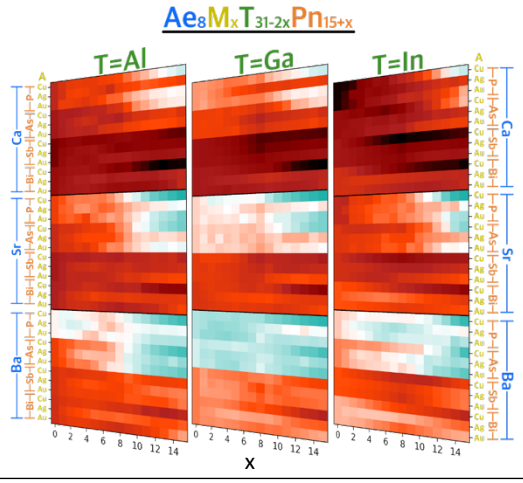

Figure 2. Stability map for the alkaline-earth (Ae), metal (M), tetrel (T), pnictide (Pn) family of clathrates. Stable compounds are indicated in teal color.

synthesized (Fig. 2). In this context, we are employing transfer learning to improve the equilibrium density and decomposition energy predictions of MEGNet for clathrates.

References

1. Liu, Y.; Wu, L.-M.; Li, L.-H.; Du, S.-W.; Corbett, J. D.; Chen, L. *The Antimony-Based Type I Clathrate Compounds $Cs_8Cd_{18}Sb_{28}$ and $Cs_8Zn_{18}Sb_{28}$.* Angew. Chem. Int. Ed. **121**, 5409–5412 (2009).
2. Cox, T.; Gvozdetskyi, V.; Bertolami, M.; Lee, S.; Shipley, K.; Lebedev, O. I.; Zaikina, J. V. *Clathrate XI $K_{58}Zn_{122}Sb_{207}$: A New Branch on the Clathrate Family Tree*. Angew. Chem. Int. Ed. **133**, 419–427 (2021).
3. Yox, P.; Cerasoli, F.; Sarkar, A.; Kyveryga, V.; Viswanathan, G.; Donadio, D.; Kovnir, K. *New Trick for an Old Dog: From Prediction to Properties of "Hidden Clathrates" $Ba_2Zn_5As_6$ and $Ba_2Zn_5Sb_6$.* J. Am. Chem. Soc. **145**, 4638–4646 (2023).
4. Ong, S. P.; Richards, W. D.; Jain, A.; Hautier, G.; Kocher, M.; Cholia, S.; Gunter, D.; Chevrier, V. L.; Persson, K. A.; Ceder, G. *Python Materials Genomics (Pymatgen): A Robust, Open-Source Python Library for Materials Analysis.* Computational Materials Science, **68**, 314–319 (2013).
5. Jain, A.; Hautier, G.; Moore, C. J.; Ping Ong, S.; Fischer, C. C.; Mueller, T.; Persson, K. A.; Ceder, G. A *High-Throughput Infrastructure for Density Functional Theory Calculations.* Computational Materials Science, 50, 2295–2310 (2020).
6. Owens-Baird, B.; Wang, J.; Wang, S. G.; Chen, Y.-S.; Lee, S.; Donadio, D.; Kovnir, K. *III–V Clathrate Semiconductors with Outstanding Hole Mobility: $Cs_8In_{27}Sb_{19}$ and $A_8Ga_{27}Sb_{19}$ (A = Cs, Rb).* J. Am. Chem. Soc. 142, 2031–2041 (2020).
7. Pyykko, P. Relativistic Effects in Structural Chemistry. Chem. Rev. 88, 563–594 (1988).
8. Chen, C.; Ye, W.; Zuo, Y.; Zheng, C.; Ong, S. P. Graph Networks as a Universal Machine Learning Framework for Molecules and Crystals. Chem. Mater. 31, 3564–3572 (2019).
9. Xie, T.; Grossman, J. C. Crystal Graph Convolutional Neural Networks for an Accurate and Interpretable Prediction of Material Properties. Phys. Rev. Lett. 120, 145301 (2018).

Publications

1. Yox, P., Cerasoli, F., Sarkar, A., Kyveryga, V., Viswanathan, G., Donadio, D., Kovnir, K. *New Trick for an Old Dog: From Prediction to Properties of "Hidden Clathrates" $Ba_2Zn_5As_6$ and $Ba_2Zn_5Sb_6$*. J. Am. Chem. Soc. **145**, 4638–4646 (2023). https://doi.org/10.1021/jacs.2c12435
2. Hong, Y., Yeon, S., Yox, P., Yunxiu, Z., Choi, M.-H., Moon, D., Ok, K.M., Kim, D.-H., Kovnir, K., Miller, G.J., You, T.-S. *Role of Eu-Doping in the Electron Transport Behavior in the Zintl Thermoelectric $Ca_{5-x-y}Yb_xEu_yAl_2Sb_6$ System*. Chem. Mater. **34**, 9903–9914 (2022). https://doi.org/10.1021/acs.chemmater.2c01810
3. Sarkar, A., Viswanathan, G., Yox, P., Harycki, S., Cerasoli, F.T., Wang, J., Perras, F.A., Gundlach-Graham, A., Donadio, D., Kovnir, K. *Evolution of structure and transport properties of the $Ba_8Cu_{16}P_{30}$ clathrate-I framework with the introduction of Ga*. Appl. Phys. Lett. **120**, 191901 (2022). https://doi.org/10.1063/5.0093646
4. Wang, J., Owens-Baird, B., Kovnir, K. *From Three-Dimensional Clathrates to Two-Dimensional Zintl Phases $AMSb_2$ (A = Rb, Cs; M = Ga, In) Composed of Pentagonal M–Sb Rings*. Inorg. Chem. **61**, 533–541 (2022). https://doi.org/10.1021/acs.inorgchem.1c03217
5. Yox, P., Lebedev, O.I., Donadio, D., Kovnir, K., 2021. *Unprecedented superstructure in the type I family of clathrates*. Chem. Commun. **57**, 13780–13783. https://doi.org/10.1039/D1CC05167A
6. Yox, P., Porter, A.P., Dorn, R.W., Kyveryga, V., Rossini, A.J., Kovnir, K. *Semiconducting silicon–phosphorus frameworks for caging exotic polycations*. Chem. Commun. **58**, 7622–7625 (2022). https://doi.org/10.1039/D2CC02304K

Pore Space Engineering and Functionalization in Porous Metal-Organic Framework Materials

PI: Pingyun Feng

Department of Chemistry, Materials Science and Engineering Program,

University of California, Riverside, CA 92521

Keywords: Crystalline Porous Materials, Pore Space Partition, Bioisosteric Replacement, Gas Adsorption, Purification and Separation

Research Scope

The research scope centers on developing innovative synthetic and structural concepts and paradigms to create advanced crystalline-porous-materials platforms. Strong efforts are devoted to synthesizing new materials with functional architectural design and chemical features. Such materials possess multi-modular framework and exceptional tolerance towards isoreticular modular replacement, making precise control of materials properties possible.[1,2] The synthesized materials have well-defined pore size and geometry that can be tuned in a large range in both small (picometer-level) and large (angstrom-level) increments to target different applications. In addition to serving as adsorbents for gas storage (e.g., C_2H_2),[3] they can improve energy efficiency in large industrial processes such as hydrocarbon purification and separation (e.g., C_2H_2/CO_2, C_6H_6/C_6H_{12}).[4] Other applications include carbon capture. The project employs innovative synthetic materials-design methods. It combines chemical and solvothermal synthesis, crystal growth and crystal structure analysis, with various property (e.g., thermal and chemical stability) studies. Sorption properties of various gases by these new materials are systematically evaluated to establish composition-structure-property correlations that are used to refine synthetic strategy to optimize porous materials for energy-related applications.

Recent Progress

Multiple significant progresses have been made. Ten manuscripts have been published. The following is a brief summary of key achievements during this period.

- Progressive Core Expansion in Pore-Space-Partitioned Metal-Organic Frameworks to Enhance Gas Uptake Capacity and Separation Efficiency[5]

A multi-stage core-expansion method is proposed and demonstrated for the optimization of both acetylene uptake and selectivity. The effectiveness of this strategy is shown through a family of eight cationic pore-partitioned materials containing three different pore-partitioning ligands and various counter-anions. The optimized structure, Co3-cpt-tph-Cl (Hcpt = 4-(p-carboxyphenyl)-1,2,4-triazole, H-tph = (2,5,8-tri-(4-pyridyl)-1,3,4,6,7,9-hexaazaphenalene) with the large surface area and high C_2H_2 uptake capacity (200 cm^3/g at 298 K), also exhibits (desirably) the low CO_2 uptake and hence the high C_2H_2/CO_2 selectivity. The successful boost in both C_2H_2 capacity and selectivity allows Co_3-cpt-tph-Cl to rank among the best crystalline porous materials, ionic MOFs in particular, for C_2H_2 uptake and C_2H_2/CO_2 experimental breakthrough separation.

- Integrative Extreme Pore Tightening and Ultrafine Pore Tuning for Dramatic Amplification of Gas Selectivity in Pore-Space-Partitioned Metal-Organic Frameworks

Ultrafine tuning of MOF structures at sub-angstrom to picometer levels can dramatically improve separation selectivity for gas pairs with subtle differences. However, for MOFs with large-enough pore size, the effect from ultrafine tuning on sorption properties can be muted. In this work, we propose and demonstrate an integrative strategy that couples together extreme pore compression with ultrafine pore tuning. Specifically, we use one module (L1) to shrink pore size to extreme minimum on the pacs platform while retaining porosity. This is followed by using another module (L2) for ultrafine pore turning. This integrative L1-L2 strategy leads to dramatically enhanced C_2H_2/CO_2 selectivity from 2.6 to 48.4 and excellent experimental breakthrough performance.

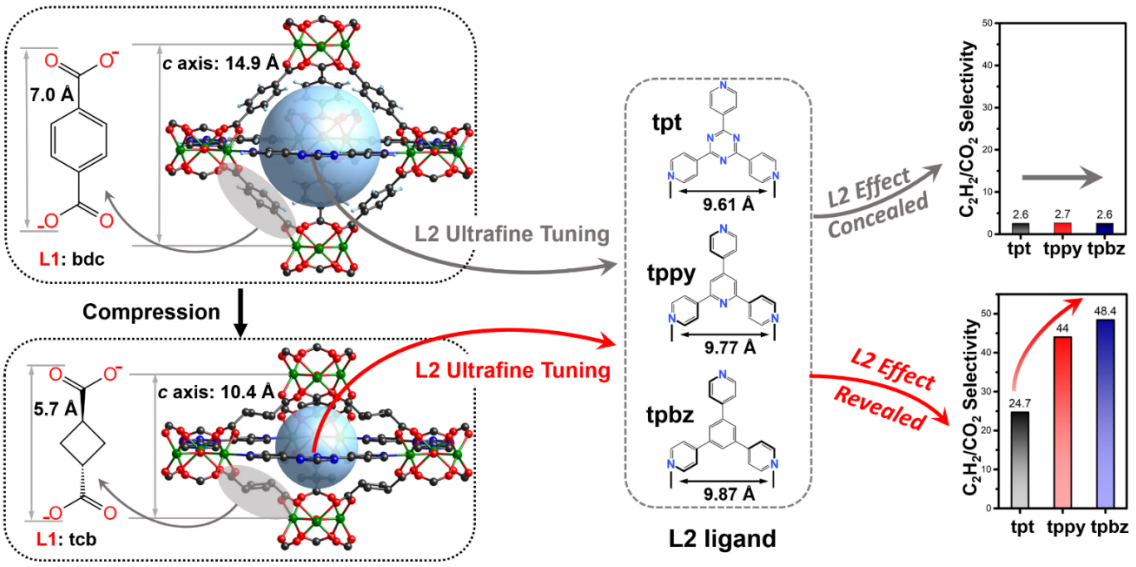

Figure 1. Illustration of extreme pore compression with L1 ligand and ultrafine pore tuning with L2 ligand and their impact or lack of impact on C_2H_2/CO_2 selectivity.

- Ultrastable Porous Materials for Applications in Harsh Chemical Conditions

We have succeeded in synthesizing Cr(III)-based porous materials that are exceptionally stable in boiling water or under either extreme acidic or extreme basic conditions with a large pH range from pH < 0 to pH >14. These materials help open up applications under harsh chemical conditions.

- Solvent-free Synthesis of Multi-Module Pore-Space-Partitioned Metal-Organic Frameworks for Gas Separation[6]

The green syntheses using solvent-free methods are generally limited to simple chemical systems usually with just one inorganic module and one organic module. In this work, we have succeeded in developing a solvent-free method to synthesize complex metal-organic framework materials with multiple modules. Such multi-module materials are more amenable to compositional and geometrical tuning and thus offer more opportunities for property

optimization. The synthesis only requires simple mixing of reactants and short reaction time. Highly porous and stable materials can be made without corrosive additives and without any energy-costing post-synthetic activation.

References

1. Zhai, Q-G; Bu, X.; Mao, C.; Zhao, X.; Daemen, L.; Cheng, Y.; Ramirez-Cuesta, A. J.; Feng, P., An Ultra-Tunable Platform for Molecular Engineering of High-Performance Crystalline Porous Materials, Nat. Commun. 2016, 7, 13645.
2. Hong, A. N.; Yang, H.; Bu, X.; Feng, P., Pore Space Partition of Metal-Organic Frameworks for Gas Storage and Separation. EnergyChem, 2022, 4, 100080.
3. Wang, Y.; Jia, X.; Yang, H.; Wang, Y.; Chen, X.; Hong, A.; Li, J.; Bu, X. Feng, P., A New Strategy for Constructing Pore Space Partitioned MOFs with High Uptake Capacity for C2 Hydrocarbons and CO2. Angew. Chem. Int. Ed. 2020, 59, 19027.
4. Yang, H.; Wang, Y.; Krishna, R.; Jia, X.; Wang, Y.; Hong, A. H.; Dang, C.; Castillo, H. E.; Bu, X.; Feng, P., Pore-Space-Partition-Enabled Exceptional Ethane Uptake and Ethane-Selective Ethane-Ethylene Separation. J. Am. Chem. Soc. 2020, 142, 2222.
5. Hong, A. N.; Wang, Y.; Chen, Y.; Yang, H.; Kusumoputro, E.; Bu, X.; Feng, P., Concurrent Enhancement of Acetylene Uptake Capacity and Selectivity by Progressive Core Expansion and Extra-Framework Anions in Pore-Space-Partitioned Metal-Organic Frameworks. Chem. Eur. J. 2023, e202203547.
6. Xiao, Y.; Chen, Y.; Hong, A. N.; Bu, X.; Feng, P., Solvent-free Synthesis of Multi-Module Pore-Space-Partitioned Metal-Organic Frameworks for Gas Separation. Angew. Chem. Int. Ed. 2023, 62, e202300721.

Publications

1. Xiao, Y.; Chen, Y.; Wang, W.; Yang, H.; Hong, A. N.; Bu, X.; Feng, P., Simultaneous Control of Flexibility and Rigidity in Pore-Space-Partitioned Metal–Organic Frameworks. J. Am. Chem. Soc. 2023, 145, 10980−10986.
2. Xiao, Y.; Chen, Y.; Hong, A. N.; Bu, X.; Feng, P., Solvent-free Synthesis of Multi-Module Pore-Space-Partitioned Metal-Organic Frameworks for Gas Separation. Angew. Chem. Int. Ed. 2023, 62, e202300721.
3. Hong, A. N.; Wang, Y.; Chen, Y.; Yang, H.; Kusumoputro, E.; Bu, X.; Feng, P., Concurrent Enhancement of Acetylene Uptake Capacity and Selectivity by Progressive Core Expansion and Extra-Framework Anions in Pore-Space-Partitioned Metal-Organic Frameworks. Chem. Eur. J. 2023, e202203547.
4. Xiao, Y.; Hong, A. N.; Chen, Y.; Yang, H.; Wang, Y.; Bu, X.; Feng, P., Developing Water-Stable Pore-Partitioned Metal-Organic Frameworks with Multi-Level Symmetry for High-Performance Sorption Applications. Small 2023, 2205119.
5. Yang, H.; Chen, Y.; Dang, C.; Hong, A. N.; Feng, P.; Bu, X., Optimization of Pore-Space-Partitioned Metal-Organic Frameworks Using Bioisosteric Concept. J. Am. Chem. Soc. 2022, 144, 20221–20226.
6. Hong, A. N.; Yang, H.; Bu, X.; Feng, P., Pore Space Partition of Metal-Organic Frameworks for Gas Storage and Separation. EnergyChem, 2022, 4, 100080.
7. Hong, A. N.; Kusumoputro, E.; Wang, Y.; Yang, H.; Chen, Y.; Bu, X.; Feng, P., Simultaneous Control of Pore-Space Partition and Charge Distribution in Multi-Modular Metal-Organic Frameworks. Angew. Chem. Int. Ed. 2022, 61, e202116064.
8. Hong, A. N.; Luong, D.; Alghamdi, M.; Liao, W. C.; Zhang, W.; Kusumoputro, E.; Chen, Y.; Greaney, P. A.; Cui, Y.; Shi, J.; Bu, X.; Fokwa, B. P. T.; Feng, P., Metal-mediated Directional-capping of Rod-packing Metal-organic Frameworks. Chem. Eur. J. 2022, e202201576.
9. Xiao, Y.; Yang, H.; Hong, A. N.; Wang, Y.; Bu, X.; Feng, P., In Situ Synthesized Homochiral Spiroborate Ester Metal-Organic Framework with Mono-, Di-, and Trivalent Cations. Chem Asian J. 2022, e202200918.
10. Hong, A. N.; Yang, H.; Li, T.; Wang, Y.; Wang, Y. X.; Jia, X.; Zhou, A.; Kusumoputro, E.; Li, J.; Bu, X.; Feng, P., Pore-Space Partition and Optimization for Propane-Selective High-Performance Propane/Propylene Separation. ACS Appl Mater Interfaces. 2021, 13, 52160-52166.

Modular Intermetallics: Materials Discovery from Chemical Pressure-Derived Principles for the Formation and Morphology of Complex Metallic Structures

Daniel C. Fredrickson and Rie T. Fredrickson, Department of Chemistry, University of Wisconsin-Madison, Madison, Wisconsin

Keywords: Intermetallic phases, design principles, chemical pressure, modular structures

Research Scope

Intermetallic phases represent a rich palette of potential materials for energy applications as they combine unparalleled diversity in both structural features and materials properties. The identification or creation of compounds optimized for specific properties—including superconductivity or other quantum phenomena, thermoelectric effects, magnetic order, and catalysis—is limited, however, by the inability to control their structures at the atomic level and develop structure-properties relationships. Here, we are addressing this need for design principles in intermetallics through a focus on complex structures derived from the assembly of units of simpler structures, as illustrated by the MAX (M= transition metal, A=group 13 or 14 element, X = C or N) phases (Figure 1).[1] Our objectives are to (1) devise and validate a predictive *theory of modular intermetallic chemistry*, in which the results of electronic structure calculations on simpler compounds are used to anticipate their compatibility for intergrowth and the preferred orientations of their domain interfaces; (2) synthetically realize unprecedented families of modular intermetallic compounds, guided by and providing feedback to the theoretical framework; and (3) evaluate structure-properties relationships and the potential new functionality arising from the modularity of the new compounds obtained. Through these endeavors, this project is creating materials that may exhibit intriguing or technologically useful behavior, as well as establishing broader guidelines for how the wide-ranging structural motifs offered by intermetallic phases can be combined in new ways.

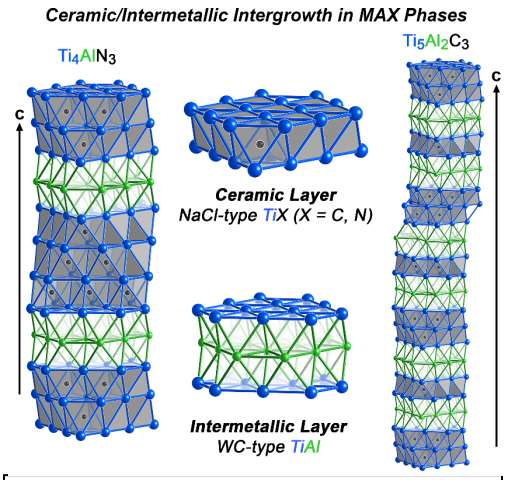

Figure 1. The MAX phases viewed as modular materials.

Recent Progress

In our resent work, we have examined the driving forces underlying a range of complex intermetallic structures derived from modular components. The structural arrangements elucidated include the intergrowth of Zintl and Laves phase units in K_3Au_5Tl;[2] the assembly of metallic glass building units in the Mo_4Hf_9B type;[3] tiling patterns of the σ-phase structure and

dodecagonal quasicrystal approximants,[4,5] Pd_5InAs,[6] and Y_2Mg_2Ni;[7] and the lamellar alteration of Laves-and $CaCu_5$-type slabs in RE-Ni intermetallics (RE = lanthanide or group 3 transition metal).[8] We uncovered a variety of mechanisms at work in these cases, such as the inclusion of buffer regions to resolve the packing issues of certain structural units (Mo_4Hf_9B type)[9] and electron transfer across domain interfaces to solve non-ideal electron counts in the parent structures (Pd_5InAs).[10] A mechanism that is particularly adaptable to synthetic design is the matching of complementary features in the DFT-Chemical Pressure (CP) schemes of the parent structures at their interfaces (the σ-phase and dodecagonal quasicrystal approximants,[11] Y_2Mg_2Ni[12]) . This effect can be visualized with the newly developed $CP_{interface}$ function,[11] as shown for the parent structures of the σ-phase type in Figure 2.

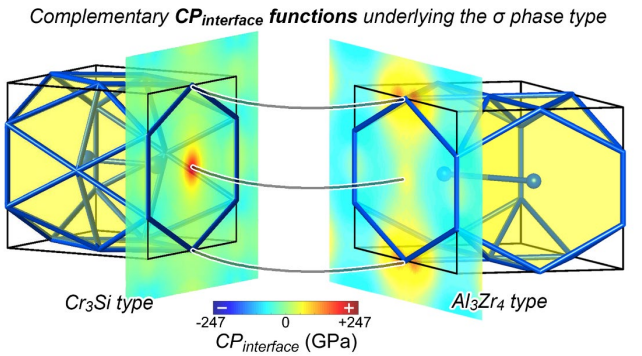

Figure 2. The $CP_{interface}$ function illustrating complementary between the CP features of the parent structures of the σ-phase structure type. Reprinted with permission from Ref.11. Copyright 2022 American Chemical Society.

Our experimental investigations have led to the discovery of a variety of modular structures of key relevance to our emerging theory of modular intermetallic chemistry. We are currently working on the final characterization and/or manuscript preparation for six new modular structures distributed over three very different ternary systems. Importantly, one is constructed from a pairing of parent structures that was predicted to be favorable from our theoretical work. We plan to present the details of these compounds in a series of publications over the next year.

DFT-CP schemes of potential parent structures and other metrics regarding bonding are the key indicators this project uses in designing the synthesis of new modular structures. The facilitate this process, we have created and released on the web the *Intermetallic Reactivity Database* (*IRD*)[12] as a repository of such data obtained in the course of this project, as well as other ongoing endeavors (user submissions are also invited). The IRD's web interface allows users to visualize and interact with CP schemes and other data overlaid on 3D structural models, as well as download entries for more detailed analysis. Our article marking its release describes four different applications of the resource, ranging from explaining or anticipating intergrowth structures, to following packing trends with elemental substitution, to assisting the development of theoretical methodology. The IRD is continuing to expand in terms of entries, data types, interface functionality, as well as incorporating key advances in the DFT-CP method enabled by this project.[13]

References

1. 1. Radovic, M.; Barsoum, M. W. MAX phases: bridging the gap between metals and ceramics. *Am. Ceram. Soc. Bull.* **2013**, *92 (3)*, 20-27.
2. 2. Li, B.; Kim, S.-J.; Miller, G. J.; Corbett, J. D. Gold Tetrahedra as Building Blocks in K_3Au_5Tr (Tr = In, Tl) and Rb_2Au_3Tl and in Other Compounds: A Broad Group of Electron-Poor Intermetallic Phases. *Inorg. Chem.* **2009**, *48*, 6573-6583.
3. 3. Hårsta, A.; Rundqvist, S. The crystal chemistry of kappa-phases. *J. Solid State Chem.* **1987**, *70*, 210-218.
4. 4. Iga, H.; Mihalkovič, M.; Ishimasa, T. Approximant of dodecagonal quasicrystal formed in Mn–Si–V alloy. *Philos. Mag.* **2011**, *91*, 2624-2633.
5. 5. Shoemaker, C. B.; Shoemaker, D. P. The crystal structure of the ν phase, $Mn_{81.5}Si_{18.5}$. *Acta Crystallogr. B* **1971**, *27*, 227-235.
6. 6. Zakharova, E. Y.; Andreeva, N. A.; Kazakov, S. M.; Kuznetsov, A. N. Ternary arsenides based on platinum–indium and palladium–indium fragments of the Cu_3Au-type: Crystal structures and chemical bonding. *J. Alloys Compd.* **2015**, *621*, 307-313.
7. 7. Hoffmann, R.-D.; Fugmann, A.; Rodewald, U. C.; Pöttgen, R. New Intermetallic Compounds Ln_2Ni_2Mg (Ln = Y, La–Nd, Sm, Gd–Tm) with Mo_2FeB_2 Structure. *Z. Anorg. Allg. Chem.* **2000**, *626*, 1733-1738.
8. 8. Parthé, E.; Lemaire, R. Structure block stacking in intermetallic compounds. I. The rhombohedral-hexagonal $M_{n+1}X_{5n-1}$ and the monoclinic-hexagonal-trigonal-orthorhombic $M_{n+1}X_{5n+2}$ structure series. *Acta Crystallogr. B* **1975**, *31*, 1879-1889.
9. 9. Lu, E.; Gressel, D. G.; Fredrickson, D. C. Buffering Octahedra in Mo_4Zr_9P: Intergrowth as a Solution to the Frustrated Packing of Tricapped Trigonal Prisms and Icosahedra. *Inorg. Chem.* **2022**, *61*, 8298-8308.
10. 10. Kraus, J. D.; Van Buskirk, J. S.; D. C. Fredrickson, D. C. The Zintl Concept Applied to Intergrowth Structures: Electron-Hole Matching, Stacking Preferences, and Chemical Pressures in Pd5InAs, *Z. Anorg. Allg. Chem.,* under revision.
11. 11. Fredrickson, R. T.; Fredrickson, D. C. Chemical Pressure-Derived Assembly Principles for Dodecagonal Quasicrystal Approximants and Other Complex Frank–Kasper Phases. *Inorg. Chem.* **2022**, *61*, 17682-17691.
12. 12. Van Buskirk, J. S.; Kraus, J. D.; Fredrickson, D. C. The Intermetallic Reactivity Database: Compiling Chemical Pressure and Electronic Metrics toward Materials Design and Discovery. *Chem. Mater.* **2023**, *35*, 3582-3591.
13. 13. Sanders, K. M.; Van Buskirk, J. S.; Hilleke, K. P.; Fredrickson, D. C. Self-Consistent Chemical Pressure Analysis: Resolving Atomic Packing Effects through the Iterative Partitioning of Space and Energy. *J. Chem. Theory Comput.* **2023**, ASAP, DOI: 10.1021/acs.jctc.1023c00368.

Publications

1. Lu, E.; Van Buskirk, J. S.; Cheng, J.; Fredrickson, D. C. Tutorial on Chemical Pressure Analysis: How Atomic Packing Drives Laves/Zintl Intergrowth in K_3Au_5Tl. *Crystals* **2021**, *11*, 906.
2. Lu, E.; Gressel, D. G.; Fredrickson, D. C. Buffering Octahedra in Mo_4Zr_9P: Intergrowth as a Solution to the Frustrated Packing of Tricapped Trigonal Prisms and Icosahedra. *Inorg. Chem.* **2022**, *61*, 8298-8308.
3. Fredrickson, R. T.; Fredrickson, D. C. Chemical Pressure-Derived Assembly Principles for Dodecagonal Quasicrystal Approximants and Other Complex Frank–Kasper Phases. *Inorg. Chem.* **2022**, *61*, 17682-17691.
4. Van Buskirk, J. S.; Kraus, J. D.; Fredrickson, D. C. The Intermetallic Reactivity Database: Compiling Chemical Pressure and Electronic Metrics toward Materials Design and Discovery. *Chem. Mater.* **2023**, *35*, 3582-3591.
5. Sanders, K. M.; Van Buskirk, J. S.; Hilleke, K. P.; Fredrickson, D. C. Self-Consistent Chemical Pressure Analysis: Resolving Atomic Packing Effects through the Iterative Partitioning of Space and Energy. *J. Chem. Theory Comput.* **2023**, ASAP, DOI: 10.1021/acs.jctc.1023c00368.
6. Kraus, J. D.; Van Buskirk, J. S.; D. C. Fredrickson, D. C. The Zintl Concept Applied to Intergrowth Structures: Electron-Hole Matching, Stacking Preferences, and Chemical Pressures in Pd_5InAs, *Z. Anorg. Allg. Chem.,* under revision.

Permanent Magnets Featuring Heavy Main Group Elements for Magnetic Anisotropy

Danna Freedman | Massachusetts Institute of Technology

Keywords: High-pressure; magnet; bismuth; spin-orbit coupling

Research Scope

Permanent magnets are the functional component of electric motors and generators found in numerous renewable energy applications. To improve energy conversion in such applications, we require fundamentally new magnets that generate higher magnetic flux per volume while retaining the properties conferred by rare-earth elements incorporated into current technologies. We hypothesize that by engendering a covalent interaction between two elements, we can access a new regime of magnetic materials where the two components of a magnetic moment—spin and orbital angular momentum—come from two separate atoms to form a complete magnetic moment.

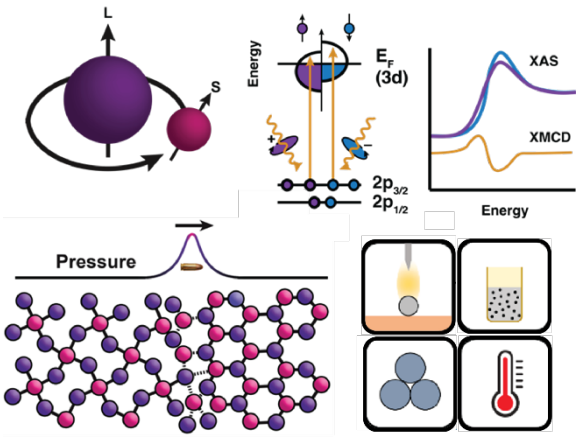

Figure 3. Our approach to new magnetic materials entails combining the orbital angular momentum (L) of heavy elements with the spin angular momentum (S) of 3d transition metals. We made progress rationalizing our magnetic response measurements of high-pressure phases via density functional theory (top right), studying the kinetics of these high-pressure transformations via shockwave experiments (bottom left) and expanded our focus to 3d–5d transition metal systems using an array of synthetic conditions (bottom right).

Our previous research utilized high-pressure conditions to discover two new candidate materials ideal for assessing this hypothesis. The first material, $FeBi_2$, enables the study of an unprecedented solid-state metal-metal bonding interaction. The second, $MnBi_2$ represents the second member of the promising Mn–Bi family known for its magnetic properties. Importantly, $MnBi_2$ is isostructural to $FeBi_2$. Together these chemically simple but magnetically rich materials provide an elegant platform for elucidating fundamental design principles of magnetic anisotropy while inspiring the synthesis of new magnetic materials. In fact, we have leveraged our understanding of magnetism in these compounds, aided by techniques such as X-ray Magnetic Circular Dichroism (XMCD), to target novel phases of interest in chemical systems composed of 3*d* and 5*d* transition metals.

Recent Progress

To fully harness the potential of solid state chemistry we need to create a window into both the structure and the properties of our high-pressure materials. To this end, we have predicted, synthesized, and magnetically probed magnet candidates through three objectives: **(1)** We performed ab initio electronic structure calculations on $MnBi_2$ and closely related magnetic compounds to elucidate the relationship between their structures and magnetic responses, **(2)** we targeted the recovery of these materials using dynamic compression, expanding our methods to include *in-situ*, time-resolved X-ray diffraction and mechanical shock using a gas-fired gun, **(3)** we synthesized new ambient-pressure phases in a 3*d*–5*d* chemical system using a wide range of preparatory conditions to access new candidate permanent magnets.

Future Plans

We initiated a new collaboration with the Institute for Soldier Nanotechnologies, providing access to their gas-fired gun (Figure 2). Laser shock stresses last several nanoseconds while projectile-impact shock stresses last at least three orders of magnitude longer. We hypothesize that the longer stress state involved in the mechanical shock loading will better enable phase transitions or reactivity compared to laser shock stresses. Within these experiments, we shoot approximately 12 gram steel bullets at approximately 300 m/s, successfully hitting our targets. Enabling the recovery of the sample after shock is a critical next step, as the sample is typically destroyed after being hit by the bullet. We expect utilizing copper sheets will protect the sample from destruction while allowing the transmission of the pressure and temperature waves. Shockwaves pull systems out of equilibrium which we expect to allow us to access new materials which are not the thermodynamic product. Alongside shocking MnBi, we have begun to target shocking oxide materials with interesting magnetic properties such as $BiFeO_3$, a multiferroic material; $BaFeO_3$, a ferromagnet; and Ce_2BiO_2, an antiferromagnet

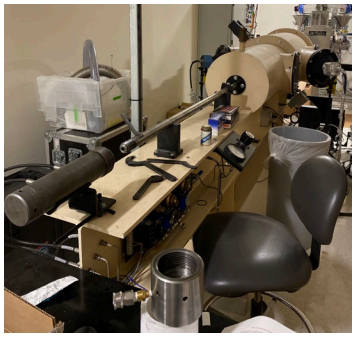

Figure 2. The gas-fired gun at the Institute for Soldier Nanotechnologies at MIT.

Permanent magnets combining 5*d* and 3*d* metal MnBi [8] and Rh_2CoSb [9] exhibit unusually hard magnetic responses in part due to the interaction between 3*d* metal unpaired spins, strongly spin-orbit coupled heavy atoms, and structural anisotropy. Taking inspiration from these chemical principles, we are pursuing new intermetallic phases with intimate contact between early 5*d* transition metals and 3*d* transition metals to elicit strong magnetocrystalline anisotropy. Such phases composed of relatively abundant elements are promising for bulk permanent

magnets, as opposed to those for magnetic memories where higher cost elements like Rh and Pt can be tolerated due to the microscopic device size.

One thrust of our efforts is directed at the W–Mn system, which is not reported to host any compounds, in contrast to nearby binary chemical systems combining 5*d* and 3*d* elements. We hypothesized this may correspond to challenges in reacting these two elements with wildly different physical properties (e.g. the boiling point of Mn is well below the melting point of W)

Compositional Control of Fundamental Electronic and Magnetic Properties of Ordered Layered Multielemental MXenes

PI: Yury Gogotsi, Co-PIs: Steven May

A.J. Drexel Nanomaterials Institute and Department of Materials Science and Engineering, Drexel University, Philadelphia, PA 19104, USA

Keywords: MXene, Electronic properties, 2D material, Synthesis

Research Scope

MXenes are a rapidly expanding family of two-dimensional transition metal carbides, nitrides, and carbonitrides. In the past decade, MXenes ($M_{n+1}X_nT_x$) family has grown to encompass various transition metals (M), carbon, nitrogen and oxygen (X), surface functional groups (T), number of layers (*n*), and a variety of structures, including solid solutions and atomic ordering [1]. This research project focuses on controlling electronic and magnetic properties of MXenes via composition. Here, we aim to modify and control the M, X, and terminations of MXenes produced using molten salt synthesis. Specifically, we focus on synthesis of carbide/nitride/carbonitride MAX phases and their corresponding MXenes that may offer magnetic properties. We also study how different surface terminations can impact the electronic and magnetic properties of MXenes, and how nitrogen at the X-site alters the electronic and magnetic properties of MXenes.

Recent Progress

Impact of M-site composition on electronic behavior: We have revealed the correlations between macroscopic electronic conductivity, M-site composition, and extrinsic factors such as flake size and *d*-spacing within the $Ti_yNb_{2-y}CT_x$ system (Fig. 1a) [2]. Through a detailed analysis of resistivity and mobility data, we discovered correlations between material parameters and macroscopic conductivity. Our key finding reveals that compositional tuning significantly impacts conductivity and mobility, potentially outweighing external factors like flake size and *d*-spacing. The consequence of intrinsic changes in electronic structure due to alloying of Ti and Nb was confirmed by hard XPS (HAXPES) (Fig. 1c). This work thus provides guidance on how both intrinsic compositional and extrinsic factors can be engineered to boost MXene conductivity and provides insights into the relative impacts of material features on electronic behavior that until now have been difficult to disentangle.

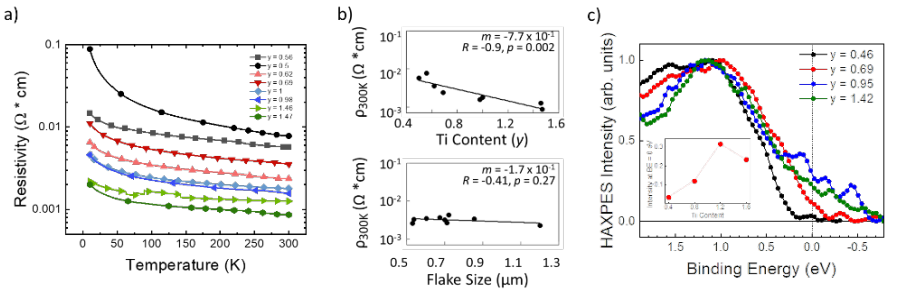

Figure 1. a) Temperature dependence of resistivity of $Ti_yNb_{2-y}CT_x$ with *y* values ranging from 0.56 to 1.47. b) Correlation plots for Ti content and flake size dependence of the RT resistivity. *m* is the slope constant that describes the dependence, *b* is the *y*-intercept value, *R* is the correlation, and *p* is the *p*-value. c) HAXPES valence band spectra.

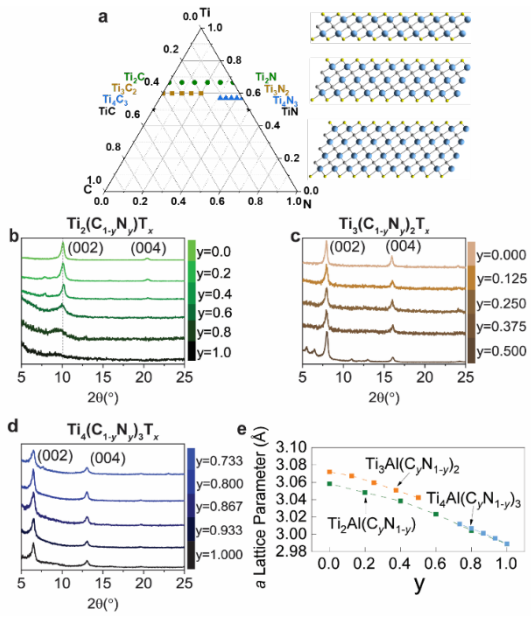

Figure 2. (a) Illustration of three families of carbonitride MXene. (b-d) X-ray diffraction patterns of the (*002*) and (*004*) reflections of $Ti_2(C_{1-y}N_y)T_x$, $Ti_3(C_{1-y}N_y)_2T_x$, and $Ti_4(C_{1-y}N_y)_3T_x$ MXenes produced. (e) The *a* lattice parameters plotted as a function of the N content.

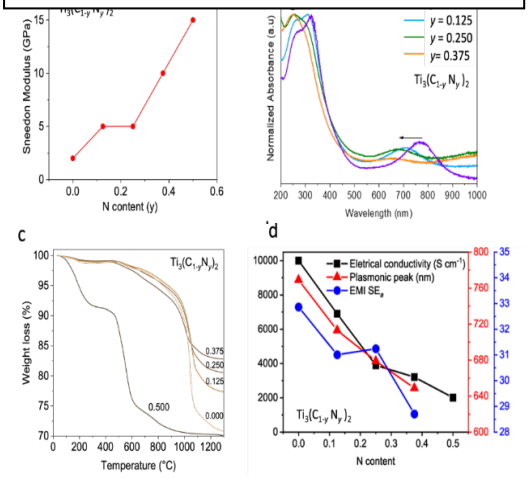

Figure 3. Dependence of physical properties on nitrogen content in $Ti_3(C_{1-y}N_y)_2T_x$ MXene. The plot of (a) Sneedon modulus, (b) UV-vis spectra, and (c) thermal gravity analysis of $Ti_3(C_{1-y}N_y)_2T_x$. (d) The plot of electrical conductivity, plasmonic peak, and Electromagnetic interface (EMI) shielding absorbance as the function of nitrogen content.

Carbonitride MXenes: After focusing on the role of M-site element on electrical properties, we systematically investigated carbonitride MXenes, determining the synthesis conditions and structural parameters of 16 X-site solid-solution MAX phases [3,4]. We synthesized carbonitride MXenes in molten chloride salts. $Ti_2Al(C_{1-y}N_y)$, $Ti_3Al(C_{1-y}N_y)_2$ and $Ti_4Al(C_{1-y}N_y)_3$ MAX phases exhibit a universal dependence of the *a*-lattice parameter on nitrogen content (Fig. 1e). Upon the removal of the Al layer, the MAX phases directly transformed into MXenes with uniform halogen terminations: $Ti_2(C_{1-y}N_y)T_x$, $Ti_3(C_{1-y}N_y)_2T_x$ and $Ti_4(C_{1-y}N_y)_3T_x$, including 11 compositions that have not been previously reported (Fig. 2a-d). Our findings reveal that solid-solution MXenes with higher nitrogen contents have shorter synthesis times, but lower stability, providing valuable insights for future exploration of solid-solution MXenes. Most notably, we observed a strong monotonic correlation between the nitrogen content and optical, mechanical, thermal and electrical properties, stability, as well as EMI shielding performance. In the $Ti_3(C_{1-y}N_y)_2T_x$ system, AFM revealed that the Sneedon modulus consistently increases with nitrogen content, to more than 8 times from $Ti_3C_2T_x$ to $Ti_3(C_{0.5}N_{0.5})_2T_x$ (Figure 3a). Analysis of UV-vis spectra demonstrated a decrease in both, absorbance wavelength and intensity in the NIR and UV regions, suggesting a correlation between the oxidation state of Ti and inter-band transitions of $Ti_3(C_{1-y}N_y)_2T_x$ (Fig. 3b) [5]. Further, thermal stability, influenced by bond enthalpy, also demonstrated dependency on nitrogen concentration (Fig. 3c). Fig. 3d portrays the impact of nitrogen concentration on electrical conductivity, EMI shielding absorbance efficiency, and the absorption peak position from UV-vis spectra. Considering that the EMI shielding effectiveness is associated with the electrical conductivity of MXenes, it is critical to isolate the impact of nitrogen concentration to understand these properties better [6]. Through our ongoing research, we aim to unravel these intricate dependencies and their implications for MXene applications.

References

1. A. Vahid Mohammadi, A.; Rosen, J.; Gogotsi, Y., The world of two-dimensional carbides and nitrides (MXenes), *Science,* 2021, 372 (6547), eabf1581.
2. Y. Yang, C. E. Shuck, M. Han, R. Sah, A. Gray, Y. Gogotsi, S. J. May, Correlating electronic properties with M-site composition in solid solution $(Ti_yNb_{1-y})_2CT_x$ MXenes, *2D Materials*, **2023**, *10*(1), 014011.
3. T. Zhang, C. E. Shuck, K Shevchuk, M Anayee Y. Gogotsi, Synthesis of Three Families of Titanium Carbonitride MXenes, *JACS,* under review.
4. M. Han, K. Maleski, C. E. Shuck, Y. Yang, J. T. Glazar, A. C. Foucher, K. Hantanasirisakul, A. Sarycheva, N. C. Frey, S. J. May, V. B. Shenoy, E. A. Stach, Y. Gogotsi. Tailoring Electronic and Optical Properties of MXenes through Forming Solid Solutions. *J. Am. Chem. Soc*., **2020**, 142, 19110-19118.
5. K. Hantanasirisakul, M. Alhabeb, A. Lipatov, K. Maleski, B. Anasori, P. Salles, C. Ieosakulrat, P. Pakawatpanurut, A. Sinitskii, S. J. May, Y. Gogotsi. Effects of Synthesis and Processing on Optoelectronic Properties of Titanium Carbonitride MXene. *Chem. Mater*., **2019**, 31, 2941.
6. Han, M. K.; Shuck, C. E.; Rakhmanov, R.; Parchment, D.; Anasori, B.; Koo, C. M.; Friedman, G.; Gogotsi, Y., Beyond $Ti_3C_2T_x$: MXenes for Electromagnetic Interference Shielding, *ACS Nano*, **2020**, 14 (4), 5008-5016.

Publications

1. Y. Yang, C. E. Shuck, M. Han, R. Sah, A. Gray, Y. Gogotsi, S. J. May, Correlating electronic properties with M-site composition in solid solution $(Ti_yNb_{1-y})_2CT_x$ MXenes, *2D Materials*, **2023**, *10*(1), 014011.
2. P. Derek, M. Shekhirev, C. Dai, P. Kim, K. Wang, P. Ashby, B.A. Helms, Y. Gogotsi, T. P. Russell, and A. Zettl. All-Liquid Reconfigurable Electronics Using Jammed MXene Interfaces. *Advanced Materials*, **2023**, *35*(13), 2208148.
3. M. Han, C. E. Shuck, A. Singh, Y. Yang, A. C. Foucher, A. Goad, B. McBride, S. J. May, V. B. Shenoy, E. A. Stach, and Y. Gogotsi, Electromagnetic Wave Absorption and Shielding with $V_{n+1}C_nT_x$ MXenes, *Cell Reports Physical Science*, **2022**, *3*(10), 101073.
4. B. Anasori, Y. Gogotsi, (2022). MXenes: Trends, growth, and future directions, *Graphene and 2D Materials*, **2022**, *7*, 75-79.
5. P. P. Michałowski 1 , M. Anayee , T.S. Mathis, S. Kozdra , A. Wójcik , K. Hantanasirisakul, I. Jóźwik , A. Piątkowska, M. Możdżonek , A. Malinowska , R. Diduszko, E. Wierzbicka and Y. Gogotsi . Oxycarbide MXenes and MAX phases identification using monoatomic layer-by-layer analysis with ultralow-energy secondary-ion mass spectrometry. *Nature Nanotechnology*, **2022**, *17*(11), 1192-1197.
6. T. Zhang, C. E. Shuck, K Shevchuk, M Anayee Y. Gogotsi, Synthesis of Three Families of Titanium Carbonitride MXenes, *JACS,* under review.
7. Y. Yang, M. Anayee, A. Pattammattel, M. Shekhirev, R. Wang, X, Huang, Y. Chu, Y. Gogotsi, S. J. May, Enhanced magnetic susceptibility in $Ti_3C_2T_x$ via Co and Ni incorporation, *in preparation*.

Elucidating and Controlling Ion Mobility at the Nanoscale in Block Polymer Electrolytes - Joint Experiment and Modeling Effort in Manipulating Ion Conduction

Prof. Lisa M. Hall (The Ohio State University) and Prof. Thomas H. Epps, III (University of Delaware)

Keywords: Polymer electrolytes, Block polymers, Ion mobility, Molecular Dynamics simulations, Polymer blends

Research Scope

As proposed, we study the links between macromolecular chemistry and architecture, nanostructure assembly, small molecule distributions in nanoscale domains, chain motion, and ultimate transport properties in nanostructured electrolytes. Work highlighted here primarily focuses on Aim 3: Probing the effect of interfacial profiles, interfacial polymer chain conformations, dielectric constant, and glass transition temperatures (T_gs) on relative ion mobility and overall molecular transport in ion-conducting BPs. In particular, we have recently compared density profiles, local ion association, and local and overall ion mobility in coarse-grained models of salt-doped versus single-ion block polymers, which will be highlighted. Experimental results and ongoing work to better map simulations to experiments also will be discussed.

Recent Progress

Single-ion polymer architectures (polymers with one of the ion types covalently bonded to the chains, leaving only one ion type free) are of interest to increase the lithium-ion transference number in polymer electrolytes.[1-5] We used coarse-grained models to compare single-ion and salt-doped block polymer electrolytes in a controlled fashion, with no chemical differences between the two architectures other than the tethering of anions. Specifically, building on model development from prior years,[6-9] we simulated lamellae-forming diblock copolymeric systems with anions free or bound to one of the copolymer types at random points, and we investigated how this tethering impacts ion structural and dynamical properties at different ion concentrations and polymer dielectric constants. We found that tethering anions to the polymer backbone can improve cation conductivity in comparison to analogous salt-doped systems, especially at moderate ion concentrations. These differences in ion dynamics can be related to the structural dispersion of ions and other structural properties, which provides some insight into general features of ions dynamics in mesostructured polymer electrolytes.

Across the several concentrations and dielectric constants (ε_r) studied, the distribution of the polymer beads within the lamellar structure was similar between systems with or without anion tethering; however, tethering more significantly impacted the distribution of ions within the lamellar domains as shown in **Figure 1**. Tethering anions (creating single-ion systems) leads to a more uniform distribution of ions within the conducting domain (on a relative basis) and leads to a slightly higher amount of ions near the interface between the conducting and non-conducting phases.

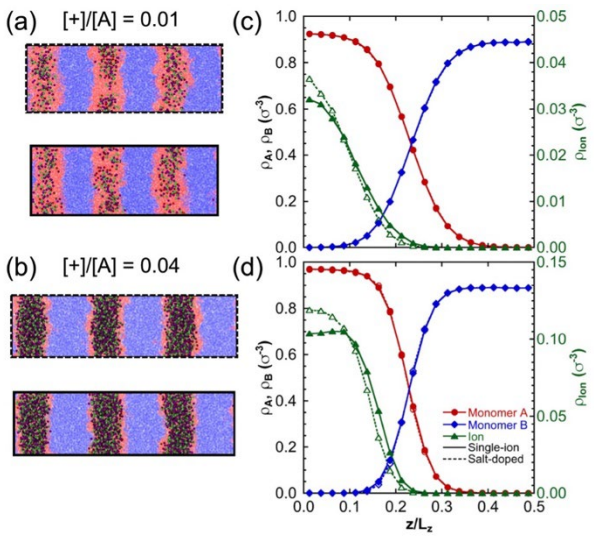

Figure 1. Reproduced from [10]. Snapshots and density profiles: (a) and (c) at [+]/[A] = 0.01 and (b) and (d) at [+]/[A] = 0.04, all at ε_r = 7.5. Top snapshots are for salt-doped and bottom are for single-ion systems, with monomers A, monomers B, cations, and anions colored transparent red, transparent blue, green, and purple, respectively. Density profiles for ions and monomers as labeled are plotted as a function of fractional distance across the half-lamellar domain; for both monomer type densities, the salt-doped and single-ion curves are overlapping.

Tethering also had a significant impact on cation dynamics. **Figure 2** shows the cation mobility for various systems studied; at high ion concentration or high ε_r, mobility increases with ion concentration and is relatively similar between the single-ion and salt-doped systems. However, at both low ion concentration and low enough ε_r, cation and anion motion becomes more correlated, reducing cation mobility. In this regime, single-ion systems have increased cation mobility versus the analogous salt-doped systems, presumably due to their more even distribution of ions.

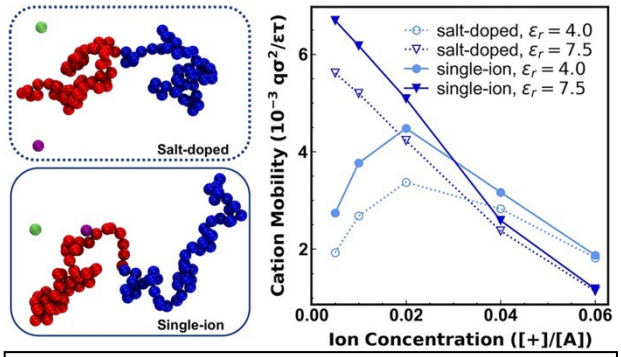

Figure 2. Reproduced from [10]. (left) Schematic of example salt-doped and single-ion polymer chains. (right) Cation mobility as a function of ion concentration for single-ion and salt-doped systems at various dielectric constants.

In ongoing work, we have included additional features in the coarse-grained models, such as polarizability, stiffness, adjusted Tg, and a comb-like architecture to match certain experimental systems of interest. Efforts in these areas allow us to more closely reproduce local dynamical features throughout the domain for better comparison with experimental results.

References

1. S. Zhao, Y. Zhang, H. Pham, J. M. Carrillo, B. G. Sumpter, J. Nanda, N. J. Dudney, T. Saito, A. P. Sokolov, and P. F. Cao, *Improved single-ion conductivity of polymer electrolyte via accelerated segmental dynamics*, ACS Applied Energy Materials **3(12)**, 12540 (2020).
2. S. Inceoglu, A. A. Rojas, D. Devaux, X. C. Chen, G. M. Stone, and N. P. Balsara, *Morphology–conductivity relationship of single-ion-conducting block copolymer electrolytes for lithium batteries*, ACS Macro Letters **3(6)**, 51 (2014).
3. E. I. Lozinskaya, D. O. Ponkratov, I. A. Malyshkina, P. Grysan, G. Lingua, C. Gerbaldi, A. S. Shaplov, and Y. S. Vygodskii, *Self-assembly of Li single-ion-conducting block copolymers for improved conductivity and viscoelastic properties*, Electrochimica Acta **413**, 140126 (2022).
4. P. Dreier, A, Pipertzis, M, Spyridakou, R. Mathes, G. Floudas, and H. Frey, *Introduction of Trifluoromethanesulfonamide Groups in Poly (ethylene oxide): Ionic Conductivity of Single-Ion-Conducting Block Copolymer Electrolytes,* Macromolecules **55(4)**, 1342 (2022).
5. J. Liu, P. D. Pickett, B. Park, S. P. Upadhyay, S. V. Orski, and J. L. Schaefer, *Non-solvating, side-chain polymer electrolytes as lithium single-ion conductors: synthesis and ion transport characterization*, Polymer Chemistry **11(2)**, 461 (2020).
6. J. R. Brown, Y. Seo, and L. M. Hall, *Ion Correlation Effects in Salt-Doped Block Copolymers*, Physical Review Letters **120(12)**, 127801 (2018).
7. Y. Seo, K.-H. Shen, J. R. Brown, and L. M. Hall, *Role of solvation on diffusion of ions in diblock copolymers: understanding the molecular weight effect through modeling,* Journal of the American Chemical Society **141**, 18455 (2019).
8. K.-H. Shen and L. M. Hall, *Effects of Ion Size and Dielectric Constant on Ion Transport and Transference Number in Polymer Electrolytes,* Macromolecules **53(22)**, 10086 (2020).
9. K.-H. Shen and L. M. Hall, *Ion Conductivity and Correlations in Model Salt-Doped Polymers: Effects of Interaction Strength and Concentration,* Macromolecules **53(10)**, 3655 (2020).
10. M. Fan, K.-H. Shen, and L. M. Hall, *Effect of Tethering Anions in Block Copolymer Electrolytes via Molecular Dynamics Simulations*, Macromolecules **55(17)**, 7945 (2022).

Publications

1. P. M. Ketkar, N. F. Pietra, A. G. Korovich, L. A. Madsen, and T. H. Epps III, *Role of intra-domain heterogeneity on ion and polymer dynamics in block copolymer electrolytes: An approach for spatially resolving dynamics and ion transport* Macromolecules, in review (2023).
2. N. F. Pietra, A. G. Korovich, L. A. Madsen, P. M. Ketkar, and T. H. Epps III, *Role of intra-domain heterogeneity on ion and polymer dynamics in block copolymer electrolytes: Investigating interfacial mobility and ion-specific dynamics and transport* Macromolecules, in review (2023).
3. M. Fan, K.-H. Shen, and L. M. Hall, *Effect of Tethering Anions in Block Copolymer Electrolytes via Molecular Dynamics Simulations*, Macromolecules **55(17)**, 7945 (2022).
4. P. M. Ketkar and T. H. Epps III, *Nanostructured block polymer electrolytes: tailoring self-assembly- to unlock the potential in lithium-ion batteries* Accounts of Chemical Research **54(23)**, 4342 (2021).
5. P. M. Ketkar, K.-H. Shen, M. Fan, L. M. Hall, and T. H. Epps III, *Quantifying the effects of monomer segment distributions on ion transport in tapered block polymer electrolytes* Macromolecules **54(16)**, 7590 (2021).

Autoxidation Mechanisms and Methods for Plastic Upcycling

PI: Ive Hermans[a]

CoPIs: Shannon Stahl, Megan Robertson, Ramanan Krishnamoorti, Sanat Kumar, Linda Broadbelt

[a] University of Wisconsin-Madison ; [b] University of Houston ; [c] Columbia University ;

[d] Northwestern University

Keywords polyolefins, oxyfunctionalization, mechanisms, chemicals, polyurethane

Research Scope

Our research interrogates and designs new methods for aerobic oxygenation of polyolefins (POs) to achieve two related goals: (1) convert mixed plastics waste into low molecular weight (MW) feedstock chemicals with high yield and selectivity and (2) prepare new polymeric materials with favorable properties. The upcycling and conversion of waste plastics within a circular carbon economy is a grand challenge. Major advantages of autoxidation methods include: (a) it is thermodynamically favorable, resulting in significant energy savings and reduced CO_2 footprint relative to pyrolysis; (b) autoxidation-based PO depolymerization is compatible with mixed plastics, minimizing or avoiding the need for pre-sorting; (c) it tolerates impurities, contaminants, and water; (d) homogeneous autoxidation catalysts offer transport kinetic advantages over heterogeneous catalysts for polymer deconstruction; and (e) catalysts and initiators that support autoxidation are composed of robust, earth-abundant, recyclable materials.[1-4]

Recent Progress

Research Aim 1: An overarching theme of this research thrust is to leverage the fundamental study of the autoxidation of PO chemical analogs including cyclohexane, cumene, *n*-decane, among others, to glean molecular insights that could inform the development of autoxidation methods for the upcycling of complex mixtures of polyolefins. Towards this end, a Taylor flow microreactor has been constructed to accurately measure the intrinsic kinetics of the autoxidation of polyolefin chemical analogs (UW-Madison). Initially, the kinetics profiles of the autoxidation of cyclohexane were collected at several temperatures. The obtained kinetics profiles are used for the development and refinement of initial microkinetic models (Northwestern University). To ensure that the modeling framework is functional and a working model can be used to calibrate the development of the more user-friendly software platform, Pickaxe, the automated mechanism generation software (NETGEN) has been deployed to replicate the results of the oxidation of *n*-decane and octane.[5] The reaction families have been

successfully tested, and unit testing aimed at ensuring that the rate-based algorithm used to generate the results obtained underway.

Research Aim 2: An overarching theme of this research thrust is the direct oxyfuctionalization of POs (i.e., isotactic polypropylene (iPP) and high-density polyethylene (HDPE)) to afford polymeric materials with favorable physical and mechanical properties (U. of Houston) as well as further conversion to value-added thermoset polymer (e.g., polyurethanes) (Columbia University). The oxidation of the iPP and HDPE was conducted with a co-rotating twin screw extruder under a constant flow of diluted oxygen in nitrogen. Following melt processing, FTIR revealed carbonyl groups and hydroxyl groups in both the oxidized iPP and HDPE and the presence of unsaturated moieties (C=C double bonds) in the oxidized iPP. NMR was used to further confirm the structures of the oxidized polymers. To prepare oxidized iPP and HDPE with higher degree of functionality, organic radical initiators were employed to accelerate the oxidation process and the impact of processing parameters on the functionalization process was explored. Furthermore, the partial oxidation of POs through oven oxidation is being explored, while characterizing the functionalization and studying its relationship with respect to processing parameters (Columbia University). Likewise, to the oxidative iPP melting processing (University of Houston), FTIR revealed iPP can be functionalized with carbonyl and hydroxyl groups along their main chain through oven oxidation. The degree of oxidation of the polymers can be controlled through variation in the oxidation environment such as temperature and reaction time.

Research Aim 3: The production of phenol from the oxidative deconstruction of polystyrene (PS) was explored (UW-Madison). Initial findings suggest deconstruction of PS proceeds via chain scission to form oligomers that are prone to oxyfunctionalization, and subsequent acid-treatment of oligomers can form phenol via Hock rearrangement. A thorough theoretical and experimental mechanistic investigation is underway. Furthermore, to afford mild reaction conditions, the photocatalyzed aerobic oxidation of polyethylene was investigated using quinones, acting as efficient photosensitizers and HAT mediators, and multiple wavelengths of light from LED arrays. The next objective is to enhance oxygen diffusion and mass transport to facilitate the efficient trapping of alkyl radicals formed from the C-H activation process to minimize cross-linking and improve oxyfunctionalization.

Conclusions: We present several strategies for the direct oxyfunctionalization and deconstruction of POs to value-added oxygenates. For example, we demonstrate phenol can be directly produced from PS. Furthermore, using strategic PO chemical analogs for the development of microkinetic models provide important mechanistic and molecular insights into C-H activation and oxyfunctionalization of aliphatic and aromatic hydrocarbons that will further inform the development of robust autoxidation methods for the deconstruction of POs.

References

1. Pifer, A.; Sen, A. *Chemical Recycling of Plastics to Useful Organic Compounds by Oxidative Degradation*. Angew. Chem. Int. Ed. 37, 3306-3308 (1998).
2. Remias, J.E.; Pavlosky, T. A.; Sen, A. *Oxidative Chemical Recycling of Polyethylene*. Comptes Rendus de l'Académie des Sciences – Series IIC – Chemistry, 3, 627-629 (2000).
3. Partenhemier, W. *Valuable Oxygenates by Aerobic Oxidation of Polymers Using Metal/Bromide Homogeneous Catalysts*. Catal. Today, 81, 117-135 (2003).
4. Backstrom, E.; Odelius, K.; Hakkarainen, M. *Trash to Treasure: Microwave-Assisted Conversion of Polyethylene to Functional Chemical*. Industrial & Engineering Chemistry Research, 56, 14814-14821 (2017).
5. Pfaendtner, J.; Broadbelt, L. J. *Mechanistic Modeling of Lubricant Degradation 2. The Autoxidation of Decane and Octane.* Industrial & Engineering Chemistry Research, 47, 2897-2904 (2008).

Publications

N/A

Porous, Lightweight, and Semiconducting Chalcogel as High Energy Density Electrode for Lithium-ion and Sodium-ion Batteries

PI: Dr. M. Saiful Islam, Dr. Misganaw Weret, and Taohedul Islam

Department of Chemistry, Physics, and Atmospheric Sciences, Jackson State University, Jackson, MS-39217, USA

Co-PI: Dr. Chad Risko, Keerthan Raghavendra Rao, and Sahar Bayat

Department of Chemistry, University of Kentucky ,125 Chemistry/Physics Building, Lexington KY 40506-0055;

Collaborators: Dr. Ruhul Amin, Electrification & Energy Infrastructure Division, Oak Ridge National Laboratory, Oak Ridge, TN-37831, USA; Kamila M. Wiaderek, Argonne National Laboratory, Lemont, IL 60439

Keywords: chalcogel, chalcocarbogel, Li-S/Na-S batteries, high capacity, and cyclic stable

Research Scope

Chalcogel is a unique class of porous amorphous metal-sulfides that consist of aggregated colloidal particles whose structural backbone, in most cases, is formed by polysulfides, and the surface of the nanoparticles are covered with a high density of (poly)sulfide species.[1–3] We hypothesize that high (poly)sulfide desity can lead to high energy density for conversion based Na(Li)-ion batteries, and the chalcogel's porosities, semiconductivity, amorphicity, and compositional diversity can offer additional advantages including faster ion kinetics, higher electrical conductivity, lower activation energy barriers during the structural rearrangements, and resistance to large volume change during the charge-discharge process. We also hypothesize that an integration of colloidal sized particle with carbonaceous species (e.g., graphene oxides (GO) and carbon nanotube (CNT)) with the chalcogenide will results in the formation of nanocomposite gels, which will attribute to superior electrical conductivity, specific capacity and decrease polysulfide dissolution. This

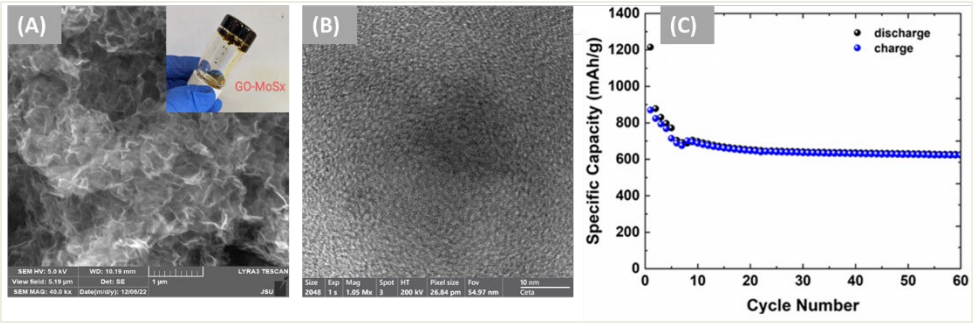

Figure 1: SEM image of the MoS_x-GO chalcocarbogel (A), inset showing the RT synthesized monolith wetgel; HRTEM showing the amorphous features of the gel particles (B); charge/discharge properties vs cyclic stability for Li ion batteries (C).

synergy of the chalcogels and carbonaceous species in the hybrid chalcocarbogels will allow us to develop high-energy desity, cycle stable, safer, cost-effective anode materials for sodium- and lithium-sulfide batteries (NaSBs and LiSBs).

Here, we introduce a new class of hybrid aerogel that integrates inorganic metal sulfide and carbonaceous species, for instance, molybdenum sulfides (MoS_4^{2-}) and graphene oxide (GO). We named them chalcocarbogels because these consist of chalcogenides and carbonaceous species. The monolith wetgel of the chalcocarbogel was synthesized at room temperature (RT) from a mixture of a solution of (MoS_4^{2-}) and highly dispersed nanoparticles of graphene oxide (GO). The MoS_x-GO chalcocarbogel is amorphous and its local structure consists of Mo_3S_{13} species as determined by synchrotron X-ray diffraction. The electrochemical charge-discharge of the MoS_x-GO xerogel reveals the initial discharge capacity of 1215 mAh g^{-1} for Li-ion half-cell and 807 mAh g^{-1} for Na-ion half-cell. Importantly, the lithium-ion half-cell retains the capacity 700 mAh g^{-1} and sodium-ion half-cell exhibits a reversible capacity of 473 mAh g^{-1} after 50 cycles. Finally, the solution processable and scalable RT synthesis of the MoS_x-GO chalcocarbogel, high electrochemical, high-energy density and superior rate performance reveal this new class of materials as promising electrode materials for Na- and Li-ion batteries for grid-scale energy storage.

Recent Progress

For high-capacity energy storage, lithium–sulfur (Li–S) batteries are considered the most promising candidate because of their high theoretical specific capacity, 1672 mAh/g.[4,5] But, the progress of this field is bottlenecked with several issues including cyclic stability. Previously, we introduced metal sulfide chalcogel (MoS_x) as sulfur equivalent electrodes that exhibits superior cyclic stability over sulfur electrodes.[6] Despite the great promise of chalcogel electrode materials, this technology is challenged by poor electron and ion kinetics, polysulfide shuttling, dendrite formation, large volume changes, loss of active materials and safety issues. Our recently, developed Chalcocargels of MoS_x-GO offers a new paradigm of sulfur based electrodes that exhibit remarkably high specific capacity and cyclic stability and thus show great potential to dominate the next generation electrodes for both Na and Li ion batteries.

References

1. J. Staszak-Jirkovský, C. D. Malliakas, P. P. Lopes, N. Danilovic, S. S. Kota, K.-C. Chang, B. Genorio, D. Strmcnik, V. R. Stamenkovic, M. G. Kanatzidis, N. M. Markovic, Design of active and stable Co–Mo–Sx chalcogels as pH-universal catalysts for the hydrogen evolution reaction *Nature Mater* **2016**, *15*, 197.
2. S. Bag, I. U. Arachchige, M. G. Kanatzidis, Aerogels from metal chalcogenides and their emerging unique properties *J. Mater. Chem.* **2008**, *18*, 3628.
3. S. Bag, P. N. Trikalitis, P. J. Chupas, G. S. Armatas, M. G. Kanatzidis, Porous Semiconducting Gels and Aerogels from Chalcogenide Clusters. Science, *Science* **2007**, *317*, 490.
4. Y. Son, J.-S. Lee, Y. Son, J.-H. Jang, J. Cho, Recent Advances in Lithium Sulfide Cathode Materials and Their Use in Lithium Sulfur Batteries *Advanced Energy Materials* **2015**, *5*, 1500110.
5. A. Manthiram, Materials Challenges and Opportunities of Lithium Ion Batteries. *J. Phys. Chem. Lett.* **2011**, *2*, 176.
6. V. V. T. Doan-Nguyen, K. S. Subrahmanyam, M. M. Butala, J. A. Gerbec, S. M. Islam, K. N. Kanipe, C. E. Wilson, M. Balasubramanian, K. M. Wiaderek, O. J. Borkiewicz, K. W. Chapman, P. J. Chupas, M.

Moskovits, B. S. Dunn, M. G. Kanatzidis, R. Seshadri, Molybdenum Polysulfide Chalcogels as High-Capacity, Anion-Redox-Driven Electrode Materials for Li-Ion Batteries *Chem. Mater.* **2016**, *28*, 8357.

Understanding Structure, Phase Behavior, and Physical Properties of Polysulfamides and Polysulfamates using Simulations, Experiments, and Machine Learning

PI: Arthi Jayaraman (University of Delaware), co-PIs: Quentin Michaudel (Texas A&M) and Ryan Hayward (University of Colorado, Boulder)

Keywords: Polysulfamides, Simulations, Machine Learning, Semi-crystalline, Characterization

Research Scope

This project aims to understand the structure, bulk phase behavior, and physical properties of a new family of polymers — polysulfamides and polysulfamates — with potential as chemically recyclable and high-performance materials. This is being accomplished using synergistic experimental and computational approaches involving polymer synthesis, structural and thermal characterization, molecular modeling, simulations, and machine learning. This project leverages our expertise and recent advances in SuFEx click polymerization, (Michaudel)[1, 2] development and use of coarse-grained polymer models for macromolecules with H-bonding interactions, (Jayaraman)[3, 4] machine learning for structural characterization, (Jayaraman)[5, 6] and solution and solid-state characterization of polymeric materials, including H-bonding systems (Hayward) to obtain a fundamental understanding on this new class of polymers.
The specific aims are: *Specific Aim 1:* To understand hydrogen-bonding driven structural ordering of polysulfamides as a function of the molecular structure of the repeat unit.
Specific Aim 2: To develop machine learning models to automate the classification and interpretation of structural characterization results.
Specific Aim 3: To extend the fundamental studies of molecular interactions and chain structure, physical properties, and bulk phase behavior to polysulfamates.

Recent Progress

During this 1st year of this project, synthesis (Michaudel), characterization (Hayward), and computational (Jayaraman) tasks under the three aims have been initiated.

In the Michaudel lab, Jiun Wei Wu (5th year PhD student) and Avinash Choudhury (1st year PhD student) have been working on the development of robust syntheses of polysulfamides based on Sulfur(VI) Fluoride Exchange (SuFEx) click chemistry[7, 8] and conducting characterization via NMR and IR spectroscopy, size-exclusion chromatography (SEC), and powder X-ray diffraction. Thus far, over 30 structurally different polysulfamides have been synthesized and fully characterized. Simultaneously, in the Jayaraman lab, Zijie Wu (5th year PhD student) and Jay Shah (1st year PhD student) have been working on development and use of a coarse-grained (CG) model of polysulfamide to link polysulfamide design to the assembled chains' orientational and

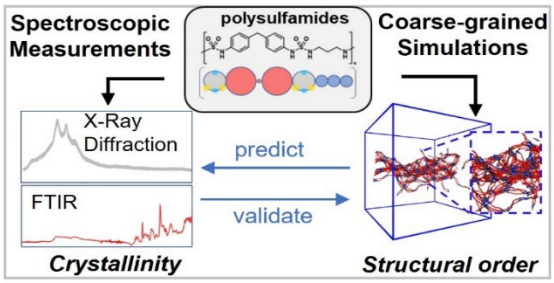

Figure: "Investigating hydrogen bond-induced self-assembly of polysulfamides using molecuzzzlar simulations and experiments", Wu, Zijie; Wu, Jiun Wei; Michaudel, Quentin; Jayaraman, Arthi (Macromolecules) accepted.zz

positional order in CG molecular dynamics (MD) simulations. CG MD simulation results have been validated through comparison with experiments; this comparison is the focus of our 1st joint publication[9] that has been accepted in *Macromolecules* in June 2023 (see Figure).

In Jayaraman lab, Shizhao Lu (4th year PhD student) has developed a machine learning (ML) approach called 'PairVAE'[10] tailored towards generation of bottleneck characterization data of materials from complementary high throughput characterization data through paired learning of two variational autoencoders (VAE). Lu used open access data sets from small angle X-ray scattering (SAXS) and scanning electron microscopy (SEM) measurements of block copolymers from a recent publication[11]. Using that data Lu trained the PairVAE to successfully predict SEM images for a given SAXS profile or a SAXS profile for a given SEM image.

The above PairVAE method from the Jayaraman lab is now being extended to characterization data from the Michaudel and Hayward labs to enable quantitative prediction of crystallinity from analogous structural characterization data. First, the Hayward lab is collecting paired structural characterization data on polymer films that, like polysulfamide, exhibit semi-crystalline morphologies, but for which parameters including the crystal structure and enthalpy of melting are well-characterized. Specifically, to serve as training data for PairVAE, Matthew Ticknor (4th year PhD student) has been generating data sets that combine multiple different characterization modalities applied to the same set of materials with systematically varying structure (e.g., degree of crystallinity) achieved through variations in thermal history and stereochemical composition. Since polysulfamides have not yet been structurally characterized in detail, we have begun with poly(L-lactic acid) (PLLA) as a simpler and more well-studied model system to validate our methodology. Simultaneously over 40 different *N,N'*-disubstituted sulfamides are being synthesized by members of the Michaudel lab and will be sent to the Hayward lab for characterization to create a polysulfamide focused structural characterization dataset for training the PairVAE. We believe PairVAE will also be valuable to the broader materials chemistry community who can use cross-reconstruction of complementary characterization data to foster more ways of generating data for design-structure-property relationships that accelerate materials design and innovation.

References

1. R. W. Kulow, J. W. Wu, C. Kim and Q. Michaudel, *Synthesis of unsymmetrical sulfamides and polysulfamides via SuFEx click chemistry*. Chemical Science **11**, 7807-7812 (2020).
2. J. W. Wu, R. W. Kulow, M. J. Redding, A. J. Fine, S. M. Grayson and Q. Michaudel, *Synthesis of Degradable Polysulfamides via Sulfur(VI) Fluoride Exchange Click Polymerization of AB-Type Monomers*. Acs Polymers Au (2023).
3. A. Kulshreshtha, R. C. Hayward and A. Jayaraman, *Impact of Composition and Placement of Hydrogen-Bonding Groups along Polymer Chains on Blend Phase Behavior: Coarse-Grained Molecular Dynamics Simulation Study*. Macromolecules **55**, 2675-2690 (2022).
4. A. Jayaraman, *100th Anniversary of Macromolecular Science Viewpoint: Modeling and Simulation of Macromolecules with Hydrogen Bonds: Challenges, Successes, and Opportunities*. ACS Macro Letters **9**, 656-665 (2020).
5. S. Lu, B. Montz, T. Emrick and A. Jayaraman, *Semi-supervised machine learning workflow for analysis of nanowire morphologies from transmission electron microscopy images*. Digital Discovery **1**, 816-833 (2022).
6. C. M. Heil, A. Patil, A. Dhinojwala and A. Jayaraman, *Computational Reverse-Engineering Analysis for Scattering Experiments (CREASE) with Machine Learning Enhancement to Determine Structure of Nanoparticle Mixtures and Solutions*. Acs Central Science **8**, 996-1007 (2022).
7. J. Dong, L. Krasnova, M. G. Finn and K. B. Sharpless, *Sulfur(VI) Fluoride Exchange (SuFEx): Another Good Reaction for Click Chemistry*. Angewandte Chemie International Edition **53**, 9430–9448 (2014).
8. A. S. Barrow, C. J. Smedley, Q. Zheng, S. Li, J. Dong and J. E. Moses, *The growing applications of SuFEx click chemistry*. Chemical Society Reviews **48**, 4731–4758 (2019).
9. Z. Wu, J. Wu, Q. Michaudel and A. Jayaraman, *Investigating hydrogen bond-induced self-assembly of polysulfamides using molecular simulations and experiments*. Macromolecules (accepted).
10. S. Lu and A. Jayaraman, *Pair-Variational Autoencoders (PairVAE) for Linking and Cross-Reconstruction of Characterization Data from Complementary Structural Characterization Techniques*. JACS Au (under review).
11. G. S. Doerk, A. Stein, S. Bae, M. M. Noack, M. Fukuto and K. G. Yager, *Autonomous discovery of emergent morphologies in directed self-assembly of block copolymer blends*. Science Advances **9** (2023).

Publications

1. S. Lu, A. Jayaraman*, Pair-Variational Autoencoders (PairVAE) for Linking and Cross-Reconstruction of Characterization Data from Complementary Structural Characterization Techniques*, JACS Au (under review)* https://arxiv.org/abs/2305.16467
2. J. Ju, A. Jayaraman, R. Hayward*, Temperature-Sensitive Micro- and Macro-phase Separation of Hydrogen-Bonded Polystyrene-Polydimethylsiloxane Blends, *Macromolecules (accepted)*
3. Z. Wu, J. Wu, Q. Michaudel*, A. Jayaraman*, Investigating hydrogen bond-induced self-assembly of polysulfamides using molecular simulations and experiments, *Macromolecules (accepted)*

Understanding the Interfaces for High-Energy Batteries using Anions as Charge Carriers

Xiulei "David" Ji (PI), Oregon State University, De-en Jiang, Vanderbilt University, Chunsheng Wang, University of Maryland, Quinton Williams, Howard University

Keywords: Anions, Transport, Interfaces, Cathode, Conversion

Research Scope

There is a pressing need to invent an alternative rechargeable battery chemistry that does not involve depleting elements and potentially provides a higher energy density. In Li-ion batteries (LIBs) and other cation battery chemistry such as Na-ion, Mg-ion, and Zn-ion, the working ions are the cations. Anion hosting can serve to enable reactions in batteries as well but is yet to receive much attention.[1] The anion-storage batteries will potentially shift the paradigm of the LIB industry. Such batteries can be more sustainable solutions for high-energy batteries because they do not need Co or Ni in the electrodes. Recent results from the PIs show that anion-storage batteries can deliver competitive energy density with cost-effective carbon or metals as the electrodes.[2,3,4] The goal of the project is to reveal the mechanisms and gain an understanding of the limiting factors in new anion battery reactions and to generate fundamental knowledge about under what conditions and with what battery constituents anion-hosting batteries can deliver high energy density with a stable cycling life. The PIs with their synergistic set of expertise will gain the predicative knowledge of anion-hosting reactions by novel materials science, electrochemical experiments, advanced characterization, and first principles simulations. In particular, the project will investigate quintessential electrode systems for hosting anions via intercalation, plating, and conversion reactions. A primary outcome is that we will identify critical descriptors to predict electrochemical behaviors and the performance of anion storage electrode systems. This predictive capability will greatly promote research interest among the community to explore anion storage. The project investigates Li-salt-composite (LSC) cathodes *that comprises a lithium salt as the source of anions and Li-ions and an oxidizable structure to host anions.*[1] The LSC cathodes are different from the cathodes in dual-ion batteries (DIBs) in that the latter gleans anions from the electrolyte during charging.[5]

The project will answer the following fundamental questions. *How do the charges of anions transport through the lattice of metal salts? What factors affect the kinetics and utilization of the anion-hosting reactions? What chemical environment of electrodes and electrolytes stabilizes their interphase? What are the limiting factors that regulate the anodic reactions of metals and non-metals in the defined chemical environments?* The project will integrate experimental design, first principles modeling, and machine learning. The new knowledge about anion storage will generate broad and profound impacts across the science and engineering disciplines of

chemistry, physics, and materials science. The new LSC batteries may re-invent LIBs in providing more sustainable energy-storage solutions.

Recent Progress

The project has made some significant progress in the proposed research area. Multiple manuscripts are under preparation. (1) We found that it is viable to use a mixture of a metal and lithium salt(s) as the starting electrodes for a rocking-chair battery. Such an electrode can be paired with conventional anode materials, including graphite and silicon; therefore, the fundamental knowledge we gain here can directly translate to practical impacts. We have explored the mixture of metal powder with different lithium salts, including LiF, LiOH, Li_2CO_3, Li_2SO_4, and Li_3PO_4. We found that the choice of salts can have a large impact on the resulting capacity, where one of our electrode formulas offers a stable cycle life and a reversible specific capacity of nearly 300 mAh/g with an average operation potential of 2.8 V vs. Li. The reversible energy density of this cathode is over 800 Wh/kg, comparable to the state-of-the-art $LiNi_xMn_yCo_zO_2$ (NMC) and $LiNi_xCo_yAl_zO_2$ (NCA) cathode systems.[6] The results support the hypothesis that solid anion diffusion can charge-compensate for the reversible corrosion reactions of metals in battery settings. We are testing the hypothesis that the enhanced anion transport properties enable better utilization of the electrodes, where the promoted kinetic properties allow the thermodynamic possibility to be realized. We also discovered that non-metals, including halogens, can be oxidized to host anions. Non-metals have been widely investigated for their cathodic redox properties in hosting alkali metal ions. In this project, we pushed the envelope of non-metal redox chemistry to the anodic side. We found that suitable electrolytes are critical to enabling the new anion-hosting electrochemical reactions. For the metal-based electrode, it is known that iron exhibits a certain extent of catalytic properties. Our initial reactions found that inhibiting iron's catalytic behavior is necessary by growing cathode electrolyte interphase (CEI) layers, where electrolyte additives are indispensable.

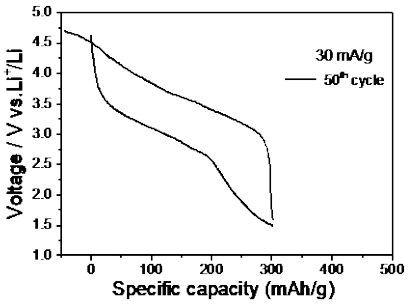

Typical charge-discharge potential profiles of a metal-based LSC cathode.

Combining density functional theory, *ab initio* molecular dynamics, and machine learning potentials to simulate ion diffusivity, we found that glassy materials such as $LiTaCl_6$ have high mobilities for cations (Li^+) and anions (Cl^-). The simulated Li-ion conductivity of 20 $mS \cdot cm^{-1}$ at room temperature and the simulated diffusion barrier of 0.16 eV for Li-ion agree well with the experiment. More important, the barrier of Cl^- diffusion (at 0.15 eV) is comparable to that of Li^+, indicating a new mechanism of superionic transport whereby superionic anion transport accelerates superionic cation transport. Hence, these materials offer important clues regarding the ion mobilities which can facilitate anion transport and storage.

References

1. Z. Huang, X. Li, Z. Chen, P. Li, X. Ji, C. Zhi, Anion Chemistry in Energy Storage. *Nature Reviews Chemistry* https://doi.org/10.1038/s41570-023-00506-w (2023)
2. C. Yang, J. Chen, X. Ji, T. P. Pollard, X. Lü, C. J. Sun, S. Hou, Q. Liu, C. Liu, T. Qing, Y. Wang, O. Borodin, Y. Ren, K. Xu, C. Wang, Aqueous Li-Ion Battery Enabled by Halogen Conversion–Intercalation Chemistry in Graphite. *Nature* **569***,* 245-250 (2019).
3. M. Yu**, Y. Sui, S**. K. Sandstrom, C.-Y. Wu, H. Yang, W. Stickle, W. Luo, X. Ji, Reversible Copper Cathode for Nonaqueous Dual-Ion Batteries. *Angew. Chem. Inter. Ed.* **61**, e202212191 (2022)
4. T. C. Gallagher, C.-Y. Wu, M. Lucero, S. K. Sandstrom, L. Hagglund, H. Jiang, W. Stickle, Z. Feng, X. Ji, From Copper to Basic Copper Carbonate: A Reversible Conversion Cathode in Aqueous Anion Batteries" *Angew. Chem. Inter. Ed.* **61**, (2022) e202203837 https://doi.org/10.1002/anie.202203837
5. T. Plake, A. Heckmann, R. Schmuch, P. Meister, K. Beltrop, M. Winter, Perspective on Performance, Cost, and Technical Challenges for Practical Dual-Ion Batteries, *Joule*, **2**, 2528, (2018)
6. W. Li, S. Lee, A. Manthiram, High-Nickel NMA: A Cobalt-Free Alternative to NMC and NCA Cathodes for Lithium-Ion Batteries. *Advanced Materials*, **32**, 2002718, (2020)

Publications

We are preparing manuscripts that are supported by this project.

Fundamental Studies of Charge Transfer in Nanoscale Heterostructures of Earth-Abundant Semiconductors for Solar Energy Conversion

Song Jin and John C. Wright (contact PI email: jin@chem.wisc.edu)

Department of Chemistry, University of Wisconsin-Madison, Madison, Wisconsin 53706

Keywords: heterostructures, halide perovskites, carrier dynamics, spectroscopy, ionic diffusion

Research Scope

Hybrid metal halide perovskites are inexpensive semiconductor materials promising for high performance solar cells and light emitting diodes (LEDs) because they are easy to make and tolerant of defects. Fundamental understanding of the factors controlling the carrier transfer mechanisms in heterostructures of halide perovskites is crucial for guiding the synthetic strategies to improve properties and device applications. To address these challenges, our collaborative team synergistically combines expertise in synthesis of new materials and nanoscale heterostructures (Jin) with the development of new ultrafast spectroscopies (Wright) to probe complex heterostructures at the single quantum state level.

Recent Progress

We developed new methods for synthesizing nanostructures of both three-dimensional (3D) perovskites and two-dimensional (2D) Ruddlesden–Popper (RP) layered perovskites, and using them to create novel and arbitrary heterostructures, such as 2D/3D perovskite and vertical and lateral 2D heterostructures, with high quality interface and tunable band alignments. Various structural characterization and time-resolved spectroscopic methods have been employed to collaboratively study the carrier transfer mechanisms between these well-defined heterostructures of 2D and 3D perovskites. Some recent highlights include:

Deterministic Fabrication and Study of Vertical Heterostructures of RP Halide Perovskites
We have developed methods for creating large-area vertical or lateral heterostructures of RP perovskites with the goal of precisely controlling the compositions and the stacking sequence of each layer. We first developed a solution growth method for synthesizing large nanosheets of a variety of phase-pure 2D RP lead halide perovskites (40+) with different LA and A cations, lateral dimensions of up to a few hundred micrometers, and thicknesses down to a monolayer.

Using a soft contact transfer method, these nanosheets can be sequentially transferred and stacked to fabricate vertical heterostructures in a deterministic fashion (see examples in Fig. 1). The self-assembled bilayer of LA cations can act as a natural diffusion barrier to slow down halide migration across the adjacent perovskite layers while maintaining stable and atomically sharp junctions. These advances enabled the deterministic fabrication of arbitrary vertical heterostructures and multi-heterostructures of different RP perovskites with unprecedented structural degrees of freedom that define the electronic structures of the heterojunctions (Fig. 1). These RP perovskite heterostructures will enable the exploration of carrier transfer dynamics and novel exciton physics. For example, we have further made heterostructures with presumed Type II band alignment and preliminarily observed the evidence for interlayer excitons. To expand the design of robust type II heterostructures, we further developed the synthesis of nanosheets for (PEA)2Csn-1PbnBr3n+1 (n = 1-6) phases and studied their basic optical properties and band positions using UPS techniques. We have also made well-defined 2D/3D perovskite heterostructures by stacking nanosheets of various 2D RP perovskites on single crystals of 3D perovskites and are studying the ionic diffusion and carrier transfer in these heterojunctions.

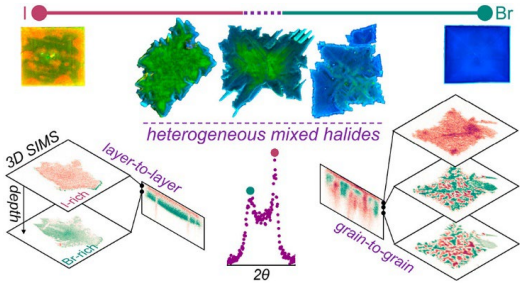

Fig. 2. Heterogeneity within mixed halide 2D RP perovskites revealed by spectral imaging and SIMs.

Lateral Heterostructures and Mixed Halide RP Halide Perovskites

We have synthesized lateral heterostructures of RP halide perovskites via halide anion exchange. Sharp halide lateral heterostructures can be formed from n = 1 and 2 RP lead iodide microplates via anion exchange with hydrogen bromide (HBr) vapor due to the low halide miscibility. Many studies of mixed-halide RPPs assume that halide mixing yields homogeneous alloys like those in 3D lead halide perovskites, with halide segregation only occurring under perturbations from light or heat. We found heterogeneous halide microscale domains in the mixed I/Br phases in solution grown microplates of three representative n = 1 and n = 2 RPP phases using X-ray diffraction and secondary ion mass spectrometry (SIMS) imaging – even in absence of photoinduced phase separation. However, photoluminescence (PL) imaging alone can falsely imply homogeneous alloy formation in heterogeneous RPPs. We then demonstrate the use of spectral imaging as an alternative high-throughput tool for accurate halide phase characterization in mixed-halide RPPs.

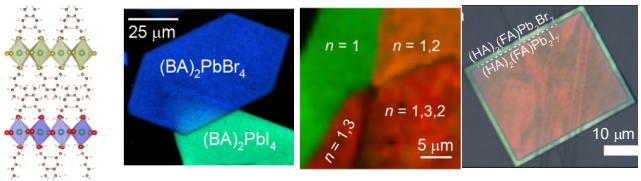

Fig. 1. Various novel vertical heterostructures, multiple hetero-structures and lateral heterostructures of 2D RP perovskites that we have fabricated and studied.

Development of New Multidimensional Spectroscopic Methods for Studying Floquet States. Charge transfer across the junction can involve coherent and incoherent dynamics and it is here that our Floquet state methodologies can spatially resolve the dynamics. Floquet states are quantum mechanical superposition states that directly access couplings between states. They form the basis for directly measuring the structure of the Brillouin zone of a material. Mapping based on Floquet states can then form the basis for observing the changes in the Brillouin zone over an entire heterostructure. Currently, angularly resolved photoelectron spectroscopy (ARPES) is the only method for measuring the Brillouin zone so the promise of an alternative Floquet state method could be a transformative methodology for materials science. We have finished construction of a widefield hyperspectral microscope that images both fully coherent output generated from a single or multiple driving fields, as well as population-based output (transient absorption) and are now doing NIR pump-SHG probe experiments on TMDC monolayers and heterostructures that will resolve the charge transfer dynamics at the interface between two TMDC monolayers. Our experiments have included the creation of Floquet states with two coupled coherences at the same k-vector in the Brillouin zone of a WS2 monolayer using two tunable 50 fs pulses to create 2D fully coherent spectra with double resonances that excite the 3.33 eV band in the Brillouin zone as well as experiments where the couplings between states can result in structural changes that are optically controllable.

References (see the next section)

Two Year List of Publications Supported by BES:

1. Ratté, J.; Macintosh, M. F.; DiLoreto, L.; Liu, J.; Mihalyi-Koch, W.; Hautzinger, M. P.; Guzei, I. A.; Dong, Z.; Jin, S.; Song, Y.: Spacer-Dependent and Pressure-Tuned Structures and Optoelectronic Properties of 2D Hybrid Halide Perovskites. *The Journal of Physical Chemistry Letters* **2023**, *14*, 403-412. DOI: 10.1021/acs.jpclett.2c03555.
2. Roy, C. R., Zhou, Y., Kohler, D. D., Zhu, Z.; Wright, J. C.; Jin, S.; Intrinsic Halide Immiscibility in 2D Mixed-Halide Ruddlesden–Popper Perovskites. *ACS Energy Letters* **2022**, *7*, 3423-3431. DOI: 10.1021/acsenergylett.2c01631.
3. Ci, P.; Zhao, Y.; Sun, M.; Rho, Y.; Chen, Y.; Grigoropoulos, C. P.; Jin, S.; Li, X.; Wu, J.: Breaking Rotational Symmetry in Supertwisted WS2 Spirals via Moiré Magnification of Intrinsic Heterostrain. *Nano Letters* **2022**, *22*, 9027-9035. DOI: 10.1021/acs.nanolett.2c03347.
4. Zhao, Y.; Jin, S.: Stacking and Twisting of Layered Materials Enabled by Screw Dislocations and Non-Euclidean Surfaces. *Acc. Mater. Res.* **2022**, *3*, 369-378. DOI: 10.1021/accountsmr.1c00245
5. Fu, Y.; Jin, S.; Zhu, X. Y.: Stereochemical expression of ns2 electron pairs in metal halide perovskites. *Nature Reviews Chemistry* **2021**, *5*, 838-852. DOI: 10.1038/s41570-021-00335-9.
6. Roy, C. R.; Pan, D.; Wang, Y.; Hautzinger, M. P.; Zhao, Y.; Wright, J. C.; Zhu, Z.; Jin, S.: Anion Exchange of Ruddlesden–Popper Lead Halide Perovskites Produces Stable Lateral Heterostructures. *J. Am. Chem. Soc.* **2021**, *143*, 5212-5221. DOI: 10.1021/jacs.1c01573.
7. Kuo, M.-Y.; Spitha, N.; Hautzinger, M. P.; Hsieh, P.-L.; Li, J.; Pan, D.; Zhao, Y.; Chen, L.-J.; Huang, M. H.; Jin, S.; Hsu, Y.-J.; Wright, J. C.: Distinct Carrier Transport Properties Across Horizontally vs Vertically Oriented Heterostructures of 2D/3D Perovskites. *J. Am. Chem. Soc.* **2021**, *143*, 4969-4978. DOI: 10.1021/jacs.0c10000.

8. Pan, D.; Fu, Y.; Spitha, N.; Zhao, Y.; Roy, C. R.; Morrow, D. J.; Kohler, D. D.; Wright, J. C.; Jin, S.: Deterministic fabrication of arbitrary vertical heterostructures of two-dimensional Ruddlesden–Popper halide perovskites. *Nat. Nanotech.* **2021**, *16*, 159-165. DOI: 10.1038/s41565-020-00802-2.

Direct Reduction of Metal Oxides to Metals for Electrowinning and Energy Storage

Paul A. Kempler,[1,2] Carl K. Brozek,[1] Nancy M. Washton,[3] J. David Bazak[3]

1. **Department of Chemistry and Biochemistry, University of Oregon**
2. **Oregon Center for Electrochemistry, University of Oregon**
3. **Pacific Northwest National Laboratory**

Keywords: Electrochemistry, energy storage, nanoparticles, NMR, electrodeposition

Research Scope

Solid/solid metal-oxide/metal conversion reactions are required for iron (Fe) and zinc (Zn) electrodes proposed for low-cost batteries and are a promising, electrified route for manufacturing metals directly from inexpensive ores. Identifying and understanding new design principles for **energy-** and **atom-efficient** conversion reactions between Fe, Zn, and their respective oxides in alkaline electrolytes would unlock **long-duration energy storage** opportunities[1] while also opening a low-carbon pathway for their fabrication.[2]

The three aims of the project are to understand the limits to nanoscale transport in solid/solid metal-oxide/metal electrowinning, measure the solvation environment of cations in alkaline, mesoporous metal oxides, and identify the structure and composition of metal/metal-oxide interfaces.

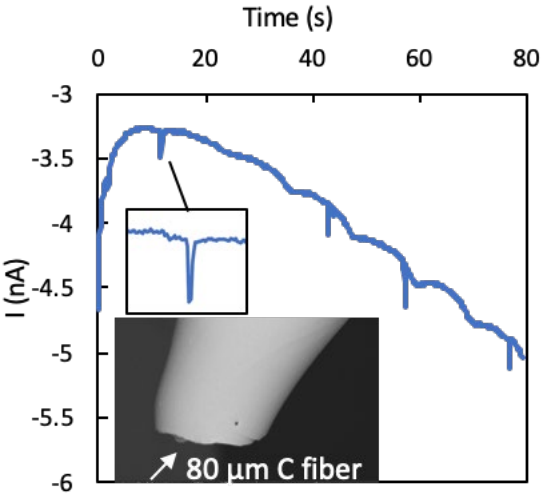

Figure 1: Current voltage data from a carbon fiber microelectrode (electron micrograph inset) in 30 wt% NaOH with 0.2 mM equivalents Fe_2O_3

Recent Progress

Nanoscale transport: Reduction reactions occuring from suspensions of metal oxide nanoparticles are mechanistically complex and poorly understood. **Kempler** is leading electrochemical studies in environments with controlled hydrodynamic transport to capture intermediates involved in the direct reduction of hematite to iron metal.

Raj Shekhar at Oregon has prepared insulated carbon-fiber microelectrodes to study nanoparticles attached or colliding with an inert microelectrode in concentrated alkaline environments. Small current spikes have been used to measure the reduction kinetics assigned to the local environment of individual nanoparticles. Additionally, rotating ring-disk electrode

studies have been used to characterize the onset of reductive dissolution from thin films of hematite.

Solvation Environment: A detailed understanding of the composition and solution structure of the evolving concentrated electrolytes in M/MO electrochemical conversion is necessary for a mechanistic description of the reaction. **Bazak** and **Washton** are conducting an NMR-focused study of both model concentrated electrolytes at high pH and ex situ samples of electrochemically generated M/MO slurries as a function of conversion level, with an emphasis on contrasting the dynamics and transport of solvated probe ions.

Mixed-cation hydroxide brines containing lithium have been shown to produce synergistic effects which promote M/MO conversion by modifying the solvation environment (**Figure 2**). Using a dynamics-centric approach, multinuclear NMR and viscometry studies at PNNL have been conducted to explore the kinetics and mass transport ramifications of this electrolyte design strategy. These initial studies on bulk electrolytes will also benchmark future efforts to quantitatively examine restricted diffusion in nanoporous metal oxide structures formed electrochemically.

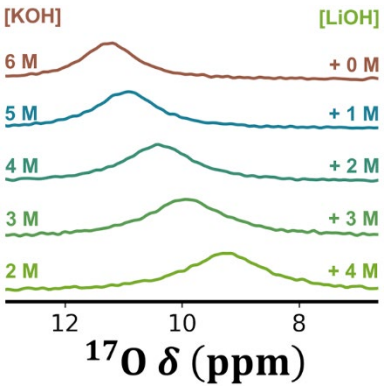

Figure 2: ^{17}O NMR for mixed cation-hydroxide brines at 6 M ionic strength.

Cation effects at complex interfaces: **Kempler** is leading a study on the mechanism of alkaline metal plating by modifying the local structure of water. The influence of cations on metal plating reactions and the competing hydrogen evolution reaction is complex.[5] Working with industry partner EnZinc, who is developing a microsponge Zn anode to serve in both mobile and stationary energy storage devices, the Oregon team has identified non-linear effects of hard cations such as Li^+ in representative electrolytes used in alkaline batteries and employed on-line gas chromatography measurements to characterize the effects on porous Zn anodes.

References

1. N. A. Sepulveda, J. D. Jenkins, A. Edington, D. S. Mallapragada, and R. K. Lester The Design Space for Long-Duration Energy Storage in Decarbonized Power Systems. Nature Energy **6** 506-516 (2021).
2. E. Pomerantseva, F. Bonaccorso, X. Feng, Y. Cui, Y. Gogotsi, *Energy Storage: The Future Enabled by Nanomaterials.* Science **366**, 6468 (2019).
3. K. Shimizu, K. Tschulik, and R.G. Compton, *Exploring the Mineral–Water Interface: Reduction and Reaction Kinetics of Single Hematite (α-Fe_2O_3) Nanoparticles.* Chemical Science **7**, 1408-1414 (2016).
4. J.D. Bazak, A.R. Wong, K. Duanmu, K.S. Han, D. Reed, and V. Murugesan, *Concentration-Dependent Solvation Structure and Dynamics of Aqueous Sulfuric Acid Using Multinuclear NMR and DFT*. *The Journal of Physical Chemistry B* **125**, 5089-5099 (2021)
5. J. T. Bender, A. S. Petersen, F. C. Østergaard, M. A. Wood, S. M. Heffernan, D. J. Milliron, J. Rossmeisl and J. Resasco, *Understanding Cation Effects on the Hydrogen Evolution Reaction*. ACS Energy Letters, **8**, 657-665 (2022).

Publications

1. B. B. Noble, L. J. Moutarlier, and P. A. Kempler, *Electrochemical Chlor-Iron Process for Iron Production from Iron Oxide and Seawater*, ChemRxiv, 10.26434/chemrxiv-2023-d22xj (2023).

Designing Chemical Disorder in Solid-State Superionic Conductors

Jae Chul Kim, Assistant Professor, Department of Chemical Engineering & Materials Science, Stevens Institute of Technology

Keywords: Solid electrolytes, Solid-state batteries, Lithium thiophosphates, Noncrystalline

Research Scope

Chemical and structural disorder present in noncrystalline states can often provide new functionalities to materials properties.[1,2] In noncrystalline materials design, however, the lack of structural descriptors makes it difficult to employ traditional materials chemistry. The objective of this project is to establish materials design principles and propose synthesis guidelines for noncrystalline solids to advance energy storage technology. Specifically, we will rationalize the development of noncrystalline lithium (Li) superionic conductors with high ionic conductivity and excellent electrochemical stability for all-solid-state battery applications. We hypothesize that chemical disorder can be introduced to systematically disrupt long range structures of crystalline Li conductors, while local symmetry (i.e., Li coordination, anion distribution, and short-range order) of the crystalline state can remain to dictate electrochemical properties of the resulting noncrystalline products.

Our model system to test this hypothesis is lithium thiophosphate (Li_3PS_4, LPS) that has multiple crystalline polymorphs with different ionic conductivities and can also be prepared noncrystalline.[3-5] High-energy ball-milling will be used to induce structural and chemical disorder in crystalline LPS and to transform crystalline LPS to noncrystalline LPS. This mechanochemical activation process will be elaborated to control the degree of disorder and stoichiometry of the material. Disorder created will be investigated by diverse structural and chemical analyses. We will also explore how local configurations and compositions of noncrystalline frameworks govern macroscopic Li conduction and electrochemical stability with reference to crystalline LPS phases to study the *ancestry* of electrochemical properties.

Recent Progress

In the first year of this project, we prepared two of the three crystalline LPS polymorphs and introduced disorder to them by high-energy ball-milling. We used solid-state methods to obtain β- and γ-polymorphs of LPS and found that β-LPS forms at lower temperature (300°C) than γ-LPS at 500°C after 5-hour firing, as similarly reported in literature.[3-5] δ-LPS that requires high pressure beyond what conventional furnaces can reach[6] cannot be obtained. β- and γ-LPS were then ball-milled to induce disorder. Fig. 1(a-c) shows XRD patterns of as-synthesized β-LPS and subsequently ball-milled β-LPS for different time periods. We monitored the intensity variation of the (221) peak at 30° and the (123) peak at 48° 2θ. The peak intensities decrease

almost immediately after short-time ball-milling for 20 min. As the ball-milling time increases to 120 min, the crystalline peaks almost disappear, but not completely even with subsequent quenching. The crystallites may originate from fast recrystallization upon ball-milling and/or incomplete crystalline-to-noncrystalline phase transitions. Similarly, another noncrystalline LPS was prepared using γ-LPS.

By comparing the XRD patterns of ball-milled LPS originating from β- and γ-LPS in Fig. 2a, we found very little difference. They are mostly amorphous whereas small peaks in which the overall pattern look alike to β- or γ-LPS appear. We will defer the rigorous phase identification of XRD results until we have access to the synchrotron resources. However, the Nyquist plot in Fig. 2b demonstrates two very distinct transport properties between the two materials. Li conductivity of LPS in the amorphous state scales with that of the crystalline parents. Noncrystalline LPS derived from β-LPS shows smaller overall resistance than noncrystalline LPS from γ-LPS.

These results confirm our hypothesis about local structural characteristics that can dictate Li transport properties for noncrystalline LPS. As a result of high-energy ball-milling, high shear stress imposed on LPS can disrupt the long-range arrangement of the PS_4 framework. As the relative arrangement of neighboring PS_4 may remain similar in the short range, the low barrier Li conduction for β-LPS parent can be inherited in its noncrystalline child to the large extent.

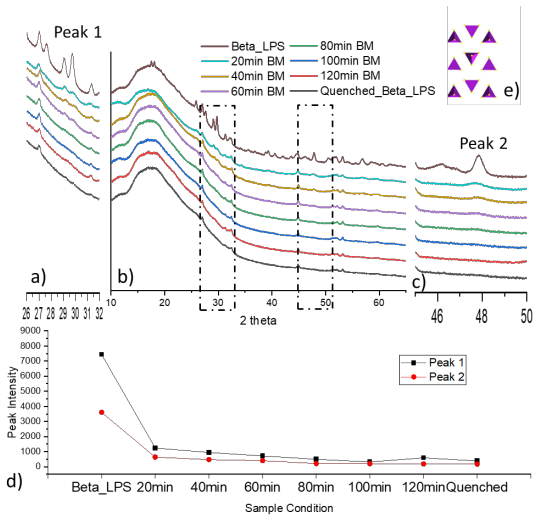

Fig. 1. (a-c) XRD patterns obtained and derived from β-LPS and (d) intensity variation for the (221) and (123) peaks. (e) The schematic illustration of PS_4 tetrahedra in β-LPS.

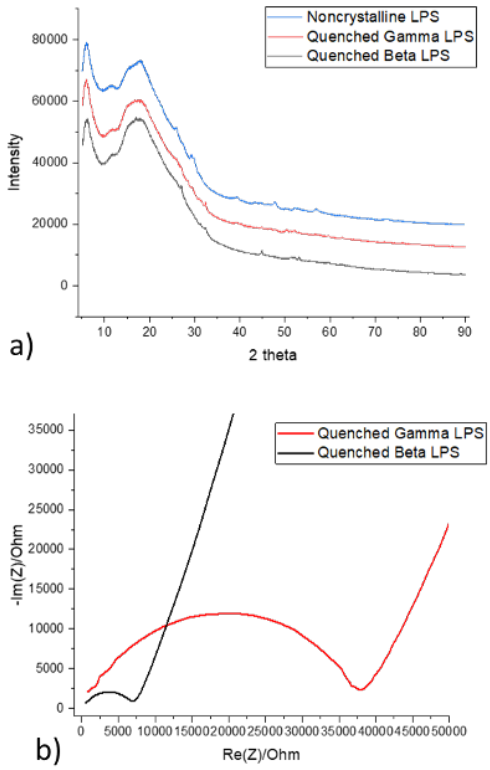

Fig. 2 (a) XRD patterns of noncrystalline LPS by direct ball-milling and from β- and γ-LPS and (b) the Nyquist plot for β- and γ-derived noncrystalline LPS.

References

1. J. Saienga, S.W. Martin, *The Comparative Structure, Properties, and Ionic Conductivity of LiI + Li_2S + Ge_S2 Glasses Doped with Ga_2S_3 and La_2S_3*. Journal of Non-Crystalline Solids **354**, p. 1475–1486 (2008).
2. S.W. Martin, R. Christensen, G. Olson, J. Kieffer, W. Wang, *New Interpretation of Na^+-Ion Conduction and the Structures and Properties of Sodium Borosilicate Mixed Glass Former Glasses*. Journal of Physical Chemistry C, **123**, p. 5853–5870 (2019).
3. A. Sakuda, A. Hayashi, M. Tatsumisago, *Sulfide Solid Electrolyte with Favorable Mechanical Property for All-Solid-State Lithium Battery*. Scientific Reports **3**, p. 2261 (2013).
4. M. Tachez, J.-P. Malugani, R. Mercier, G. Robert, *Ionic Conductivity of and Phase Transition in Lithium Thiophosphate Li_3PS_4*. Solid State Ionics **14**, p. 181–185 (1984).
5. Z. Zhang, H. Li, K. Kaup, L. Zhou, P.-N. Roy, L.F. Nazar, *Targeting Superionic Conductivity by Turning on Anion Rotation at Room Temperature in Fast Ion Conductors*. Matter **2**, p. 1667–1684 (2020).
6. S. Iikubo, K. Shimoyama, S. Kawano, M. Fujii, K. Yamamoto, M. Matsushita, T. Shinmei, Y. Higo, H. Ohtani, *Novel stable structure of Li3PS4 predicted by evolutionary algorithm under high-pressure*. AIP Advances 8, p. 015008 (2018).

Publications

None.

Multilength-Scale Synthesis of Silicon Materials

Rebekka S. Klausen, Johns Hopkins University

Keywords: polymers, silicon, mesoscale, hierarchical materials, synthesis

Research Scope

The Objectives of this project are to:

(1) Prepare hierarchically structured materials from existing cyclosilane building blocks (e.g. 1,3Si6, 1,4Si6) using covalent strategies.
(2) Rationally design novel cyclosilane building blocks to achieve targeted properties, while also expanding the scope of architectures achievable under Objective One.
(3) Leverage mechanism-driven insights to achieve control of poly(cyclosilane) microstructure, crystallinity, and mechanical properties.

Recent Progress

The goal of this project is to synthesize hierarchically structured silicon materials with precision from the atomic level to the bulk. The central hypothesis is that cyclosilane building blocks (synthesized atom-by-atom) can be linked together in specific, well-defined polymerization reactions to yield bulk materials with structural definition at multiple length scales. As described under Research Scope, achieving these goals is structured around three major Objectives that include elaboration of known building blocks, constructing an expanded set of building blocks, and understanding structure-property relationships in materials synthesized under this project.

Objective One. Polymers based on main group elements find application as solution-processable precursors to ceramics (polymer-derived ceramics, PDCs).[1,2] To understand microstructure-dependent polycyclosilane pyrolysis, three distinct polymers differing in connectivity (1,3 or 1,4) and architecture (linear or cyclic) were synthesized.[3] The thermal decomposition was studied by thermogravimetric analysis (TGA). Thermal decomposition began ca. 250 ˚C, while the weight became constant above 550 ˚C. A black solid residue remained in the sample pan after the TGA measurement, consistent with ceramization. While all samples provided char yields between 50-60%, higher than linear polymers e.g., poly($SiMe_2$), the highest char yield was found for the cyclic polymer, consistent with lower degrees of volatilization due to the need for multiple Si–Si bond homolysis events to occur to produce volatile byproducts.

In addition to the synthesis of ceramics, we developed approaches to the synthesis of ordered hierarchical structures through functionalization of Si–H bonds of cyclosilane molecules and

polymers. While the addition of a Si–H bond to an unsaturated bond (hydrosilylation) is a widely used reaction in the synthesis of industrially relevant silicones, platinum-based catalysts are known to react with Si–Si bonds. After a survey of catalysts, $RuHCl(CO)(PPh_3)_3$ was identified as a highly chemo-, regio-, and stereoselective catalyst for the addition of cyclosilanes to alkynes, yielding new conjugated materials.[4] We further showed Kumada polycondensation of a thienylcyclosilane, affording a unique *stereoregular conjugated polymer*.

Adding to this suite of chemoselective Si–H functionalizations, borane-catalyzed dehydrocoupling of thiophenols with cyclosilanes proceeded with high chemoselectivity for Si–H bonds in the presence of Si–Si bonds.[5] Isomeric cyclosilanes afforded isomeric cyclosilane thioethers that differed in chair or twist-boat conformation as demonstrated by both X-ray crystal structures and density functional theory (DFT) calculations. We expect these works to together establish a set of design principles for cyclosilane hierarchical materials synthesis.

Objective Two. While it has long been appreciated that the optical properties of polysilanes are conformation dependent,[6] efforts to control polysilane global conformation have exclusively focused on organic side chains. We reported the first example of using cyclosilane connectivity and conformation to control delocalization.[7] We found that 1,3-linked cyclosilanes can adopt a favorable *anti* conformation unavailable to 1,4-linked cyclosilanes. In addition, we carried out extensive TD-DFT calculations to understand the structural basis of polycyclosilane absorption. Critical long-term impacts of this study include the possibility of preparing materials in which every single Si atom contributes to conjugation and the possibility of computationally predicting new targets with enhanced optical absorption.

Objective Three. A significant challenge in the bottom-up synthesis of hierarchical materials is structure determination: can the hypothesized long-range order and structural regularity be conclusively determined? To address this challenge in silane materials, we reported a model system for determining relative configuration by NMR spectroscopy via isomer-specific long range ^1H-^1H coupling.[8]

Several studies investigating the synthesis of new cyclosilane building blocks were pursued. Towards the synthesis of a tricyclic silane building block for complex polysilanes, we sought to prepare a 1,2-dichlorocyclohexasilane functionalized with sterically bulky tert-butyl groups. However, during a Na-promoted reductive cyclization, instead of the desired six-membered ring, we obtained a five-membered ring resulting from silylene (or silylenoid) elimination.[9] In collaboration with the Lin group (Cornell),[10] we reported a general approach for the synthesis of disilanes as well as linear and cyclic oligosilanes via the reductive activation of readily available chlorosilanes. In comparison to the traditional Wurtz coupling, our method features milder

conditions and improved chemoselectivity, broadening the functional groups that are compatible in oligosilane preparation.

References

1. Ackley, B. J.; Martin, K. L.; Key, T. S.; Clarkson, C. M.; Bowen, J. J.; Posey, N. D.; Ponder, J. F.; Apostolov, Z. D.; Cinibulk, M. K.; Pruyn, T. L.; et al. Advances in the Synthesis of Preceramic Polymers for the Formation of Silicon-Based and Ultrahigh-Temperature Non-Oxide Ceramics. *Chem. Rev.* **2023**, *123* (8), 4188–4236.
2. Birot, M.; Pillot, J. P.; Dunoguès, J. Comprehensive Chemistry of Polycarbosilanes, Polysilazanes, and Polycarbosilazanes as Precursors of Ceramics. *Chem. Rev.* **1995**, *95*, 1443–1477.
3. Jiang, Q.; Wong, S.; Klausen, R. S. Effect of Polycyclosilane Microstructure on Thermal Properties. *Polym. Chem.* **2021**, *12* (33), 4785–4794.
4. Jiang, Q.; Gittens, A. F.; Wong, S.; Siegler, M. A.; Klausen, R. S. Highly Selective Addition of Cyclosilanes to Alkynes Enabling New Conjugated Materials. *Chem. Sci.* **2022**, *13* (25), 7587–7593.
5. Gittens, A. F.; Jiang, Q.; Siegler, M. A.; Klausen, R. S. Conjugation in Isomeric Cyclosilane Thioethers. *Organometallics* **2022**, *41* (23), 3762–3769.
6. Miller, R. D.; Hofer, D.; Rabolt, J.; Fickes, G. N. Anomalously Long-Wavelength Electronic Transition in Conformationally Locked Organosilane High Polymers. *J. Am. Chem. Soc.* **1985**, *107* (7), 2172–2174.
7. Fang, F.; Jiang, Q.; Klausen, R. S. Poly(Cyclosilane) Connectivity Tunes Optical Absorbance. *J. Am. Chem. Soc.* **2022**, *144* (17), 7834–7843.
8. Ferguson, J. T.; Jiang, Q.; Marro, E. A.; Siegler, M. A.; Klausen, R. S. Long-Range Coupling in Cyclic Silanes. *Dalt. Trans.* **2020**, *49* (42), 14951–14961.
9. Ballestero-Martínez, E.; Ferguson, J. T.; Siegler, M. A.; Klausen, R. S. Isolation of a Cyclopentasilane from Magnesium Reduction of a Linear Hexasilane. *European J. Org. Chem.* **2021**, *2021* (33), 4641–4646.
10. Guan, W.; Lu, L.; Jiang, Q.; Gittens, A. F.; Wang, Y.; Novaes, L. F. T.; Klausen, R. S.; Lin, S. An Electrochemical Strategy to Synthesize Disilanes and Oligosilanes from Chlorosilanes. *Angew. Chemie Int. Ed.* **2023**, e202303592.

Publications

1. Q. Jiang, S. Wong, R. S. Klausen, *Effect of Polycyclosilane Microstructure on Thermal Properties*, Polym. Chem. **12**, 4785 (2021).
2. E. Ballestero–Martínez, J. T. Ferguson, M. A. Siegler, R. S. Klausen, *Isolation of a Cyclopentasilane from Magnesium Reduction of a Linear Hexasilane*, Eur. J. Org. Chem. **22**, 4641 (2021).
3. R. S. Klausen, E. Ballestero–Martínez, *Organosilicon and Related Group 14 Polymers*, Comprehensive Organometallic Chemistry IV, 135 (2022).
4. Q. Jiang, A. F. Gittens, S. Wong, M. A. Siegler, R. S. Klausen, *Highly Selective Addition of Cyclosilanes to Alkynes Enabling New Conjugated Materials*, Chem. Sci. 13, 1407 (2022)
5. F. Fang, Q. Jiang, R. S. Klausen, *Polycyclosilane Connectivity Tunes Optical Absorbance*, J. Am. Chem. Soc. **144**, 7834 (2022).
6. A. F. Gittens, Q. Jiang, M. A. Siegler, R. S. Klausen, *Conjugation in Isomeric Cyclosilane Thioethers*, Organometallics **41**, 3762 (2022).
7. W. Guan, L. Lu, Q. Jiang, A. F. Gittens, Y. Wang, L. F. T. Novaes, R. S. Klausen, S. Lin, *An Electrochemical Strategy to Synthesize Disilanes and Oligosilanes from Chlorosilanes*, Angew. Chem. Int. Ed. e202303592 (2023).

Crystal Growth and Quantum Phases of Frustrated Rare Earth Oxides DE-SC0020071

Joseph W Kolis, Department of Chemistry, Clemson University

Kate Ross, Department of Physics, Colorado St. University

Keywords: Magnetic Frustration, Quantum Liquids, Pyrochlores, Hydrothermal, Crystal Growth

Research Scope

Magnetically frustrated materials are a rich hunting ground for quantum materials. In particular they can display persistent disorder down to the lowest temperatures.[1] This leads to massively degenerate ground states and non-classical behavior such as quantum spin ices and quantum spin liquids (QSL). Most work on frustrated systems focuses on planar 2-D lattices such as Kagome nets. In order to identify next generation of quantum materials we are extending our study to 3-D systems with frustrated lattices particularly pyrochlores. These can potentially display quantum phases such as QSLs, as well as other effects such as quantum order-by-disorder.[2] These cubic lattices containing rare earth ions in highly symmetric magnetically frustrated sites. They are structurally flexible and can be substituted by many types of metal ions displaying a wide range of frustrated magnetic behavior. Such situations are ripe for emergent nonclassical behaviors such as quantum spin liquids and Kitaev exchange.[3,4] The Kolis lab employs a hydrothermal technology to grow materials at the relatively low temperatures of 600-700˚C in high pressure aqueous fluids.[5] The relatively low growth temperatures are particularly useful in solving two significant problems that persists in traditional high temperature synthesis and crystal growth of pyrochlores. These problems are oxide defects from nonstoichiometry in the lattice, and disorder between the A and B metal sites of the pyrochlore.[6] At present we are specifically targeting a series of cubic pyrochlores $A_2B_2O_7$ across the range of rare earths (A = Ce – Yb and B are the magnetically silent tetravalent ions Ge and Sn). Our hydrothermal approach can minimize these problems leading to much better sample quality and improved chances of observing new physical phenomena. The magnetic properties are structures appear to be extremely complex, so the use of single crystals in neutron scattering and diffraction is a particular focus of this work. A broader goal of this program is to enhance the collaborative potential between synthetic chemistry and an experimental physics to address a big idea challenge (rational design of quantum materials) within the DoE. [7]

Recent Progress:

Large single crystals of both $Er_2Sn_2O_7$ and $Yb_2Sn_2O_7$ were grown using the hydrothermal method, and careful X-ray diffraction and heat capacity measurement indicated that they are well ordered with minimal lattice defects.[8,9] We also grew single crystals of the tetragonal phase of $Er_2Ge_2O_7$ and obtained some very interesting magnetic and neutron scattering data.[10] We also grew single crystals of *cubic* $Yb_2Ge_2O_7$ in sufficient quantity and quality to obtain detailed INS data.[11] We were able to use these to determine exchange interactions and also to place this material in the universal phase diagram of the pyrochlores. The $Yb_2Ge_2O_7$ shows long range antiferromagnetic order but no well-defined spin wave excitations from this state, which is highly

unconventional, but is similar to $Yb_2Ti_2O_7$ even though $Yb_2Ti_2O_7$ is a ferromagnet. Neutron scattering data shows the lack of conventional spin waves in the ordered state. We grew single crystal $Er_2Sn_2O_7$ and obtained field-dependent low temperature specific heat data in three high-symmetry directions and also obtained single crystal neutron scattering data.[12] This helped develop the theory to support our findings of "re-entrant" phase diagrams that indicates that the ordered phase, an antiferromagnet, becomes more thermodynamically stable as the field increases. (Fig. 1)

We are now making a special effort to focus on Ce^{3+} pyrochlores including large single crystals of, which has been postulated theoretically to form a range of quantum spin liquids. The cerates have small effective magnetic moments and reduced neutron scattering signals, so larger quantities are needed for INS measurements, requiring significant experimental effort. We grew large single crystals of $Ce_2Sn_2O_7$ performed an array of detailed XRD and neutron scattering experiments to demonstrate that they have minimal defects and site disorder. A detailed neutron scattering study at ORNL to demonstrated evidence for a remarkable dipolar spin with an all-in all-out ground state showing "order by disorder" induced by quantum effects.[13] This behavior is significantly different from that reported for powders prepared by high temperature solid state synthesis. It definitively shows that the interpretation of phase behavior is highly sensitive to sample preparation.

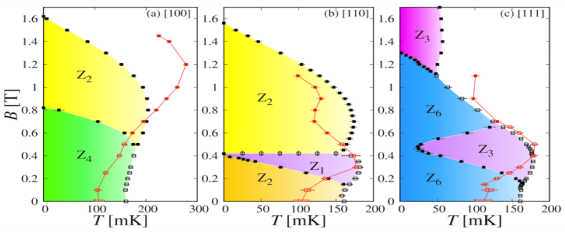

Figure 1. Observing the reentrant phase of $Er_2Sn_2O_7$ by employing oriented single crystal to identify the phases relative to the three cubic orientations [100], [110] and [111].

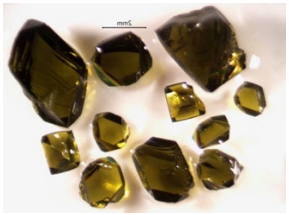

Figure 2. High quality single crystals of $Ce_2Sn_2O_7$ (2-4mm)

We grew large single crystals which are scheduled for single crystal neutron diffraction at both HFIR ($WAND^2$) and SNS (CNCS) at ORNL this spring to provide more detailed information about this puzzle. (Fig. 2)

In addition we are just beginning to systematically investigate the synthesis and growth of double perovskites, again using Ge and Sn as magnetically silent building blocks where the rare earth ions can be varied across the whole row. One unexpected initial result using germanate is the isolation of a novel 1-D phase with the adelite structure $MRE(GeO_4)(OH)$ (M^{2+} = Co, Ni, Zn). The initial properties of this very rich system are also very interesting. [14]

References

1. J.E. Greedan *Geometrically frustrated magnetic materials* J. Mat. Chem.**11** 37-53 (2001).
2. J. S. Gardner, M. J.Gingras, J. E. Greedan *Magnetic pyrochlore oxides.* Rev. Mod. Phys. **82**, 53 (2010).
3. K. A. Ross, L. Savary, B. D. Gaulin, L. Balents *Quantum excitations in quantum spin ice.* Phys. Rev. X. **1**, 021002 (2011).

4. S. T. Bramwell, M. J. Gingras *Spin ice state in frustrated magnetic pyrochlore materials.* Science., **294,** 1495-501 (2001).
5. J. W. Kolis, C. D. McMillen, *High Temperature Hydrothermal Synthesis of Inorganic Compounds* in Comprehensive Inorganic Chemistry III Reedijik, J.; Poeppelmeier, K. (eds.) Elsevier (2023)**.**
6. G. Sala, D. D, Maharaj, M. B. Stone, H. A. Dabkowska, B. D. Gaulin *Crystal field excitations from Yb^{3+} ions at defective sites in highly stuffed Yb_2Ti_2O7.* Physical Review B. **97** 224409 (2018).
7. J.E. Moore, A. Aspuru-Guzik, B. Bauer, S. Coppersmith, W. B. de Jong, T. Devereaux, M. Fernandez-Serra. G. Galli, R. Harrison. P. Love, T. Maier *Basic Energy Sciences Roundtable: Opportunities for Quantum Computing in Chemical and Materials Sciences*. USDOE Office of Science (SC) (United States); (2017).
8. M. Powell, L. D. Sanjeewa, C. D. McMillen, K. A. Ross, C. Sarkis, J. W. Kolis *Rare Earth Tin Pyrochlores, $RE_2Sn_2O_7$ (RE = La-Lu): Site Ordered, Low Defect Single Crystals.* Cryst. Growth Des. **19** 4920-4926 (2019)
9. L. D. Sanjeewa, K. A. Ross, C. L. Sarkis, H. S. Nair, C. D. McMillen, J. W. Kolis *Single crystals of cubic rare-earth pyrochlore germanates: $RE_2Ge_2O_7$ (RE= Yb and Lu) grown by a high-temperature hydrothermal technique.* Inorganic Chemistry. **57** 12456-60 (2018).
1. D. M. Pajerowski, K. M. Taddei, D. L. Sanjeewa, A. T. Savici, M. B. Stone, J. W. Kolis *Quantification of local-Ising magnetism rare-earth pyrogermanates $Er_2Ge_2O_7$ and $Yb_2Ge_2O_7$* Phys. Rev. B **101** 014420. (2020)
10. C.L. Sarkis, J. G. Rau, L. D. Sanjeewa, M. Powell, J. Kolis, J. Marbey, S. Hill, J. A. Rodriguez-Rivera, H. S. Nair, D. R. Yahne, S. Säubert, M. J. P. Gingras, K. A. Ross *Unravelling competing microscopic interactions at a phase boundary: A single-crystal study of the metastable antiferromagnetic pyrochlore $Yb_2Ge_2O_7$* Phys. Rev. B, 102 134418 (2020).
11. D. R. Yahne, D. Pereira, L. D. C. Jaubert, L. D. Sanjeewa, M. Powell, J. W. Kolis, Guangyong Xu, M. Enjalran, M. J. P. Gingras, K. A. Ross. *Understanding Reentrance in Frustrated Magnets: the Case of the $Er_2Sn_2O_7$ Pyrochlore.* Phys. Rev. Lett. **127** 277206 (2021).
12. D. R. Yahne, B. Placke, R. Schafer, O. Benton, R. Moessner, M. Powell, J. W Kolis, C. M. Pasco, A. F. May, M. D. Frontzek, E. M. Smith, B. D. Gaulin, S. Calder, K. A. Ross, *Dipolar spin ice regime proximate to an all-in-all-out Néel ground state in the dipolar-octupolar pyrochlore $Ce_2Sn_2O_7$* Phys. Rev. X (2023) under review. arXiv:2211.15140.
13. M. Powell, J.W. Kolis manuscript in preparation.

Publications

1. J. W. Kolis, C. D. McMillen, *High Temperature Hydrothermal Synthesis of Inorganic Compounds* in Comprehensive Inorganic Chemistry III Reedijik, J.; Poeppelmeier, K. (eds.) Elsevier (2023)**.**
2. D. R. Yahne, D. Pereira, L. D. C. Jaubert, L. D. Sanjeewa, M. Powell, J. W. Kolis, Guangyong Xu, M. Enjalran, M. J. P. Gingras, K. A. Ross. *Understanding Reentrance in Frustrated Magnets: the Case of the $Er_2Sn_2O_7$ Pyrochlore.* Phys. Rev. Lett. **127** 277206 (2021).
3. D. R. Yahne, D. L. Jaubert, L. D. Sanjeewa, J. W, Kolis, D. Pereira, M. Enjalran. M. J. Gingras, K. A. Ross *Magnetic phase competition in the XY pyrochlore $Er_2Sn_2O_7$* Bull. Am. Phys. Soc. **Oct**. 64. (2019).
4. D. R. Yahne. *Understanding Reentrance in Frustrated Magnets: The Case of the $Er_2Sn_2O_7$ Pyrochlore*. CIFAR Quantum Materials Summer School. (2021)
5. D. M. Pajerowski, K. M. Taddei, D. L. Sanjeewa, A. T. Savici, M. B. Stone, J. W. Kolis *Quantification of local-Ising magnetism rare-earth pyrogermanates $Er_2Ge_2O_7$ and $Yb_2Ge_2O_7$* Phys. Rev. B **101** 014420. (2020)
6. C.L. Sarkis, J. G. Rau, L. D. Sanjeewa, M. Powell, J. Kolis, J. Marbey, S. Hill, J. A. Rodriguez-Rivera, H. S. Nair, D. R. Yahne, S. Säubert, M. J. P. Gingras, K. A. Ross *Unravelling competing microscopic interactions at a phase boundary: A single-crystal study of the metastable antiferromagnetic pyrochlore $Yb_2Ge_2O_7$* Phys. Rev. B, 102 134418 (2020).

7. C. L. Sarkis, J. Rau, D. L. Sanjeewa, M. Powell, J. W. Kolis, J. Marbey, S. Hill, J. A. Rodriguez-Rivera, H. S. Nair, M. J. P.Gingras, K. A. Ross *Single crystal neutron scattering study of the pyrochlore $Yb_2Ge_2O_7$*. Bull. Am. Phys. Soc. **Mar.** 65 (2020).
8. D. R. Yahne, B. Placke, R. Schafer, O. Benton, R. Moessner, M. Powell, J. W Kolis, C. M. Pasco, A. F. May, M. D. Frontzek, E. M. Smith, B. D. Gaulin, S. Calder, K. A. Ross, *Dipolar spin ice regime proximate to an all-in-all-out Néel ground state in the dipolar-octupolar pyrochlore $Ce_2Sn_2O_7$* Phys. Rev. X (2023) under review. arXiv:2211.15140.
9. S. Yang, M. Powell, J. W. Kolis, A. Navrotsky *Thermochemistry of Rare Earth Oxyhydroxides, REOOH (RE =Eu-Lu)* J. Solid State Chem. **287** 121344. (2020).
10. D. R. Yahne, L. D. Sanjeewa, A. S. Sefat, B. S. Stadelman, J. W. Kolis, S. Calder, K. A. Ross *Pseudospin versus magnetic dipole moment ordering in the isosceles triangular lattice material $K_3Er(VO_4)_2$*. Phys. Rev. B **102** 104423 (2020).

Janus 2D Material Platform Enabled by Atomic-Layer Substitution

Jing Kong, Massachusetts Institute of Technology

Program Scope

This project aims at using the atomic layer substitution (ALS) strategy developed in our previous DOE BES supported research to continue the development of a variety of revolutionary 2D Janus materials and structures that have never been obtained before. In addition, for the Janus materials/structures that have already been demonstrated by our group, there is a great need to characterize their properties and develop their applications. Our proposed research can be divided into three areas: (1) For the already developed Mo- and W- based, S- or Se- Janus structures, we plan to carry out in depth characterizations and further investigations on the conversion process, so that the reaction can be extended to Te- Janus and 1T' Janus materials; (2) We plan to use our ALS method to develop a set of novel Janus structures based on new TMD host materials and study their interesting properties; (3) based on our current understanding on the ALS process, we propose to extend such a process to wider range of 2D materials, beyond TMD.

Recent Progress

Under the support of this project, during the past year, we have made the following progress:

1. During the previous research period, we worked with Prof. Ju Li's group on the theoretical prediction that monolayer Janus TMDs in the 1T' phase possess colossal nonlinear photoconductivity owing to their topological band mixing, strong inversion symmetry breaking, and small electronic bandgap, our work was published in npj Computational Materials in 2021. It was predicted that 1T' Janus TMDs have inverted bandgaps on the order of 10 meV and are exceptionally responsive to light in the terahertz (THz) range. The shift current conductivity can be as large as 2300 nm μA V^{-2}, equivalent to a photo-responsivity of 2800 mA/W. The circular current (CC) conductivity of 1T' Janus TMDs is as large as$\sim 10^4$ nm μA V^{-2}. As a follow up on this work, we continued to collaborate with Prof. Ju Li (MIT)'s group and started to work with Prof. Aaron Lindenberg (Stanford)'s group on the characterization of non-linear optical properties of the Janus 1T' MoSSe via high harmonic generation (HHG), THz emission and second harmonic generation measurements. It was found that indeed 1*T'* MoSSe shows orders of magnitude enhancement in THz nonlinearities (e.g., it has > 50 times higher than 2*H* MoS2 for 18th order harmonic generation; and it shows > 20 times higher than 2*H* MoS2 for terahertz emission). These results confirmed our 2021 theoretical prediction and indicated the potential for the 1T' Janus TMD in nonlinear optical applications such as scalable attosecond sources. These results have

been written up and a manuscript submitted to Nature Communications has recently been accepted.

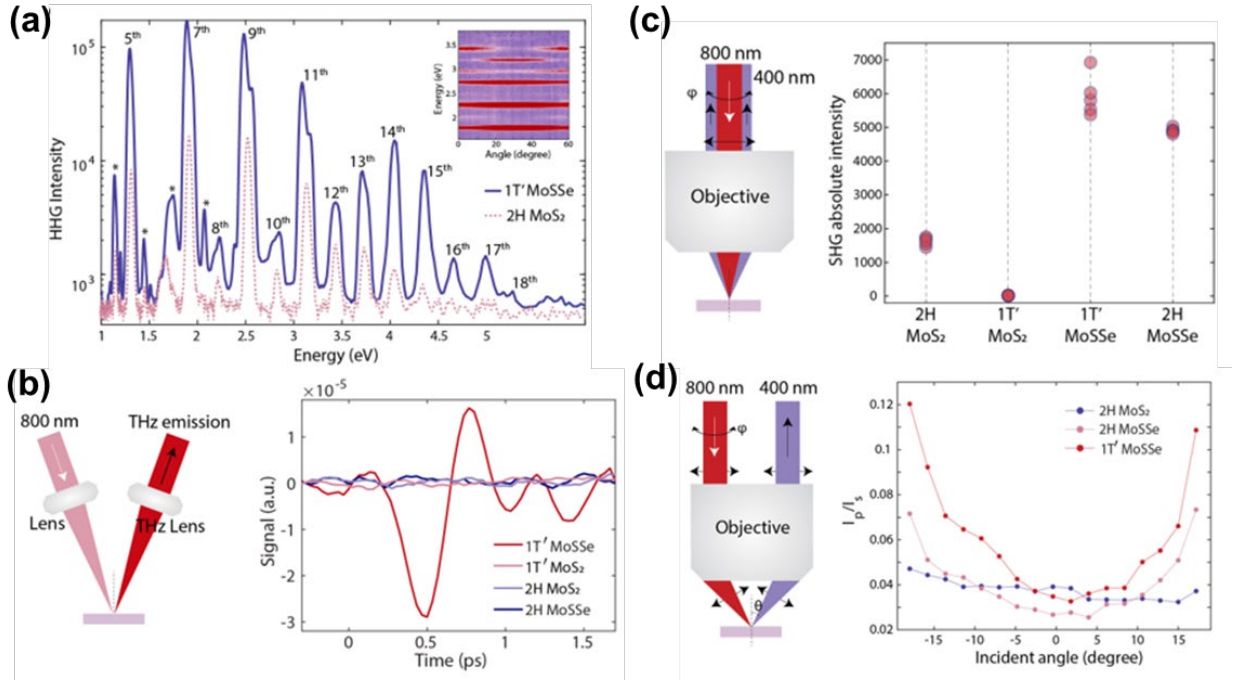

Figure 1. (a) Mid-Infrared (MIR) HHG spectrum of 1*T′* MoSSe shown in the blue curve is over an order of magnitude stronger than the HHG from macroscopic monolayer 2*H* MoS_2 shown as the red dashed line. HHG extends up to ~ 5 eV and is limited mainly by the cutoff of detection optics (e.g., aluminum mirrors and grating). The inset shows 1T′ MoSSe HHG intensity as a function of MIR incident polarization angles. The cancellation of a few orders at some polarization angles indicates the signal is generated from a single flake. (b) Left plot shows a schematic of THz emission setup. 1T′ MoSSe shows a dramatically enhanced THz emission signal compared with three other types of monolayer TMDs. (c) Left plot shows a schematic of second harmonic generation with normally incident 800-nm excitation. The right plot shows SHG intensity statistics of five different flakes in each sample and shows SHG is enhanced in 1T′ MoSSe and 2H MoSSe compared with 1T′ MoS_2 and 2H MoS_2. (d) The left plot shows the schematic of the angle-resolved SHG setup that measures out-of-plane dipole. The beam position at the objective back aperture is scanned perpendicular to the incident beam direction with a motorized stage, which tunes the incident angle accordingly. The right plot shows the angle-dependent SHG intensity ratio between p and s polarization (Ip and Is) in 1T′ MoSSe, 2H MoSSe, and 2H MoS_2. In the 1T′ MoSSe and 2H MoSSe, the Ip/Is ratio increases at non-normal incidence angles, indicative of out-of-plane dipoles. In 2H MoS_2, almost no

2. We have continued our collaborations with Prof. Shengxi Huang's group on the characterizations of MoSSe/MoS_2 heterobilayers, during the past year we have also worked with Prof. Riichiro Saito in Tohuku University in Japan on the theoretical understandings on the nonlinear optical responses of these heterobilayers optimized by stacking order and strain. From the theoretical calculation, we found that the non-linear susceptibility, χ_2, of the AA stacking MoSSe/MoS_2 is three times as large as AB stacking (AA: 550pm/V; AB: 170pm/V) due to the

broken inversion symmetry in AA. Further, a relatively large, two-dimensional strain (0.04) that breaks C_{3v} point group symmetry of the MoSSe/MoS2, enhances the χ_2 values for both AA (900pm/V) and AB (300pm/V) stacking by 1.6 times as large as that without strain. Our results show that the lack of inversion symmetry of the Janus MoSSe/MoS_2 leads to the nonzero of the nonlinear susceptibility components, $\chi^{(2)}_{xxx} = -\chi^{(2)}_{xyy} = -\chi^{(2)}_{yxy} = -\chi^{(2)}_{yyx} \neq 0$. The nonlinear susceptibilities χ_2 of MoSSe/MoS_2 can be controlled by stacking and strain engineering due to breaking the mirror and in-plane symmetries, respectively. MoSSe/MoS2 heterobilayer exhibits good mechanical properties with the ideal strain up to $\sim$ 20%, making MoSSe/MoS_2 as a flexible material for the optoelectronic and nonlinear optical applications, such as the bulk photovoltaic or four-wave mixing. This manuscript has been submitted to ACS Nano, and it currently under review.

3. During the past year we have also worked on SnSe multilayer flakes, a material we planned to carry out our Janus conversion and explore novel structures beyond TMD in the future. SnSe itself is a very interesting material, it shows in-plane ferroelectric domains and the multilayer stacks demonstrate much higher second harmonic generation (SHG) signal than typical monolayer TMDs such as MoS_2 and WS_2, which we understood from our cross-sectional STEM analysis that this is due to the stacking of the layers (in the ferroelectric stacking instead of the more energetically favorable anti-ferroelectric stacking). Through the collaboration with Dr. Bill Wilson's group in Harvard Center for nanoscale systems (CNS), anisotropic exciton polariton propagation through these ferroelectric domains were also revealed using scanning near field microscopy. When an electric field is applied, the polarization of the domains can be switched, thus the propagation of the exciton polariton can be tuned actively by the external electric field. These works have been published in Advanced Materials, Advanced Electric Materials, and Nature Nanotechnology this year.

4. During the course of this project, Dr. Nannan Mao and Dr. Tianyi Zhang (who have been supported by this project) have also carried out collaborations within our own group or outside our group, with one publication in Nano Letters and another one in Nature Nanotechnology. Even though these progresses are not in the direction of Janus materials, they are important progresses in the field acknowledging the support of this project.

Future Plans

In the coming year, and also the following few years, we are planning to carry out the following investigations:

1. The incorporation of Se atoms into MoS_2 structure causes a strain in the lattice. Researchers have proposed to utilize the strain to form interesting Origami and Kirigami structures. However, the strain in the Janus structure has not been well studied yet due to the

limitation of obtaining the samples. We are planning to work with Prof. Yimo Han's group at Rice University to use STEM to characterize the strain in MoSSe and also at the interface between lateral heterostructures of MoS_2 and MoSSe.

2. The intrinsic properties of the Janus TMDs have not been thoroughly explored. We are currently collaborating with Dr. Andrey Krayev in Horiba Scientific to characterize these Janus TMD with tip enhanced Raman spectroscopy. We have observed some interesting results that need further investigation. We anticipate there will be a lot of new findings in the coming year through this collaboration.

3. Previously interesting single photon emission (SPE) behaviors were found in WSe_2 monolayers [1, 2]. Researchers have also identified that by straining the TMD lattice, SPE can be controllably introduced [3]. Since intrinsic strains were introduced into the WSSe lattice, we are interested in investigating SPEs in these WSSe structures. During the past year we sent samples to Prof. Dirk Englund's group for such characterization. We are planning to carry out some low temperature measurements to see if there are SPE from these Janus monolayers.

4. In our collaboration with Prof. Ju Li's group, we have identified the fascinating properties of 1T' MoSTe. Up to now, we had limited success for the conversion of MoS_2 to MoSTe, possibly due to the weaker bonding between Mo and Te compared to Mo with S. During the past year we have used MoTe2 samples to convert to MoSTe and have received some preliminary results. In the coming year we are planning to continue in this and explore the interesting properties of 1T' MoSTe.

5. We have developed Au-assisted transfer technique to obtain a variety of other monolayer TMDs, together with our CVD synthesis, we now have PtS_2 or $PtSe_2$, $NbSe_2$, TaS_2. In addition, we have SnSe multilayer flakes. In the coming year we are planning to study the Janus conversion of these 2D materials.

References

1. M. Koperski, K. Nogajewski, A. Arora, V. Cherkez, P. Mallet, J.-Y. Veuillen, J. Marcus, P. Kossacki & M. Potemski, "Single photon emitters in exfoliated WSe_2 structures", Nature Nanotech 10, 503–506 (2015)
2. Yu-Ming He, Genevieve Clark, John R. Schaibley, Yu He, Ming-Cheng Chen, Yu-Jia Wei, Xing Ding, Qiang Zhang, Wang Yao, Xiaodong Xu, Chao-Yang Lu & Jian-Wei Pan, "Single quantum emitters in monolayer semiconductors", Nature Nanotech 10, 497–502 (2015)
3. Carmen Palacios-Berraquero, Dhiren M. Kara, Alejandro R.-P. Montblanch, Matteo Barbone, Pawel Latawiec, Duhee Yoon, Anna K. Ott, Marko Loncar, Andrea C. Ferrari & Mete Atatüre, "Large-scale quantum-emitter arrays in atomically thin semiconductors", Nat Commun 8, 15093 (2017).

Publications

List of publications SUPPORTED BY BES:

1. Nannan Mao, Yue Luo, Ming-Hui Chiu, Chuqiao Shi, Xiang Ji, Tymofii S Pieshkov, Yuxuan Lin, Hao-Lin Tang, Austin J Akey, Jules A Gardener, Ji-Hoon Park, Vincent Tung, Xi Ling, Xiaofeng Qian, William L Wilson, Yimo Han, William A Tisdale, Jing Kong, "Giant Nonlinear Optical Response via Coherent Stacking of In-Plane Ferroelectric Layers", Advanced Materials, 2210894, (2023) DOI: https://doi.org/10.1002/adma.202210894
2. Ming-Hui Chiu, Xiang Ji, Tianyi Zhang, Nannan Mao, Yue Luo, Chuqiao Shi, Xudong Zheng, Hongwei Liu, Yimo Han, William L. Wilson, Zhengtang Luo, Vincent Tung, Jing Kong, "Growth of Large-Sized 2D Ultrathin SnSe Crystals with In-Plane Ferroelectricity", Advanced Electronic Materials, 2201031, (2023) DOI: https://doi.org/10.1002/aelm.202201031
3. Yue Luo, Nannan Mao, Dapeng Ding, Ming-Hui Chiu, Xiang Ji, Kenji Watanabe, Takashi Taniguchi, Vincent Tung, Hongkun Park, Philip Kim, Jing Kong, William L Wilson, "Electrically switchable anisotropic polariton propagation in a ferroelectric van der Waals semiconductor", Nature Nanotechnology, (2023) DOI: https://doi.org/10.1038/s41565-022-01312-z.
4. Jiadi Zhu, Ji-Hoon Park, Steven A. Vitale, Wenjun Ge, Gang Seob Jung, Jiangtao Wang, Mohamed Mohamed, Tianyi Zhang, Maitreyi Ashok, Mantian Xue, Xudong Zheng, Zhien Wang, Jonas Hansryd, Anantha Chandrakasan, Jing Kong, Tomás Palacios, "Low thermal budget synthesis of monolayer molybdenum disulfide for silicon back-end-of-line integration on 200 mm platform", Nature Nanotechnology, 18, 456–463 (2023) DOI: https://doi.org/10.1038/s41565-023-01375-6
5. Shuai Fu, Ji-Hoon Park, Hongyan Gao, Tianyi Zhang, Xiang Ji, Tianda Fu, Lu Sun, Jing Kong, Jun Yao, “Two-Terminal MoS2 Memristor and the Homogeneous Integration with a MoS2 Transistor for Neural Networks”, Nano Letters, Accepted.
6. Jiaojian Shi, Haowei Xu, Christian Heide, Changan HuangFu, Chenyi Xia, Felipe de Quesada, Hao Zhou, Tianyi Zhang, Leo Yu, Amalya Johnson, Fang Liu, Enzheng Shi, Liying Jiao, Tony Heinz, Shambhu Ghimire, Ju Li, Jing Kong, Yunfan Guo, Aaron M. Lindenberg, “Giant room-temperature nonlinearities from a monolayer Janus topological semiconductor”, Nature Communications, accepted
7. Nguyen T. Hung, Kunyan Zhang, Vuong V. Thanh, Yunfan Guo, Alexander A. Puretzky, David B. Geohegan, Jing Kong, Shengxi Huang, Riichiro Saito, “Nonlinear Optical Responses of Janus MoSSe/MoS2 Heterobilayers Optimized by Stacking Order and Strain”, submitted to ACS Nano.
8. Tianyi Zhang, Jiangtao Wang, Peng Wu, Jing Kong, “Vapor Phase Deposition of Two-Dimensional Layered Chalcogenides”, Nature Reviews Materials, submitted.

Novel Strategies for Direct Air Capture and Conversion of CO_2 Using Dual-Function Materials

Debasish Kuila and Aleksandrs Prokofjevs

Department of Chemistry, North Carolina Agricultural and Technical State University, Greensboro, NC 27411, USA

Jianzhong Lou

Department of Chemical Biological & Bioengineering, North Carolina Agricultural and Technical State University, Greensboro, NC 27411, USA

William A. Goddard III

Materials and Process Simulation Center (MSC), California Institute of Technology Pasadena, California 91125, USA

Keywords: CO_2 capture, Phosphines, Membranes, Adsorbents, Electrochemical conversion

Research Scope

The objective of the project is the development of new phosphine structures for CO_2 capture, release, and conversion [1]. This involves the synthesis of air-stable phosphine compounds featuring highly electron rich ligands and assess their interaction with CO_2. This series of studies was initiated by Density Functional Theory (DFT) screening over an array of electron-rich phosphines, resulting in the discovery of several phosphines with high affinities for CO_2. Subsequently, various mesoporous adsorbents will be functionalized with the synthesized phosphines. Accordingly, mesoporous solid adsorbents will be synthesized which possess uniform pore size distribution, high surface area, and large pore volume to accommodate the phosphine groups and enable rapid CO_2 diffusion within the pore structure. The lower energy requirement of the phosphine will lead to facile CO_2 desorption and adsorbent regeneration unlike amine which has strong binding energy [2, 3]. The adsorbents will be thoroughly characterized using SEM, XRD, FTIR, BET, TGA and surface analysis. Finally, electrochemical potential will be applied to facilitate the desorption of the captured CO_2 from the adsorbent and its conversion to valuable chemicals.

Recent Progress

1. An initial DFT screening of several novel phosphines revealed that molecules bearing either 1,1,3,3-tetramethylguanidinium (TMG) or BH_3^- ligands were capable of strongly binding CO_2. [pub. 1] Further modification of the TMG ligand with hydrogen-bonding motifs further improved CO_2 binding strength, indicating that gas phase CO_2 can be stabilized via hydrogen-bonding and

charge transfer environments. We have now carried a follow-up study to assess CO_2 binding affinities to other phosphine-borane complexes. Our results indicate that the combination of both the TMG and BH_3^- moieties on a phosphine can dramatically improve CO_2 binding strength, making a most promising candidate for phosphine-catalyzed CO_2 reduction towards energy-dense fuels. Our best new CO2 capture candidate is: $Li(TMG)_2P(BH_3)$ which is predicted to have a free energy for CO_2 binding of ΔG=-31.5 kcal/mol at 298K in MeCN. (See Fig. 1)

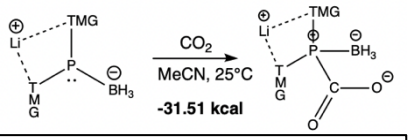

Figure 4 Best CO2 binding complex.

2. Based on these DFT calculations, we are performing attempts towards synthesis of a phosphoborane anionic complex, in which P atom is bound to two methyl groups and a BH_3^- group. Accordingly, various batches of experiments were performed to obtain pure dimethyl phosphine borane (DMPB).

3. Various phosphine oxide containing monomers have been synthesized for incorporation in polymeric membranes for CO_2 separation from various gas mixtures. The work involved:

- Synthesized bis(4-methoxylphenyl) phenyl phosphine oxide (BMPPO)
- Synthesized bis(4-hydroxylphenyl) phenyl phosphine oxide (BHPPO) monomer
- Synthesized bis(4-methoxyphenyl) ethyl phosphine oxide (BMEPO)
- Synthesized bis(4-hydroxylphenyl) ethyl phosphine oxide (BHEPO) monomer

4. The polysulfones containing the phosphine oxide was incorporated in polyimide polymeric matrix by solution casting. The mixed matrix membranes were assessed for CO_2 separation from CO_2/N_2 and CO_2/O_2 gas mixtures. The permeability of CO_2 decreased with increasing time and the selectivity of CO_2/O_2 was less than one. Phosphine oxide is expected to interact with CO_2 strongly. Therefore, according to membrane theory, the solubility of CO_2 in phosphine oxide polymer should be high, leading to increased permeability of CO_2. However, the results up to date are the opposite. See Fig. 2. Our next step is to fabricate membrane by incorporating high molecular weight polysulfones containing the phosphine oxide groups and investigate CO_2 separation.

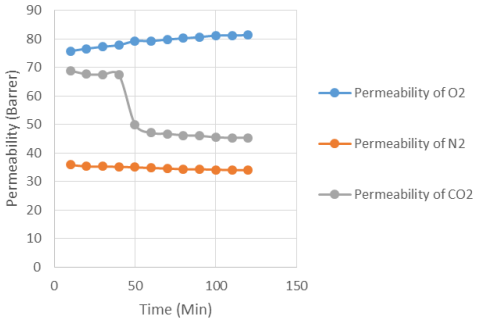

Figure 2: Transport pattern of O_2, N_2 and CO_2 through 10 wt. % Phosphine Oxide in Polyimide membrane.

5. Synthesis of porous metal-organic framework (MIL-101(Cr) and mesoporous silica (SBA-15) composites for CO_2 capture upon amine as well as phosphine impregnation. The composites resulted in efficient CO_2 capture from concentrated as well as dilute (400 ppm) gas streams. The composite showed enhanced mesopore volume of 1.62 cm^3/g compared to nascent MOF (0.65 cm^3/g). This increased the CO_2 adsorption to 2.1 mmol/g in case of MIL-101(Cr)/SBA-15 compared to nascent SBA-15 (0.8 mmol/g) and MIL-101(Cr) (1.3 mmol/g) at 303 K and 1 bar. See Fig. 3. The composite was impregnated with polyethyleneimine (PEI) which further increased the adsorption capacity to 3.2 mmol/g for pure CO_2 and 1.6 mmol/g for 400 ppm CO_2.This hierarchical composite will be further functionalized using the phosphine based compounds and used for CO_2 adsorption.

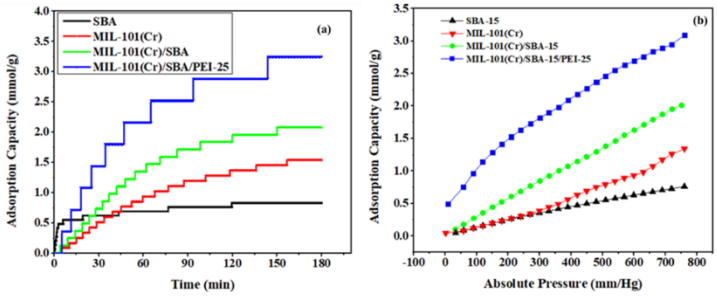

Figure 3: Pure CO_2 adsorption capacity estimated using (a) TGA; (b) BET of SBA-15, MIL-101(Cr), MIL-101(Cr)/SBA-15, MIL-101(Cr)/SBA-15/PEI-25

6. Electrochemical CO_2 reduction has been performed in a H type two-compartment cell containing Ag/AgCl reference electrode, Ag sheet as working electrode, platinum mesh as the counter electrode and 0.1M $KHCO_3$ as the electrolyte. Nafion-212 membrane was used between the junction of the anode and cathode. Reduction of CO2 using 0.1M KHCO3 solution within potential range varying from 1V to -1V RHE accompanied with successful chronoamperometry and CV curves were obtained. Phosphine based composites will be used as a working electrode in the future studies.

References

1. F. Buß, P. Mehlmann, C. Mück-Lichtenfeld, K. Bergander, F. Dielmann, *Reversible Carbon Dioxide Binding by Simple Lewis Base Adducts with Electron-Rich Phosphines,* Journal of the American Chemical Society, **138** (6), 1840-1843, (2016).
2. M. Abu-Zahra, L.H.J. Schneiders, JPM Niederer, PHM Feron, F. Geert, *CO_2 capture from power plants: Part I. A parametric study of the technical performance based on monoethanolamine,* International Journal of Greenhouse Gas Control, **1**, 37-46, (2007).
3. F. A. Chowdhury, H. Yamada, T. Higashii, K. Goto, M. Onoda, *CO_2 capture by tertiary amine absorbents: a performance comparison study,* Industrial & engineering chemistry research, **52** (24), 8323-8331, (2013).
4. K. M. G. Langie, K. Tak, C. Kim, H. W. Lee, K. Park, D. Kim, ……, Lee, U. *Toward economical application of carbon capture and utilization technology with near-zero carbon emission,* Nature Communications, **13** (1), 7482, (2022).

Publications

1. C. B. Musgrave III, A. Prokofjevs, and W. A. Goddard III, *Phosphine Modulation for Enhanced CO2 Capture: Quantum Mechanics Predictions of New Materials*. The Journal of Physical Chemistry Letters, **13**(48), 11183-11190 (2022).
2. D. Mukherjee, S. Hassan, J. Shajahan, A. Prokofjevs, D. Kuila, *Synergistic Enhancement of CO_2 Capture via Amine Decorated Hierarchical MIL-101(Cr)/SBA-15 Composites.* [Manuscript submitted]
3. M. Chowdhury, J. Lou, D. Kuila, "Separation of CO_2 and N_2 using polydimethylsiloxane mixed matrix membrane", Manuscript in preparation.

Design Exciton and Spin Functionalities in Halide Perovskite Epitaxial Heterostructures

Letian Dou and Libai Huang; Purdue University

Keywords: Halide Perovskites, Epitaxial growth, Exciton transport, Ultrafast Microscopy

Research Scope

Two-dimensional (2D) organic-inorganic halide perovskites have emerged as an exciting new class of optoelectronic materials, supporting strongly bound excitons with large oscillator strength.[1-8] The large spin–orbit coupling endowed by the heavy elements such as Pb also leads to great potentials for future spintronic and spin-optoelectronic applications.[9-13] These unique properties have inspired substantial research efforts in exploring exciton and spin properties in these materials in recent years. Their unique properties along with highly programmable structures make them great candidates for constructing heterostructures to control the dynamics and transport of both the charge and spin degrees of freedom. However, the current synthesis and characterization methods both lack the necessary precision for controlling the interfaces and interactions, hindering the realization of a "materials-by-design" approach for heterostructures based on 2D halide perovskites.

To bridge this research gap, we plan to develop well-controlled and atomically precise halide perovskite epitaxial heterostructures as a material platform for long-range exciton and spin transport. We will design lateral and vertical heterostructures to form interfacial excitons with long lifetimes and many-body interactions favorable for long-range transport. Furthermore, lattice symmetry and interfacial strain will be tuned synthetically to suppress spin relaxation and to enhance spin transport. The active feedback between materials synthesis and ultrafast microscopy measurements will elucidate structure-property relationship to provide guidelines for designing perovskite heterostructures for optoelectronic and spintronic applications.

Recent Progress

Over the past two years, we have carried out fundamental research on the synthesis and optical characterization of novel 2D halide perovskite heterostructures. Two representative works are discussed briefly below.

Two-dimensional perovskite crystals have attracted intensive interest for their diverse optoelectronic characteristics owing to their superior semiconducting properties. However, most studies to date have been limited to single crystals, which are difficult to implement into integrated device arrays due to their incompatibility with selective growth or typical lithography

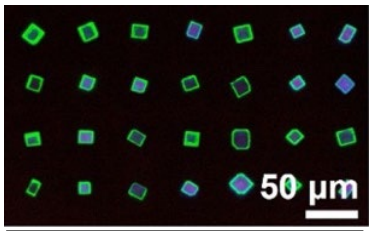

Fig. 1. PL image of the heterostructure 2D perovskite crystals array.

processes. In our recent work, we demonstrated a facile one-step solution process for synthesizing 2D perovskite crystal arrays through the meniscus-guided coating on patterned substrates (**Fig. 1**). We further utilize this novel method for the synthesis of lateral heterostructure crystal arrays. Six different 2D perovskite crystal arrays including epitaxial heterostructures are successfully realized. Structural and optical characterizations demonstrate that the crystals display excellent crystallinity and optical properties. Moreover, this method is further employed to prepare high-performance 2D perovskite crystal photosensor arrays. This strategy can be utilized as a guideline for the fundamental investigation of optical properties and development of high-performance optoelectronics of perovskite materials including photosensors and displays. (*ACS Nano* 2023, under revision)

In another work, we focused on vertical heterostructures of two thin 2D perovskites sheets and examined their twist-angle dependent excitonic properties. Moiré superlattices of 2D materials have recently emerged as a new platform for studying strongly correlated and topological quantum phenomena. 2D organic-inorganic halide perovskites with programmable structures and strongly bound excitons are excellent candidates for creating moiré structures featuring square lattices. Moiré flat bands have been predicted in twisted 2D perovskites; however, their experimental realization is absent owing to a variety of synthetic and fabrication challenges, including difficulties in creating a ultra-thin perovskite sheet free from bulky organic ligands, and in transferring and stacking of these thin sheets that have soft ionic lattices. In our recent work, we overcome these obstacles via a new synthetic pathway and demonstrate moiré superlattices based on twisted ultra-thin ligand-free 2D hybrid perovskites. Moiré superlattices are clearly visualized through high-resolution transmission electron microscopy (HRTEM) and moiré flat bands are revealed by density functional theory. (**Fig. 2a**) Localization of excitons and charge carriers by the moiré potential near a twist angle of 9~11° is observed using both transient photoluminescence microscopy and electrical characterizations, which are excellent agreements with theoretical calculations (**Fig. 2b**). Further, more than one order of magnitude enhancement of photoluminescence intensity is observed due to the increased density of states from the moiré flat bands. Different from previously reported twisted bilayers, moiré interactions in halide perovskites are long-range (beyond unit-cell-thick sheets), which is likely a result of the strong

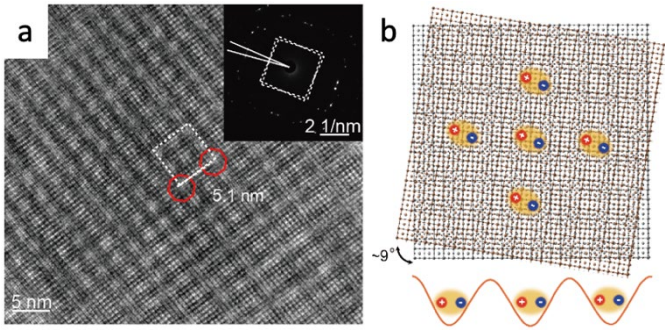

Fig. 2. (a) A high-resolution TEM image of twisted ligand-free 2D perovskite bilayers. (b) Illustration of localized moiré excitons in a 9° twisted bilayer heterostructure.

ionic interactions. Our findings provide a new tunable family of 2D ionic semiconducting materials for exploring moiré flat bands at room temperature. (Under revision)

References

1. Mitzi, D. B.: Synthesis, structure, and properties of organic-inorganic perovskites and related materials. In *Progress in Inorganic Chemistry*; Karlin, K. D., Ed.; John Wiley & Sons, Inc., 2007; pp 1-121.
2. Dou, L.; Wong, A. B.; Yu, Y.; Lai, M.; Kornienko, N.; Eaton, S. W.; Fu, A.; Bischak, C. G.; Ma, J.; Ding, T.; Ginsberg, N. S.; Wang, L. W.; Alivisatos, A. P.; Yang, P. Atomically thin two-dimensional organic-inorganic hybrid perovskites. *Science* 2015, *349*, 1518-1521.
3. Blancon, J. C.; Stier, A. V.; Tsai, H.; Nie, W.; Stoumpos, C. C.; Traoré, B.; Pedesseau, L.; Kepenekian, M.; Katsutani, F.; Noe, G. T.; Kono, J.; Tretiak, S.; Crooker, S. A.; Katan, C.; Kanatzidis, M. G.; Crochet, J. J.; Even, J.; Mohite, A. D. Scaling law for excitons in 2D perovskite quantum wells. *Nature Communications* 2018, *9*, 538.
4. Ishihara, T.; Takahashi, J.; Goto, T. Exciton state in two-dimensional perovskite semiconductor (C10H21NH3)2PbI4. *Solid State Communications* 1989, *69*, 933-936.
5. Meresse, A.; Daoud, A. Bis(n-propylammonium) tetrachloroplumbate. *Acta Crystallographica Section C* 1989, *45*, 194-196.
6. Mitzi, D. B.; Feild, C. A.; Harrison, W. T. A.; Guloy, A. M. Conducting tin halides with a layered organic-based perovskite structure. *Nature* 1994, *369*, 467-469.
7. Papavassiliou, G. C. Three- and low-dimensional inorganic semiconductors. *Progress in Solid State Chemistry* 1997, *25*, 125-270.
8. Kinigstein, E. D.; Tsai, H.; Nie, W.; Blancon, J.-C.; Yager, K. G.; Appavoo, K.; Even, J.; Kanatzidis, M. G.; Mohite, A. D.; Sfeir, M. Y. Edge States Drive Exciton Dissociation in Ruddlesden–Popper Lead Halide Perovskite Thin Films. *ACS Materials Letters* 2020, *2*, 1360-1367.
9. Jana, M. K.; Song, R.; Liu, H.; Khanal, D. R.; Janke, S. M.; Zhao, R.; Liu, C.; Valy Vardeny, Z.; Blum, V.; Mitzi, D. B. Organic-to-inorganic structural chirality transfer in a 2D hybrid perovskite and impact on Rashba-Dresselhaus spin-orbit coupling. *Nature Communications* 2020, *11*, 1757.
10. Long, G.; Jiang, C.; Sabatini, R.; Yang, Z.; Wei, M.; Quan, L. N.; Liang, Q.; Rasmita, A.; Askerka, M.; Walters, G.; Gong, X.; Xing, J.; Wen, X.; Quintero-Bermudez, R.; Yuan, H.; Xing, G.; Wang, X. R.; Song, D.; Voznyy, O.; Zhang, M.; Hoogland, S.; Gao, W.; Xiong, Q.; Sargent, E. H. Spin control in reduced-dimensional chiral perovskites. *Nature Photonics* 2018, *12*, 528-533.
11. Zhai, Y.; Baniya, S.; Zhang, C.; Li, J.; Haney, P.; Sheng, C.-X.; Ehrenfreund, E.; Vardeny, Z. V. Giant Rashba splitting in 2D organic-inorganic halide perovskites measured by transient spectroscopies. *Science Advances* 2017, *3*, e1700704.
12. Kagan, C. R.; Mitzi, D. B.; Dimitrakopoulos, C. D. Organic-Inorganic Hybrid Materials as Semiconducting Channels in Thin-Film Field-Effect Transistors. *Science* 1999, *286*, 945.
13. Lanty, G.; Jemli, K.; Wei, Y.; Leymarie, J.; Even, J.; Lauret, J.-S.; Deleporte, E. Room-Temperature Optical Tunability and Inhomogeneous Broadening in 2D-Layered Organic–Inorganic Perovskite Pseudobinary Alloys. *The Journal of Physical Chemistry Letters* 2014, *5*, 3958-3963.

Publications

1. Yoon Ho Lee, Jee Yung Park, Peiran Niu, Hanjun Yang, Dewei Sun, Libai Huang, Jianguo Mei and Letian Dou*, “One-Step Solution Patterning for Two-Dimensional Perovskite Nanocrystal Arrays”, *ACS Nano* 2023, under revision.

2. Shuchen Zhang, Linrui Jin, Yuan Lu, Linghai Zhang, Jiaqi Yang, Qiuchen Zhao, Dewei Sun, Joshua J. P. Thompson, Biao Yuan, Ke Ma, Akriti, Jee Yung Park, Yoon Ho Lee, Zitang Wei, Blake P. Finkenauer, Daria D. Blach, Sarath Kumar, Hailin Peng, Arun Mannodi-Kanakkithodi, Yi Yu, Ermin Malic, Gang Lu, Letian Dou*, Libai Huang*, "Square Moiré Superlattices in Twisted Two-Dimensional Halide Perovskites", Under revision.
3. Jee Yung Park, Ruyi Song, Jie Liang, Linrui Jin, Kang Wang, Shunran Li, Enzheng Shi, Yao Gao, Matthias Zeller, Simon J. Teat, Peijun Guo, Libai Huang*, Yong Sheng Zhao*, Volker Blum*, Letian Dou*, "Dimensionality-Controlled Organic Semiconductor-Incorporated Perovskite Quantum Wells", *Nature Chemistry* 2023, Accepted.
4. Ao Liu, Huihui Zhu*, Sai Bai, Youjin Reo, Mario Caironi, Annamaria Petrozza, Letian Dou, Yong-Young Noh*; "*Pursuing high-performance metal halide perovskite transistors*." *Nature Electronics* 2023, accepted.
5. Songhao Guo, Yahui Li, Yuhong Mao, Weijian Tao, Kejun Bu, Tonghuan Fu, Chang Zhao, Hui Luo, Qingyang Hu, Haiming Zhu, Enzheng Shi, Wenge Yang, Letian Dou*, Xujie Lü*; "Reconfiguring band-edge states and charge distribution of organic semiconductor–incorporated 2D perovskites via pressure gating" *Science Advances* 2022, 8, eadd1984.
6. Daria D Blach, Victoria A Lumsargis, Daniel E Clark, Chern Chuang, Kang Wang, Letian Dou, Richard D Schaller, Jianshu Cao, Christina W Li*, Libai Huang*; "Superradiance and Exciton Delocalization in Perovskite Quantum Dot Superlattices" Nano Letters 2022, 22, 7811-7818.
7. Colton Fruhling, Kang Wang, Sarah Chowdhury, Xiaohui Xu, Jeffrey Simon, Alexander Kildishev, Letian Dou, Xiangeng Meng, Alexandra Boltasseva, Vladimir M. Shalaev*; "Coherent Random Lasing in Subwavelength Quasi-2D Perovskites" Laser & Photonics Reviews 2023, 17, 2200314.
8. Kang Wang, Zih-Yu Lin, Zihan Zhang, Ke Ma, Aidan H. Coffey, Linrui Jin, Harindi R. Atapattu, Yao Gao, Jee Yung Park, Zitang Wei, Blake P. Finkenauer, Chenhui Zhu, Xiangeng Meng, Sarah N. Chowdhury, Zhaoyang Chen, Tauguy Terlier, Yan Yao, Kenneth R. Graham, Alexandra Boltasseva, Tzung-Fang Guo, Libai Huang, Hanwei Gao, Brett M. Savoie, Letian Dou*, "Suppressing Phase Disproportionation in Quasi-2D Perovskite Light-Emitting Diodes", *Nature Communications 2023, 14, 397. (Featured in Editor's Highlight*)
9. Wenhao Shao, Seok Joo Yang, Kang Wang, Letian Dou*; "Light-Emitting Organic Semiconductor-Incorporated Perovskites: Fundamental Properties and Device Applications" The Journal of Physical Chemistry Letters 2023, 14, 2034-2046.
10. Ke Ma, Jiaonan Sun, Harindi R. Atapattu, Bryon W. Larson, Hanjun Yang, Dewei Sun, Ke Chen, Kang Wang, Yoonho Lee, Yuanhao Tang, Anika Bhoopalam, Libai Huang, Kenneth R. Graham, Jianguo Mei, Letian Dou*; "Holistic energy landscape management in 2D/3D heterojunction via molecular engineering for efficient perovskite solar cells." *Science Advances* 2023, 9, eadg003.

Research Project on the Recruitment, Retention and Promotion of Women in STEM Fields

Jean Stockard, PhD., Professor Emerita, Interim Co-Director COACh

Keywords: Graduate education, research, Women in Chemistry, Minorities in Chemistry, Professional Development

Research Scope

Recent events prompted scientist in the United States and throughout the world to consider how systematic racism and gender inequities are affecting the scientific enterprise. This is happening at a time when our domestic talent pool in STEM fields continues to be inadequate in developing the solutions that we face in areas such a climate change, new technologies and infectious diseases. The country and the STEM enterprise needs to make a more concerted effort in the recruitment and retention of all the talent that this country has to offer. Given that a significant fraction of the research and development that the Department of Energy (DOE) supports occurs in research universities and its National Laboratories, DOE has a vested interest in making certain that we are recruiting adequate talent for its energy research effort, and to provide an environment that will allow all creative ideas to flourish and innovation to emerge in unexpected areas.

The primary objective of this project is aiding the Department of Energy's efforts in recruiting a science and engineering workforce that mirrors the demographics of this country. This proposal requests funding for important and high-impact research-based projects conducted by the COACh organization at the University of Oregon that focuses on increasing the number, retention and career success of women and other underrepresented groups in both academic institutions and the DOE laboratories. Fueled by funding from the DOE Basic Energy Sciences since 2000, the Committee on the Advancement of Women Chemists (COACh) has grown into an internationally recognized organization that has had a positive impact on the careers of over 25,000 scientists and engineers in fields that include chemistry, physics, engineering, math, computer science, materials science, geology and biology.

This project supports important and high-impact research-based projects that are aimed at (1) supporting, evaluating and improving COACh programs, (2) understanding the issues that are leading to the continuing low percentage of STEM women and URMs in our academic institutions, our national laboratories, and at different stages of the career path, (3) examining the impact of COVID-19 on career plans and aspirations of STEM women and URMs, (4) providing data-driven mentorship programs to assist STEM women and URMs in navigating and succeeding in often hostile environments, (5) continuing research and coaching efforts at the DOE national laboratories, (6) expansion of virtual COACh career workshops and the COACh-the-COACHes

program in partnership with academic departments, national laboratories, and professional societies and (7) continued development and expansion of COACh networking and mentoring activities through outreach and social media.

The research and outreach activities will be conducted by the experienced COACh social science research team and COACh Advisory Board members consisting of leading women STEM researchers and educators. This effort is in partnership with the leadership ranks of the Department of Energy Laboratories. In the academic arena COACh will continue its related survey and data collection efforts including assessment of its career building programs for underrepresented groups, partnering with academic institutions and professional societies.

Recent Progress

COACh outreach activities have been increasing since COVID-19, more in-person workshops are being scheduled at professional society meetings, academic institutions, and government laboratories. Virtual presentations have been held as well.
Details of the current status of each of the research-related activities follow:

1 – Evaluations of workshops: This crucial element of COACh's work has encompassed there areas: First, the surveys used to evaluate the short-term impact of COACh-sponsored workshops have been revised using a format that can be adapted for each workshop topic. Second, in winter 2023, we conducted the third study of the long-term impact of COACh, and data analysis is proceeding. Third, we completed a COACh technical report (Stockard 2022) that summarizes feedback from participants in workshops in Africa. Completion of a research article that combines findings from all the international COACh workshops is planned for completion in 2023 or 2024.

2 – Graduate Student Experiences and concerns: Our work related to graduate student experiences, using data gathered by the American Chemical Society (ACS) in 2013 (Stockard, et al. 2021; Stockard et al., 2022; Rohlfing, et al, 2022) continues to receive attention, with an invited presentation at the 2022 Biennial Conference on Chemistry Education and an interview for a video channel dedicated to promoting interests in STEM among teen-agers and young adults. In spring 2023 the ACS agreed to provide access to data gathered from graduate students in 2019, and analysis of these data is proceeding. The analysis focuses on comparing student views with those given in 2013 and with data that we gathered in the fall of 2022, as described below. Preliminary results of these analyses are included in a presentation at the Gordon Conference in July 2023 (Stockard 2023).

3 –COVID-related work - Research related to the impact of the COVID-19 pandemic has involved two avenues. First, as anticipated in the proposal, we have surveyed former COACh participants from around the world regarding the impact of the COVID-pandemic on their professional lives. Data collection ceased in the spring of 2023 and analysis is proceeding. Second, in response to a request from the ACS, we conducted a survey of graduate students in the chemical sciences

regarding the impact of the pandemic on their educational experience and career plans. The survey was distributed in fall of 2022. Results of the survey and comparisons to the data gathered in 2013 and 2019 are summarized in a COACh technical report (Stockard, et al. 2023) and included in the presentation to the Gordon Conference (Stockard 2023). It is anticipated that articles from these works will be submitted for publication within the coming year.

4. Experiences of Post-Doctoral Fellows – While the original proposal called for COACh to gather data from post-doctoral fellows, we plan, instead, to examine data gathered by the ACS from fellows in 2019. These data have not yet been analyzed, and understanding findings from that work is essential before proceeding with any additional surveys.

References

1. The National Laboratories Diversity & Inclusion. https://nationallabs.org/staff/diversity/ (accessed August 5, 2018.)
2. How Diversity Makes Us Smarter. https://www.scientificamerican.com/article/how-diversity-makes-us-smarter/ (accessed August 14 2018).
3. Digest of Education Statistics 2015. https://nces.edu.gov/pubs2016/2016014.pdf (accessed August 5, 2018 2018).
4. *To Recruit and Advance Women Students and Faculty in U.S. Science and Engineering*; National Academy Press: Washington, DC, 2006.
5. To Advance Science, It's time to Tackle Unconscious Bias. https://www.livescience.com/55026-scientists-tackle-unconscious-bias.html (accessed August 13 2018).

Publications

1. J. Stockard, M. Noviski, C. M. Rohlfing, G. Richmond., P. Lewis, "The Chemistry Graduate Student Experience: Findings from an ACS Survey." *Journal of Chemical Education*, 2022, 99(1), 461-468 (on web October 28,2021), DOI: 10.1021/acs.jchemed.1c00610
2. C. M. Rohlfing, G. Richmond., M. Noviski, P. Lewis, J. Stockard,"Policies and Practices to Improve the Chemistry Graduate Student Experience: Implications of the ACS Survey of Graduate Students.", *Journal of Chemical Education.* 2022, 99 (1), pp. 10-13; on web October 29, 2021, DOI: 10.1021/acs.jchemed.1c00611
3. J. Stockard, C. M. Rohlfing, G. Richmond "Equity for Women and Underrepresented Minorities in STEM: Graduate Experiences and Career Plans.", *Proceedings of the National Academy of Science*, 2021, 118(4), https://doi.org/10.1073/pnas.2020508118
4. G. Richmond, C. M. Rohlfing, J. Stockard, J. Tucker, B. Butterfield, M. Noviski, P. Lewis , *"Needed Improvements in Standards and Transparency for Staff Promotion". 2021.* National Institute of Standards and Technology. NIST GCR 21-029, (Chapters 2-7) https://doi.org/10.6028/NIST.GCR.21-029

COACh Reports:

1. The Impact of the COVID-19 Pandemic on Graduate Students and Programs in the Chemical Science: Results from an ACS-Sponsored Survey – June 2023 – A COACh technical report
2. Stockard, J. 2022. COACh Workshops in Africa: An Analysis of Feedback from Participants. University of Oregon: COACh Technical Report.

When Covalent Organic Frameworks Meet Cross-coupling Reactions: Directed Synthesis, Mechanistic Investigation, and Energy Application

Xinle Li, Clark Atlanta University

Keywords: covalent organic frameworks; topochemical polymerization; cross-coupling reaction; irreversible reaction; photocatalysis

Research Scope

The objective of this research is to translate irreversible cross-coupling reactions into the realm of covalent organic frameworks (COFs) through a feedback loop of topochemical synthesis, mechanistic investigation, and photocatalytic application. The goal is to free bulk COF synthesis from the constraints of reversible reactions. Toward this goal, structurally analogous COFs are employed as templates to reticulate monomers through cross-coupling reactions, giving rise to as-yet-undiscovered robust COFs. To expedite the condition screening process and circumvent the lengthy reaction time (typically 3 days) associated with the traditional solvothermal synthesis of COFs, microwave-assisted and mechanochemical synthesis techniques have been employed. These resulting COFs have exhibited exceptional activity in photocatalysis, surpassing the performance of their COF templates. Alongside directed synthesis, the research aims to unravel the formation mechanism of novel COFs using a combination of experimental and computational approaches, such as *ex situ* kinetic studies and computational simulations. This research aligns directly with the Material Chemistry Program in Basic Energy Sciences (BES) as it seeks to produce new COFs by gaining mechanistic insights and precise control over synthetic pathways.

Recent Progress

We have for the first time established a versatile template-directed methodology, enabling the synthesis of bulk sp^2c-conjugated COFs (sp^2c-COFs) using the classic irreversible cross-coupling reaction, Heck reaction. In this work, we employed a structurally analogous imine-linked COF as a seed and template to guide the nucleation and polymerization of a C3-symmetric knot and a C2-symmetric linker. Subsequently, we selectively etched the template, resulting in the formation of new sp^2c-COFs. Notably, template-free polymerization only yielded amorphous polymers, highlighting the significance of the template in achieving the desired COF structures. We have conducted thorough characterizations of the obtained novel sp^2c-COFs (termed Heck-CAU-COF-1). Solid-state ^{13}C NMR and FTIR analyses confirmed the removal of the imine COF template. Scanning electron microscopy showed that Heck-CAU-COF-1 adopted a dramatically different morphology compared to the imine COF template. In addition, the chemical stability of CAU-COF-1 was far superior to the imine COF template. Heck-CAU-COF-1 retained the PXRD

pattern after being treated in hexylamine at 120 °C for 3 hours, whereas the imine COF was completely degraded, highlighting the superiority of olefin linkage over imine.[2]

In investigating the formation mechanism underlying the template-directed methodology, we discovered that the pore size of the COF template plays a crucial role in the synthesis of sp^2c-COFs. Smaller-pore-sized COF templates failed to yield the desired sp^2c-COFs. Furthermore, the obtained Heck-CAU-COF-1 exhibited remarkable efficiency (>99% yield in 2 hours) for the oxidative hydroxylation of various substituted arylboronic acids using blue light (450 nm) at room temperature, with air as the oxidant, N, N-diisopropylethylamine as the sacrificial agent, and acetonitrile as the solvent. They outperformed most reported imine COFs,[3] benzoxazole COFs,[4,] and olefin-linked COFs.[5]

This study not only establishes a versatile synthetic toolkit for the synthesis of unprecedented sp^2c-COFs but also highlights their immense potential for energy applications. Ongoing efforts are focused on expanding the scope of this unique strategy, providing molecular-level mechanistic insights into the photocatalytic properties of sp^2c-COFs, and unraveling the detailed mechanisms of COF formation.

References

1. E. Jin, K. Geng, K. H. Lee, W. Jiang, J. Li, Q. Jiang, S. Irle and D. Jiang, Topology-templated synthesis of crystalline porous covalent organic frameworks, *Angew. Chem. Int. Ed.*, **132**, 12260-12267 (2020).
2. X. Li, sp^2 carbon-conjugated covalent organic frameworks: synthesis, properties, and applications, *Mater. Chem. Front.*, **5**, 2931-2949 (2021)
3. X. Yan, H. Liu, Y. Li, W. Chen, T. Zhang, Z. Zhao, G. Xing and L. Chen, Ultrastable Covalent Organic Frameworks via Self-Polycondensation of an A2B2 Monomer for Heterogeneous Photocatalysis, *Macromolecules*, **52**, 7977-7983 (2019).
4. P.-F. Wei, M.-Z. Qi, Z.-P. Wang, S.-Y. Ding, W. Yu, Q. Liu, L.-K. Wang, H.-Z. Wang, W.-K. An, and W. Wang, Benzoxazole-Linked Ultrastable Covalent Organic Frameworks for Photocatalysis, *J. Am. Chem. Soc.*, **140**, 4623-4631 (2018).
5. S. Bi, P. Thiruvengadam, S. Wei, W. Zhang, F. Zhang, L. Gao, J. Xu, D. Wu, J.-S. Chen and F. Zhang, Vinylene-Bridged Two-Dimensional Covalent Organic Frameworks via Knoevenagel Condensation of Tricyanomesitylene, *J. Am. Chem. Soc.*, **142**, 11893-11900 (2020).

Publications

1. Ziad Alsudairy, Normanda Brown, Chongqing Yang, Songliang Cai, Fazli Akram, Abrianna Ambus, Conrad Ingram, and Xinle Li. Facile Microwave-Assisted Synthesis of 2D Imine-Linked Covalent Organic Frameworks for Exceptional Iodine Capture, *Precision Chemistry*, 2023, https://doi.org/10.1021/prechem.3c00006
2. Ziad Alsudairy, Normanda Brown, Allea Campbell, Abrianna Ambus, Bianca Brown, Kayla Smith-Petty, and Xinle Li. Covalent Organic Frameworks in Heterogeneous Catalysis: Recent Advances and Future Perspective, *Materials Chemistry Frontiers*, 2023, DOI: 10.1039/D3QM00188A.

Multi-Scale Study of Self-Healing Polymers to Enhance Carbon Dioxide Removal

Jihong A. Ma, University of Vermont (UVM)

Jason E. Bara, University of Alabama (UA)

Dryver Huston, University of Vermont (UVM)

Keywords: Self-Healing Polymers, Polymer Synthesis, Simulation, Characterization, Gas Transport

Research Scope

In this proposed project, we set our overarching goal to enhance carbon dioxide (CO_2) capture capabilities by using high-performance self-healing (SH) polymers as gas separation membranes with optimized polymer structures. This study seeks to develop durable, high-performance CO_2 separation systems by obtaining an atomistic understanding of the gas transport and SH mechanisms of a group of polyamide ionene (PA-ionene) membranes, which have been designed to be able to self-heal upon mechanical wear and tear (e.g., punctures, tears), and to possess high CO_2 permeability and selectivity relative to other gases [1].

To achieve our overarching goal, we will address the three specific objectives to establish a composition-structure-property relationship of PA-ionene membranes by building upon an existing collaboration between the University of Vermont (UVM), University of Alabama (UA), and Oak Ridge National Laboratory (ORNL).

Objective 1 - Establish the relationship between the chemical compositions of SH PA-ionenes and their dynamic structural information.

Objective 2 - Identify the gas transport and SH mechanisms of PA-ionenes using the structural information acquired from Objective 1.

Objective 3 – Understand extreme operation conductions, such as creep and cyclic loads, on the structure and performance of PA-ionene membranes.

Our long-term goal is to establish a multi-scale framework from fundamental materials discovery to industrial-level applications.

Recent Progress

We have conducted a combination of polymer synthesis and atomistic simulations to establish the composition-structure-property relationship of PA-ionene membranes to mainly achieve Objective 1. Specifically, PI Bara at UA has successfully synthesized our proposed PA-ionene containing a spirobisindane (SBI), which has been associated with polymers of intrinsic microporosity (PIMs). The molecular structure of the first PA-ionene backbone is shown in Fig. 1. The polymer was thoroughly characterized via NMR, while MALDI-TOF MS indicated that the

number average molecular weight (MN) was 43.5 kDa. Digital photographs of the membranes are shown in Fig. 2.

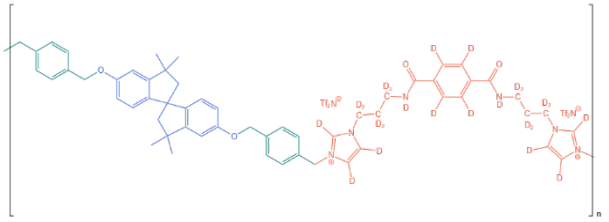

Figure 1. Example of PIM-PA-ionene bearing high permeability SBI segments (blue) and self-healing segments (red) with linking groups (green).

We found that the addition of "free" ionic liquid (IL) ([C_4mim][Tf_2N]) has the effect of increasing membrane flexibility (with an associated decrease in glass transition temperature). The combination of amide H-bonding and ionic interactions has been postulated to be responsible for the SH behaviors [3]. The first gas permeability studies are currently underway. The team at UA is also testing the mechanical properties of the materials, enabled by 3D printing of tensile bars.

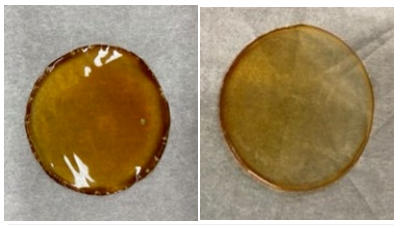

Figure 2. Photographs of 60 mm diameter membranes formed from the PA-ionene. The neat polyme is shown on the left, and the polymer + 1.0 molar equivalents of added IL is shown on the right.

PI Ma at UVM and her ORNL collaborator, Dr. Stephan Irle, conducted a computational methodology study to confirm the applicability of the proposed atomistic simulation method to the ionic polymeric systems of interest, *i.e.*, the linear-scaling fragment molecular orbital (FMO) based on long-range corrected (LC) density-functional tight-binding (DFTB) theory, or the FMO-LC-DFTB method [4], which is proposed to be highly suitable for studying PIM-PA-ionenes, as the FMO linear-scaling methodology allows for large-scale full quantum-chemical MD simulations of up to one million atoms within weeks [5].

Meanwhile, to avoid delays in the computational effort, large-scale molecular dynamics (MD) simulations using LAMMPS on PA-ionenes with and without the PIM parts with various chain lengths have been performed by PI Ma and her graduate student. The density of the PA-ionenes obtained from the MD simulations agrees very well with the one experimentally measured by the UA team. Additionally, the MD simulations reveal that the spirobisindane (aka "PIM") part of the polymer creates 30-40% fractional free volume (FFV), indicating a likelihood of achieving a high CO_2 permeability. We also reveal that the density of the PA-ionenes decreases as temperature increases, while that of the PIM-PA-ionene presents a reversed trend, as shown in Fig. 3. Our structural analysis via radial distribution function calculation reveals that the spacings of imidazolium decrease as the temperature increases. Experimental validation is underway.

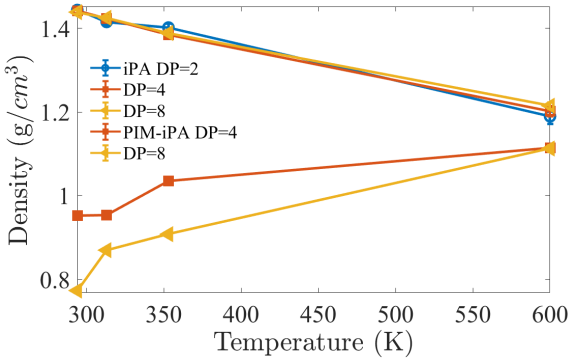

Figure 5. Density change with temperature for different polymers (iPA and PIM-iPA) with different degrees of polymerization (DP).

References

1. K. E. O'Harra, I. Kammakakam, D. M. Noll, E. M. Turflinger, G. P. Dennis, E. M. Jackson, and J. E. Bara, *Synthesis and Performance of Aromatic Polyamide Ionenes as Gas Separation Membranes*, Membranes **10**, 51 (2020).
2. I. Kammakakam, K. E. O'Harra, J. E. Bara, and E. M. Jackson, *Spirobisindane-Containing Imidazolium Polyimide Ionene: Structural Design and Gas Separation Performance of "Ionic PIMs*," Macromolecules **55**(11), 4790-4802 (2022).
3. A. Abedini, E. Crabtree, J. E. Bara, and C. H. Turner, *Molecular simulation of ionic polyimides and composites with ionic liquids as gas-separation membranes*, Langmuir **33**(42), 11377-11389 (2017).
4. V. Q. Vuong, Y. Nishimoto, D. G. Fedorov, B. G. Sumpter, T. A. Niehaus, and S. Irle, *The Fragment Molecular Orbital Method Based on Long-Range Corrected Density-Functional Tight-Binding*, Journal of Chemical Theory and Computation **15**, 3008 (2019).
5. Y. Nishimoto, H. Nakata, D. G. Fedorov, and S. Irle, *Large-Scale Quantum-Mechanical Molecular Dynamics Simulations Using Density-Functional Tight-Binding Combined with the Fragment Molecular Orbital Method*, The Journal of Physical Chemistry Letters **6**, 5034 (2015).
6. A. P. Thompson, H. M. Aktulga, R. Berger, D. S. Bolintineanu, W. M. Brown, P. S. Crozier, P. J. in't Veld, A. Kohlmeyer, S. G. Moore, T. D. Nguyen, R. Shan, M. J. Stevens, J. Tranchida, C. Trott, and S. J. Plimpton, *LAMMPS-a flexible simulation tool for particle-based materials modeling at the atomic, meso, and continuum scales*, Computer Physics Communications **271**, 108171 (2022).

Publications

Project awarded in 10/2022. No publications yet.

Materials and Interfacial Chemistry for Next-Generation Electrical Energy Storage

John B. Goodenough and Arumugam Manthiram, University of Texas at Austin

Keywords: sodium-ion cells, sodium-sulfur cells, solid-state cells, interface, single crystals

Research Scope

With growing demand for energy storage and global supply-chain challenges, we must look for alternative battery chemistries free from lithium and other scarcely available metals. Sodium-based cell chemistries are appealing in this regard, but they are met with numerous basic science challenges. The goal of this project is to develop an in-depth understanding of the materials and interfacial chemistry of sodium-based batteries. The project currently focuses on (i) delineating the relationships among surface facets, reactivity, and particle cracking in layered sodium oxides, (ii) interfacial control with advanced electrolytes in sodium-based cells, and (iii) solid-state sodium cells with polymer-ceramic composite and oxysulfide glassy solid electrolytes.

Recent Progress

Layered Cathodes: Layered Na_xMO_2 (M = transition metal and $0 < x \leq 1$) with high electronic and ionic conductivity are promising, but they suffer from fast capacity fade due to phase transitions and particle cracking. To overcome this challenge, we synthesized single crystals of both O3-type and P2-type Na_xMO_2 and assessed the effects of intragranular vs. intergranular cracks on capacity fade. Single-crystal particles showed improved cyclability, suggesting that intragranular cracking is the dominant degradation mechanism.[1]

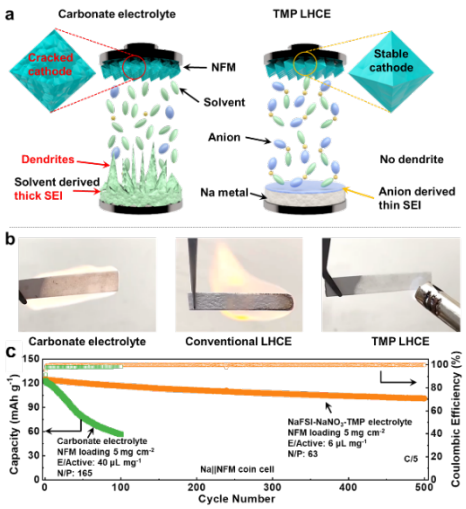

Figure 1: (a) Stabilization mechanisms of TMP-based LHCE with coordinated solvent. (b) Flammability test for the electrolytes. (c) Cycling data of Na | NFM343 cells.

Parasitic surface reactions with electrolyte is another significant degradation pathway. Localized high concentration electrolytes (LHCEs) use an inert liquid diluent to form a fluid solvation complex and create stable solid-electrolyte interfaces (SEIs), but the liquid diluents used are often highly flammable and expensive. We instead used $NaNO_3$ as an inexpensive solid diluent with sodium bis(fluorosulfonyl)imide (NaFSI) in trimethyl phosphate (TMP). The LHCE solvation structure of the $NaNO_3$-NaFSI-TMP electrolyte was confirmed with FTIR and ^{31}P NMR spectroscopies. Cells with the developed LHCE, layered $NaNi_{0.3}Fe_{0.4}Mn_{0.3}O_2$ (NFM343) cathode, and Na-metal anode exhibited superior cyclability due to the stable SEI formed on both

electrodes as revealed by time-of-flight secondary ion mass spectrometry (TOF-SIMS) (**Figure 1a,c**). Additionally, our designed electrolyte is nonflammable in contrast to the highly flammable carbonate electrolytes and the conventional LHCE (**Figure 1b**).[2]

Sodium-Sulfur Cells: Sodium-sulfur cells are a low-cost option, but they suffer from Na dendrites and polysulfide (PS) shuttling.[3] To address these issues, we developed an intercalation-conversion hybrid material based on $MoTe_2$-graphene sheet (MTG) that suppresses PS shuttling and improves the sulfur redox kinetics. The MTG not only functions as adsorptive sites to chemically confine sulfur species and catalyze the sulfur conversion reaction, but also offers enhanced ion mobility for the sulfur redox reaction (**Figure 2 a-b)**. Additionally, we have developed a novel electrolyte by incorporating bismuth triflate and 1,3,2-dioxathiolane 2,2-dioxide (DTD) into a conventional ether-based electrolyte that is compatible with both Na-metal anode and sulfurized polyacrylonitrile (SPAN) cathode (**Figure 2c-d**). Bismuth triflate enables a facile dissolution of sodium triflate based on a salt-in-solvent mechanism and effectively prevents the decomposition of the solvent and additive.

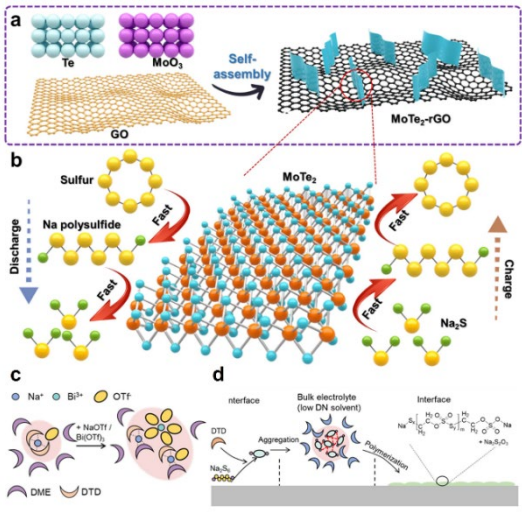

Figure 2. (a) Illustration of the synthetic route for MTG and (b) fast electrochemical reaction kinetics of Na-S cells with MTG. (c) Illustration of the solvation structure induced by Bi^{3+} cation and (d) CEI formation process in DME-based solvent.

Solid-State Cells: Development of optimal solid-state electrolytes (SSE) is critical to tap the full potential of solid-state cells. With this goal, we have developed fiber-based composite solid electrolytes to obtain thin, flexible, large area format SSE separators. We obtained them by infiltrating a polyethylene glycol diacrylate (PEGDA)-based solution into a glass-fiber paper and polymerizing with UV-light. The use of PEG plasticizer and NaFSI salt was found to form stable electrode interfaces, suppress dendrites, and enable cell cycling with layered $Na_{0.67}Ni_{0.33}Mn_{0.67}O_2$ cathode and Na-metal anode. In addition, we have investigated the effects of glassy $Na_{2x}PO_{2.5+x}$ precursors on the synthesis and properties of oxysulfide $Na_3PS_{4-x}O_x$ glassy solid electrolytes. Raman and ^{31}P NMR spectroscopies reveal the glass is comprised of both PS_4^{3-} and PS_3O^{3-} anions, which is critical for performance and electrochemical stability.[4]

Future Work

- Molten-salt synthesis of doped oxides, Na-ion dynamics in SSEs with ^{23}Na MAS NMR, Na-S cell interfaces with $Na_3PS_{4-x}O_x$ SSEs, and catalytic effects of cathode on SSE degradation.

References

1. K. Wang, P. Yan, and M. Sui, *Phase Transition Induced Cracking Plaguing Layered Cathode for Sodium-ion Battery*, Nano Energy **54,** 148-155 (2018).
2. A. Swiderska-Mocek, P. Jakobczyk, E. Rudnicka, and A. Lewandowski, *Flammability Parameters of Lithium-ion Battery Electrolytes*, Journal of Molecular Liquids **318**, 113986 (2020).
3. A. Bhargav and A. Manthiram, *Li-S batteries, What's Next?*, Next Energy **1**, 100012 (2023).
4. X. Chi, Y. Zhang, F. Hao, S. Kmiec, H. Dong, R. Xu, K. Zhao, Q. Ai, T. Terlier, L. Wang, L. Zhao, L. Guo, J. Lou, H. L. Xin, S. Martin and Y. Yao, *An Electrochemically Stable Homogeneous Glassy Electrolyte Formed at Room Temperature for All-Solid-State Sodium Batteries,* Nature Communications **13**, 2854 (2022).

Publications

1. S. Nanda and A. Manthiram, *Delineating the Lithium-electrolyte Interfacial Chemistry and the Dynamics of Lithium Deposition in Lithium-sulfur* Batteries, Advanced Energy Materials **11**, 2003293: 1-13 (2021).
2. J. He, A. Bhargav, W. Shin, and A. Manthiram, *Stable Dendrite-Free Sodium–Sulfur Batteries Enabled by a Localized High-Concentration Electrolyte*, Journal of the American Chemical Society **143**, 20241-20248 (2021).
3. J. Lamb and A. Manthiram, *Stable Sodium-based Batteries with Advanced Electrolytes and Layered-oxide Cathodes*, ACS Applied Materials & Interfaces **14**, 28865–28872 (2022).
4. D. Guo, D. B. Shinde, W. Shin, E. Abou-Hamad, A.-H. Emwas, Z. Lai, and A. Manthiram, *Foldable Solid-state Batteries Enabled by Electrolyte Mediation in Covalent Organic Frameworks*, Advanced Materials **34***,* 2201410: 1-19 (2022).
5. H. Sul, A. Bhargav, and A. Manthiram, *Sodium Trithiocarbonate Cathode for High-performance Sodium-sulfur Batteries*, Journal of Materials Chemistry A **11**, 130-140 (2022).
6. R. Fang, Y. Li, N. Wu, B. Xu, Y. Liu, A. Manthiram, and J. B. Goodenough, *Ultra-thin Single-particle-layer Sodium Beta-alumina-based Composite Polymer Electrolyte Membrane for Sodium-metal Batteries,* Advanced Functional Materials **33**, 2211229 (2022).
7. J. Darga and A. Manthiram, *Facile Synthesis of O3-type $NaNi_{0.5}Mn_{0.5}O_2$ Single Crystals with Improved Performance in Sodium-ion Batteries,* ACS Applied Materials & Interfaces **14**, 52729-52737 (2022).
8. D. Guo, J. Wang, T. Lai, G. Henkelman, and A. Manthiram, *Electrolytes with Solvating Inner Sheath Engineering for Practical Na-S Batteries,* Advanced Materials **35**, 2300841: 1-9 (2023).
9. S. Kmiec, E. Ruoff, J. Darga, A. Bodratti, and A. Manthiram, *Scalable Glass-fiber-polymer Composite Solid Electrolytes for Solid-state Sodium-metal Batteries,* ACS Applied Materials & Interfaces, **15**, 20946-20957 (2023).
10. Y Ren, T. Lai, Su, and A. Manthiram, *High-performance Sodium-sulfur Batteries enabled by a Moderately Concentrated Ether-based Electrolyte with a Synergistic Dual Additive,* ACS Energy Letters, **8**, 2746-2752 (2023).

Dynamic Properties of Nanostructured Porous Materials

Adam J. Matzger; Department of Chemistry and the Macromolecular Science and Engineering Program; University of Michigan; 930 North University Avenue, Ann Arbor, MI 48109-1055

Keywords: metal-organic frameworks, coordination chemistry, adsorbents, separations, gas storage materials

Research Scope

The overarching goal for this project is to develop an enhanced understanding of dynamic phenomena in metal-organic frameworks (MOFs), and to harness this knowledge to explain and optimize MOF creation and behavior.

Recent Progress

The activation of MOFs to access permanent porosity has been a central challenge in the field and a major focus of our work over the years of DOE-BES support. Activation is a two-step process that involves solvent exchange and solvent evacuation in order to access the porosity of the MOF. Many reports in the literature have expressed preference for low boiling point – low surface tension solvents because of the delicacy and thermal sensitivity of some structures. Dimethyl ether (DME) presents itself as an attractive activation solvent due to its low boiling point and low surface tension, along with its ability to displace solvents that are in the pores and/or coordinated to the framework (these latter MOFs are referred to as CUS-MOFs).[1]

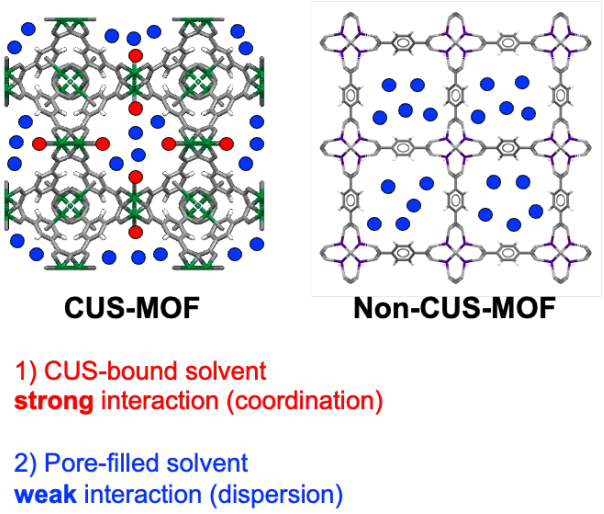

We demonstrated during this last project period that exchange and evacuation with dimethyl ether allows for the reproducible activation of HKUST-1 at a much reduced temperature 120 °C.[2] Encouraged by these results, we have now explored other thermally sensitive- high surface area MOFs that could not previously be activated by existing methods. These systems include DUT-34 and UMCM-151. In the case of DUT-34 other employed methods, including the previous state-of-the-art method of supercritical CO2 treatment, result in the collapse of the MOF, but using DME yields an average surface area of 1600 m2/g. This is the difference between being able to achieve a high surface area MOF with potential for selective separations and catalysis vs. a collapsed structure of little practical use. UMCM-151 was first reported in our laboratory in 2010[3] and we were never able to activate the

material substantially with existing methods. Through comparison of activation methods: conventional solvent exchange, supercritical CO2, and DME the following surface areas were obtained: 263, 455, and 950 m2/g respectively. These data further validate that this new method can outcompete existing activation techniques. The simplicity of the methods means that it will be simple for other labs to implement. The solvent also has shown special efficacy for MOFs with coordinatively unsaturated metal sites, creating more candidates for activation that once appeared impossible. Furthermore, this method has also shown applicability towards both micro- and mesoporous systems. This method is the culmination of years of research under DOE-BES support and represents the best method for activating some of the most troublesome MOFs, those with CUS, providing a path to further elevate the performance of MOFs that are central for hydrogen storage and selective separations mediated by metal cluster coordination.

In addition to understanding the final exchange step and ultimate evacuation of MOFs to reveal porosity, we have examined the step of exchanging out synthesis solvent. As the most prominent example of a MOF with a copper paddlewheel, HKUST-1 was investigated to elucidate the exchange kinetics at this common metal cluster. During solvent exchange. The rate of solvent exchange of HKUST-1 from N,N-dimethylformamide (DMF) to ethanol (EtOH) was compared to the rate of exchange of DMF to dichloromethane (DCM). The concentration of DMF in the solution above the MOF crystals was monitored to quantify the release pattern of DMF out of MOF through spectroscopic measurement to track the exchange process via in situ Raman and ^{1}H NMR spectroscopy. Exchange kinetics in a single MOF crystal was also monitored during replacement of the synthesis solvent based on the change in Cu^{2+} coordination that occurs upon the exchange of solvent at the copper paddlewheel. Further, the quantity of remnant DMF was analyzed through ^{1}H NMR spectroscopy of digested HKUST-1 after solvent exchange. Ultimately it is the amount of residual solvent that is particularly important to ensure that MOF activation is complete and, therefore, that properties of the MOF will be optimal. The change in CUS coordination environment is elucidated directly by tracking the shift in the Cu–Cu stretch of a single crystal during solvent exchanges, which shows the inability of DCM to replace DMF at the paddlewheel, but displays the coordination environment change in EtOH exchange. This spectroscopic observation agrees with residual solvent analysis on bulk samples. The rate law of DMF release from the framework follows first order kinetics for DCM exchange and zero order kinetics for EtOH exchange. This indicates that the pore-filled solvent exchange is dependent on the concentration of DMF in pores, but the exchange of CUS-solvent is independent of the concentration of CUS-bound DMF. The insights gained in this study provide a basis for understanding solvent exchange in MOFs more broadly since the copper paddlewheel motif is among the most common; implementing robust exchange protocols informed by mechanism is a crucial step for maximizing the surface area and harnessing the full application potential of MOFs.[4,5]

References

1. Boissonnault, J. A.; Wong-Foy, A. G.; Matzger, A. J., “Purification of Chloromethane by Selective Adsorption of Dimethyl Ether on Microporous Coordination Polymers” Langmuir, 2016, 32, 9743-9747..
2. Wright, K. R.; Nath, K.; Matzger, A. J., “Superior Metal-Organic Framework Activation with Dimethyl Ether” *Angew. Chem. Int. Ed.* **2022**, *61* (52), e202213190.
3. Schnobrich, J. K.; Lebel, O.; Cychosz, K. A.; Dailly, A.; Wong-Foy, A. G.; Matzger, A. J., “Linker-Directed Vertex Desymmetrization for the Production of Coordination Polymers with High Porosity” *J. Am. Chem. Soc.* **2010**, *132* (39), 13941–13948.
4. Dodson, R. A.; Matzger, A. J., “Resolvation-Based Damage to Metal–Organic Frameworks and Approaches to Mitigation” *ACS Mater. Lett.* **2019**, *1* (3), 344–349.
5. Dodson, R. A.; Wong-Foy, A. G.; Matzger, A. J., “The Metal–Organic Framework Collapse Continuum: Insights from Two-Dimensional Powder X-Ray Diffraction” *Chem. Mater.* **2018**, *30* (18), 6559–6565.

Publications

1. Du Bois, D. R.; Matzger A. J., “Reagent Reactivity and Solvent Choice Determine Metal–Organic Framework Microstructure during Postsynthetic Modification” *J. Am. Chem. Soc.*, **2021**, *143*, 671–674.
2. Du Bois, D. R.; Wright, K. R.; Bellas, M. K.; Wiesner, N.; Matzger, A. J., “Linker Deprotonation and Structural Evolution on the Pathway to MOF-74” *Inorg. Chem*. **2022**, *61*, 4550–4554.
3. Suresh, K. Kalenak, A. P.; Sotuyo, A.; Matzger, A. J., “Metal-Organic Framework (MOF) Morphology Control by Design” *Chem. Eur. J.*, **2022**, *28*, e202200334.
4. Harris, J. T.; de la Garza, G. D.; Devlin, A. M.; McNeil, A. J., "Rapid Removal of Poly- and Perfluoroalkyl Substances with Quaternized Wood Pulp" *ACS EST Water*, 2022, ***2***, 349
5. Du Bois, D. R.; Matzger, A. J., “Metal-Organic Framework Seeding to Drive Phase Selection and Overcome Synthesis Limitations” *Cryst. Growth. Des.*, **2022**, *22*, 6379–6383.
6. Wright, K. R.; Nath, K.; Matzger, A. J., “Superior Metal-Organic Framework Activation with Dimethyl Ether” *Angew. Chemie Int. Ed.*, **2022**, *61*, e2022131

Fundamental Understanding of Electrochemical – Mechanical Driven Instability of Sodium Metal

Partha P. Mukherjee (PI, Purdue University), David Mitlin (Co-PI, The University of Texas at Austin), Yu-chen Karen Chen-Wiegart (Co-PI, Stony Brook University)

Keywords: sodium metal, interface instability, failure mechanism, dendrite-SEI interaction, heterogeneity.

Research Scope

Sodium metal anodes are a key driver in the emerging landscape of "beyond-lithium" electrochemical energy storage systems.[1-3] However, sodium metal exhibits unstable morphological growth across different electrolytes and current densities, accompanied by various limiting mechanisms such as dendrite growth,[4,5] solid electrolyte interphase (SEI) failure,[6-8] and the formation of dead metal.[9] It is becoming clear that existing paradigms cannot account for this behavior and new ways of examining the problem are necessary.[10] While established models have largely focused on ionic transport through the electrolyte, the missing aspects in the current understanding concern the interdependent roles of ionic transport through the SEI, electrochemically generated stresses, and metal wetting energetics. To address these existing knowledge gaps in sodium metal anodes, we aim to examine underpinning mechanistic aspects such as the coupled electrochemical-mechanical interactions and ionic transport in the SEI, dynamic metal wetting/dewetting on the current collector, and the influence of heterogeneities at the sodium-metal/electrolyte interface and SEI structure. The mechanistic coupling amongst such electrochemical, transport and mechanical processes will be mapped to critical descriptors such as the nucleation response, dendrite onset, SEI stability, stripping behavior, and the associated electrochemical signature. Toward gaining a comprehensive understanding of such aspects, a wide range of mechanistic modeling, synthesis, electrochemical, and in situ/operando characterization activities will be performed in this project.

Recent Progress

As part of the BES-sponsored research, two fundamental research themes pertaining to the mechanistic attributes of interface instability in sodium metal were studied. The first thrust was focused on interrogating the heterogeneity-

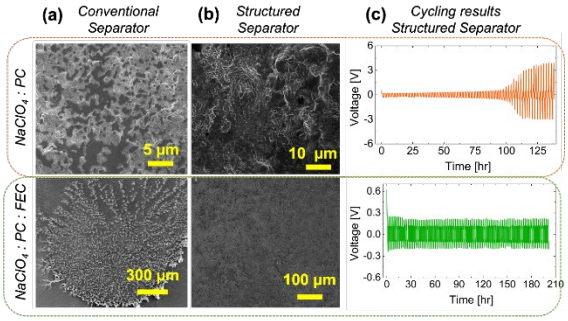

Figure 1. (a-b) Deposition morphology in $NaClO_4$:PC and $NaClO_4$:PC:FEC, and (c) the associated electrochemical response with the structured separator.

induced SEI-mediated interactions and dendrite growth in sodium anodes. Using propylene carbonate (PC) based electrolytes as a model system, we probed the nucleation characteristics and chemical evolution of the SEI, to reveal their influence on the degradation response. While fluoroethylene carbonate (FEC) can potentially improve the ionic conductivity, we identify that it can lead to inhomogeneity in the SEI composition, resulting in local dendritic growth. To counter the heterogeneity and synergistically leverage the FEC-driven transport improvement, we incorporate a flux-homogenizing separator with FEC, to enable improved interface stability (Figure 1). Furthermore, using a sodiophilic current collector based on sodium-chalcogenide intermetallics as a model system, we probed the relationship between substrate-metal interactions and nucleation, and the underlying mechanisms that dictate the sodium metal morphology (Figure 2). While sodium exhibits a filament-like structure on unmodified copper foams, electrodeposition on the modified substrate, due to the enhanced wetting, is dense, smooth, and free of dendrites or pores.

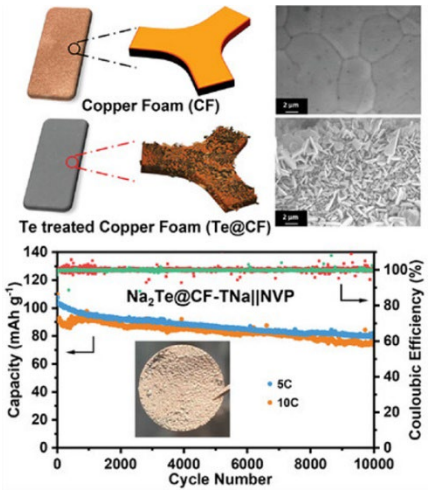

Figure 2. Modified current collector based on sodium-chalcogenide intermetallics and Cu particles enables enhanced metal wetting and electrochemical

As an integral part of the research progress, we have developed a mechanistic modeling framework that captures the interface instability in sodium metal anodes, cognizant of the mechanical and transport characteristics of the SEI. The modeling framework incorporates the implication of structural, chemical and transport heterogeneities in the SEI, on the reaction landscape and morphological growth of sodium metal. The role of such heterogeneities on the onset of dendrite growth and mechanical failure of the SEI, the correlation between mechanical stress distribution and the underpinning transport response and reaction kinetics, and the influence of non-uniform SEI morphology on ionic flux distribution, overpotential response and interface evolution, has been analyzed through the modeling efforts.

The second research thrust was focused on examining the fundamental science of metal-support interactions and dendrite growth. Using a combination of synchrotron X-ray nanotomography imaging, cryogenic electron microscopy and mechanistic modeling, we studied how the current collector wetting influences the three-dimensional deposition morphology, microstructure, and SEI properties in metal electrodes. We investigate the critical role of the substrate-metal interactions on planar versus dendritic growth, explaining the correlation between wetting behavior, electrochemical performance, and electrodeposition morphology. Our work is focused on examining the relationship of metal wettability and substrate-metal energetics and the relevant effect on the morphological attributes of the metal electrode. Building on these research

thrusts, our future work will focus on further investigation of the coupled interactions between ionic transport, mechanical response, SEI structure and wetting behavior, and their relationship with the failure mechanisms and instability onset in sodium metal anodes.

References

1. Y. Zhao, K. R. Adair, and X. Sun, *Recent developments and insights into the understanding of Na metal anodes for Na-metal batteries*, Energy & Environmental Science, **11**, 2673 (2018).
2. X. Zheng, C. Bommier, W. Luo, L. Jiang, Y. Hao, and Y. Huang, *Sodium metal anodes for room-temperature sodium-ion batteries: Applications, challenges and solutions*, Energy Storage Materials, **16**, 6 (2019).
3. Y. Wang, Y. Wang, Y.-X. Wang, X. Feng, W. Chen, X. Ai, H. Yang, and Y. Cao, *Developments and perspectives on emerging high-energy-density sodium-metal batteries*, Chem, **5**, 2547 (2019).
4. F. Hao, A. Verma and, P. P. Mukherjee, *Electrodeposition stability of metal electrodes*, Energy Storage Materials, **20**, 1 (2019).
5. Q. Liu, L. Zhang, H. Sun, L. Geng, Y. Li, Y. Tang, P. Jia, Z. Wang, Q. Dai, and T. Shen, *In situ observation of sodium dendrite growth and concurrent mechanical property measurements using an environmental transmission electron microscopy–atomic force microscopy (ETEM-AFM) platform*, ACS Energy Letters, **5**, 2546 (2020).
6. C. Bao, B. Wang, P. Liu, H. Wu, Y. Zhou, D. Wang, H. Liu, and S. Dou, *Solid electrolyte interphases on sodium metal anodes*, Advanced Functional Materials, **30**, 2004891 (2020).
7. W. Liu, P. Liu and D. Mitlin, *Review of emerging concepts in SEI analysis and artificial SEI membranes for lithium, sodium, and potassium metal battery anodes*, Advanced Energy Materials, **10**, 2002297 (2020).
8. S. Sarkar, M. J. Lefler, B. S. Vishnugopi, R. B. Nuwayhid, C. T. Love, R. Carter, and P. P. Mukherjee, *Fluorinated ethylene carbonate as additive to glyme electrolytes for robust sodium solid electrolyte interface*, Cell Reports Physical Science, **4**, 101356 (2023).
9. B. Lee, E. Paek, D. Mitlin, and S. W. Lee, *Sodium metal anodes: emerging solutions to dendrite growth*, Chemical reviews, **119**, 5416 (2019).
10. H. Wang, E. Matios, J. Luo and, W. Li, *Combining theories and experiments to understand the sodium nucleation behavior towards safe sodium metal batteries*, Chemical Society Reviews, **49**, 3783 (2020).

Publications

1. Y. Wang, H. Dong, N. Katyal, B. S. Vishnugopi, M. K. Singh, H. Hao, Y. Liu, P. Liu, P. P. Mukherjee, G. Henkelman, J. Watt, and D. Mitlin, *Intermetallics Based on Sodium Chalcogenides Promote Stable Electrodeposition–Electrodissolution of Sodium Metal Anodes.* Advanced Energy Materials, 2204402 (2023).
2. P. Liu, D. Yen, B. S. Vishnugopi, V. R. Kankanallu, D. Gürsoy, M. Ge, J. Watt, P. P. Mukherjee, Y. K. Chen-Wiegart, and D. Mitlin, *Influence of Potassium Metal-Support Interactions on Dendrite Growth*. Angewandte Chemie, **62**, e202300943 (2023).
3. S. Sarkar, B. S. Vishnugopi, R. Carter, C. T. Love, J. Watt, D. Mitlin, and P. P. Mukherjee, *Mechanistic Origin of Dendrite Growth though SEI Heterogeneity in Sodium Metal Anodes*, (ready for submission), (2023).

Discovering Dopable, Next-Generation Defect Tolerant Hybrid Semiconductors

James R Neilson, Department of Chemistry, Colorado State University

Obadiah G Reid, Renewable and Sustainable Energy Institute, University of Colorado Boulder

Keywords: Semiconductor, hybrid perovskite, crystallography, defects

Research Scope

This project seeks to discover new defect tolerant and dopable semiconductors, as such new materials are needed for myriad energy-relevant technologies. In this project, the overarching goal is to discover new hybrid inorganic-organic semiconductors, by way of understanding how organic cation-based materials chemistry influences self-regulation of point defects,[1] charged impurities, and doping. The major goals of the project are to understand how organic cations influence the formation and organization of point defects in hybrid halide semiconductors and how the chemistry of the organic cation influences the electronic transport through modification of the charge carrier concentration. These goals are accomplished by the synthesis of materials with well-defined compositions, identification of their often-disordered atomistic structures,[2] interrogation of the electronic properties using microwave conductivity and bulk transport,[3] and discovery of the composition-structure-property relationships. Selective control over the concentration and mobility of defects *and* carriers has potential to enable new and emerging technologies requiring next-generation semiconductors.

Recent Progress

Hybrid tin halide perovskites exhibit non-trivial relationships between the structure, defect equilibria, and carrier transport, as carrier localization plays significant role in the electronic properties. Examination of $CH_3NH_3SnBr_3$, $CsSnBr_3$, and their solid solutions by microwave conductivity experiments reveals a decreasing trend carrier mobility with increasing amounts of cesium. This defies our predictions from band transport and phonon scattering mechanisms. The role of polaron-dressed carriers in these materials is predicted to play a large role in governing the electronic transport of these materials,[4] particularly as the materials exhibit large high-amplitude distortions of the local atomistic structure from our analysis of X-ray total scattering experiments. Polaron-based electron localization reduces carrier mobility but has the potential to extend carrier lifetimes due to reduced overlap of the electron and hole wavefunctions. Understanding how the materials chemistry affects this balance is essential.

Chemical substitution also influences the localization of ionic defects. For example, substitution of ethylenediammonium for methylammonium in $CH_3NH_3SnI_3$ yields disordered vacancies,[5] while substitution with diammoniumheptane yields crystallographically-ordered vacancies.[6] These materials are distinct from the coalescence of "vacancies" in the structures with dimensionally-confined electronic structures resembling the Ruddlesden-Popper and Dion-Jacobsen perovskites. In this project, we discovered that the partial substitution of SCN for I in $(CH(NH_2)_2)PbI_3$ yields a superstructure of columnar vacancies.[7] In this case, the isovalent substitution yields the vacancy-ordered superstructure to accommodate the steric interactions of the larger SCN instead of charge compensation as found with the divalent organic cations. Twinned crystals with ordered columnar vacancies form a coincident-site lattice resembling the unsubstituted phase. This appears to stabilize the unsubstituted, metastable $(CH(NH_2)_2)PbI_3$ as inferred from thermodiffraction studies on biphasic samples. This provides a foundational materials chemistry understanding for the role of SCN "additives" used in device processing.

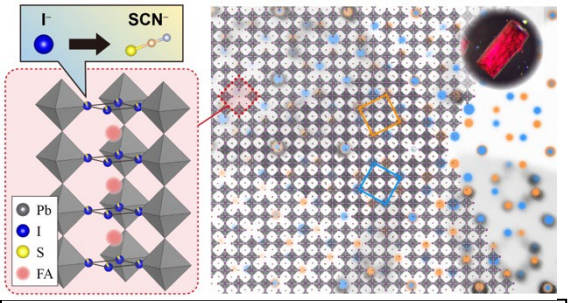

Substitution of SCN for I in $(CH(NH_2)_2)PbBr_3$ yields a superstructure that forms coincident column defect lattices that coincide with and stabilize $(CH(NH_2)_2)PbBr_3$.

References

1. A. Walsh, D. O. Scanlon, S. Chen, X. G. Gong, S.-H. Wei, *Self-Regulation Mechanism for Charged Point Defects in Hybrid Halide Perovskites*. Angew. Chem., **127**, 1811–1814 (2015).
2. E. M. Mozur, J. R. Neilson, *Cation Dynamics in Hybrid Halide Perovskites*, Ann. Rev. Mater. Res., **51**, 269-291 (2021).
3. O. G. Reid, D. T. Moore, Z. Li, D. Zhao, Y. Yan, K. Zhu, G. Rumbles, *Quantitative analysis of time-resolved microwave conductivity data*. J. Phys. D: Appl. Phys., **50**, 493002 (2017).
4. H.Ouhbi, F. Ambrosio, F. De Angelis, J. Wiktor, *Strong Electron Localization in Tin Halide Perovskites*. J. Phys. Chem. Lett., **12**, 5339–5343, (2021).
5. I. Spanopoulos, W.Ke, C. C. Stoumpos, E. C. Schueller, O. Y. Kontsevoi, R. Seshadri, M. G. Kanatzidis, *Unraveling the Chemical Nature of the 3D "Hollow" Hybrid Halide Perovskites.* J. Am. Chem. Soc, **140**, 5728–5742, (2018).
6. J. Guan, Z. Tang, A. M. Guloy, *$[H_3N(CH_2)_7NH_3]_8(CH_3NH_3)_2Sn(IV)Sn(II)_{12}I_{46}$ - A Mixed-Valent Hybrid Compound with a Uniquely Templated Defect-Perovskite Structure,* Chem. Commun., **1**, 48-50 (2005).

Publications

1. T. Ohmi, I. W. H. Oswald, J. R. Neilson, N. Roth, S. Nishioka, K. Maeda, K. Fujii, M. Yashima, M. Azuma, T. Yamamoto, *Thiocyanate-Stabilized Pseudo-Cubic Perovskite $CH(NH_2)_2PbI_3$ from Coincident Columnar Defects Lattices*, Under Revision (2023).

Passive and Enhanced Capture and Conversion of CO_2 by d/f^0 Molecules and Materials

May Nyman, Department of Chemistry, Oregon State University, Corvallis, OR 97330
Tim Zuehlsdorff, Department of Chemistry, Oregon State University, Corvallis, OR 97330
Ahmet Uysal, Heavy Elements/Separation Sciences Group, Chemical Sciences and Engineering Division, Argonne National Laboratory, Lemont, IL, 60439

Keywords: CO_2, carbon dioxide, peroxide, vanadium, uranyl, DAC

Research Scope

In this project, we are developing an understanding of direct air capture (DAC) of CO_2 by high-valent transition metal and actinide molecules, referred to as d/f^0 complexes or peroxometalates. These include transition metals (d^0) Ti^{IV}, V^V, Nb^V, Ta^V, Mo^{VI}, W^{VI}, and actinide (f^0) U^{VI}. While we recognize weakly radioactive depleted uranium is problematic for major industrial use, much of our understanding of the CO_2 capture behavior of these complexes originally came from studies of U^{VI}. Moreover, we observe that CO_2 capture trends and phenomena of V^V are remarkably similar to that of U^{VI}, providing unique opportunities to broaden understanding of the periodic table, the relationship between early transition metals and early actinides in particular. Finally, the uranyl peroxide molecule is the only peroxometalate complex we have studied thus far that retains its peroxide ligands in water, rather than exchanging them for oxide/hydroxide ligands. This will also allow for studies at the aqueous-air interface, particularly valuable for surface spectroscopies.

Recent Progress

DAC behavior of uranyl peroxides. In prior studies, we observed that uranyl triperoxide, formulated $UO_2(O_2)_3^{4-}$ (denoted **U_1** in this narrative), undergoes conversion to $UO_2(CO_3)_3^{4-}$ via an unknown intermediate by a poorly understood mechanism. Interestingly, the reaction is countercation-dependent; specifically, the reactivity increases with increasing size of the alkali. We have recently studied the intermediate of the reaction of the Cs-salt (denoted **Cs-U_1**) in detail, and several lines of evidence suggest this intermediate is a metastable pentavalent uranium phase, meaning peroxide becomes a reducing agent under prescribed conditions. Therefore, the formation of the carbonate via DAC is a mechanism to stabilize reactive U^V. The conditions that invoke U^{VI} to U^V reduction are simply removing the formed crystals of **Cs-U_1** from their mother liquor and allowing them to dry in

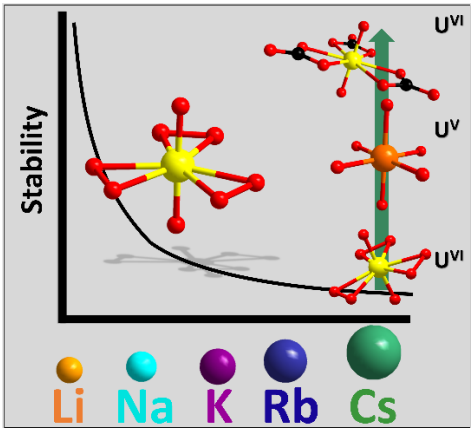

Figure 1. Summary of reactivity of alkali uranyl triperoxide compounds, and the studied reaction pathway of Cs-U_1 to a U^V compound, that rapid converts to uranyl tricarbonate.

ambient conditions. The intermediate was first identified by powder X-ray diffraction (PXRD), as a close match to $CsUO_3$ perovskite, a phase predicted by the Materials Project, but never synthesized. Given the hygroscopic nature of this phase, as well as its observed instability, it is not surprising that it has not been observed experimentally, although the lighter alkali analogues $NaUO_3$ and KUO_3 have been synthesized. In studies this year, we confirmed the identity of the U^V intermediate by XPS (X-ray photoelectron spectroscopy) and Raman spectroscopy. We also performed a time-dependent PXRD study that clearly shows the short-lived nature of the intermediate pentavalent uranium phase and rapid formation of the carbonate phase. EPR (electron paramagnetic resonance) spectroscopy identifies either small molecule free-radicals or U^V, and these studies are ongoing. We are also investigating the effect of light on the reaction, which represents an inconsistent parameter in these experiments, and more broadly DAC mechanisms that may involve free-radical species.

DAC of transition metal peroxides. We have synthesized and surveyed DAC of peroxometalates including Ti^{IV}, V^V, Nb^V, Ta^V, Mo^{VI}, W^{VI}. In this survey study, the K^+ salt of V^V ($V(O_2)_4^{3-}$) proved to be the 'goldilocks compound'; reactive enough to study its DAC mechanism in ambient conditions. PXRD, ^{51}V solid state NMR, FTIR, single-crystal X-ray diffraction (SCXRD) and tandem TGA-MS (thermogravimetry-mass spectrometry) show $VO(CO_3)(O_2)_2^{3-}$ (K-salt) to be the direct product of DAC. Up to one additional equivalent of CO_2 per vanadium (i.e. two CO_2 per vanadium) is captured via the vanadium center for all the studied salts (Li, Na, K, Rb, Cs), and eventual conversion of the final product to VO_3^{1-} plus alkali bicarbonate was observed (**Figure 2**). Computational studies (DFT) show a mechanism of forming a peroxycarbonate intermediate. While SCXRD indicates a chelating bonding mode of carbonate to vanadium, computational studies suggest monodentate coordination is favored in the absence of lattice-packing. Newly-

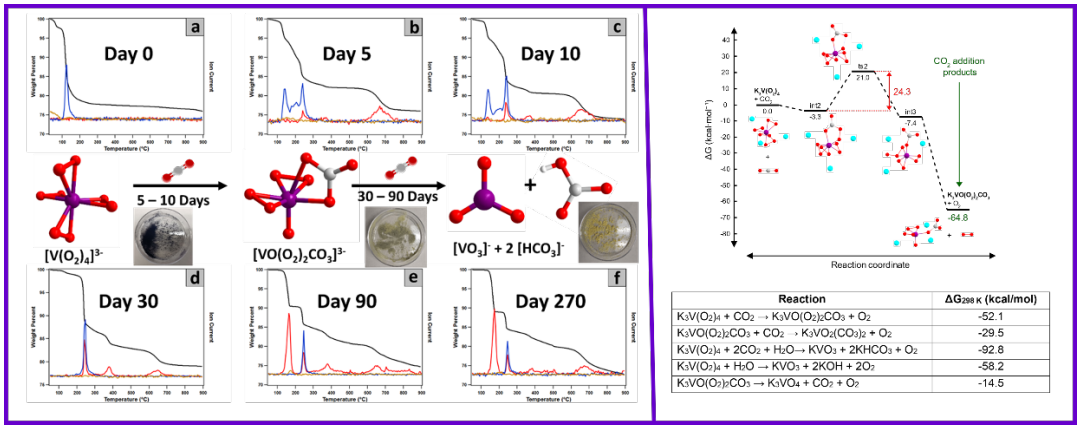

Figure 2. Experimental (left) and computational (right) summary of the tetraperoxovanadate CO_2 capture behavior. The data shown is TGA-MS of $K_3V(O_2)_4$ aged on a benchtop. Black is the thermogravimetric signal, red and blue are respectively CO_2 and O_2 by tandem mass spectrometry. Right, bottom summarizes the calculated energies of the reaction steps.

synthesized $Ti(O_2)_4^{4-}$ compounds also capture considerable CO_2 per Ti-center, but yet direct bonding of carbonate to titanium is never observed by the above-described mechanisms.
Finally, studies of aqueous VO_4^{3-} via SFG Raman Spectroscopy (with and without added amines) provides opportunity to investigate the DAC reaction at the air-water interface, with and without added amines to enhance organization and concentration of the DAC molecules at the interface.

Publications

1. A. Arteaga, Trevor Arino, G.C. Moore, J.L. Bustos, M.K. Horton, K.A. Persson, J. Li, W.F. Stickle, T.A. Kohlgruber, R.G. Surbella, M. Nyman, *'The Role of Alkalis in Orchestrating Uranyl-peroxide Reactivity'* Chemistry: A European Journal **in review**, page (2023).
2. E.G. Ribó, Z. Mao, J.S. Hirschi, T. Linsday, C.R. Simons, T.J. Zuehlsdorff, May Nyman, *'Implementing Vanadium Peroxides as Direct Air Carbon Capture Materials'* Chemical Science **in review**, page (2023).

Chemo-Mechanically Driven In Situ Hierarchical Structure Formation in Mixed Conductors

PI: Nicola H. Perry, UIUC Department of Materials Science & Engineering

Keywords: crystallization, combinatorial films, conductivity, oxygen surface exchange kinetics

Research Scope

The overarching goal of the project is to monitor, understand, and direct structure across multiple length scales to achieve hierarchical, highly active mixed ionic/electronic conducting oxides (MIECs). MIECs enable a variety of energy, synthesis, sensing, and electronic applications by their dual ability to exchange oxygen with the gas phase (catalyzing electrochemical reactions) at the surface and conduct ionic and electronic species within the bulk[1]. However, conventional MIECs are processed at high temperatures, causing coarsening and segregation of non-active cations, leading to sluggish surface exchange kinetics[2]. We are developing a new, low temperature, non-equilibrium pulsed laser deposition method that leverages MIEC chemo-mechanical coupling to create hierarchical structures with high surface reactivity and good mixed transport. Amorphous films are fabricated by low temperature pulsed laser deposition and actuated into hierarchical structures at mild temperatures by chemical contractions induced by crystallization and oxidation[3]. We focus on monitoring, understanding, and controlling the emerging hierarchical structure and functional properties via this new approach in (Sr,La)(Ti,Ga,Fe,Co)$O_{3-\delta}$ perovskites.

In phase 1, we observe and interpret the interplay of chemo-mechanical coupling and hierarchical structure evolution, correlating changes across multiple length scales. In phase 2, we learn how PLD growth conditions and crystallization stimuli can be tuned to tailor the resulting hierarchical structure. In phase 3, we measure and understand transport and surface reactivity changes during hierarchical transformation. This final task involves developing a new 2-dimensional optical transmission relaxation (2D-OTR) technique for high throughput monitoring of surface catalytic activity and applying methods to separate ionic and electronic conductivity.

Recent Progress

Our first work on this project demonstrated that hierarchical transformation during crystallization of various MIECs led to emergence of unprecedented surface catalytic activity and kinetics of oxygen exchange, critical for MIEC efficiency[4]. Using angle-resolved XPS, synchrotron XANES, TEM, and in-situ ac impedance spectroscopy, we then showed that the ultra-fast kinetics arose from a) pristine surface chemistry absent of segregation that is ubiquitous in conventional MIEC processing, and b) favorable bulk defect chemistry for surface charge transfer, the likely rate-limiting step[5]. The inherent chemo-mechanical coupling of MIECs promotes oxidation during crystallization-induced densification, and this stoichiometry change drives local increases in

transition metal coordination number and polyhedral alignment that promote hierarchical microstructural evolution and increase hole concentration and mobility[5]. We also advanced a contact-free optical method for monitoring the catalytic activity (oxygen surface exchange coefficient) continuously during crystallization, which avoids the problematic contribution of metal current collectors to measured catalytic activity[6,7].

Our most recent work has focused on phases 2 and 3. In phase 2, given that oxygen content increased during crystallization, we studied the impact of oxygen chemical potential (or oxygen availability) during crystallization on the local atomic and nanoscale structure. Detailed synchrotron EXAFS studies have shown trends in local structural evolution (coordination numbers, bond lengths) with respect to gas atmosphere and temperature during crystallization[8]. Ongoing 4D-STEM (electron nanobeam diffraction) and STEM-EDS studies are observing dramatic changes in elemental distributions when oxygen chemical potential is instead modified by solid-state electrochemical pumping during crystallization[9]. In phase 3, we focus on technique development for in-situ monitoring of functional properties. We have finished developing our new 2D-OTR capability that now allows us to monitor crystallization and oxygen surface exchange kinetics on each part of a 1x1 cm^2 film simultaneously without contacts. We have developed combinatorial library growth capability and have mapped crystallization temperatures and surface exchange coefficients vs. temperature across combinatorially graded composition libraries for the first time[10]. We have also applied this 2D-OTR method to map oxygen exchange kinetics as a function of distance from a current collector, demonstrating that the metal does indeed enhance the apparent kinetics even mm away from the nominal interface[11]. Lastly we have developed a thin film blocking electrode cell design to isolate changes in ionic vs. electronic conductivity during crystallization. By coupling *in-situ* synchrotron GIXRD with simultaneous ac impedance spectroscopy, blocking electrode studies, and dc polarization, we have demonstrated the possibility to turn a material from a pure ionic conductor into a pure electronic conductor (with every ratio of ionic : electronic conductivity in between), through crystallization[12]. Both ionic and electronic conductivity increase orders of magnitude during crystallization, but the electronic portion shows the more

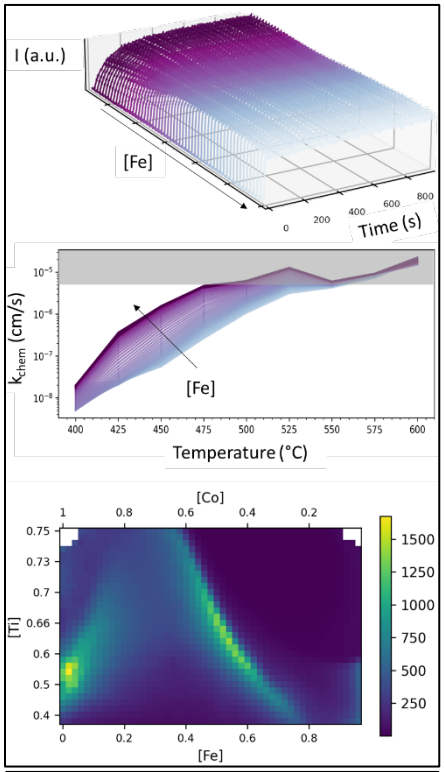

Figure 6 – high T 2D-OTR Results. Top: Simultaneous optical relaxations induced by pO_2 step on combinatorial library; middle: oxygen surface exchange coefficients vs. composition and T; bottom: oxygen exchange time constants of ternary library at 450C

dramatic change. This last aspect is being supported by MD simulations of the impact of crystallinity on ionic transport via collaboration.

References

1. N. H. Perry, and T. Ishihara, *Roles of bulk and surface chemistry in the oxygen exchange kinetics and related properties of mixed conducting perovskite oxide electrodes*, Materials, **9**(10), 858 (2016); H. J. M. Bouwmeester, H. Kruidhof, and A. J. Burggraaf, *Importance of the surface exchange kinetics as rate limiting step in oxygen permeation through mixed-conducting oxides,* Solid state ionics, **72**, 185-194 (1994); P. J. Gellings, and H. J. Bouwmeester, *Ion and mixed conducting oxides as catalysts,* Catalysis Today, **12**(1), 1-101 (1992); U. Balachandran, B. Ma, P. S. Maiya, R. L. Mieville, J. T. Dusek, J. J. Picciolo, J. Guan, S. E. Dorris, and M. Liu, *Development of mixed-conducting oxides for gas separation,* Solid State Ionics **108** (1-4), 363-370 (1998).
2. B. Koo, K. Kim, J. K. Kim, H. Kwon, J. W. Han, and W. Jung, *Sr segregation in perovskite oxides: why it happens and how it exists*, Joule, **2**(8), 1476-1499 (2018); Y. Li, W. Zhang, Y. Zheng, J. Chen, B. Yu, Y. Chen, and M. Liu, *Controlling cation segregation in perovskite-based electrodes for high electro-catalytic activity and durability*, Chemical Society Reviews, **46**(20), 6345-6378 (2017).
3. T. Chen, G. F. Harrington, K. Sasaki, and N. H. Perry, *Impact of microstructure and crystallinity on surface exchange kinetics of strontium titanium iron oxide perovskite by in situ optical transmission relaxation approach*, Journal of Materials Chemistry A, **5**(44), 23006-23019 (2017).
4. T. Chen, G. F. Harrington, J. Masood, K. Sasaki, and N. H. Perry, *Emergence of rapid oxygen surface exchange kinetics during in situ crystallization of mixed conducting thin film oxides*, ACS applied materials & interfaces, **11**(9), 9102-9116 (2019).
5. H. B. Buckner, Q. Ma, J. Simpson-Gomez, E. J. Skiba, and N. H. Perry, *Multi-scale chemo-mechanical evolution during crystallization of mixed conducting $SrTi_{0.65}Fe_{0.35}O_{3-\delta}$ films and correlation to electrical conductivity*, Journal of Materials Chemistry A, **10**(5), 2421-2433 (2022).
6. E. J. Skiba, T. Chen, and N. H. Perry, *Simultaneous Electrical, Electrochemical, and Optical Relaxation Measurements of Oxygen Surface Exchange Coefficients: $Sr(Ti,Fe)O_{3-d}$ Film Crystallization Case Study*, ACS Applied Materials & Interfaces, **12**(43), 48614-48630 (2020).
7. H. B. Buckner and N. H. Perry, *In situ optical absorption studies of point defect kinetics and thermodynamics in oxide thin films*, Advanced Materials Interfaces, **6**(15), 1900496 (2019).
8. E. Skiba, Q. Ma, H. B. Buckner, and N. H. Perry, *Evolution of local ion environments as a function of crystallinity in $Sr(Ti,Fe)O_{3-x}$ films* and *Impact of gas-controlled oxygen chemical potential on atomic structure evolution during crystallization of $Sr(Ti,Fe)O_{3-x}$ perovskite* (2 papers in preparation for submission this summer)
9. H. B. Buckner, et al., J. Zuo, and N. H. Perry, *Effects of electrochemically tailored oxygen chemical potential on crystallization: a 4D-STEM study of $Sr(Ti,Fe)O_{3-x}$* (in preparation for submission in fall)
10. E. Skiba, A. Popescu, K. Arsky, and N. H. Perry, *Combinatorial analysis of oxygen surface exchange kinetics and crystallization by 2D optical transmission relaxation on $Sr(Ti,Co,Fe)O_{3-x}$ libraries* (in preparation for submission this summer)
11. E. J. Skiba and N. H. Perry, *High-Temperature 2D Optical Relaxation Visualizes Enhanced Oxygen Exchange Kinetics at Metal-Mixed Conducting Oxide Interfaces*, ACS Applied Materials & Interfaces, **14**(42), 47659-47673 (2022).

12. H. B. Buckner, K. Rubartsch, A. Bonkowski, R. De Souza, and N. H. Perry, *Turning an ionic conductor into an electronic conductor via crystallization: in-situ study of transference numbers and evolving structure in (La,Sr)(Ga,Fe)O_{3-x} perovskite* (in preparation for submission this summer)

Publications (Past 2 Years)

1. H. B. Buckner, Q. Ma, J. Simpson-Gomez, E. J. Skiba, and N. H. Perry, *Multi-scale chemo-mechanical evolution during crystallization of mixed conducting $SrTi_{0.65}Fe_{0.35}O_{3-\delta}$ films and correlation to electrical conductivity*, Journal of Materials Chemistry A, **10**(5), 2421-2433 (2022).
2. E. J. Skiba and N. H. Perry, *High-Temperature 2D Optical Relaxation Visualizes Enhanced Oxygen Exchange Kinetics at Metal-Mixed Conducting Oxide Interfaces*, ACS Applied Materials & Interfaces, **14**(42), 47659-47673 (2022).
3. N. Kim, B. J. Blankenau, T. Su, N. H. Perry, and E. Ertekin, *Multisublattice cluster expansion study of short-range ordering in iron-substituted strontium titanate*, Computational Materials Science, **202**, 110969 (2022).

Five other publications in preparation for submission in coming months, as listed in references section.

Hierarchical Hybrid Multifunctional Materials through Interface Engineering

PI : Dr. Pierre Ferdinand Poudeu; Department of Materials Science and Engineering, University of Michigan; ppoudeup@umich.edu
Co-PI: Dr. Ctirad Uher; Department of Physics, University of Michigan; cuher@umich.edu

Keywords: Entangled Nanocomposites, Polymorphism, Nanostructuring, Defects Hybridization, Electronic Transition

Research Scope

This project focuses on the development of *stimuli-responsive hybrid multifunctional materials*. We emphasize a strong coupling between electronic and optical properties through hierarchical structural entanglement of two semiconductors: a narrow band gap (NBG), Cu_2Se, and a range of wider band gap (WBG) phases such as $CuMSe_2$ (M = Al, Ga, In, Fe) and Cu_4NSe_4 (N = Ti, Si, Ge). Our goal is to understand the correlation between the *hierarchical microstructure* (chemical composition and structure, mole fraction, size, and shape of the coexisting phases and their distribution at multiple length scale) of the resulting (1-x)Cu_2Se/(x)WBGS *bulk composites* and the multi*functional properties* (quantum electronic transition, ultrahigh optical absorption, giant negative photoconductivity, p to n type electronic transition) that may arise from the hybrid electronic band structure resulting from the multiscale (atomic, nanometer and micrometer) interaction of native electronic defects and chemical bonding in these materials.

Recent Progress

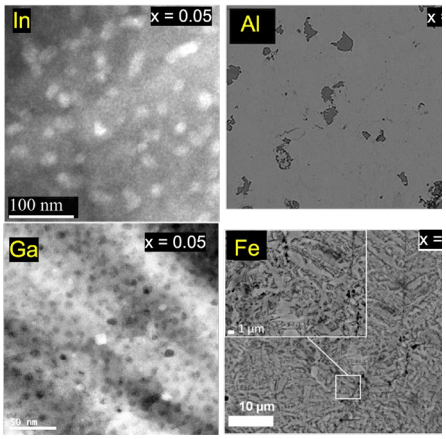

Fig.1: Microstructure evolution of (x) Cu_2Se/(1-x)$CuMSe_2$ composites (M = In, Ga, Al, Fe).

We have completed the synthesis and characterization of the microstructure of several composites within the material systems, (1-x)Cu_2Se/(x)$CuMSe_2$ (M = Al, In, Fe, Ga), which revealed a strong variation of the microstructure with the chemical composition of the $CuMSe_2$ phase (Fig.1). [1-5] The exploration of the full composition range for the (1) (1-x)Cu_2Se/(x)$CuMSe_2$ and (1-x)Cu_2Se/(x)$CuGaSe_2$ systems showed that both the Cu_2Se and $CuInSe_2$ ($CuGaSe_2$) phases coexist at multiple length scales, ranging from sub-ten nanometer to several micrometers, leading to the formation of a hybrid hierarchically entangled microstructure [4, 6]. Astonishingly, the electronic phase diagram (Fig 2 and 3) of the (1-x)Cu_2Se $-$ (x)$CuMSe_2$ hierarchical composites remarkably deviates from the trend normally expected for composites between a heavily doped semiconductor (Cu_2Se) and a poorly conducting phase

($CuMSe_2$). A sudden increase in the carrier concentration is observed for composites at the vicinity of equimolar composition ($48\% \leq x \leq 52\%$) in both In and Ga composites. The atypical electronic behavior is rationalized in the light of the formation of an inter-band (IB) within the band gap, which may arise from the hybridization of native acceptor electronic point defects such as (i) copper vacancies in Cu_2Se ($[V_{Cu}]_{CS}$); $CuInSe_2$ ($[V_{Cu}]_{CIS}$); and $CuGaSe_2$ ($[V_{Cu}]_{CGS}$); (ii) anti-site defects in $CuInSe_2$ ($[Cu_{In}]_{CIS}$); and $CuGaSe_2$ ($[Cu_{Ga}]_{CGS}$); and (iii) In-vacancy in $CuInSe_2$ ($[V_{In}]_{CIS}$); and Ga-vacancy in $CuGaSe_2$ ($[V_{Ga}]_{CGS}$) in the resulting hierarchical composites (Fig. 3).[7, 8] The density as well as the energy distribution of these electronic defects depend on the fraction of $CuInSe_2$ ($CuGaSe_2$) phase. Surprisingly, Hall effect data revealed a transition from p-type to n-type electronic conduction in In-containing composites, whereas such transition is not observed for the Ga-containing samples. Interestingly, the temperature, $T_{p\text{-}n}$, of the electronic transition depends on the $CuInSe_2$ phase fraction and follows a similar trend as the carrier density (Fig. 2C). This surprising electronic behavior can be rationalized by considering the density as well as the energy distribution of both donor and acceptor shallow and deep electronic defects in Cu_2Se, $CuInSe_2$ and $CuGaSe_2$. In $Cu_2Se/CuInSe_2$ composites, the activation at high temperatures of both shallow donor $[In_{Cu}]_{CIS}$ (E_d~100 meV) and shallow acceptor defects ($[V_{Cu}]_{CS}$; $[V_{Cu}]_{CIS}$; and $[V_{Cu}]_{CGS}$ with E_a < 6 meV) results in compensated charge carrier transport. By contrast, the $[Ga_{Cu}]_{CGS}$ donor defect in $CuGaSe_2$ is located deeper in the band gap (E_d~400 meV) and is therefore difficult to activate, which may explain the absence of p to n transition in Ga containing composites.[8] These results point to a new strategy to modulate the electronic structure of semiconductor composites to maximize interaction and coupling between two fundamentally contrasting properties. This enables access to electronic hybrid systems with interactive and stimuli-responsive multifunctional properties paving the way for potential applications in quantum computing, memory, sensing, and detection electronic devices.

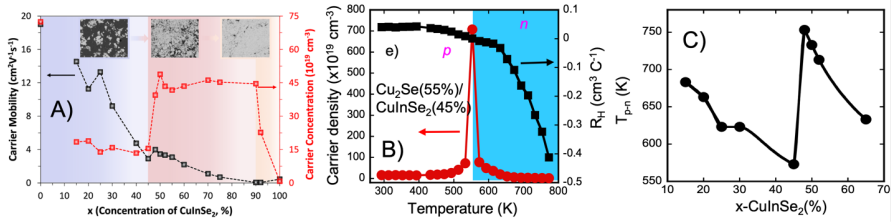

Fig. 2: (A) Electronic phase diagram of (1-x)Cu_2Se — (x)$CuInSe_2$ composites. (B) temperature dependent carrier density showing p to n transition at temperature $T_{p\text{-}n}$; and (C) Dependence of $T_{p\text{-}n}$ with phase composition.

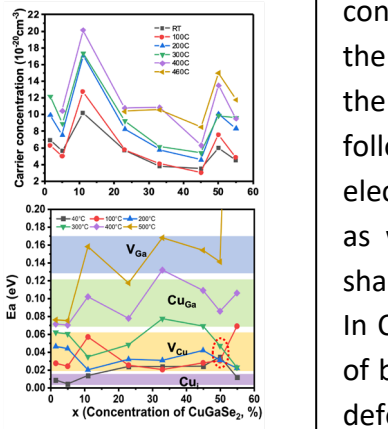

Fig. 3: (A) Electronic phase diagram of (1-x)Cu_2Se — (x)$CuGaSe_2$ composites. (B) Energy distribution of native electronic defects.

Reference

1. R. M. Lu, A. Olvera, T. P. Bailey, C. Uher, P. F. P. Poudeu, *$CuAlSe_2$ Inclusions Trigger Dynamic Cu^+ Ion Depletion from the Cu_2Se Matrix Enabling High Thermoelectric Performance*. ACS Appl Mater Inter **12**, 58018−58027 (2020).
2. R. M. Lu, A. Olvera, T. P. Bailey, C. Uher, P. F. P. Poudeu, *Nanoscale Engineering of Polymorphism in Cu_2Se-Based Composites*. ACS Appl Mater Inter **12**, 31601-31611 (2020).
3. R. M. Lu, A. Olvera, T. P. Bailey, C. Uher, P. F. P. Poudeu, *Ultrafine Interwoven Dendritic $Cu_2Se/CuFeSe_2$ Composites with Enhanced Thermoelectric Performance*. *ACS Appl Energ Mater* **3**, 9133-9142 (2020).=
4. A. Olvera, N. A. Moroz, P. Sahoo, P. Ren, T. P. Bailey, A. A. Page, C. Uher, P. F. P. Poudeu, *Partial indium solubility induces chemical stability and colossal thermoelectric figure of merit in Cu_2Se*, Energ Environ Sci **10**, 1668-1676 (2017).
5. Y. Chen, Y. Zhang, C. Uher, P.F.P. Poudeu, *Carrier Mobility Modulation in Cu_2Se Composites Using Coherent Cu_4TiSe_4 Inclusions Leads to Enhanced Thermoelectric Performance*, ACS Appl. Mater. Interfaces **14**, 56817–56826 (2022).
6. Y. Chen, Y. Zhang, R. Lu, T.P. Bailey, C. Uher, P.F.P. Poudeu, *Unusual electronic transport in (1− x) Cu_2Se–(x)$CuInSe_2$ hierarchical composites*, Nanoscale Advances **4**, 4279-4290 (2022).
7. S. B. Zhang, S.-H. Wei, and A. Zunger, *Defect physics of the $CuInSe_2$ chalcopyrite semiconductor*, Phys. Rev B, **57**, 9642 (1998).
8. C. Spindler, F. Babbe, M. H. Wolter, F. Ehre, K. Santhosh, P. Hilgert, F Werner, S. Siebentritt, *Electronic defects in Cu(In,Ga)Se_2: Towards a comprehensive mode,l* Physical Review Materials 3, : 090302 (2009).

Publications

1. Y. Chen, Y. Zhang, C. Uher, P.F.P. Poudeu, *Carrier Mobility Modulation in Cu_2Se Composites Using Coherent Cu_4TiSe_4 Inclusions Leads to Enhanced Thermoelectric Performance*, ACS Appl. Mater. Interfaces **14**, 56817–56826 (2022).
2. Y. Chen, Y. Zhang, R. Lu, T.P. Bailey, C. Uher, P.F.P. Poudeu, *Unusual electronic transport in (1− x) Cu_2Se–(x)$CuInSe_2$ hierarchical composites*, Nanoscale Advances **4**, 4279-4290 (2022)
3. R. Lu, A. Olvera, T. P. Bailey, J. Fu, X. Su, I. Veremchuk, Z.Yin, B. Buchanan, C. Uher, X. Tang, Y. Grin, P. F.P. Poudeu, *High carrier mobility and ultralow thermal conductivity in the synthetic layered superlattice $Sn_4Bi_{10}Se_{19}$* Mater. Adv. **2**, 2382 (2021).
4. . Chae, K. Mengle, K. Bushick, J.Lee, N. Sanders, Z. Deng, Z.n Mi, P. F. P. Poudeu, H. Paik, J. T. Heron, and E. Kioupakis; *Perspective: Towards the predictive discovery of ambipolarly dopable ultra-wide-band-gap semiconductors: the case of rutile GeO_2;* Appl. Phys. Lett. **118**, doi: 10.1063/5.0056674 (2021)

Metal-Organic Frameworks: Structure, Function and Design via Hyperpolarized NMR Spectroscopy: Collaborative Proposal, DE-SC0020635

PI: Jeff Reimer, UC Berkeley reimer@berkeley.edu
Alexander Pines, UC Berkeley pines@berkeley.edu
Carlos Meriles, CCNY cmeriles@ccny.cuny.edu
Co-Investigator: Ashok Ajoy, UC Berkeley ashokaj@berkeley.edu

Keywords: metal-organic frameworks, optical-nuclear polarization.

Research Scope.

Our objectives are to develop magnetic resonance and optical spectroscopy methods to investigate the spin dynamics of metal organic frameworks (MOFs), with special attention to using optical pumping schemes(1) to improve detection sensitivity of nuclear spin polarization in MOFs as well as the development and application of new MOF structures to quantum information science. Critical to these objectives are developing instrumentation and materials to optically prepare long-lived triplet states in MOFs, then transfer the highly athermal electron spin polarizations to the MOFs themselves.

Recent Progress

We report progress on three objectives: a theoretical description of methods to transfer polarizations amongst spins in MOF systems, two major experimental apparatuses to show polarization transfer in condensed spin systems, and the design and synthesis of MOFs that are expected to exhibit optical-nuclear polarization.

Spin methods development. The triplet-state in optically excited MOFs create a lattice of coupled electron and nuclear spins; such systems a notoriously complex to access with magnetic

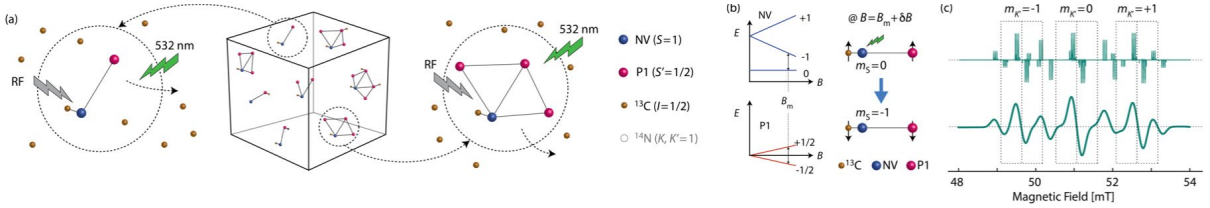

Figure 1. Here the NV defect in diamond serves as the test-bed for exploring clusters of spins may be optically pumped. (a) Randomly occurring paramagnetic centers (NVs, P1s) and 13C nuclei in the diamond lattice (as well as the 14N hosts of each point defect) can be grouped into hybrid clusters of strongly interacting spins. RF excitation resonant with hyperfine transitions in the cluster allows us to single out those nuclei most effectively contributing to the transfer of polarization to bulk carbons. (b) Electron Zeeman levels for the P1 and NV defects; this work was conducted at magnetic fields where the P1 Zeeman splitting approximately matches one of the NV transitions (left energy diagrams). Slight detuning of this field provides the energy difference required to polarize the nuclear spin, as most clearly seen in a three-spin model (right schematics). (c) Calculated nuclear spin polarization pattern as a function of the applied magnetic field assuming the three-spin 13C−NV−P1 model in (b). Dashed boxes indicate sections of the pattern preferentially associated with each spin projection of the P1 14N host. The lower trace derives from a convolution with a Gaussian.

resonance methods. We have recently shown that clusters of electron-nuclear spins can be detected and manipulated via spectroscopic methods (R. Pigliapochi et. al. 2023). This and temperature jump methods (Meriles et. al. 2022) suggest that there may be new dynamic polarization transfer (*"cross-polarization"*) methods ideally suited to preparing hyperpolarized nuclei in MOFs (Figure 1).

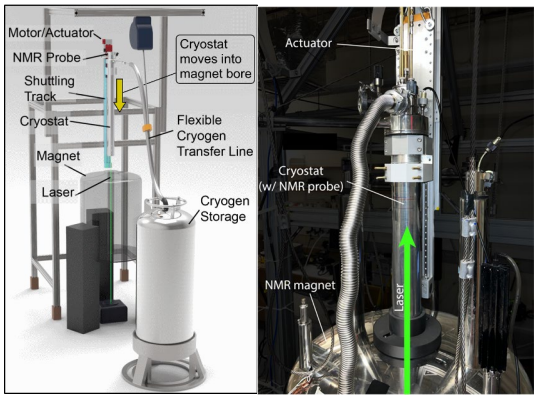

Figure 2. Left: Shuttling instrument designed and built for optical nuclear DNP in MOFs. Right: Detailed photograph showing laser excitation in an NMR probe in the magnet fringe field.

Instrumentation design and construction. We have developed a novel instrument that allows for optical dynamic nuclear polarization (ODNP) and nuclear interrogation at a range of cryogenic temperatures (4K-RT). It utilizes an Oxford Spectrostat NMR cryostat under continuous flow cooling which is mechanically moved ("shuttled") from lower fields of a few mT into a 9.4T NMR magnet (Oxford). Optical hyperpolarization is carried out in the fringe field of the magnet through an optical window at the cryostat bottom. Hyperpolarized nuclei are detected via spin-locking NMR sequences with >1M pulses, yielding a continuously interrogated NMR signal for up to t=180s (see Figure 2) In addition, an *x*-band pulsed EPR system with optical access, cryogenic temperature control, and (0.3T) hydrogen and ^{13}C NMR has been assembled to provide triplet lifetimes and quantitate hyperfine interactions so as to develop the experimental protocols for optical DNP apparatus described above.

Materials synthesis. Critical to the application of ODNP to MOFs is the chemical design and synthesis of MOFs that are anticipated to support long-lived triplet states. Based upon molecular analogs, MOFs with linkers containing pyrene/naphthalene/pentacene or porphyrin moieties are anticipated to be useful. Toward that end we have synthesized in multi-gram quantities two pyrene-based linker for MOFs $[Mg_{1.5}(HTBAPy)(H_2O)_2]\cdot 3DMF$ (a.k.a Sion-7, a pyrene linker(2), Figure 3) and $[Al_2(OH)_2(TBAPy)]\cdot 4DMF\cdot 3H_2O$ (a.k.a. AlPyrMOF (3)). Synthesis of a pentacene-based linker in an aluminum MOF has been partly successful, with further optimization this should be accessible. There are dozens of porphyrin-based MOFs in the literature, and we have hydrothermally synthesized PCN-224 by coordinating tetra-kis(4-carboxyphenyl)porphyrin (TCPP) ligands with zirconium. Finally, molecular analogs to test and quantitate our

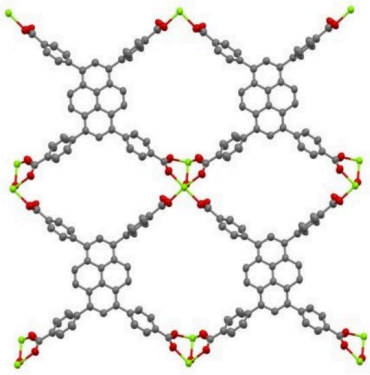

Figure 3. SION7,$[Mg_{1.5}(HTBAPy)(H_2O)_2]\cdot 3DMF$. Top portion of a 2- dimensional layer constructed from HTBAPy3– ligands joined together by Mg3-clusters. Color code: Mg: green, O: red, C: gray.

ODNP protocols require Bridgeman-type crystallization methods, and toward that end have constructed such an apparatus and can routinely prepare multi-gram quantities of e.g., pentacene. Optically detected magnetic resonance (ODMR) demonstrated our ability to create these materials and characterize them.

References

1. James Eills, Dmitry Budker, Silvia Cavagnero, Eduard Y. Chekmenev, Stuart J. Elliott, Sami Jannin, Anne Lesage, Jörg Matysik, Thomas Meersmann, Thomas Prisner, Jeffrey A. Reimer, Hanming Yang, and Igor V. Koptyug, *"Spin Hyperpolarization in Modern Magnetic Resonance,"* Chemical Reviews, **2023** 123, 4, 1417–1551.
2. Gładysiak, A.; Nguyen, T. N.; Bounds, R.; Zacharia, A.; Itskos, G.; Reimer, J. A.; Stylianou, K. C. Temperature-Dependent Interchromophoric Interaction in a Fluorescent Pyrene-Based Metal–Organic Framework. *Chemical Science* **2019**, *10*, 6140–6148.
3. Boyd, P. G.; Chidambaram, A.; García-Díez, E.; Ireland, C. P.; Daff, T. D.; Bounds, R.; Gładysiak, A.; Schouwink, P.; Moosavi, S. M.; Maroto-Valer, M. M.; *et al.* Data-Driven Design of Metal–Organic Frameworks for Wet Flue Gas CO2 Capture. *Nature* **2019**, *576*, 253–256.

Publications

1. R. Pigliapochi, D. Pagliero, L. Buljubasich, P.R. Zangara, C.A. Meriles, "Dynamic-nuclear-polarization-weighted spectroscopy of multi-spin electronic-nuclear clusters", Phys. Rev. B 107, 214202 (2023). 2. S. Bussandri, G. Sequeiros, R.H. Acosta, P.R. Zangara, C.A. Meriles, "Information-guided dynamic nuclear polarization", Phys. Rev. Appl. 18, 034039 (2022).3. C.A. Meriles, P.R. Zangara, "Microwave-free dynamic nuclear polarization via sudden thermal jumps," Phys. Rev. Lett. 128, 037401 (2022).
2. G.I. López-Morales, M. Li, A. Hampel, S. Satapathy, N.V. Proscia, H. Jayakumar, A. Lozovoi, D. Pagliero, G.E. Lopez, V.M. Menon, J. Flick, C.A. Meriles, "Investigation of photon emitters in Ce-implanted hexagonal boron nitride", Opt. Mater. Exp. 11, 3478 (2021).
3. S. Bussandri, P.R. Zangara, R.H. Acosta, C.A. Meriles, "Non-Hermitian dynamics of spin chains with loss and gain", Phys. Rev. B 103, 214409 (2021).

Reversible Electrochemical Capture/Release of Carbon Dioxide Mediated by Electrostatically-Enhanced Charge Transfer

Joaquín Rodríguez López, University of Illinois Urbana-Champaign (Principal Investigator)
Veronica Augustyn, North Carolina State University (Co-Investigator)
Jahan Dawlaty, University of Southern California (Co-Investigator)
Keywords: Electrochemical Interface, Capacitance, CO_2, Direct Air Capture, Modified Electrode

Research Scope

The major goal of this project is to use electric fields at the electrochemical interface to capture and release CO_2 molecules to develop a novel CO_2 storage and release mechanism with low energy consumption and high efficiency. Our overarching hypothesis is that controllable nucleophilicity of a tethered capture motif via electro-induction will lead to modified CO_2 adduct equilibria that will permit the on-demand capture and release of CO_2 for its effective separation from other substances in air. To this end, we have advanced the understanding of molecular event characterization at polarized carbon electrodes, characterized the interactions of CO_2 with electrodes by observing changes in capacitive properties, and correlating the spectroscopic signatures of adducted CO_2 with capture motifs such as anilines.

Recent Progress

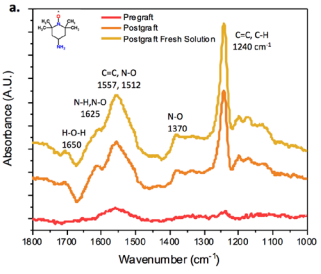

Figure 1. SEIRAS of TEMPO grafted on graphene-on-Au electrode.

Characterization of CO_2-binding processes at practical and model electrodes for DAC applications, such as carbon and gold, respectively, first requires a versatile toolset to probe our hypothesis. Two of our methods of choice are electrochemical surface enhanced infrared absorption spectroscopy (EC-SEIRAS) and electrochemical surface enhanced Raman scattering (EC-SERS). With previous work indicating the possibility of carrying out EC-SERS on graphene-on-metal electrodes,[1] we set out to demonstrate the possibility of SEIRAS on carbon materials through the grafting of molecular motifs such as TEMPO on these surfaces.[2,3] In the SEIRAS spectra, we see an increase of peaks at 1512 cm^{-1} and 1370 cm^{-1} which correspond to N-O stretches of the TEMPO molecule (Figure 1). These signals are not observed on pristine graphene electrodes, and no grafting is observed on pure metal electrodes, indicating a strong synergy of our approach to detect molecular species. Our recent experiments have also aimed at exploring the electrochemical and analytical spectroscopic window to detect surface events optimally – for example by characterizing the CO_2-binding properties of amines in alcohols rather than on aqueous solutions. Under these

conditions, complications due to the speciation of CO_2 in water may be avoided,[4] while also providing fewer interfering spectroscopic signals that will facilitate testing our hypothesis.

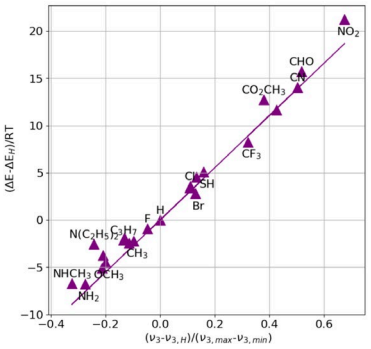

Figure 2. Correlation between scaled vibrational frequencies of the antisymmetric stretch of CO_2 and the computed energies of the carbamate bond.

Elucidating CO_2 interactions with molecular motifs at electrodes requires predictoing spectroscopic signatures. We showed that the energy of the carbamate bond (the bond between the amine and the captured CO_2) depends on the electron-withdrawing/donating strength of the substituents on the para position of aniline. Secondly, the strength of this bond correlates very well with the experimental and computational vibrational frequency of the anti-symmetric stretch of the adducted CO_2 (Figure 2). Electron donating groups typically enhance the driving force of carbamate formation by transferring more charge to the adducted CO_2 and thus increasing the occupancy of the anti-bonding orbital in the carbon-oxygen bonds. Increased occupancy of the anti-bonding orbital within adducted CO_2 weakens the bond, leading to a red shift in the characteristic carbamate frequency. We expect analogous trends in other amine-CO_2 capture systems, especially those placed on electrodes.

Additionally, it is critical to characterize the baseline interactions of electrodes with CO_2 – i.e., how this gas affects capacitive phenomena even in the absence of molecular motifs. Supercapacitive swing adsorption of CO_2 is proposed as a high energy efficiency and low cost electrochemical method for CO_2 capture.[5,6] However, the mechanism of supercapacitive swing adsorption is poorly understood. For example, in aqueous electrolytes, it is not clear whether capture occurs from the adsorption of neutral CO_2 or of the charged bicarbonate and carbonate ions. To answer these questions, we compared the capacitance changes of a planar gold electrode in saturated Ar and CO_2 aqueous electrolytes (Figure 3) while varying the electrolyte concentration, salt, and pH. During this project period, we completed this study and in doing so, determined the aqueous electrolyte features that maximize CO_2 capture. We propose that the observed reduction in capacitance occurs from the replacement of adsorbed cations with CO_2 molecules. Therefore, the extent of capacitance reduction is related to the surface charge density of the electrode as well as the applied potential. A model is proposed to account for the mechanism for CO_2 capture on bare electrode surfaces.

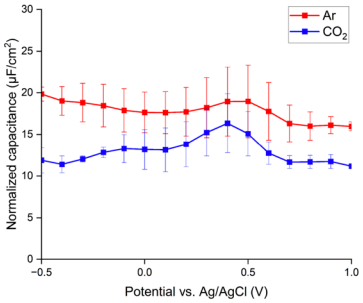

Figure 3. Effect of CO2 on capacitance on Au electrode in aqueous 5 mM Li_2SO_4.

References

1. K.O. Hatfield, S.T. Putnam, J. Rodriguez-López, J. *Inducing SERS Activity at Graphitic Carbon Using Graphene-Covered Ag Nanoparticle Substrates: Spectroelectrochemical Analysis of a Redox-Active Adsorbed Anthraquinone* J. Chem. Phys., **158**, 014701 (2023).
2. B. Yuan, C. Xu, D. Zhang, R. Zhang, H. Su, P. Guan, J. Nie, C. Fernandez. E*lectrografting of Amino-TEMPO on Graphene Oxide and Electrochemically Reduced Graphene Oxide for Electrocatalytic Applications.* Electrochem. Commun*.* **81**, 18–23 (2017).
3. K. Barman, G. Askarova, R. Jia, G. Hu, M. V. Mirkin. *Efficient Voltage-Driven Oxidation of Water and Alcohols by an Organic Molecular Catalyst Directly Attached to a Carbon Electrode*. J. Am. Chem. Soc*.* **145 (10),** 5786–5794 (2023).
4. R. V. Said, J. M. Kolle, K. Essalah, B. Tangour, A. Sayari. *A Unified Approach to CO_2–Amine Reaction Mechanisms.* ACS Omega, **5 (40),** 26125–26133 (2020).
5. S. Voskian, T. A. Hatton. *Faradaic Electro-Swing Reactive Adsorption for CO_2 Capture.* Energy Environ. Sci. **12 (12)**, 3530–3547 (2019).
6. M. Bilal, J. Li, H. Guo, K. Landskron. *High-voltage supercapacitive swing adsorption of carbon dioxide*. Small, 2207834 (2023).

Publications

Accepted for publication:

1. B. Delibas, K. Kron, D. Cotton, S. Sharada, J. Dawlaty, *Inferring Energetics of CO_2 -Aniline Adduct Formation from Vibrational Spectroscopy*. J. Phys. Chem. A. **In Press** (2023).

In preparation (2023):

1. R. Ding, J. Dawlaty, J. Rodríguez-López, V. Augustyn. *Understanding the mechanism of supercapacitive swing adsorption*.
2. A.R. Siddiqui, J. N'Diaye, K. Martin, J. Dawlaty, V. Augustyn, J. Rodríguez-López. *Surface-Enhanced Infrared Reflection-Absorption Spectroscopy on Graphitic Materials Enabled by Graphene-Metal Interfaces: Monitoring the Electrografting of 4-Amino-TEMPO.*

The Synthesis of Metal Superhydrides through Extreme Temperature/Pressure Conditions: towards Room Temperature Superconductivity

Ashkan Salamat, University of Nevada, Las Vegas

Keywords: Superconductivity, superhydrides, stoichiometry, characterization, spectroscopy

Research Scope

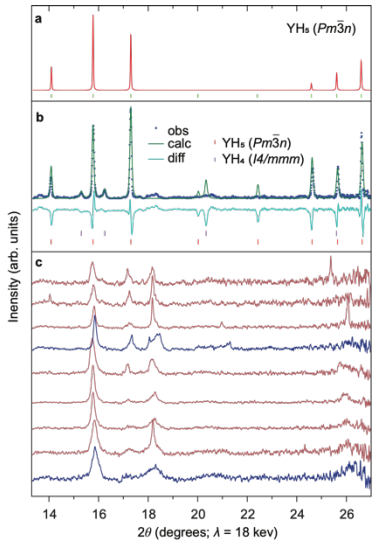

Figure 7: Accessibility of non-equilibrium yttrium-hydrogen compounds via ultrafast X-ray induced chemistry (a) theoretical pattern of A15 yttrium hydride system (b) Structural refinement of A15 structure after exposure to XFEL at 125 GPa (c) X-ray diffraction as a function of time per XFEL pulse

Controlling the formation and stoichiometric content of desired phases of materials has become a central interest for the study of a variety of fields, notably high temperature superconductivity under extreme pressures. The further possibility of accessing metastable states by initiating reactions by x-ray triggered mechanisms over ultra-short timescales is enabled with the development of x-ray free elections (XFEL). Utilizing the exceptionally high brilliance x-ray pulses from the EuXFEL, we report the synthesis of a previously unobserved yttrium hydride under high pressure, along with non-stoichiometric changes in hydrogen content as probed at a repetition rate of 4.5 MHz using time-resolved x-ray diffraction. Exploiting non-equilibrium pathways we synthesize and characterize a hydride with yttrium cations in an A15 structure type at 125 GPa, predicted using crystal structure searches, with a hydrogen content between 4.0--5.75 hydrogens per cation, that is enthalpically metastable on the convex hull. I will demonstrate a tailored approach to changing hydrogen content using changes in x-ray fluence that is not accessible using conventional synthesis methods, and reveals a new paradigm in metastable chemical physics. In addition, we have been utilizing machine learning methods to permit a deeper appreciation of correlations in higher order parameter space and be trained to behave as a predictive tool in the exploration of new materials. We have applied this approach in our search for new high temperature superconductors by incorporating models which can differentiate structural polymorphisms, in a pressure landscape, a critical component for understanding high temperature superconductivity.

Recent Progress

The discovery of high‐temperature superconductivity in metal hydrides under high pressures has revitalized the possibility of, and the race for, higher temperature superconductivity at lower pressure conditions [1]. This experimental breakthrough came after the pioneering suggestion from Ashcroft that hydrogen‐rich materials could have a large electron‐phonon coupling due to a high density of states at the Fermi level and high‐energy phonon modes;[2] each driven by the hydrogen content. The realization of these materials requires the application of high pressure conditions for driving reactions towards higher metal oxidation states that cannot be accessed through other synthesis routes.[3] Thus, driving the formation of materials that are hydrogen‐rich compared to those formed at ambient conditions. A major challenge I have identified and have attempt to address as part of this project is the synthesis of metal superhydrides and driving ever more hydrogen atoms to coordinate with a metal center. Hydrogen is challenging to work with as it is highly diffusive, and reactions can be sluggish. Heating the metal and hydrogen reactants can improve reaction rates at high pressures, and is typically achieved by focused near‐infrared (Nd:YAG or similar) lasers.[4] Laser heating in this fashion preferentially heats near the surface of the metal through direct absorption, in a similar manner to what would be achieved by heating thermally to an equilibrium state. Ultimately, this heating method has limited success due to the difficulty in dissociating molecular hydrogen and the sluggishness of hydrogen diffusion into the metal. While the advantage of laser‐based heating is that it is readily accessible, synthesis of these types of systems remains quite challenging. For example, many of the most interesting proposed hydrides have yet to be synthesized.[5] The prime example of this is the sought after cubic phase of YH10 which has been predicted to be dynamically stable with a high‐Tc at 300 GPa, on the convex hull at and above 300 GPa, not on the convex hull at 300 GPa and not on the convex hull but thermally stabilized above 1000 K and 350 GPa.[6] I have been investigating less conventional methods for inducing reactions are emerging which are far from equilibrium. In particular, synthesis via x‐ray irradiation shows great promise for allowing the synthesis of materials which otherwise could not have formed under normal thermodynamic conditions. When high energy photons interact with matter, electrons and even atoms with very high velocities can be produced, creating unique energetic pathways that can lead to the formation of products.

References

1. N Dasenbrock-Gammon, E Snider, R McBride, et. al., Evidence of near-ambient superconductivity in a N-doped lutetium hydride Nature 615 (7951), 244-250 (2023)
2. N. W. Ashcroft, Physical Review Letters 92, 187002 (2004)
3. L. Ma, K. Wang, Y. Xie, X. Yang, Y. Wang, M. Zhou, H. Liu, X. Yu, Y. Zhao, H. Wang, G. Liu, and Y. Ma, Physical Review Letters 128, 167001 (2022),

4. P. Kong, V. S. Minkov, M. A. Kuzovnikov, A. P. Drozdov, S. P. Besedin, S. Mozaffari, L. Balicas, F. F. Balakirev, V. B. Prakapenka, S. Chariton, D. A. Knyazev, E. Greenberg, and M. I. Eremets, Nature Communications 12, 5075 (2021),
5. T. Bi, N. Zarifi, T. Terpstra, and E. Zurek, Molecular Sciences and Chemical Engineering (Elsevier, 2019)
6. F. Peng, Y. Sun, C. J. Pickard, R. J. Needs, Q. Wu, and Y. Ma, Physical Review Letters 119, 107001 (2017) publisher:

Publications

1. S Villa-Cortés, D la Peña-Seaman, KV Lawler, A Salamat, The Isotope Effect and Critical Magnetic Fields of Superconducting YH: A Migdal-Eliashberg Theory Approach, arXiv preprint arXiv:2302.12988 (2023)
2. H Pasan et. al., Observation of conventional near room temperature superconductivity in carbonaceous sulfur hydride, arXiv preprint arXiv:2302.08622 (2023)
3. L Novakovic, A Salamat, KV Lawler, Machine learning using structural representations for discovery of high temperature superconductors, arXiv preprint arXiv:2301.10474 (2023)
4. AL Cornelius, KV Lawler, A Salamat, Understanding hydrogen rich superconductors: importance of effective mass and dirty limit, arXiv preprint arXiv:2202.04254 (2023)
5. L Novakovic, D Sayre, D Schacher, RP Dias, A Salamat, KV Lawler, Dispersion interactions in proposed covalent superhydride superconductors, Physical Review B 105 (2), 024512 (2022)
6. G. A Smith, I. E Collings, E. Snider, D. Smith, S. Petitgirard, J. S Smith, M. White, E. Jones, P/ Ellison, K. V Lawler, R. P Dias, A. Salamat, Carbon content drives high temperature superconductivity in a carbonaceous sulfur hydride below 100 GPa Chemical Communications 58, 65, 9064-9067 (2022)

Hybrid Metal Halides: Advancing Optoelectronic Materials

Ram Seshadri,[1] Michael Chabinyc,[1] and Mercouri Kanatzidis[2]

[1]Materials Department, University of California, Santa Barbara, CA 93106

[2]Department of Chemistry, Northwestern University, Evanston IL 60208

Keywords: Halide Materials, Perovskites, Semiconductors, Luminescence, Magnetism

Research Scope: Main-group halide compounds with the perovskite crystal structure (exemplified by methylammonium lead iodide $MAPbI_3$, with MA = $CH_3NH_3^+$, **Figure 1**), have recently attracted immense attention for their remarkable optoelectronic properties. Halide perovskites exhibit great chemical flexibility, leading to diverse structure and function. Beyond PV, the scope has broadened substantially to include the pursuit of lead-free materials, bromides, and mixed halides for light emission and detection applications. Key aspects regarding the origins of the remarkable functionality of these materials remain enigmatic. There has also been a great need for the advancement of new materials and new chemistries beyond the simple perovskites to expand this class of materials. This project has a strong focus on the creation of new materials, as well as developing fundamental understanding of the materials science of these hybrid metal halides. Some of the questions driving the project include: *How does the interaction between the organic and inorganic sublattices influence the structural transitions and lattice dynamics in halide perovskites? Can the domain of known functional hybrid metal halides be expanded through the creation of novel materials? What is the nature of film growth and the impact of structural defects on electronic properties, and how does structure and chemistry influence charge carriers?* A targeted multidisciplinary approach has been adopted towards answering these key questions to inform new chemical design principles for defect-tolerant semiconductors, produce new materials with enhanced stability and optimized performance, and enable materials with large, tunable bandgaps and high mobilities.

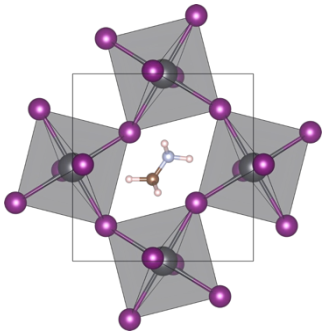

Figure 1: Depiction of the crystal structure of $MAPbI_3$ with ordered MA cations.

Recent Progress: (i) Cation size and stability in halide compounds: Cations that lie outside the acceptable range of some structural tolerance factor usually result in reduced-dimensional structures in hybrid halides. Connectivity within the inorganic network can be retained when the links among the metal-halide octahedra are rearranged to fit the large cations. New hybrid 3D bromide compounds of Pb^{2+} incorporating linear organic diammonium *A* cations APb_2Br_6 have been reported (structure types depicted in **Figure 2**) and rules for these compounds have been

proposed.[1] Size arguments have been examined in the context of expanding the cage of the organic ammonium cations in layered hybrid halide perovskites.[2] Separately, tolerance factor and size arguments have been employed to address the question of why halide double perovskites $A_2MM'X_6$ are so rare when for X = I.[3] Such compounds would be highly desirable since in contrast to the Cl and Br congeners, the band gaps ad dispersions of the iodides could be better suited for several optoelectronic applications.

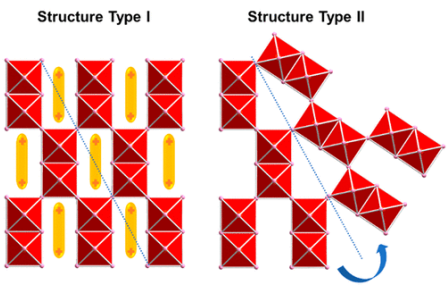

Figure 2: Crystal structure types of the APb$_2$Br$_6$ type structures with linear diammonium cations.

(ii) Layered perovskites with short inter-layer contacts: Within this collaboration, two layered hybrid lead iodide perovskites have been reported that possess unusually short interlayer distances: $(IPA)_2(MA)Pb_2I_7$ and (ACA)(MA)PbI_4} (IPA = isopropylammonium, MA = methylammonium, ACA = acetamidinium).[4] These compounds, prepared from mixing small organic cations, crystallize in a Ruddlesden–Popper type structure, or in a previously reported (by some of us) structure type with alternating cations in the interlayer space,[5] respectively. The crystal structures of these compounds were established and have been compared in detail with related structures, with the electronic structures analyzed using density functional theory-based calculations suggesting significant dispersion even between the layers, due to the short non-bonded contacts between the iodides.

(iii) Optical emission control in thin films: A method for extinguishing or enhancing different emission features has been demonstrated for the family of 2D Ruddlesden–Popper perovskites $(EA_{1-x}FA_x)_4Pb_3Br_{10}$ (EA = ethylammonium, FA = formamidinium). When grown from aqueous hydrobromic acid, crystals retain all the emission features of their parent compound, $(EA)_4Pb_3Br_{10}$. Surprisingly, when grown from dimethylformamide (DMF), an emission feature, likely self-trapped exciton (STE), near 2.7 eV is missing. Extinction of this feature is correlated with DMF being incorporated between the 2D Pb-Br sheets, forming a material with DMF inclusions. Without FA, films grown from DMF form $(EA)_4Pb_3Br_{10}$, retain little solvent, and have strong emission near 2.7 eV. Slowing the kinetics of film growth strengthens a different emission feature, likely a different type of STE, which is much broader and present in all compositions. Films of DMF-included materials have large, micron-sized domains and homogeneous orientation of the semiconducting sheets, resulting in low electronic disorder near the absorption edge. The ability to selectively strengthen or extinguish different emission features in films of these R-P materials reveals a pathway to tune the emission color in these compounds.[6]

References

1. 1. X. Li, M. Kepenekian, L. Li, H. Dong, C. C. Stoumpos, R. Seshadri, C. Katan, P. Guo, J. Even, and M. G. Kanatzidis. *Tolerance Factor for Stabilizing 3d Hybrid Halide Perovskitoids Using Linear Diammonium Cations,* J. Am. Chem. Soc. **144**, 3902–3912 (2022).
2. X. Li, S. A. Cuthriell, A. Bergonzoni, H. Dong, B. Traore, C. C. Stoumpos, P. Guo, J. Even, C. Katan, R. D. Schaller, and M. G. Kanatzidis, *Expanding the Cage of 2D Bromide Perovskites by Large A-Site Cations*, Chem. Mater. **34**, 1132–1142 (2022).
3. P. Vishnoi, R. Seshadri, and A. K. Cheetham, *Why are Double Perovskite Iodides so Rare?* J. Phys. Chem. C 125, 11756–11764 (2021).
4. L. Mao, E. E. Morgan, A. Li, R. M. Kennard, M. J. Hong, Y. Liu, C. J. Dahlman, J. G. Labram, M. L. Chabinyc, and R. Seshadri, *Layered Hybrid Lead Iodide Perovskites with Short Interlayer Distances*, ACS Energy Lett. **7**, 2801–2806 (2022).
5. C. M. M. Soe, C. C. Stoumpos, M Kepenekian, B Traore, H Tsai, W Nie, B Wang, C Katan, R Seshadri, A D. Mohite, J Even, T.. J. Marks, and M. G. Kanatzidis, *New Type of 2D Perovskites with Alternating Cations in the Interlayer Space, $(C(NH_2)_3)(CH_3NH_3)_nPb_nI_{3n+1}$: Structure, Properties, and Photovoltaic Performance*, J. Am. Chem. Soc. **139**, 16297–16309 (2017).
6. R. M. Kennard, C. J. Dahlman, E. E. Morgan, G. Wu, J. Chung, B. L. Cotts, A. Mikhailovsky, L. Mao, J. R. A. Kincaid, R. A. DeCrescent, K. H. Stone, S. Panuganti, N. R. Venkatesan, Y. Mohtashami, S. Assadi, M. G. Kanatzidis, A. Salleo, J. A. Schuller, R. Seshadri, and M. L. Chabinyc, *Enhancing and Extinguishing the Different Emission Features of Two-Dimensional $(EA_{1-x}FA_x)4Pb_3Br_{10}$ Perovskite Films*, Adv. Opt. Mater. **5**, 2200547 (2022).

10 Publications

1. S. A. Cuthriell, C. D. Malliakas, M. G. Kanatzidis, and R. D. Schaller, *Cyclic versus Linear Alkylammonium Cations: Preventing Phase Transitions at Operational Temperatures in 2D Perovskites*, J. Am. Chem. Soc. **145**, 11710–11716 (2023).
2. S. Panuganti, S. A. Cuthriell, A. A. Leonard, M. A. Quintero, C. C. Laing, B. Guzelturk, X. Zhang, L. X. Chen, M. G. Kanatzidis, and R. D. Schaller, *Transient X-Ray Diffraction Reveals Nonequilibrium Phase Transition in Thin Films of $CH_3NH_3PbI_3$ Perovskite*, ACS Energy Lett. **8**, 691–698 (2023).
3. P. Raval, R. M. Kennard, E. S. Vasileiadou, C. J. Dahlman, I. Spanopoulos, M. L. Chabinyc, M. Kanatzidis, and G. N. M. Reddy, *Understanding Instability in Formamidinium Lead Halide Perovskites: Kinetics of Transformative Reactions at Grain and Subgrain Boundaries,* ACS Energy Lett. **7**, 1534–1543 (2022).
4. A. K. Cheetham, R. Seshadri, and F. Wudl, Chemical Synthesis and Materials Discovery, Nature Synth. **1**, 514–520 (2022).
5. K. Jayanthi, I. Spanopoulos, N. Zibouche, A. A. Voskanyan, E. S. Vasileiadou, M. S. Islam, A. Navrotsky, and M. G. Kanatzidis, *Entropy Stabilization Effects and Ion Migration in 3D "Hollow" Halide Perovskites,* J. Am. Chem. Soc. **144**, 8223–8230 (2022).
6. P. Vishnoi, J. Pratap; X. Li, D. C. Binwal, K. Wyckoff, L. Mao, L. Kautzsch, G. Wu, S. D. Wilson, M. G. Kanatzidis, R. Seshadri and A. K. Cheetham, *Hybrid Layered Double Perovskite Halides of Transition Metals*, J. Am. Chem. Soc. 144, 6661–6666 (2022).
7. S. Wang, E. E. Morgan, S. Panuganti, L. Mao, P. Vishnoi, G. Wu, Q. Liu, M. G. Kanatzidis, R. Schaller, and R. Seshadri, *Ligand Control of Structural Diversity in Luminescent Hybrid Copper (I) Iodides*, Chem. Mater. **34**, 3206–3216 (2022).

8. C. Chen, E. E. Morgan, Y. Liu, J. Chen, R. Seshadri, and L. Mao, "*Breathing" Organic Cation to Stabilize Multiple Structures in Low-Dimensional Ge-, Sn-, and Pb-Based Hybrid Iodide Perovskites,* Inorg. Chem. Frontiers **9**, 4892–4898 (2022).
9. G. Laurita and R. Seshadri, *Chemistry, Structure, and Function of Lone Pairs in Extended Solids*, Acc. Chem. Res. **55**, 1004–1014 (2022).
10. S. Li, X. Li, C. A. Kocoj, X. Ji, S. Yuan, E. C. Macropulos, C. C. Stoumpos, F. Xia, L. Mao, M. G. Kanatzidis, and P. Guo. *Ultrafast Excitonic Response in Two-Dimensional Hybrid Perovskites Driven by Intense Midinfrared Pulses*, Phys. Rev. Lett. **129**, 177401 (2022).

Carbon-Based Clathrates as a New Class of sp^3-Bonded Framework Materials

Timothy Strobel, Carnegie Institution for Science

Keywords: carbon clathrate, covalent framework, diamond-like, superconductor

Research Scope

This program is focused on developing novel carbon-based clathrates, which are extended guest–host materials comprised of tetrahedral carbon frameworks that trap metal atoms in polyhedral cages. The scope of the research includes determining the range of possible framework types and guest/host substitutions, determining the critical parameters that dictate thermodynamic stability, and determining/optimizing physical properties. Given the large range of possible guest/host elemental substitutions, carbon-based clathrates represent a large family of light-weight, diamond-like materials with tunable electronic structures, and may thus impact a wide range of energy materials from thermoelectrics to superconductors.

Recent Progress

Since the initial discovery of the first boron–carbon clathrate, SrB_3C_3 in the bipartite (type-VII) sodalite structure,[1] significant progress has been made in further developing these materials. Given the broad range of possible elemental guest substitutions within the framework cages, a large number of materials properties may be achieved within a robust, diamond-like lattice. Within the type-VII framework this currently includes metallicity and possible high-T_c superconductivity,[2] electron-precise semiconducting materials,[3] and ferromagnetic/ferroelectric structures.[4-6] Thus, we have established a wide range of tunable physical properties possible for type-VII C–B clathrate compounds.

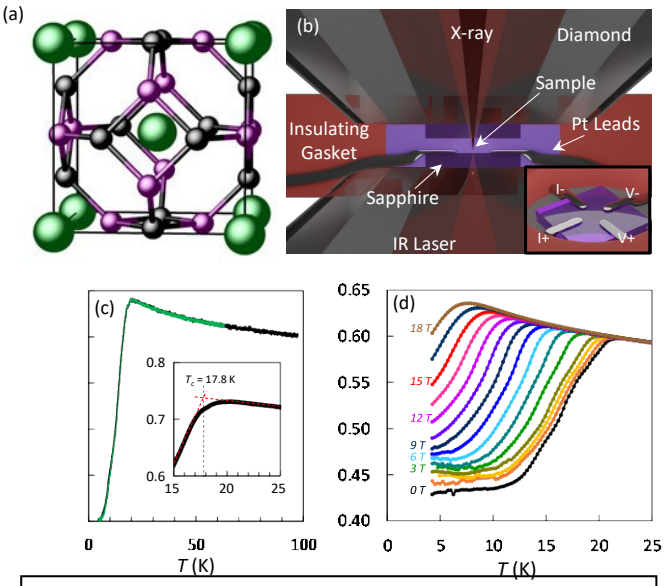

Figure 1. (a) SrB_3C_3 clathrate. (b) Experimental configuration for in situ synthesis and transport measurements. (c) Resistance drop on cooling. (d) Transition suppressed by magnetic field.

Longstanding predictions suggest that carbon-based clathrate compounds may exhibit high-T_c superconductivity.[7] Type-VII SrB_3C_3 clathrate is a hole conductor with an appreciable density of states at the Fermi energy, and we predict ambient-pressure superconductivity between 27–43 K for Coulomb pseudopotential values of $\mu^* = 0.17–0.10$, respectively.[2] To test these predictions,

we developed a novel technique for *in situ* electrical transport measurements of samples that require extreme synthesis conditions (*e.g.*, 50 GPa and >3000 K).[2] In this case, electrical leads are placed on top of a sapphire crystal within the cell, and SrB_3C_3 is synthesized between the electrical probes without damaging the contacts (Figure 1). After *in situ* high-pressure synthesis, the samples were placed into an open-flow cryostat for electrical transport measurements at low temperature. Upon cooling, a sharp drop in the electrical resistance was observed with no detectable hysteresis upon heating, consistent with superconductivity. This transition is suppressed under applied magnetic fields. In addition, when the pressure was decreased, the observed resistance drop shifted to higher temperature, consistent with the calculated trend in superconductivity when μ^*=0.15. The results suggest that SrB_3C_3 is a moderately high-temperature superconductor comparable to other covalent metals like MgB_2.

While SrB_3C_3 is a superconducting with a transition temperature comparable to MgB_2, the electronic density of states (DOS) for type-VII materials suggests that T_c could be increased significantly through electron or hole doping. Two peaks exist in the DOS on either side of the Fermi energy at +0.25 e^- and -0.5 e^-, which could enable significantly higher superconducting transition temperatures if the system was doped so that the Fermi energy was shifted to lie within one of these peaks (Figure 2). To probe the possibility of enhanced superconductivity in the Type-VII structures, we examined binary clathrate compounds with two guest metals (M1, M2) that possess difference valences. This way, the total electron count may be shifted to move the Fermi level.[8] The initial study focused on a M1:M2 ratio of 1:1 and included a systematic study of +1, +2 and +3 guest metals. After systemic study of many binary guest pairs, several systems were found to exhibit remarkably high superconducting transition temperatures (Figure 2). For example, T_c = 88 K for $KPbB_6C_6$, T_c = 78 K for $RbSrB_6C_6$, and T_c = 77 K for $KCaB_6C_6$, and all these structures were calculated to be dynamically stable at 1 atm. These results suggest that superconducting transition temperatures are highly tunable by variable guest atom substitution within the Type-VII structure, and a very large phase space becomes available for additional compositions. Initial experimental results indicate the formation of mixed-guest structures, and experimental transport measurements are in progress to validate the impact on T_c.

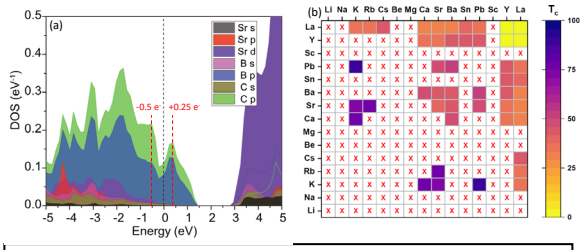

Figure 2. (a) Electronic DOS for SrB_3C_3 clathrate with peaks for electron and hole doping. (b) Calculated transition temperatures for binary type-VII clathrates.

In addition to the type-VII structure, major progress has been made in understanding the stability and optimal boron doping to create new structure types.

References

1. L. Zhu, G. M. Borstad, H. Liu, P. A. Guńka, M. Guerette, J.-A. Dolyniuk, Y. Meng, E. Greenberg, V. B. Prakapenka, B. L. Chaloux, A. Epshteyn, R. E. Cohen, and T. A. Strobel, *Carbon-Boron Clathrates as a New Class of sp^3-Bonded Framework Materials*, Sci. Adv., **6**, eaay8361 (2020).
2. L. Zhu, H. Liu, M. Somayazulu, Y. Meng, P.A. Guńka, T.B. Shiell, C. Kenny-Benson, S. Chariton, V.B. Prakapenka, H. Yoon, J.A. Horn, J. Paglione, R. Hoffmann, R.E. Cohen, T.A. Strobel, *Superconductivity in SrB_3C_3 Clathrate*, Phys. Rev. Research, **5**, 013012 (2023).
3. T.A. Strobel, L. Zhu, P.A. Guńka, G.M. Borstad, M. Guerette, *A Lanthanum-Filled Carbon–Boron Clathrate*, Angew. Chem. Int. Ed., **133**, 2913-2917 (2021).
4. T. Bi, M. Hansen, T.A. Strobel, *Prediction and synthesis of a ferroelectric boron–carbon clathrate, In Preparation*, (2023).
5. L. Zhu, T.A. Strobel, R.E. Cohen, *Prediction of an Extended Ferroelectric Clathrate*, Phys. Rev. Lett., **125**, 127601 (2020).
6. Z. Tan, H. Zhang, X. Wu, J. Xing, Q. Zhang, J. Zhu, *New High-Performance Piezoelectric: Ferroelectric Carbon-Boron Clathrate*, Phys. Rev. Lett., **130**, 246802 (2023).
7. F. Zipoli, M. Bernasconi, and G. Benedek, *Electron-phonon coupling in halogen-doped carbon clathrates from first principles*, Phys. Rev. B, **74**, 205408 (2006).
8. N. Geng, K.P. Hilleke, L. Zhu, X. Wang, T.A. Strobel, E. Zurek, *Conventional High-Temperature Superconductivity in Metallic, Covalently Bonded, Binary-Guest C–B Clathrates*, J. Am. Chem. Soc., **145**, 1696-1706 (2023).

Publications

1. T.A. Strobel, L. Zhu, P.A. Guńka, G.M. Borstad, M. Guerette, *A Lanthanum-Filled Carbon–Boron Clathrate*, Angew. Chem. Int. Ed., **133**, 2913-2917 (2021).
2. L. Zhu, Y. Lin, R.E. Cohen, T.A. Strobel, *Stability of Carbon-Silicon Clathrates*, Applied Phys. A, **128**, 448 (2022).
3. L. Zhu, H. Liu, M. Somayazulu, Y. Meng, P.A. Guńka, T.B. Shiell, C. Kenny-Benson, S. Chariton, V.B. Prakapenka, H. Yoon, J.A. Horn, J. Paglione, R. Hoffmann, R.E. Cohen, T.A. Strobel, *Superconductivity in SrB_3C_3 Clathrate*, Phys. Rev. Research, **5**, 013012 (2023).
4. N. Geng, K.P. Hilleke, L. Zhu, X. Wang, T.A. Strobel, E. Zurek, *Conventional High-Temperature Superconductivity in Metallic, Covalently Bonded, Binary-Guest C–B Clathrates*, J. Am. Chem. Soc., **145**, 1696-1706 (2023).
5. T. Bi, B. Eggers, R.E. Cohen, B.J. Campbell, T.A. Strobel, *Computational Screening and Stability of Boron-Substituted Carbon Clathrate Structures*, Submitted (2023).
6. T.A. Strobel, T. Bi, P.A. Guńka, J.M. Hübner, M.F. Hansen, S.G. Dunning, S. Chariton, V.B. Prakapenka, Y. Meng, *Synthesis of Carbon Clathrate Structures Stabilized by Boron*, Submitted (2023).
7. T. Bi, M. Hansen, T.A. Strobel, *Prediction and synthesis of a ferroelectric boron–carbon clathrate, In Preparation*, (2023).

Kinetics and Thermodynamics of Gaseous Mixtures in Nano-Confined Environments

Timo Thonhauser (WFU), Jing Li (Rutgers), Kui Tan (UNT)

Keywords: Metal-organic frameworks, gas mixtures, co-adsorption, kinetics, thermodynamics

Research Scope

Our program investigates the kinetics and thermodynamics of *gaseous mixtures* in nano-confined environments. The nano-confinement can tip the thermodynamic vs. kinetic balance, and current understanding and theory can lead to incorrect predictions for gaseous mixtures [1–4]. This is of particular interest in real-world applications, where gases are typically mixed or contain impurities and are often exposed to humid conditions. Our approach integrates intensive *in situ* characterization, *ab initio* modeling, and tailored synthesis. Our objectives are (i) to disentangle kinetic from thermodynamic effects by a series of sequential and simultaneous gas loading experiments; (ii) to identify the interactions between gas molecules of the mixture as well as between gas molecules and the host; and (iii) to develop nano-porous materials that are stable in reactive humid mixture environments, such as flue gases. Due to their structural diversity, functional flexibility, and design freedom, metal organic frameworks (MOFs) will be the main platform and serve as our nano-confined environments to address our objectives.

Recent Progress

We developed a novel strategy to increase the gas selectivity of MOFs by co-adsorbing other molecules—e.g. the addition of NH_3 in MOF-74 dramatically alters its adsorption behavior of C_2H_2 and C_2H_4. Combining *in situ* IR and *ab initio* calculations, we find that co-adsorbing NH_3 causes C_2H_2 to bind stronger and diffuse faster than C_2H_4. Remarkably, C_2H_4 is excluded from the MOF during simultaneous loading of mixed C_2H_2/C_2H_4, which is due to C_2H_2 occupying the space adjacent to metal-bound NH_3 and thus forming additional diffusion barriers for C_2H_4. Our finding dispels the belief that strongly co-adsorbed species in MOFs undermine their performance in adsorbing/separating weakly bound target molecules. Furthermore, it suggests a new route to tune the selectivity of MOFs by harnessing the interactions among co-adsorbed guests [5].

Given that the competition of NH_3 and H_2O within MOFs is rarely explored and only poorly understood due to challenges in characterization, we combined *in situ* IR with *ab initio* calculations to unveil the competitive adsorption of NH_3 and H_2O for adsorption sites in the representative MOF-74 by analyzing the molecular exchange process inside the nanochannel. Through applying sequential loading, we find that the incoming NH_3 can displace the metal-bound H_2O, moving it to secondary adsorption sites due to the stronger binding of NH_3. Interestingly, the reverse process of H_2O displacing metal-bound NH_3 is also possible upon increasing H_2O concentration. We show that this process is driven by a reduced kinetic barrier,

the formation of an energetically favorable water cluster, and H-bonding between the metal-coordinated H_2O and displaced NH_3. Our finding emphasizes that the description of gas mixtures in MOFs cannot simply be established by single-component studies; rather, intermolecular interactions such as H-bonding can greatly affect molecular distributions. We further show that vibrational modes of adsorbed NH_3 are markedly perturbed upon contact with H_2O, due to the freezing of NH_3 vibrations by co-adsorbed H_2O. Our study sheds light on co-adsorption processes in MOFs and helps assess NH_3 removal efficiency of MOFs under realistic humid conditions [6].

Using our sequential loading method, we also studied the co-adsorption of H_2O and CO_2 in TiFSIX-3-Ni—a high CO_2 affinity hybrid ultra-microporous material (HUM)—and find that slow H_2O sorption kinetics can enable CO_2 uptake and release using shortened adsorption cycles with retention of 90% of dry CO_2 uptake. Further insight into co-adsorption is provided by *in situ* IR and *ab initio* calculations, which examined the binding sites and sorption mechanisms, revealing that both CO_2 and H_2O molecules occupy the same ultra-micropore through favorable interactions between them at low water loading. An energetically favored water network displaces CO_2 molecules at higher loading. Our results offer design principles and insight into co-adsorption that is relevant across the full spectrum of carbon capture sorbents to better address the challenge posed by humidity to gas capture [7].

We also made an interesting discovery concerning the defect termination of UiO-66 materials, which has been a long-standing debate since the structure was reported. We show that missing-linker defects in an ambient environment are compensated with both carboxylate and co-adsorbed water. In contrast to the prevailing assumption that the monocarboxylate groups (COO^-) of the modulators form bidentate bonding with two Zr^{4+} sites, we find that co-existing H_2O readily inserts and breaks Zr–O–C bonds, resulting in COO^- coordinating to the open Zr^{4+} sites in an unidentate mode. This finding provides new understanding of defect termination in UiO-66 and sheds light on the origin of its enhanced physicochemical properties [8].

Finally, separation of gas and/or vapor mixtures by porous solids provides an energy-efficient alternative compared to energy-intensive distillations. Particularly, the separation of linear hexane isomers from its branched counterparts is crucial to obtain premium grade gasoline and high-quality feedstock for ethylene production. We synthesized a new, flexible Zn-MOF, $[Zn_5(\mu_3\text{-}OH)_2(adtb)_2(H_2O)_5 \cdot 5\ DMA]$ (Zn-adtb), constructed from a butterfly shaped carboxylate linker with underlying (4,8)-connected scu topology. It is capable of separating the C_6 alkane isomers based on their branching. The sorbate–sorbent interactions and separation mechanisms were investigated and analyzed through *in situ* FTIR, solid state NMR and *ab initio* modeling. Our study reveals that Zn-adtb discriminates the nHEX/3MP isomer pair through a kinetic separation mechanism and the nHEX/23DMB isomer pair through a molecular sieving mechanism. Column breakthrough measurements further demonstrate the extraordinary separation of linear nHEX from its mono- and di-branched isomers under conditions similar to industrial settings [9].

References

1. H. Wang, M. Warren, J. Jagiello, S. Jensen, S.K. Ghose, K. Tan, L. Yu, T. J. Emge, T. Thonhauser, and J. Li, *Crystallizing Atomic Xenon in a Flexible MOF to Probe and Understand Its Temperature Dependent Breathing Behavior and Unusual Gas Adsorption Phenomenon*, J. Am. Chem. Soc. **142**, 20088 (2020).
2. K. Tan, S. Jensen, H. Wang, L. Feng, K. Wei, H.C. Zhou, J. Li, and T. Thonhauser, *Thermally Activated Adsorption in Metal-Organic Frameworks with a Temperature-Tunable Diffusion Barrier Layer*, Angew. Chem. Int. Ed. **59**, 18468 (2020).
3. K. Tan, S. Jensen, S. Zuluaga, E.K. Chapman, H. Wang, R. Rahman, J. Cure, T.-H. Kim, J. Li, T. Thonhauser, and Y.J. Chabal, *Role of Hydrogen Bonding on Transport of Co-adsorbed Gases in Metal-Organic Framework Materials*, J. Am. Chem. Soc. **140**, 856 (2018).
4. K. Tan, S. Zuluaga, Q. Gong, Y. Gao, N. Nijem, J. Li, T. Thonhauser, and Y.J. Chabal, *Competitive co-adsorption of CO_2 with H_2O, NH_3, SO_2, NO, NO_2, N_2, O_2, and CH_4 in M-MOF-74 (M = Mg, Co, Ni): The role of hydrogen bonding*, Chem. Mater. **27**, 2203 (2015).
5. E. Chapman, S. Ullah, H. Wang, L. Feng, K. Wang, H.-C. Zhou, J. Li, T. Thonhauser, and K. Tan, *Tuning the Adsorption Properties of Metal-Organic Frameworks through Co-adsorbed Ammonia*, ACS Appl. Mater. Interfaces **13**, 43661 (2021).
6. K. Tan, S. Ullah, H. Pandey, E.M. Cedeño-Morales, H. Wang, K. Wang, H.-C. Zhou, J. Li, and T. Thonhauser, *Competitive Adsorption of NH_3 and H_2O in Metal-Organic Framework Materials: MOF-74*, Chem. Mater. **34**, 7906 (2022).
7. S. Ullah, K. Tan, D. Sensharma, N. Kumar, S. Mukherjee, A.A. Bezrukov, J. Li, M.J. Zaworotko, and T. Thonhauser, *CO_2 Capture by Hybrid Ultramicroporous TiFSIX-3-Ni under Humid Conditions Using Non-Equilibrium Cycling*, Angew. Chem. Int. Ed. **61**, e202206613 (2022).
8. K. Tan, H. Pandey, H. Wang, E. Velasco, K.-Y. Wang, H.-C. Zhou, J. Li, and T. Thonhauser, *Defect Termination in the UiO-66 Family of Metal-Organic Frameworks: The Role of Water and Modulator*, J. Am. Chem. Soc. **143**, 6328 (2021).
9. E. Velasco, S. Xian, H. Wang, S.J. Teat, D.H. Olson, K. Tan, S. Ullah, T.M. Osborn Popp, A.D. Bernstein, K.A. Oyekan, A.J. Nieuwkoop, T. Thonhauser, and J. Li, *Flexible Zn-MOF with Rare Underlying scu Topology for Effective Separation of C_6 Alkane Isomers*, ACS Appl. Mater. Interfaces **13**, 51997 (2021).

Publications

1. H. Pandey, H. Wang, L. Feng, K.-Y. Wang, H.-C. Zhou, J. Li, T. Thonhauser, and K. Tan, *Revisiting Competitive Adsorption of Small Molecules in the Metal-Organic Framework Ni-MOF-74*, Inorg. Chem. **62**, 950 (2023).
2. Y. Ye, S. Xian, H. Cui, K. Tan, L. Gong, B. Liang, T. Pham, H. Pandey, R. Krishna, P.C. Lan, K.A. Forrest, B. Space, T. Thonhauser, J. Li, and S. Ma, *Metal-Organic Framework Based Hydrogen-Bonding Nanotrap for Efficient Acetylene Storage and Separation*, J. Am. Chem. Soc. **144**, 1681 (2022).
3. L. Yu, S. Ullah, H. Wang, Q. Xia, T. Thonhauser, and J. Li, *High-Capacity Splitting of Mono- and Dibranched Hexane Isomers by a Robust Zinc-Based Metal-Organic Framework*, Angew. Chem. Int. Ed. **61**, e202211359 (2022).
4. X. Li, J. Liu, K. Zhou, S. Ullah, H. Wang, J. Zou, T. Thonhauser, and J. Li, *Tuning Metal-Organic Framework (MOF) Topology by Regulating Ligand and Secondary Building Unit (SBU) Geometry: Structures Built on 8-Connected M_6 (M = Zr, Y) Clusters and a Flexible Tetracarboxylate for Propane-Selective Propane/Propylene Separation*, J. Am. Chem. Soc. **144**, 21702 (2022).

5. Y. Lin, L. Yu, S. Ullah, X. Li, H. Wang, Q. Xia, T. Thonhauser, and J. Li, *Temperature-Programmed Separation of Hexane Isomers by a Porous Calcium Chloranilate Metal-Organic Framework*, Angew. Chem. Int. Ed. **61**, e202214060 (2022).
6. S. Ullah, K. Tan, D. Sensharma, N. Kumar, S. Mukherjee, A.A. Bezrukov, J. Li, M.J. Zaworotko, and T. Thonhauser, *CO_2 Capture by Hybrid Ultramicroporous TiFSIX-3-Ni under Humid Conditions Using Non-Equilibrium Cycling*, Angew. Chem. Int. Ed. **61**, e202206613 (2022).
7. K. Tan, S. Ullah, H. Pandey, E.M. Cedeño-Morales, H. Wang, K. Wang, H.-C. Zhou, J. Li, and T. Thonhauser, *Competitive Adsorption of NH_3 and H_2O in Metal-Organic Framework Materials: MOF-74*, Chem. Mater. **34**, 7906 (2022).
8. L. Yu, X. Han, H. Wang, S. Ullah, Q. Xia, W. Li, J. Li, I. da Silva, P. Manuel, S. Rudić, Y. Cheng, S. Yang, T. Thonhauser, and J. Li, *Pore Distortion in a Metal-Organic Framework for Regulated Separation of Propane and Propylene*, J. Am. Chem. Soc. **143**, 19300 (2021).
9. K. Tan, H. Pandey, H. Wang, E. Velasco, K.-Y. Wang, H.-C. Zhou, J. Li, and T. Thonhauser, *Defect Termination in the UiO-66 Family of Metal-Organic Frameworks: The Role of Water and Modulator*, J. Am. Chem. Soc. **143**, 6328 (2021).
10. E. Chapman, S. Ullah, H. Wang, L. Feng, K. Wang, H.-C. Zhou, J. Li, T. Thonhauser, and K. Tan, *Tuning the Adsorption Properties of Metal-Organic Frameworks through Co-adsorbed Ammonia*, ACS Appl. Mater. Interfaces **13**, 43661 (2021).

Exploration of Radial Conjugation Pathways in Pi-Electron Materials

John D. Tovar, PI, Department of Chemistry, Johns Hopkins University; Ramesh Jasti, co-PI, Department of Chemistry, University of Oregon; Miklos Kertesz, co-PI, Department of Chemistry, Georgetown University

Keywords: Pi-electron materials, radial conjugation, delocalization

Research Scope

This project involves hypothesis-driven exploratory research on new manifestations of pi-electronic delocalization relevant to organic electronics via building onto hitherto unused structural subunits that invoke different degrees of aromaticity, conjugation, radical character and strain. Our team consists of three interrelated groups specializing in *pi-conjugated organic electronic systems with unusual properties well beyond the conventional arsenal of organic semiconductors with linear conjugation topologies present on planar pi-electron backbones*. These systems combine unusual bonding patterns, unusual curvatures, and unusual charge states in new ways that have yet to be tapped for emerging electronics applications. The synthetic and physical organic activities of Tovar and Jasti are simultaneously supported by and driven by the computational activities of Kertesz to understand molecules with novel spin systems, novel electronic delocalization and novel aromaticities. Our objectives for this research program are to (1) design and characterize new energy materials that access unusual spin states and pi-electron delocalization in curved carbon structures and (2) examine through-space delocalization as encouraged by mechanical bonding of curved components.

Recent Progress

This project has led to the creation of several novel types of polymeric materials based upon radially conjugated cycloparaphenylene (CPP) "nanohoops". Our initial work in this regard led to the creation of norbornene-fused CPP monomers that could be polymerized via ring-opening metathesis polymerization into new partially unsaturated polymer backbones able to foster fullerene detection (Figure 1).[1] It also realized the initial development of new and as yet unexplored conjugated polymers that incorporate a hybrid blend of standard linear pi-conjugation along with the radial delocalization inherent to the nanohoop CPP architecture (Figure 2 top).[2] New electronic states emerged in these new polymers that were not simple additive contributions from the

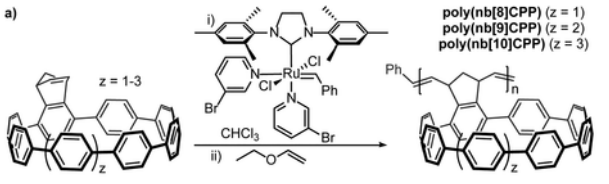

Figure 1. ROMP as a method to create polymerized but non-conjugated CPPs.

linear and radial components but rather represented hybrid delocalization spread over both linear and radial features.

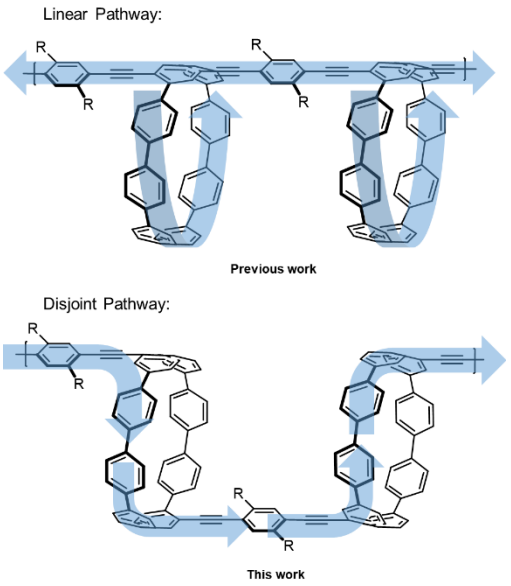

Figure 2. Linear (top) and disjoint (bottom) conjugation pathways.

In our prior design, we recognized the prospect for selective localization or conjugation through the phenyl group of the CPP that bore the two chain-extending alkyne substituents (Figure 2 bottom). We therefore extended this concept to a new monomer design whereby the two chain extending alkynes were placed on different phenyl rings of the CPP nanoring.[3] With this molecular design, the intra-polymer conjugation pathway necessarily engages both the radial CPP nanohoop and the linearly conjugated pi-linkers. We demonstrated the nature of this hybrid radial-linear conjugation pathway using spectroscopic and computational studies of the disjoint polymers and oligomers alongside critical comparison with carefully designed model systems that captured key aspects of the disjoint conjugation path but without the radial delocalization. Our current investigations entail the development of new synthetic pathways in order to facilitate molecular and polymeric tailoring of linear-radial electronic structure.

This project has also consists of quantum chemical exploration of quinonoid repeat units in π-conjugated oligomers and polymers,[4] which have promising characteristics by providing unique structures and electronic properties, including, according to our recent work, varying degrees of ground state open shell diradical character and small band gaps.[5] So far, quinonoid ground state polymers were rarely identified, and one of the goals of this work was to expand the portfolio of such systems in which a diverse set of repeat units were considered, about half preferred a quinonoid (a) and half preferred aromatic structures (b) (Figure 3). The dependency of the diradical character as a function of size and composition opens a rich space to discover trends affecting the aromaticity and diradical character. Homo-polymers with quinonoid ground states show a high diradical character, while those with the aromatic ground state behave as closed-shell systems with no or a very small diradical character. The diradical character of quinonoid

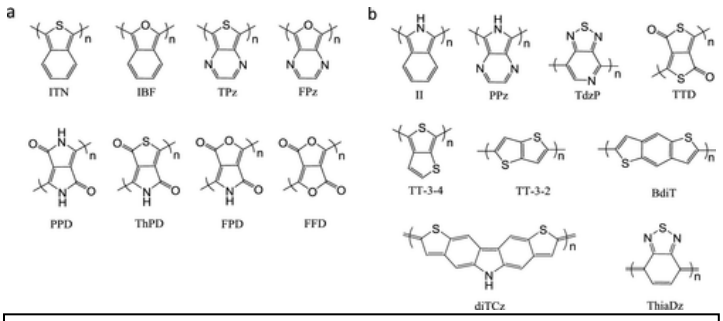

Figure 3. Quinonoid (a) and aromatic (b) ground state π-conjugated polymers

systems significantly increases with the size of the oligomer.[5] Work in progress builds on our novel insights into systematic external perturbations to reduce the bandgap of quinonoid π-conjugated polymers to previously unseen values.

References

1. R. L. Maust, P. Li, B. Shao, S. M. Zeitler, P. B. Sun, H. W. Reid, L. N. Zakharov, M. R. Golder, and R. Jasti, *Controlled Polymerization of Norbornene Cycloparaphenylenes Expands Carbon Nanomaterials Design Space*, ACS Central Science **7**, 1056-1065 (2021)
2. G. M. Peters, G. Grover, R. Maust, C. Colwell, H. Bates, W. Edgell, R. Jasti, M. Kertesz, and J. D. Tovar, *Linear and radial conjugation in extended pi-electron systems*, Journal of the American Chemical Society **142**, 2293-2300 (2020).
3. E. Peterson, R. L. Maust, R. Jasti, M. Kertesz and J. D. Tovar, *Splitting the ring: impact of ortho and meta pi conjugation pathways through disjointed [8]cycloparaphenylene electronic materials*, Journal of the American Chemical Society **144**, 4611-4622 (2022).
4. G. Grover, G. M. Peters, J. D. Tovar, and M. Kertesz, *Quinonoid vs. aromatic structures of heteroconjugated polymers from oligomer calculations*, Physical Chemistry Chemical Physics **22**, 11431-11439 (2020).
5. G. Grover, J. D. Tovar, and M. Kertesz, *Quinonoid versus Aromatic π-Conjugated Oligomers and Polymers and Their Diradical Characters*, The Journal of Physical Chemistry C **126**, 5302-5310 (2022).

Publications

1. R. L. Maust, P. Li, B. Shao, S. M. Zeitler, P. B. Sun, H. W. Reid, L. N. Zakharov, M. R. Golder, and R. Jasti, *Controlled Polymerization of Norbornene Cycloparaphenylenes Expands Carbon Nanomaterials Design Space*, ACS Central Science **7**, 1056-1065 (2021)
2. E. Peterson, R. L. Maust, R. Jasti, M. Kertesz and J. D. Tovar, *Splitting the ring: impact of ortho and meta pi conjugation pathways through disjointed [8]cycloparaphenylene electronic materials*, Journal of the American Chemical Society **144**, 4611-4622 (2022).
3. G. Grover, J. D. Tovar, and M. Kertesz, *Quinonoid versus Aromatic π-Conjugated Oligomers and Polymers and Their Diradical Characters*, The Journal of Physical Chemistry C **126**, 5302-5310 (2022).

iClick Enabled Synthesis of Porous Organometallic Polymers (POMPs) and Soft Materials

PI: Adam S. Veige, University of Florida

Co-PI: Kirk S. Schanze, University of Texas San Antonio

Keywords: metallopolymer, porous polymer, iClick, inorganic click

Program Scope

iClick is a synthetic technique that links metal ions through a triazolate bridge. Originally, inorganic click (iClick) was defined as the cycloaddition reaction between a metal-azide and metal-alkyne (Eq. 1). iClick now includes the cycloaddition of a metal-azide and an organic alkyne or a metal-acetylide and an organic azide. This presentation further expands iClick to the synthesis of porous organometallic polymers and post-polymerization functionalization of polymers.

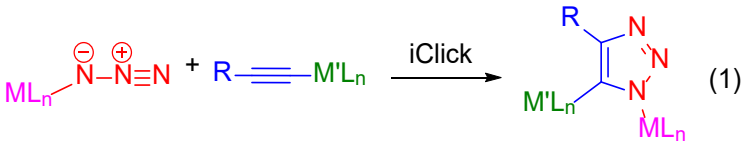

(1)

Recent Progress

Project 1: Porous Organometallic Polymers (POMP)

Heterogeneous catalysts are useful in industrial processes due to their advantageous sustainability, recyclability, robustness, and ease of catalyst/product separation. Porous organic polymers (POPs) have numerous applications in catalysis, medicine, gas separation, CO_2 capture, and as sorbents. POPs are highly selective catalysts and can lower process costs. Over the past decades, some reports of porous organic polymers containing metal ions were published; however, the ligands incorporating the metal centers were limited to polypyridines, phthalocyanine, and porphyrins. This presentation will discuss the successful synthesis of porous organometallic polymers (POMP) via iClick. The results of this work were published in Dalton Transactions, **2022**, 51, 18520-18527.

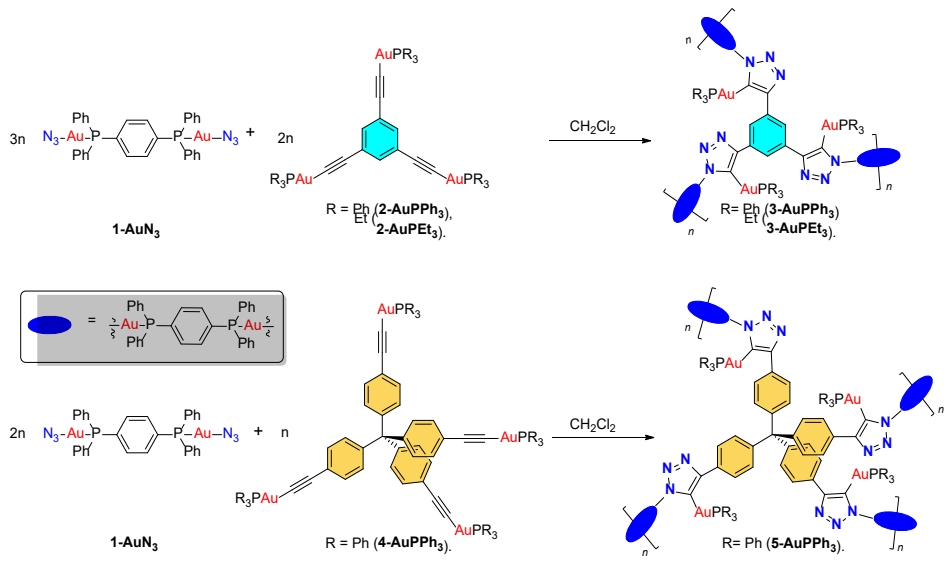

Scheme 1. Idealized structure of the iClick network metallopolymers (**3-AuPPh$_3$**, **3-AuPEt$_3$**, and **5-AuPPh$_3$**).

Confirmation of the iClick network metallopolymers comes from FTIR, ^{13}C solid-state cross-coupling magic angle spinning (CPMAS) NMR spectroscopy, thermogravimetric analysis (TGA), differential scanning calorimetry (DSC), and nitrogen and CO_2 sorption analysis. Model complexes of the repeat unit in the metallopolymer networks provide structural insights due to the insolubility of iClick network metallopolymers.

Project 2: iClick Dynamic Aurophilic Bonding Induced Polymer Crosslinks, Aggregation and Self-Assembly.

iClick can also create porous organometallic polymers or networks via Au-Au crosslinking. One of the objectives was to synthesize copolymers that feature a random coil segments comprised of polystyrene and a **Au$_2$** functionalized segments prepared by metalation/iClick of ethynyl-substituted polystyrene repeats (Scheme 2). These polymers will display novel and interesting macromolecular self-assembly properties resulting from aggregation induced by aurophilic interactions of the Au_2--> Au_4 conversion. The presentation will outline the successful metalation of polystyrene copolymers, iClick functionalization, and preliminary photophysical characterization of the polymers.

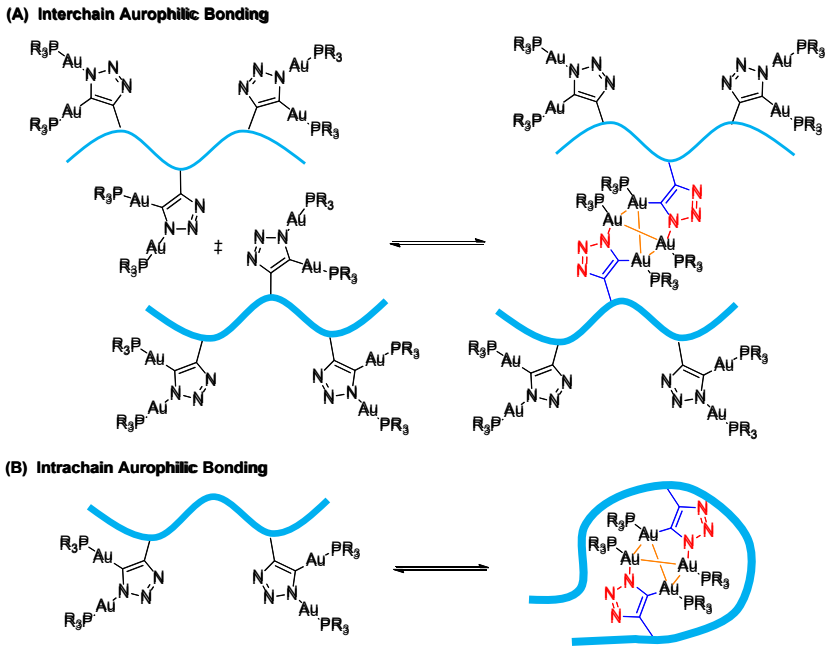

Scheme 2. Proposed (A) Interchain and Intrachain (B) aurophilic bonding via Au_2 → Au_4 formation.

Publications:

1. Shen, Y-H; Ghiviriga, I.; Abboud, K. A.; Schanze, K. S.;* and Veige. A. S.* *iClick Synthesis of Network Metallopolymers*. *Dalton Trans.* **2022**, 51, 18520-18527.
2. Li, Y.; Shen, Y-H.; Esper, A. M.; Tidwell, J. R.; Veige, A. S.*; Martin, C. D.* *Probing borafluorene B-C bond insertion with gold acetylide and azide*. *Dalton Trans*, **2022**, 52, 668-674.
3. He, R.; Chakraborty, J.; Islam, T.; Arman, H. D.; Griffith, W. P.; Veige, A. S.;* Schanze, K. S.* *N-heterocyclic carbene platinum-butadiyne Click/iClick complexes. Towards blue-violet phosphorescence*. *J. Organomet. Chem*. **2022**, 122440.
4. Shen, Y-H.; Esper, A. M.; Ghiviriga, I.; Abboud, K. A.; Schanze, K. A.; Ehm, C.*; Veige, A. S.* *SPAAC iClick: Progress towards a biorthogonal reaction incorporating metal ions*. *Dalton Trans.* **2021**, *50*, 12681-12691.
5. Makal, T. A.; Veige, A. S.* *Development of Inorganic Click (iClick) and Related Cycloaddition Chemistry*, *Comprehensive Coordination Chemistry III*, Elsevier, **2021**, 1086-1100.

Molecular mechanisms of moisture-driven DAC within charged polymers (MissionDAC)

J. Wade, Northern Arizona University, NAU; H. Feigenbaum, NAU; M. Yacaman, NAU; J. Flory, Arizona State University, ASU; P. Fromme, ASU; M. Green, ASU; K. Lackner, ASU; H. Zhuang, ASU; B. Freeman, University of Texas at Austin

Keywords: Direct Air Capture, Moisture Swing, Sorption, Transport, Chemo-Mechanic

Research Scope

The goals of the MissionDAC project are to reveal the thermodynamic, kinetic, and chemo-mechanical drivers of the moisture-swing CO_2 separation in charged polymers to inform the development of new materials for direct air capture (DAC; **Fig. 1**). Inherent to all our investigations is an understanding of the interactions between water, ions, and polymer structures in nano-confined domains as a function of water activity. The broader goals of our team are addressed through three objectives. 1) *Reveal thermodynamic drivers of the moisture driven CO_2 capture/release; 2) Reveal and probe intrinsic reaction rate and transport limitations of MS materials*; and 3) *Reveal chemo-mechanical coupling for fast, reactive function and durability.*

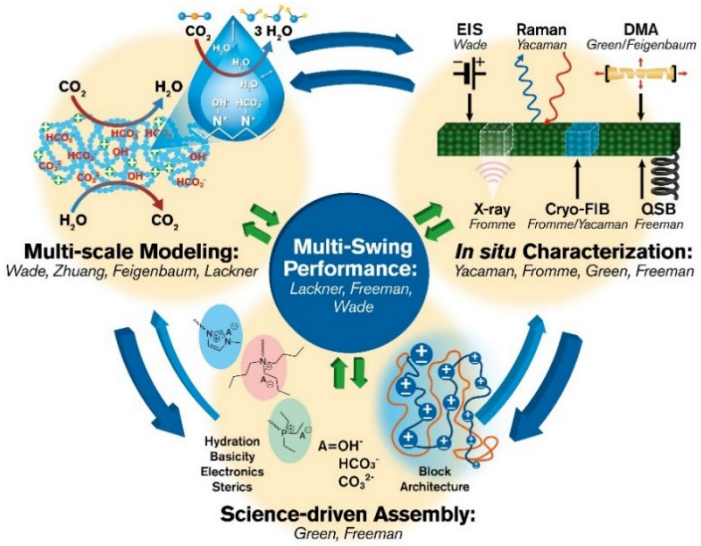

Figure 1. MissionDAC Overview

Recent Progress

Early work established standard materials and methods with two moisture responsive commercial anion exchange polymers, i) a polystyrene resin with quaternary ammonium sites charge balanced with mobile bicarbonate anions (QA-HCO_3), and ii) a polyphenylene oxide membrane with similar QA-HCO_3 active sites. The standardization ensures a clear understanding of results and phenomena observed across a diversity of investigations from which new understandings of MS sorption, transport and chemo-mechanics in these charged polymers will be revealed and lead to improved materials for carbon capture applications and beyond.

Obj. 1 Thermodynamics: CO_2 capacity and kinetics of moisture swing sorption were measured in isothermal open flow experiments with infrared gas detection. This work confirms that larger swings in RH lead to greater CO_2 capacity, building the experimental validation for the moisture dependent isotherms (solubility) models. Further, density functional theory and molecular

dynamic models have been established to compare simulated energetics of the moisture swing chemistry to published values [1], and newly acquired sorption and calorimetric data.

A key hypothesis of the MS mechanism is the influence of microstructure on the stability of the hydrated reactive anions (OH^-, CO_3^{2-}, HCO_3^-). Microstructural characteristics were investigated using Cryo-FIB tomography and electron microscopy. Early images of the membrane materials confirm the macroscopic dimensions and show distinct lamella structures (Fig. 2c) that show anisotropic swell upon hydration (not shown). The cryo-FIB imaging has been conducted in coordination with i) 2D microscopy coupled with electron diffraction (Fig. 2a), and ii) molecular dynamic (MD) structural models (Fig. 2c). Combined, this effort supports the evidence of a periodic structure that is expected to influence both ion transport and MS sorption in this anion exchange membrane.

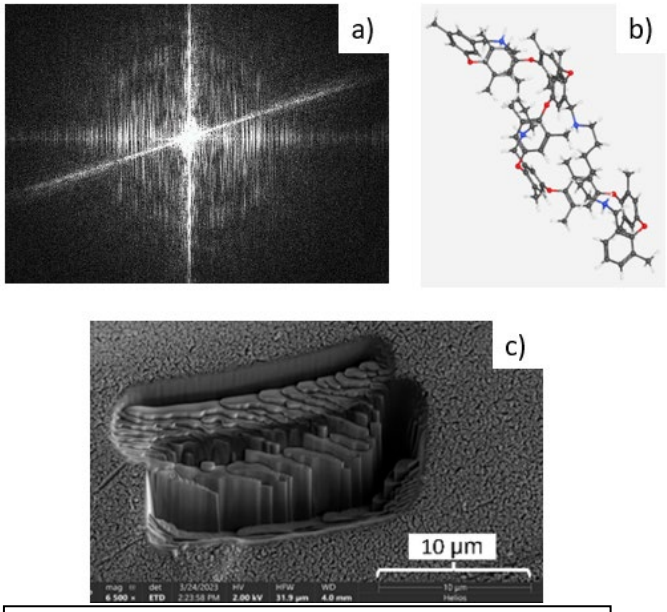

Figure 2. MS membrane characterization.

Obj. 2 Kinetics: The rates of CO_2 sorption and permeability in the membrane-based MS standards were evaluated experimentally and through simulation. A humidified sweep cell was used to measure CO_2 permeability as a function of relative humidity. CO_2 permeability increased two to fourfold when feed CO_2 partial pressure decreased from 101 kPa to 8 kPa. Increased permeability with decreasing feed partial pressure is a well-documented phenomenon in facilitated transport literature [2], [3]. In addition to MS responsive materials, dry CO_2 and N_2 permeabilities were measured for phosphonium based ionic liquids with aprotic heterocylic anions with variable CO_2 binding strength, revealing exponentially higher CO_2 permeabilities and CO_2/N_2 perm-selectivity at lower CO_2 pressures, again illustrative of a facilitated transport mechanism that may best be exploited in low pressure applications, like DAC. Simulation efforts validated from sorption experiments suggest that kinetics of MS CO_2 adsorption/desorption are likely limited by a reactive resistance, not ion mass transport [4].

Obj. 3 Chemo-mechanics: Moisture swing polymers are challenged by competing objectives for affordable and scalable CO_2 capture: fast reactivity, high capacity, and mechanical toughness. Tuning mechanical properties across water vapor activity, without a major compromise on CO_2 capacity and kinetics will enable manufacturable materials with longer lifetimes. Measurements of mechanical strain in the membrane-based MS materials were taken as a function of relative humidity to approximate the swell coefficient and cyclic loading behavior due to swelling/shrinking during water and CO_2 sorption to inform temporal chemo-mechanical models. Results thus far show that the material swells approximately equally in the plane of the

membrane, about 13–15%, but significantly less in the out-of-plane direction, 1–4%, consistent with cryoFIB imaging with and without hydration. Finally, new QA functionalized polymer films have been synthesized using grafting techniques onto porous polymer supports.

References

1. X. Shi, H. Xiao, X. Liao, M. Armstrong, X. Chen, and K. S. Lackner, *Humidity effect on ion behaviors of moisture-driven CO_2 sorbents*, **J. Chem. Phys.**, vol. 149, no. 16, p. 164708, Oct. 2018, doi: 10.1063/1.5027105.
2. J. Liao *et al.*, Fabrication of high-performance facilitated transport membranes for CO_2 separation, **Chem. Sci.**, vol. 5, no. 7, pp. 2843–2849 (2014).
3. L. Ansaloni, Y. Zhao, B. T. Jung, K. Ramasubramanian, M. G. Baschetti, and W. S. W. Ho, F*acilitated transport membranes containing amino-functionalized multi-walled carbon nanotubes for high-pressure CO2 separations*, **J. Memb. Sci.**, vol. 490, pp. 18–28, (2015).
4. J. Wade, H. Marques-Lopez, W. Wang, J. Flory, and B. Freeman, B., *Moisture Driven CO_2 Pump for Direct Air Capture.* **J. Memb. Science.** In Review, (2023). http://ssrn.com/abstract=4442166

Publications

1. Y. Kaneko and K.S. Lackner, *A General Binary Isotherm Model for Amines Interacting with CO_2 and H_2O.* **Physical Chemistry Chemical Physics. 25,** 13877-13891 (2023).
2. J.L. Wade, H. Marques-Lopez, W. Wang, J. Flory, and B. Freeman, B., *Moisture Driven CO_2 Pump for Direct Air Capture.* **Journal of Membrane Science.** In Review. (2023). http://ssrn.com/abstract=4442166

Largely pi-Extended Molecular Systems: Porphyrins Fused with PAHs

Hong Wang, Francis D'Souza, Department of Chemistry, University of North Texas

Keywords: Pi-Extended Porphyrins, Acenes, Aromatic Heterocycles, Charge Transfer/Separation, Transient Spectroscopy

Research Scope

This proposed project focuses on the design and synthesis of largely π-extended porphyrins fused with polycyclic aromatic hydrocarbons (PAHs), and the study of their electronic and photophysical properties. Largely π-extended structures represent one most fascinating yet very challenging frontiers in chemistry and materials science. Incorporating both porphyrins and polycyclic aromatic hydrocarbons to obtain largely π-extended multichromophoric systems is especially attractive as the resulted largely π-extended systems are reminiscent of "nanographenes" doped with heteroatoms.(1, 2) Fused PAH-porphyrin systems are expected to possess highly active intramolecular electronic interactions, thus open the opportunities to discover unprecedented electronic, optical and photophysical properties. Incorporating both porphyrins and PAHs to obtain largely π-extended multichromophoric systems is challenging due to synthetic limitations.(3, 4) In order to address the synthetic challenge, the Wang group has been engaged in developing new synthetic methodologies for π-extended porphyrins.(5-9) The availability of these methods provides the possibility to further extend the porphyrin π-system with other aromatic systems such as extended PAHs. The purpose of this proposed project is threefold. First, concise and versatile synthetic methods will be developed to further extend the porphyrin π-system. Second, different types of PAH-fused porphyrins including extended PAH-fused, acene-fused, and cyclooctatetraene-fused π-extended porphyrins will be designed and prepared using these methods. Third, the optical-, electronic-, and photophysical properties of these compounds will be studied using DFT calculations, UV-Vis/fluorescence spectroscopy, electrochemistry and spectroelectrochemistry, femto- and nanosecond transient absorption spectroscopy.

Recent Progress

New synthetic methods to fuse different type of aromatic rings to the porphyrin periphery was developed in the past two years. Novel large π-extended molecular structures incorporating both porphyrins and other aromatic components including acenaphtho[1,2-*b*]pentacene-, benzoimidazo-isoindole-, naphthodithiophene-fused porphyrins have been designed and synthesized (Figure 1). (10-13) Fully conjugated porphyrin oligomers including dimers and trimers were also obtained through these developed methods.(14) Porphyrin-fused acenes displayed unusual stability with a half-life > 25 days and nickel inserted in the porphyrin core was confirmed

to play the major role in stabilizing these long acenes.(12, 15) Reactivity investigation of the benzoimidazo-isoindole-fused porphyrins reveals a new organic transformation in the presence of methyl iodide, resulting in the ring-opening of isoindole with the formation of an aldehyde and dimethylation of the benzoimidazo component.(11) The fused benzoimidazo-isoindole component acted as a good ligand to bind platinum (II), forming novel homobimetallic and heterobimetallic porphyrin complexes. Time-resolved emission and transient absorption spectroscopy reveal stable excited state species of the benzoimidazo-isoindole fused porphyrins. The zinc benzoimidazo-isoindole-fused porphyrins promoted excited state electron transfer upon coordinating an electron acceptor, C_{60}, generating a long-lived charge-separated state, in the order of 37.4 μs.(11) The formation of the exceptionally long-separated state is attributed to the involvement of both singlet and triplet excited states, which is rarely reported in literature. The oligomeric porphyrins show strong excitonic coupling and the occurrence of efficient singlet-singlet energy transfer (>95% efficiency and rate constant > 10^{12} s^{-1}).(14) Excited state charge separation from both singlet and triplet excited states of zinc porphyrin oligomers has also been established. The Lifetime of the charge-separated state was in the 30-40 μs range revealing charge stabilization. An unusual trend was observed in the florescence quantum yield upon converting benzoporphyrin **2VTP** to naphtho[1,2-*b*:4,3-*b'*]dithiophene-fused porphyrin (**F2VTP**).(13) NICS analysis revealed different impact of the two isomeric naphthodithiophenes on the global aromaticity upon fusion to porphyrin (**F2VTP** and **F3VTP**).

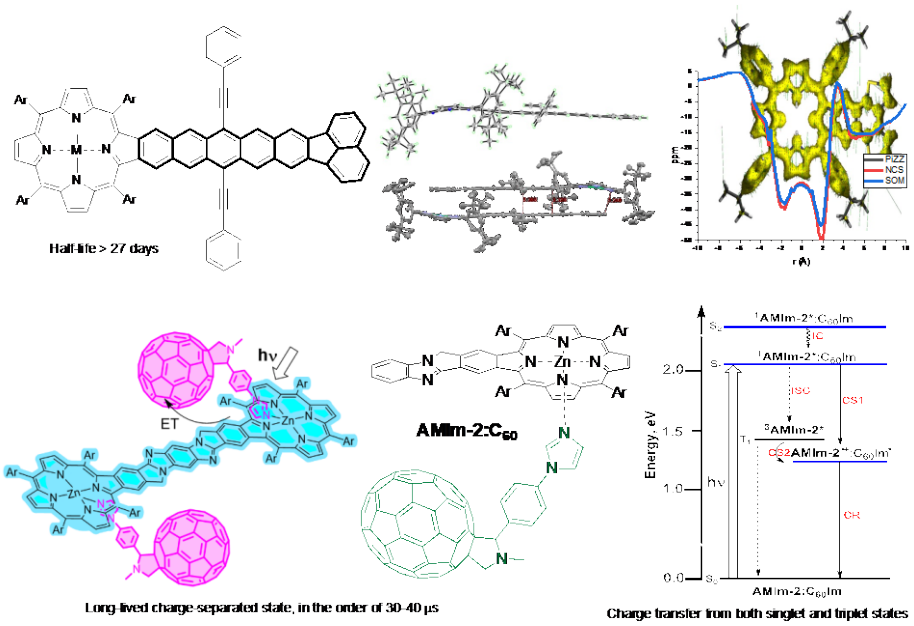

Figure 1. Selected Examples of π-Extended Porphyrins.

Future Plans

Synthetic methodologies are being developed to fuse 7- and 8-membered rings to the porphyrin periphery. Largely pi-extended structures will be designed and synthesized using these methods. The impact of the ring and ring dynamics on their aromaticity and excited state dynamics are under investigation.

References

1. M. Stepien, E. Gonka, M. Zyla, N. Sprutta, Heterocyclic Nanographenes and Other Polycyclic Heteroaromatic Compounds: Synthetic Routes, Properties, and Applications. *Chem. Rev.* **117**, 3479-3716 (2017).
2. A. Narita, X. Y. Wang, X. Feng, K. Mullen, New advances in nanographene chemistry. *Chem Soc Rev* **44**, 6616-6643 (2015).
3. J. D. Spence, T. D. Lash, Porphyrins with Exocyclic Rings. 14.1 Synthesis of Tetraacenaphthoporphyrins, a New Family of Highly Conjugated Porphyrins with Record-Breaking Long-Wavelength Electronic Absorptions. *J. Org. Chem.* **65**, 1530-1539 (2000).
4. J. P. Lewtak, D. T. Gryko, Synthesis of pi-extended porphyrins via intramolecular oxidative coupling. *Chem. Commun.* **48**, 10069-10086 (2012).
5. L. Jiang, J. T. Engle, L. Sirk, C. S. Hartley, C. J. Ziegler, and H. Wang, Triphenylene-Fused Porphyrins. *Org. Lett.* **13**, 3020-3023 (2011).
6. L. Jiang, R. A. Zaenglein, J. T. Engle, C. Mittal, C. S. Hartley, C. J. Ziegler, and H. Wang, Water-soluble ionic benzoporphyrins. *Chem Commun (Camb)* **48**, 6927-6929 (2012).
7. S. Kumar, X. Jiang, W. Shan, R. G. W. Jinadasa, K. M. Kadish and H. Wang beta-Functionalized trans-A2B2 push-pull tetrabenzoporphyrins. *Chem Commun (Camb)* **54**, 5303-5306 (2018).
8. L. Jiang, J. T. Engle, R. A. Zaenglein, A. Matus, C. J. Ziegler, H. Wang, M. J. Stillman, Pentacene-fused diporphyrins. *Chem. Eur. J.* **20**, 13865-13870 (2014).
9. S. Kumar, W. A. Webre, C. Stewart, F. D'Souza, H. Wang, A Synthetic Approach to beta-Functionalized Naphtho[2,3]porphyrins. *Org. Lett.* **22**, 7078-7082 (2020).
10. A. Moss, D. E. Nevonen, Y. Hu, V. N. Nesterov, V. Nemykin and H. Wang, Unsymmetric Pentacene- and Pentacenequinone-Fused Porphyrins: Understanding the Effect of Cross- and Linear-Conjugation. *ACS Phys. Chem. Au* **2**, 468-481 (2022).
11. A. Moss, Y. Jang, J. Arvidson, V. N. Nesterov, F. D'Souza and H. Wang, Aromatic heterobicycle-fused porphyrins: impact on aromaticity and excited state electron transfer leading to long-lived charge separation. *Chem. Sci.* **13**, 9880-9890 (2022).
12. A. M. Jacob Arvidson, Hong Wang, Francis D'Souza, acenaphtho[1,2-b]pentacene-fused porphyrin: syntheis, characterization, and singlet fission. *unpublished results*.
13. C. Cooper, A. Alsaleh, S. Kumar, W. Rackers, V. N. Nesterov, F. D'Souza, S. A. Vinogradov and H. Wang Naphthodithiophene-Fused Porphyrins: Synthesis, Characterization, and Impact of Extended Conjugation on Aromaticity *ChemSusChem*, to be submitted.
14. A. Moss, Y. Jang, H. Wang, F. D'Souza, Porphyrin Dimers with Conjugated Linker Exhibiting Charge-Transfer and Excitonic Coupling Characteristics. *ChemSusChem* (2023).
15. Y. Hu, M. B. Thomas, W. A. Webre, A. Moss, R. G. W. Jinadasa, V. N. Nesterov, F. D'Souza and H.Wang, Nickel(II) Bisporphyrin-Fused Pentacenes Exhibiting Abnormal High Stability. *Angew. Chem. Int. Ed.* **59**, 20075-20082 (2020).

Publications

1. Y. Hu, A. Alsaleh, O. Trinh, F. D'Souza, H. Wang, β-Functionalized push–pull opp-dibenzoporphyrins as sensitizers for dye-sensitized solar cells: the push group effect. *J. Mater. Chem. A* **9**, 27692-27700 (2021).
2. T. Han, Y. Jang, J. Arvidson, F. D'Souza, H. Wang, Optical and photophysical properties of platinum benzoporphyrins with C2v and D2h symmetry. *J. Porphyrins Phthalocyanines* **26**, 458-468 (2022).
3. A. Moss, Y. Jang, J. Arvidson, V. N. Nesterov, F. D'Souza and H. Wang, Aromatic heterobicycle-fused porphyrins: impact on aromaticity and excited state electron transfer leading to long-lived charge separation. *Chem. Sci.* **13**, 9880-9890 (2022).
4. A. Moss, D. E. Nevonen, Y. Hu, V. N. Nesterov, V. Nemykin and H. Wang, Unsymmetric Pentacene- and Pentacenequinone-Fused Porphyrins: Understanding the Effect of Cross- and Linear-Conjugation. *ACS Phys. Chem. Au* **2**, 468-481 (2022).
5. A. Moss, Y. Jang, H. Wang, F. D'Souza, Porphyrin Dimers with Conjugated Linker Exhibiting Charge-Transfer and Excitonic Coupling Characteristics. *ChemSusChem,* in press, e202202289 (2023).

New Synthetic Approaches Towards Atomically Precise π–d Conjugated Materials

Dianne J. Xiao, Department of Chemistry, University of Washington, Seattle

Keywords: metal–organic frameworks, conjugated materials

Research Scope

Two-dimensional conjugated metal–organic frameworks (MOFs), which are structurally reminiscent of graphene, have attracted significant recent attention due to their potential to host unique reactivity and physical phenomena, as well as by the presence of well-defined porosity, which enables the rapid transport, storage, and conversion of molecular and ionic guests.[1] The objective of our work is to expand the functional and structural scope of π–d conjugated metal–organic materials beyond existing 2D architectures, as well as to better understand their fundamental formation mechanisms. To accomplish this broader goal, three complementary research directions were undertaken over the past two years: 1) expand the structural scope of conjugated metal–organic materials beyond 2D planar architectures (e.g., 0D macrocycles, 1D chains); 2) understand how structure across length scales influences function in conjugated metal–organic materials; and 3) understand the formation mechanisms of metal–organic materials, specifically the role of ligand oxidation.

Recent Progress

Over the past two years, we have successfully truncated 2D π–d conjugated frameworks into 0D macrocycles and 1D chains. Beyond serving as model systems for 2D MOFs, these materials may reveal new physical properties due to their lower dimensionality. We have synthesized conjugated copper-based metal–organic macrocycles that resemble fragments of $Cu_3(HHTP)_2$ (HHTP = hexahydroxytriphenylene), a 2D framework (**Fig. 1a**).[2,3] Despite their dramatically truncated structures, these macrocycles preserve many of the desirable properties of MOFs, including π-stacked nanochannels (**Fig. 1b**) and high out-of-plane electrical conductivity (10^{-3} S/cm pellet conductivities). However, unlike metal–organic frameworks, macrocycles are fully solution processable. By lengthening the peripheral side chains, we can achieve macrocycles that are soluble in organic solvents (e.g. THF, toluene, $CHCl_3$) and are readily spin coated onto substrates for device fabrication (**Fig. 1c**).

We have also synthesized a family of fully conjugated 1D metal–organic chains.[4] Because 1D chains more readily form large single crystals, they can offer insight into the structure and bonding of more complex 2- and 3D conjugated analogues. Using a diphenyl-derivatized

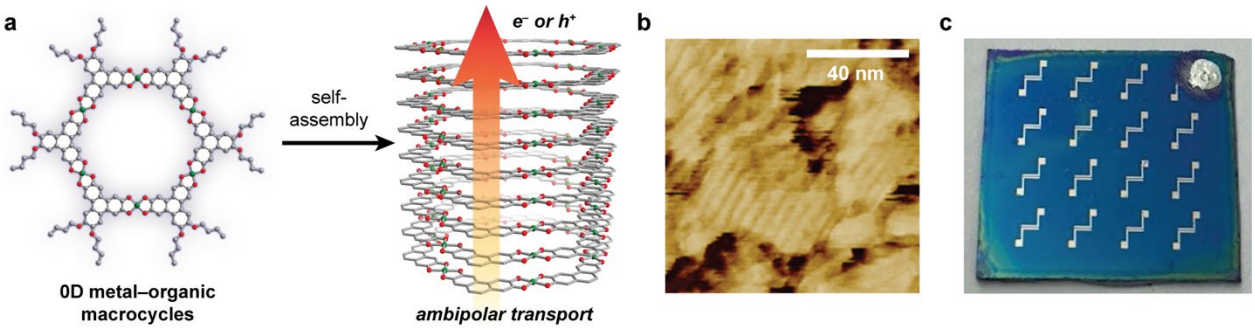

Fig. 1. a) Synthesis of conjugated metal–organic macrocycles. (**b**) Atomic force microscopy images confirm the formation of π-stacked nanotubes. (**c**) Thin-film field effect transistor devices fabricated using a C18-derivatized copper macrocycle as the active layer.

tetraoxolene ligand (H_2Ph_2dhbq), we showed that the steric profile of the coordinating solvent controls whether linear or helical 1D chains are exclusively formed. Despite similar ligand environments, only the helical chain displays temperature-dependent valence tautomerism, switching from (Fe^{II})(Ph_2dhbq^{2-}) to (Fe^{III})($Ph_2dhbq^{3\cdot-}$) at temperatures below 203 K. The stabilization of ligand radicals leads to exceptionally strong magnetic exchange coupling (J = −230 ± 4 cm^{-1}). Meanwhile, the linear chains are more amenable to oxidative doping, leading to an increase in electrical conductivity by nearly three orders of magnitude. This work illustrates how altering the metal–ligand connectivity can be a powerful tool for tuning materials properties.

Finally, we have also probed the formation mechanisms of conjugated metal–organic materials, specifically the role of ligand oxidation. We have developed a new synthetic route to form $Cu_3(HHTP)_2$ that uses solid chemical oxidants rather than air.[5] Using our new synthetic route, we have shown that the particle aspect ratio can be dramatically altered, from long rods to short flakes, simply by controlling how and when the chemical oxidant is introduced (**Fig. 2**). The initial ligand and metal oxidation state also plays an important role in the formation of 1D chains. For the helical chain, we found that using the fully reduced, tetrahydroxy ligand in combination with Fe(III) salts under N_2 led to significantly larger crystallite sizes. In contrast, using the same approach for the linear iron chain led to partial oxidative doping of the chains. Together, these studies show that oxidation of the redox-active ligand is a critical and often overlooked parameter to controlling both the morphology and composition of conjugated metal–organic materials.

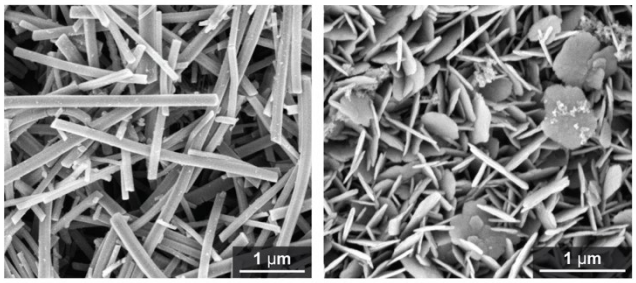

Fig. 2. Rod (left) and flake-like (right) $Cu_3(HHTP)_2$ particles can be achieved by controlling when and how quickly the ligand is oxidized.

References

1. L. S. Xie, G. Skorupskii, M. Dincă, *Electrically Conductive Metal–Organic Frameworks*, Chem. Rev. **120**, 8536 (2020).
2. M. Hmadeh, Z. Lu, Z. Liu, F. Gándara, H. Furukawa, S. Wan, V. Augustyn, R. Chang, L. Liao, F. Zhou, E. Perre, V. Ozolins, K. Suenaga, X. Duan, B. Dunn, Y. Yamamto, O. Terasaki, O. M. Yaghi, *New Porous Crystals of Extended Metal-Catecholat*es, J. Am. Chem. Soc. **24**, 3511 (2012).
3. L. B. Zasada, L. Guio, A. A. Kamin, D. Dhakal, M. Madison, G. T. Seidler, C. K. Luscombe, D. J. Xiao, *Conjugated Metal–Organic Macrocycles: Synthesis, Characterization, and Electrical Conductivity,* J. Am. Chem. Soc. **144**, 4515 (2022).
4. A. A. Kamin, I. P. Moseley, J. Oh, E. J. Brannan, P. M. Gannon, W. Kaminsky, J. M. Zadrozny, D. J. Xiao, *Geometry-dependent valence tautomerism, magnetism, and electrical conductivity in 1D iron–tetraoxolene chains*, Chem. Sci. **14**, 4083 (2023).
5. K. M. Snook, L. B. Zasada, D. Chehada, D. J. Xiao, *Oxidative control over the morphology of Cu3(HHTP)2, a 2D conductive metal–organic framework*, Chem. Sci. **13**, 10472 (2022).

Publications

1. L. B. Zasada, L. Guio, A. A. Kamin, D. Dhakal, M. Madison, G. T. Seidler, C. K. Luscombe, D. J. Xiao, *Conjugated Metal–Organic Macrocycles: Synthesis, Characterization, and Electrical Conductivity,* J. Am. Chem. Soc. **144**, 4515 (2022).
2. K. M. Snook, L. B. Zasada, D. Chehada, D. J. Xiao, *Oxidative control over the morphology of Cu3(HHTP)2, a 2D conductive metal–organic framework*, Chem. Sci. **13**, 10472 (2022).
3. A. A. Kamin, I. P. Moseley, J. Oh, E. J. Brannan, P. M. Gannon, W. Kaminsky, J. M. Zadrozny, D. J. Xiao, *Geometry-dependent valence tautomerism, magnetism, and electrical conductivity in 1D iron–tetraoxolene chains*, Chem. Sci. **14**, 4083 (2023).

Organic/Inorganic Nanocomposites

Ting Xu, Yi Liu, Robert O. Ritchie, Miquel Salmeron, Gregory Su, Jie Yao

Lawrence Berkeley National Laboratory

Keywords: nanocomposite, nanoparticle, self-assembly, topochemical polymerization, entropy-driven phase behavior,

Research Scope

We aim to establish design rules to synthesize functional organic/inorganic nanocomposites by holistically understanding the effects of molecular chemistry, thermodynamics governing phase behaviors of complex blends, and kinetic pathways of hierarchical assembly using state-of-art characterization techniques. These fundamental studies lead to chemistry-structure-function relationship to realize their technological potential for clean energy harvesting, storage and utilization. Our team efforts led to successful synthesis and assembly of polymer grafted nanoparticles into superlattices, covalent organic framework (COF) nanospheres into high performance dielectrics, and supramolecular nanocomposites with defect control as barrier materials.

Recent Progress

1. High performance barrier materials by programming entropy-driven nanosheet growth. Our inability to translate nanosheets to functional coatings is not unique and reflects deficiencies in current self-assembly designs. Instead of focusing on a small subset of characteristics under idealized conditions, we must holistically synthesize nanomaterials at the system level. Here, we leverage emerging entropy-driven phase behaviors in complex blends[1] and XPCS technique to quantify system mobility[2]. We successfully realized a micro-first-nano-later pathway to synthesize composite films with control over defect density and defect type and to correlate structure and chemistry of stacking nanosheets to the macroscopic barrier property.

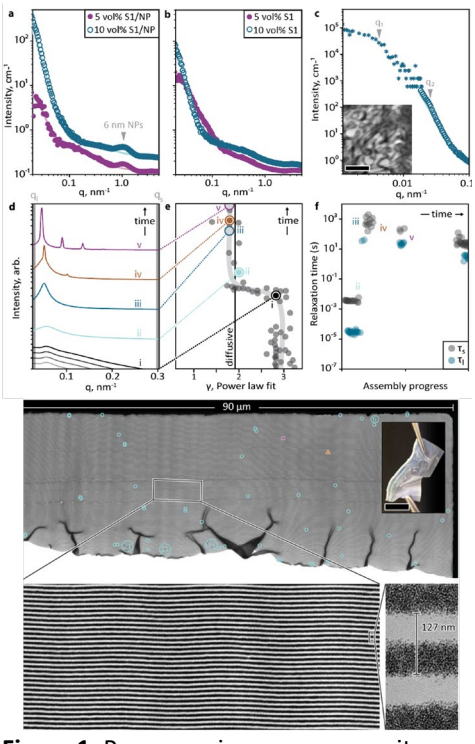

Figure 1. Programming nanocomposite synthesis based on system mobility can lead to defect control.

2. Polymer-grafted nanoparticles (PGNPs) as artificial atoms. PGNPs offer immense potential for fabricating nanoparticle-based superlattices with the ease of

tuning interactions through polymeric ligands and achieving diverse structures reminiscent of alloys.[3] We systematically investigated binary PGNP assemblies at the liquid-air interface to delineate kinetic pathway, proceeding with nanoscale microphase separation followed up surface-induced PGNP reorganization. The stacking of PGNP layers act as precursors for crystallization as the thickness of the PGNP film increases. These studies explain the formation of AlB2-, AuCu3- and NaZn13-type binary nanoparticle superlattices (BNSLs) with distinct orientations and provide guidelines to fabricate PGNP BNSLs over macroscopic distances. In parallel, we are developing polarized resonant soft x-ray scattering (p-RSoXS) techniques coupled with simulations to spatially resolve the conformation and orientation of polymers grafted to nanoparticles.

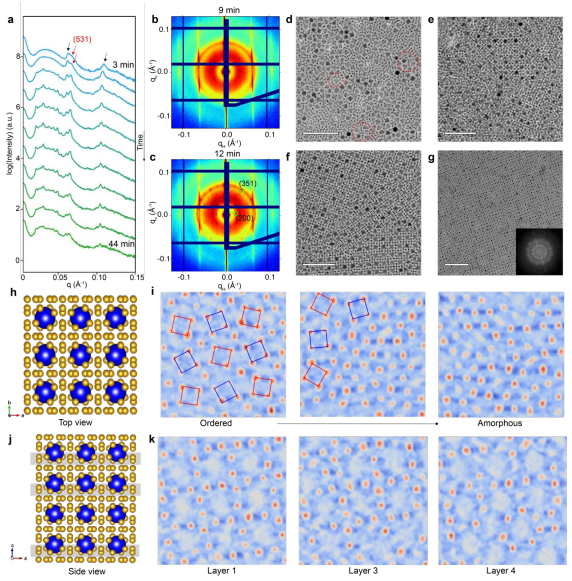

Figure 2. Kinetic pathways of binary PGNP interfacial assembly.

3. Nanocomposites as high performance dielectric materials in harsh thermal and electrical environments. We successfully incorporated rigid covalent organic framework (COF) nanospheres into thin films of soft terpolymers using an in situ synthesis and layer-by-layer solution casting method.[4] The resulting all-organic thin films displayed high dielectric constant, enhanced breakdown strength, superior energy density, mechanical self-supporting capability, and excellent mechanical flexibility. In parallel, we designed and synthesized polysulfates through sulfur(VI) fluoride exchange (SuFEx) "click chemistry" and tested their performance as dielectric polymers.[5] These polysulfates, processed into thin films via solution methods, exhibit insulating properties and stability at elevated temperatures. Electrostatic film capacitors based on these polysulfates sandwiched with two ultrathin alumina coatings achieve high breakdown strength and record-high discharged energy density at 150°C, surpassing current state-of-the-art dielectric materials.

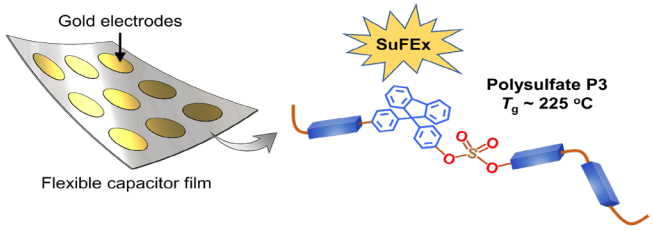

Figure 3. Flexible capacitor film achieved from SuFEx "click chemistry" with high thermal stability and record-high energy density at elevated temperatures.

References

1. L. Ma, H. J. Huang, E. Vargo, J. Y. Huang, C. L. Anderson, T. Chen, I. Kuzmenko, J. Ilavsky, C. Wang, Y. Liu, P. Ercius, A. Alexander-Katz, T. Xu, *Diversifying Composition Leads to Hierarchical Composites with Design Flexibility and Structural Fidelity*, ACS Nano, **15**, 14095 (2021).
2. M. Chu, J. Li, Q. Zhang, Z. Jiang, E. M. Dufresne, A. Sandy, S. Narayanan, N. Schwarz. *pyXPCSviewer: an open-source interactive tool for X-ray photon correlation spectroscopy visualization and analysis*. J. Synchrotron Radiat. **29**, 1122 (2022).
3. Y. Qian, A. da Silva, E. Yu, C. L. Anderson, Y. Liu, W. Theis, P. Ercius, T. Xu, *Crystallization of Nanoparticles Induced by Precipitation of Trace Polymeric Additives*, Nat Communication, **12**, 2767 (2021).
4. H. Li, Z. Xie, C. Yang, J. Kwon, A. Lainé, C. Dun, A. V. Galoustian, X. Li, P. Liu, J. J. Urban, Z. Peng, M. Salmeron, R. O. Ritchie, T. Xu, Y. Liu, *Flexible All-Organic Nanocomposite Films Interlayered with In Situ Synthesized Covalent Organic Frameworks for Electrostatic Energy Storage*, Nano Energy **113**, 108544 (2023)
5. H. Li, B. S. Chang, H. Kim, Z. Xie, A. Lainé, L. Ma, T. Xu, C. Yang, J. Kwon, S. W. Shelton, L. M. Klivansky, V. Altoé, B. Gao, A. M. Schwartzberg, Z. Peng, R. O. Ritchie, T. Xu, M. Salmeron, R. Ruiz, K. B. Sharpless, P. Wu, Y. Liu, *High-Performing Polysulfate Dielectrics for Electrostatic Energy Storage Under Harsh Conditions*, Joule **7**, 95 (2023).

Publications

1. P. F. Pieters, A. Lainé, H. Li, Y.-H. Lu, Y. Singh, L.-W. Wang, Y. Liu, T. Xu, A. P. Alivisatos and M. Salmeron, *Multiscale Characterization of the Influence of the Organic–Inorganic Interface on the Dielectric Breakdown of Nanocomposites*, ACS Nano **16**, 6744 (2022).
2. A. S. Abbas, E. Vargo, V. Jamali, P. Ercius, P. F. Pieters, R. M. Brinn, A. Ben-Moshe, M. G. Cho, T. Xu and A. P. Alivisatos, *Observation of an Orientational Glass in a Superlattice of Elliptically-Faceted CdSe Nanocrystals*, ACS Nano **16**, 9339 (2022).
3. J. Kwon, C. DelRe, P. Kang, A. Hall, D. Arnold, I. Jayapurna, L. Ma, M. Michalek, R. O. Ritchie and T. Xu, *Conductive Ink with Circular Life Cycle for Printed Electronics*, Advanced Materials 34, 2202177 (2022).
4. E. Vargo, J. C. Dahl, K. M. Evans, T. Khan, P. Alivisatos and T. Xu, *Using Machine Learning to Predict and Understand Complex Self-Assembly Behaviors of a Multicomponent Nanocomposite*, Advanced Materials **34**, 2203168 (2022).
5. L. Ma, H. Huang, P. Ercius, A. Alexander-Katz and T. Xu, *Symmetry-Breaking and Self-Sorting in Block Copolymer-Based Multicomponent Nanocomposites*, ACS Nano **16**, 9368 (2022).
6. C. L. Anderson, H. Li, C. G. Jones, S. J. Teat, N. S. Settineri, E. A. Dailing, J. Liang, H. Mao, C. Yang, L. M. Klivansky, X. Li, J. A. Reimer, H. M. Nelson and Y. Liu, *Solution-processable and functionalizable ultra-high molecular weight polymers via topochemical synthesis*, Nature Communications **12**, 6818 (2021).
7. Emma Vargo, Katherine M. Evans, Qingjun Wang, Andrew Sattler, Yiwen Qian, Jie Yao, Ting Xu Orbital Angular Momentum from Self-Assembled Concentric Nanoparticle Rings, Advanced Materials 33, 40, 2103563 (2021).
8. Lainé, R. Parmar, M. Amati, L. Gregoratti, G. M. Su, T. Xu, and M. Salmeron, *Damage-free X-ray spectroscopy characterization of oxide thin films*, Appl. Surf. Sci. **634**, 157335 (2023).
9. H. Li, Z. Xie, C. Yang, J. Kwon, A. Lainé, C. Dun, A. V. Galoustian, X. Li, P. Liu, J. J. Urban, Z. Peng, M. Salmeron, R. O. Ritchie, T. Xu, Y. Liu, *Flexible All-Organic Nanocomposite Films Interlayered with In Situ Synthesized Covalent Organic Frameworks for Electrostatic Energy Storage*, Nano Energy **113**, 108544 (2023)
10. H. Li, B. S. Chang, H. Kim, Z. Xie, A. Lainé, L. Ma, T. Xu, C. Yang, J. Kwon, S. W. Shelton, L. M. Klivansky, V. Altoé, B. Gao, A. M. Schwartzberg, Z. Peng, R. O. Ritchie, T. Xu, M. Salmeron, R. Ruiz, K. B. Sharpless, P. Wu, Y. Liu, *High-Performing Polysulfate Dielectrics for Electrostatic Energy Storage Under Harsh Conditions*, Joule **7**, 95 (2023).

Building Artificial Layered Solids from the Bottom-up: Materials by Design to Enable New Energy Technologies

Guihua Yu, The University of Texas at Austin

Keywords: 2D assembly, anisotropic growth, electrocatalysis, energy conversion

Research Scope

The properties of inorganic nanostructures can be fundamentally differentiated depending on how the atoms are structurally arranged in dimension. Owing to the reduced dimensionality and concomitant anisotropy, two-dimensional (2D) materials demonstrate distinctly different characteristics from their 3D bulk counterparts, providing a number of exciting scientific and technological opportunities.[1-2] The controlled synthesis, advanced structural characterization, and theoretical modeling of electronic properties of inorganic 2D nanostructures will enable the design and control of nanoscale energy conversion systems with great precision.[3-9] Herein, our program focuses on self-assembly and molecular engineering of structure-controlled 2D inorganic solids, with emphasis on their design, synthesis, and fundamental electrocatalytic properties and mechanisms. This effort will enable better control of electrocatalytic characteristics in novel 2D nanosheets and deeper understanding of their structure-functionality correlations that make possible next-generation electrochemical energy devices with unprecedented characteristics.

Recent Progress

The objective of achieving spatially well-defined functional nanomaterials and sophisticated architectures through nanoparticle assembly has been a subject of great scientific interest, while achieving a long-range ordering of assembly to create macroscopic structures has proven challenging, primarily due to the limitations of relying solely on interparticle interactions. We have demonstrated a strategy to produce large nanosheets with lateral dimensions of several millimeters by confining a uniformly dispersed metal-cyano colloidal suspension at the interface between ice and water, followed by the removal of ice crystals (Fig. 1). The formation of these millimeter-sized nanosheets can be attributed to the balanced electrostatic forces between dispersed

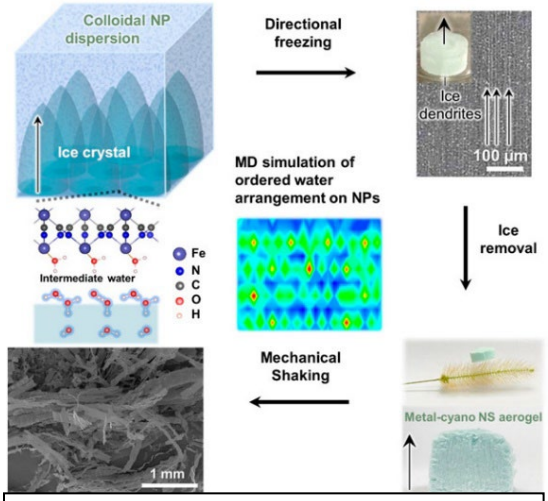

Figure 1. Schematic illustration of the mechanism of nanosheet formation via directional freezing.

nanoparticles, coupled with the appropriate hydrodynamic size of the nanoparticles, the potential lattice matching between nanoparticles and ice crystals, and the presence of intermediate water at the ice-particle interface. The highly anisotropic growth of ice crystals guides the two-dimensional assembly of nanoparticles in a long-range order, resulting in well-defined nanosheets with a two-dimensional structure. This finding highlights the potential of nanoparticle assembly at larger length scales, offering possibilities for designing various large two-dimensional nanoarchitectures for practical applications.

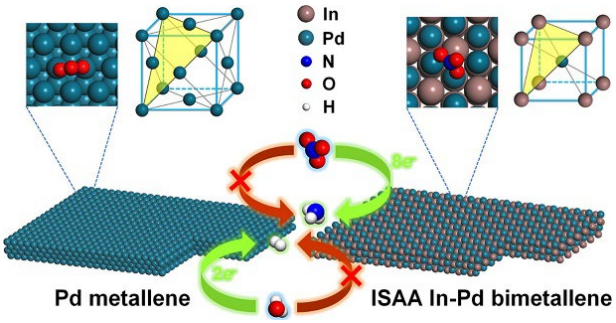

Figure 2. Phase engineering of metallene with isolated surface active sites towards ammonia synthesis.

2D assembly of atoms originated from metal-ligand complex molecules achieved by kinetic control over metal ions reduction enables anisotropic growth of metals with distinctive 2D nanostructures and intrinsically improved electrocatalytic properties. By engineering 2D atomic crystals made of metals with a thickness of a few atomic layers (Metallene) via precisely controlled lattice expansion or amorphization, a simultanous modulation over thickness, surface morphology, crystallinity, and electronic structure can be achieved, improving their electrocatalytic performance towards electrochemical energy conversions. More significantly, we tuned the crystal phase of 2D metallene to achieve an intermetallic single-atom alloys (ISAAs) structure, which features 2D isolated active sites coordinated with host metal atoms for the enhancement of electrocatalytic activity and selectivity towards ammonia synthesis (Fig. 2). The results illustrated the ultrathin morphology of the 2D metallene with a thickness of ~six atomic layers and surface single-atom sites of the highest density, by which the selectivity of ammonia can be essentially enhanced to provide a well-design platform for the structure-property study.

We demonstrated the dual electrocatalytic functionality with this designed Fe-cyano-R as a 2D nanostructure platform via ice templating method towards ammonia production and water splitting. The 2D Fe-cyano-R electrocatalyst demonstrated a strong adsorption of nitrate on Fe active sites and superhydrophilic surface with increased active sites, resulting from 2D topotactic conversion and in situ electroreduction. In addition, the above-mentioned ISAA bimetallene features downshifted surface valence states with narrowed energy band and thus significantly increased electron density with narrowed p−d hybridization around Fermi level, reducing the energy barrier of potential determining steps for the formation of the key reaction intermediate *NHO in ammonia synthesis. The two studies above highlight the important impacts of 2D assembly and molecular engineering on the design of electrocatalysts with improved performance.

References

1. V. Nicolosi, M. Chhowalla, M. G. Kanatzidis, M. S. Strano, J. N. Coleman, Liquid Exfoliation of Layered Materials. Science **340**, 1226419 (2013).
2. F. Bonaccorso, L. Colombo, G. Yu, M. Stoller, V. Tozzini, A. C. Ferrari, R. S. Ruoff, V. Pellegrin, Graphene, related two-dimensional crystals, and hybrid systems for energy conversion and storage. Science **347**, 1246501 (2015).
3. Q. H. Wang, K. Kalantar-Zadeh, A. Kis, J. N. Coleman, M. S. Strano, Electronics and optoelectronics of two-dimensional transition metal dichalcogenides. Nature Nano. **7**, 699 (2012).
4. L. Peng, Y. Zhu, X. Peng, Z. Fang, W. Chu, Y. Wang, Y. Xie, Y. Li, J. Cha, G. Yu, Effective Interlayer Engineering of 2D VOPO4 Nanosheets via Organic Intercalation for Improving Alkali Ion Storage. Nano Lett. **17**, 6273 (2017).
5. Z. Ju, S. T. King, X. Xu, X. Zhang, K. U. Raigama, K. J. Takeuchi, A. C. Marschilok, L. Wang, E. S. Takeuchi, G. Yu, Vertically assembled nanosheet networks for high-density thick battery electrodes. Proc. Nat. Acad. Sci. 119, e2212777119 (2022).
6. P. Prabhu, J. Lee, Metallenes as functional materials in electrocatalysis. Chem. Soc. Rev. **50**, 6700 (2021).
7. M. Xie, S. Tang, B. Zhang, G. Yu, Metallene-Related Materials for Electrocatalysis and Energy Conversion. Mater. Horiz. **10,** 407 (2023).
8. W. Zhu, L. Zhang, P. Yang, C. Hu, Z. Luo, X. Chang, Z. Zhao, J. Gong, Low-coordinated edge sites on ultrathin palladium nanosheets boost carbon dioxide electroreduction performance. Angew. Chem. **57**, 11544 (2018).
9. J. Fan, J. Wu, X. Cui, L. Gu, Q. Zhang, F. Meng, B.-H. Lei, D. J. Singh, W. Zheng, Hydrogen stabilized RhPdH 2D bimetallene nanosheets for efficient alkaline hydrogen evolution. J. Amer. Chem. Soc. **142**, 3645 (2020).

Publications

1. Z. Fang, Z. Jin, S. Tang, P. Li, P. Wu, G. Yu, Porous Two-dimensional Iron-Cyano Nanosheets for High-rate Electrochemical Nitrate Reduction. ACS Nano 16, 1072 (2021).
2. Z. Fang, S. Tang, Z. Wang, M. An, G. Yu, General Synthesis of Large Inorganic Nanosheets via 2D Confined Assembly of Nanoparticles. ACS Central Science 8, 627 (2022).
3. M. Xie, B. Zhang, Z. Jin, P. Li, G. Yu, Atomically reconstructed palladium metallene by intercalation-induced lattice expansion and amorphization for highly efficient electrocatalysis. ACS Nano 16, 13715 (2022).
4. M. Xie, S. Tang, Z. Li, M. Wang, Z. Jin, P. Li, X. Zhan, H. Zhou, G. Yu, Intermetallic Single-Atom Alloy In−Pd Bimetallene for Neutral Electrosynthesis of Ammonia from Nitrate. Journal of American Chemical Society 145, 13957 (2023).

Understanding and Controlling Aggregation Processes in Mixed-Molecular Solids, DE-SC0018021

Jeramy D. Zimmerman, Colorado School of Mines

Keywords: Atom Probe Tomography, HAADF-STEM, Organic Light Emitting Diodes, molecular clustering, spatial statistics

Research Scope

Despite decades of development and commercial deployment, most aspects of molecular clustering morphology in organic light emitting diodes (OLEDs) remain unknown. The goal of this project is to reveal these hidden morphologies and understand their impact on device efficiency and energy loss & degradation mechanisms using atom probe tomography (APT) and high-angle annular-dark-field scanning transmission electron microscope (HAADF-STEM) imaging.

In this project, we have developed APT techniques that extend its applicability to organic molecular solids. APT combines point-projection microscopy with time-of-flight mass spectrometry to provide an unparalleled nm-scale three dimensional (3D) spatial resolution with concurrent mass-to-charge based chemical discrimination of <1 Da, while HAADF-STEM is used to probe two-dimensional (2D) projections of the materials from nm-to-µm scales. Our developments in spatial statistics enable quantitative analysis of the microscopy data to understand clustering. This gives the ability to probe morphologies previously unattainable and develop new structure-property relationships for solid-state blends of molecules.

Recent Progress

We first focused on development of APT for molecular organic materials. We have shown that APT can be applied to molecular organic systems, where it can have a mass resolution of < 1 Da, a spatial resolution of ~0.3 nm in z and as good as ~1 nm in x-y, an analytic sensitivity of ~50 ppm, and we observe little fragmentation of molecules, making APT a very compelling technique for characterizing the morphology of small-molecule organic semiconducting systems.[1]

In the subsequent years, our primary goal has been to develop structure-property relationships for these OLED materials and relate these to the morphology data. We have also continued to

develop APT processes, including understanding molecular fragmentation mechanisms during APT analysis.[2] To understand morphology data, we continue to develop our spatial statistics analysis framework, including machine learning-based approaches that enable extracting significantly more information about morphology than is possible using the commercial APT software or open code.[3,4]

We have most recently explored morphology measurement performed using HAADF-STEM imaging of conventional phosphorescent guests (e.g., $Ir(ppy)_3$ and $Ir(ppy)_2(acac)$) in various host materials (user proposal at ORNL/CNMS, Michael Zachman), see Figure 1. The morphology measurements are analyzed using 2D/3D spatial statistical analyses, such as Ripley's K-function and the G-function, and compared against statistical simulations of morphology to identify various features. To analyze the HAADF-STEM data, we simulate various morphologies in 3D, collapse them into 2D (to make comparable to STEM data), and evaluate the sptial statistics.[3,5,6] We find direct evidence for stacking of guest molecules in the film in all guest-host combinations evaluated ($Ir(ppy)_3$ and $Ir(ppy)_2(acac)$ in several non-polar hosts). The stacking is more vertical than the most vertical pairs in a random close-packed morphology, indicating that stacking is occurring during film growth to alleviate dipole fields originating from the polar emissive molecules and that the host material fills in around the stacked guests as film growth continues. Models suggest that for $Ir(ppy)_3$ and $Ir(ppy)_2(acac)$ guests in mCBP and TCP hosts, that roughly half of the guests are in vertical dimers, trimers, or tetramers while the remaining half of the guests are isolated monomers. We see relatively uniform guest densities for $Ir(ppy)_3$, over length scales of >2nm however, we also see variations in guest density over 5-10 nm scales in $Ir(ppy)_2(acac)$, an emissive guest with a dipole moment roughly 1/3 that of $Ir(ppy)_3$. The smaller dipole moment reduces the Debye interaction with the non-polar host, decreasing the barrier to diffusion, enabling increased

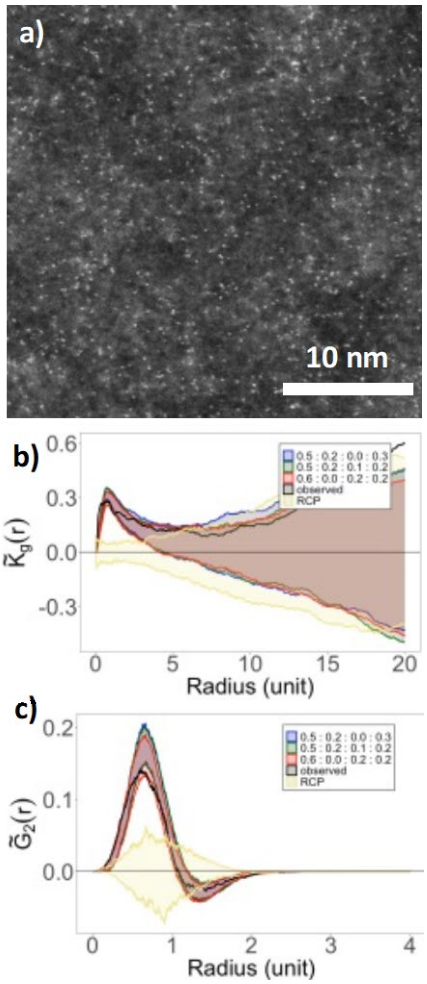

Figure 1. a) HAADF TEM image of 10nm thick layer of 10% $Ir(ppy)_3$ in mCBP. b) large-scale clustering analysis with Ripley's K-function and c) 2nd nearest neighbor G-function analysis for the best matches to various distributions of random monomers, vertical dimers, vertical trimers and vertical tetramers.

surface diffusion. Future work will explore how these morphologies change as the substrate deposition temperature is changed and effects of using a host with a larger dipole moment.

References

1. A. P. Proudian, M. B. Jaskot, D. R. Diercks, B. P. Gorman, and J. D. Zimmerman, "*Atom Probe Tomography of Molecular Organic Materials: Sub-Dalton Nanometer-Scale Quantification*" Chem. Mater. **31** (7), 2241 (2019).
2. J. T. Bingham, A. P. Proudian, S. Vyas, and J. D. Zimmerman, "*Understanding Fragmentation of Organic Small Molecules in Atom Probe Tomography*" J Phys Chem Lett **12** (42), 10437 (2021).
3. G. B. Vincent, A. P. Proudian, and J. D. Zimmerman, "*Three dimensional cluster analysis for atom probe tomography using Ripley's K-function and machine learning*" Ultramicroscopy **220**, 113151 (2021).
4. R. A. Bennett, A. P. Proudian, and J. D. Zimmerman, "*Cluster characterization in atom probe tomography: Machine learning using multiple summary functions*" Ultramicroscopy **247**, 113687 (2023).
5. A Baddeley, E Rubak, and R Turner, *Spatial Point Patterns*. (Chapman and Hall/CRC, 2016).
6. A. P. Proudian, R package for APT data processing (2019) https://github.com/aproudian2/rapt.

Publications

1. G. B. Vincent, A. P. Proudian, and J. D. Zimmerman, "*Three dimensional cluster analysis for atom probe tomography using Ripley's K-function and machine learning*" Ultramicroscopy **220**, 113151 (2021).
2. J. T. Bingham, A. P. Proudian, S. Vyas, and J. D. Zimmerman, "*Understanding Fragmentation of Organic Small Molecules in Atom Probe Tomography*" J Phys Chem Lett **12** (42), 10437 (2021).
3. P.Niyonkuru, A. P.Proudian, M. B.Jaskot, J. D. Zimmerman, "An intermediate model for fitting triplet–triplet annihilation in phosphorescent organic light emitting diode materials." Journal of Applied Physics **132**(9): 095501 (2022).
4. R. A. Bennett, A. P. Proudian, and J. D. Zimmerman, "*Cluster characterization in atom probe tomography: Machine learning using multiple summary functions*" Ultramicroscopy **247**, 113687 (2023).

Author Index

Participant List

First Name	Last Name	Email	Organization
Ashok	Ajoy	ashokaj@berkeley.edu	University of California, Berkeley
Chibueze	Amanchukwu	chibueze@uchicago.edu	University of Chicago
Ananda	Amarasekara	asamarasekara@pvamu.edu	Prairie View A&M University
Veronica	Augustyn	vaugust@ncsu.edu	North Carolina State University
Michael	Aziz	maziz@harvard.edu	Harvard University
Marc	Baldo	baldo@mit.edu	Massachusetts Institute of Technology
Jason	Bara	jbara@eng.ua.edu	University of Alabama
Svilen	Bobev	bobev@udel.edu	University of Delaware
David	Bock	dbock@bnl.gov	Brookhaven National Laboratory
Albina	Borisevich	albinab@ornl.gov	Oak Ridge National Laboratory
Bryan	Boudouris	boudouris@purdue.edu	Purdue University
Arthur	Bragg	artbragg@jhu.edu	Johns Hopkins University
Paul	Braun	pbraun@illinois.edu	University of Illinois, Urbana-Champaign
Craig	Bridges	bridgesca@ornl.gov	Oak Ridge National Laboratory
Carl	Brozek	cbrozek@uoregon.edu	University of Oregon
Richard	Brutchey	brutchey@usc.edu	University of Southern California
Ozgur	Capraz	ocapraz@okstate.edu	Oklahoma State University
Robert	Cava	rcava@princeton.edu	Princeton University
Michael	Chabinyc	mchabinyc@engineering.ucsb.edu	University of California, Santa Barbara
Matthew	Chagnot	mschagno@ncsu.edu	North Carolina State University
Qian	Chen	qchen20@illinois.edu	University of Illinois, Urbana-Champaign
Wei	Chen	wchen@anl.gov	Argonne National Laboratory
Ying	Chen	chen675@pnnl.gov	Pacific Northwest National Laboratory
Yingwen	Cheng	ycheng@niu.edu	Northern Illinois University
Yu-chen Karen	Chen-Wiegart	Karen.Chen-Wiegart@stonybrook.edu	Stony Brook University
Christopher	Chervin	christopher.chervin@science.doe.gov	U.S. Department of Energy

First Name	Last Name	Email	Organization
Sanchari	Chowdhury	sanchari.chowdhury@nmt.edu	New Mexico Institute of Mining and Technology
Seth	Cohen	scohen@ucsd.edu	University of California, San Diego
E. Bryan	Coughlin	ebc@umass.edu	University of Massachusetts, Amherst
Yi	Cui	yicui@stanford.edu	Stanford University/SLAC National Accelerator Laboratory
Sheng	Dai	dais@ornl.gov	Oak Ridge National Laboratory
Siddhartha	Das	sidd@umd.edu	University of Maryland
Emily	Davidson	edavidson@princeton.edu	Princeton University
Juan	De Pablo	depablo@uchicago.edu	University of Chicago
Mircea	Dinca	mdinca@mit.edu	Massachusetts Institute of Technology
Changwoo	Do	doc1@ornl.gov	Oak Ridge National Laboratory
Davide	Donadio	ddonadio@ucdavis.edu	University of California, Davis
James	Donahue	donahue@tulane.edu	Tulane University
Letian	Dou	dou10@purdue.edu	Purdue University
Egor	Evlyukhin	egor.evlyukhin@unlv.edu	University of Nevada, Las Vegas
Randy	Ewoldt	ewoldt@illinois.edu	University of Illinois, Urbana-Champaign
Omar	Farha	o-farha@northwestern.edu	Northwestern University
Pingyun	Feng	pingyun.feng@ucr.edu	University of California, Riverside
Jeffrey	Foster	fosterjc@ornl.gov	Oak Ridge National Laboratory
Glenn	Fredrickson	ghf@ucsb.edu	University of California, Santa Barbara
Daniel	Fredrickson	danny@chem.wisc.edu	University of Wisconsin, Madison
Danna	Freedman	danna@mit.edu	Massachusetts Institute of Technology
Hiroyasu	Furukawa	furukawa@berkeley.edu	University of California, Berkeley
Aura	Gimm	aura.gimm@science.doe.gov	U.S. Department of Energy
Yury	Gogotsi	yg36@drexel.edu	Drexel University
Karen	Goldberg	kig@sas.upenn.edu	University of Pennsylvania

First Name	Last Name	Email	Organization
John	Goodenough	jgoodenough@mail.utexas.edu	University of Texas, Austin
Matthias	Graf	matthias.graf@science.doe.gov	U.S. Department of Energy
Kenneth	Graham	kenneth.graham@uky.edu	University of Kentucky
Greg	Grason	grason@mail.pse.umass.edu	University of Massachusetts, Amherst
Lisa	Hall	hall.1004@osu.edu	The Ohio State University
Kelsey	Hatzell	kelsey.hatzell@princeton.edu	Princeton University
Ryan	Hayward	ryan.hayward@colorado.edu	University of Colorado, Boulder
David	Heldebrant	david.heldebrant@pnnl.gov	Pacific Northwest National Laboratory
Brett	Helms	bahelms@lbl.gov	Lawrence Berkeley National Laboratory
Craig	Henderson	craig.henderson@science.doe.gov	U.S. Department of Energy
Ive	Hermans	hermans@chem.wisc.edu	University of Wisconsin, Madison
Noah	Holzapfel	npholzap@ncsu.edu	North Carolina State University
Yan-Yan	Hu	yhu@fsu.edu	Florida State University
Wenyu	Huang	wy.huang@gmail.com	Ames National Laboratory
Harold	Hwang	hyhwang@stanford.edu	SLAC National Accelerator Laboratory
Muhammad Saiful	Islam	muhammad.s.islam@jsums.edu	Jackson State University
Alex	Ivanov	ivanova@ornl.gov	Oak Ridge National Laboratory
Santa	Jansone-Popova	jansonepopos@ornl.gov	Oak Ridge National Laboratory
Arthi	Jayaraman	Arthij@udel.edu	University of Delaware
Samson	Jenekhe	jenekhe@uw.edu	University of Washington
Xiulei David	Ji	david.ji@oregonstate.edu	Oregon State University
Song	Jin	jin@chem.wisc.edu	University of Wisconsin, Madison
Hannibal	Joma	hannibal.joma@science.doe.gov	U.S. Department of Energy
Ishita	Kamboj	ikamboj@ncsu.edu	North Carolina State University
Mercouri	Kanatzidis	m-kanatzidis@northwestern.edu	Northwestern University
Chenfeng	Ke	chenfeng.ke@dartmouth.edu	Dartmouth College
Paul	Kempler	pkempler@uoregon.edu	University of Oregon

First Name	Last Name	Email	Organization
Justin	Kennemur	jkennemur@fsu.edu	Florida State University
Helen	Kerch	helen.kerch@science.doe.gov	U.S. Department of Energy
Jae Chul	Kim	jkim7@stevens.edu	Stevens Institute of Technology
Rebekka	Klausen	klausen@jhu.edu	Johns Hopkins University
Takeshi	Kobayashi	takeshi@ameslab.gov	Ames National Laboratory
Joseph	Kolis	kjoseph@clemson.edu	Clemson University
Jing	Kong	jingkong@mit.edu	Massachusetts Institute of Technology
Kirill	Kovnir	kovnir@iastate.edu	Iowa State University
Marisa	Kozlowski	marisa@sas.upenn.edu	University of Pennsylvania
Debasish	Kuila	dkuila@ncat.edu	North Carolina A&T State University
Youngmin	Lee	youngmin.lee@nmt.edu	New Mexico Institute of Mining and Technology
Sangbok	Lee	slee@umd.edu	University of Maryland
Jing	Li	jingli@rutgers.edu	Rutgers University
Xinle	Li	xli1@cau.edu	Clark Atlanta University
Yi	Liu	yliu@lbl.gov	Lawrence Berkeley National Laboratory
Jeffrey	Long	jrlong@berkeley.edu	Lawrence Berkeley National Laboratory
Jihong	Ma	Jihong.Ma@uvm.edu	University of Vermont
Arumugam	Manthiram	rmanth@mail.utexas.edu	University of Texas, Austin
Michael	Markowitz	mike.markowitz@science.doe.gov	U.S. Department of Energy
Amy	Marschilok	amarschilok@bnl.gov	Brookhaven National Laboratory
Jarad	Mason	mason@chemistry.harvard.edu	Harvard University
Adam	Matzger	matzger@umich.edu	University of Michigan
Steven	May	smay@drexel.edu	Drexel University
John	McCoy	john.mccoy@nmt.edu	New Mexico Institute of Mining and Technology
Carlos	Meriles	cmeriles@ccny.cuny.edu	City University of New York
Claudia	Mewes	claudia.mewes@science.doe.gov	U.S. Department of Energy
Quentin	Michaudel	quentin.michaudel@chem.tamu.edu	Texas A&M University

First Name	Last Name	Email	Organization
David	Mitlin	david.mitlin2@utexas.edu	University of Texas, Austin
David	Mitzi	david.mitzi@duke.edu	Duke University
Seongbak	Moon	smoon5@ncsu.edu	North Carolina State University
Jeff	Moore	jsmoore@illinois.edu	University of Illinois, Urbana-Champaign
Partha	Mukherjee	mukher28@purdue.edu	Purdue University
Paul	Nealey	pnealey@anl.gov	Argonne National Laboratory
James	Neilson	james.neilson@colostate.edu	Colorado State University
May	Nyman	may.nyman@oregonstate.edu	Oregon State University
Simon	Pang	pang6@llnl.gov	Lawrence Livermore National Laboratory
Pietro	Papa Lopes	plopes@anl.gov	Argonne National Laboratory
Parans	Paranthaman	paranthamanm@ornl.gov	Oak Ridge National Laboratory
Aaron	Peng	apeng@uchicago.edu	University of Chicago
John	Perdew	perdew@tulane.edu	Tulane University
Frederic	Perras	fperras@ameslab.gov	Ames National laboratory
Nicola	Perry	nhperry@illinois.edu	University of Illinois, Urbana-Champaign
Pierre	Poudeu	ppoudeup@umich.edu	University of Michigan
Michael	Pravica	michael.pravica@unlv.edu	University of Nevada, Las Vegas
Obadiah	Reid	obadiah.reid@colorado.edu	University of Colorado, Boulder
Jeffrey	Reimer	reimer@berkeley.edu	University of California, Berkeley
Joaquin	Rodriguez Lopez	joaquinr@illinois.edu	University of Illinois, Urbana-Champaign
Aaron	Rossini	arossini@iastate.edu	Ames National Laboratory
Gary	Rubloff	rubloff@umd.edu	University of Maryland
Saeed	Saeed	smsaeed@ncsu.edu	North Carolina State University
Tomonori	Saito	saitot@ornl.gov	Oak Ridge National Laboratory
Ashkan	Salamat	Ashkan.salamat@unlv.edu	University of Nevada, Las Vegas
Regina	Sanchez	rsanchez@anl.gov	Argonne National Laboratory

First Name	Last Name	Email	Organization
Bayram	Saparov	saparov@ou.edu	University of Oklahoma
Brett	Savoie	bsavoie@purdue.edu	Purdue University
Charles	Schroeder	cms@illinois.edu	University of Illinois, Urbana-Champaign
Robert	Schurko	rschurko@fsu.edu	Florida State University
Kenneth	Schweizer	kschweiz@illinois.edu	University of Illinois, Urbana-Champaign
Ram	Seshadri	seshadri@mrl.ucsb.edu	University of California, Santa Barbara
Charles	Sing	cesing@illinois.edu	University of Illinois, Urbana-Champaign
Andrew	Stack	stackag@ornl.gov	Oak Ridge National Laboratory
Timothy	Strobel	tstrobel@carnegiescience.edu	Carnegie Institution for Science
Gregory	Su	gsu@lbl.gov	Lawrence Berkeley National Laboratory
Sophia	Suarez	snsuarez@brooklyn.cuny.edu	Brooklyn College
Bobby	Sumpter	sumpterbg@ornl.gov	Oak Ridge National Laboratory
Xiao-Guang	Sun	sunx@ornl.gov	Oak Ridge National Laboratory
Emad	Tajkhorshid	emad@illinois.edu	University of Illinois, Urbana-Champaign
Kenneth	Takeuchi	ktakeuchi@bnl.gov	Brookhaven National Laboratory
Alec	Talin	aatalin@sandia.gov	Sandia National Laboratory
Kui	Tan	Kui.Tan@unt.edu	University of North Texas
Mauricio	Terrones	mut11@psu.edu	Pennsylvania State University
Bishnu	Thapaliya	Prasadthapab@ornl.gov	Oak Ridge National Laboratory
Edwin L.	Thomas	elt@tamu.edu	Texas A&M University
Samuel	Thomas	sam.thomas@tufts.edu	Tufts University
Timo	Thonhauser	thonhauser@wfu.edu	Wake Forest University
Matthew	Tirrell	mtirrell@anl.gov	Argonne National Laboratory
Sarah	Tolbert	tolbert@chem.ucla.edu	University of California, Los Angeles
J. D.	Tovar	tovar@jhu.edu	Johns Hopkins University
Adam	Veige	veige@chem.ufl.edu	University of Florida
Gabriel	Veith	veithgm@ornl.gov	Oak Ridge National Laboratory

First Name	Last Name	Email	Organization
Javier	Vela	vela@iastate.edu	Ames National Laboratory
John	Vohs	vohs@seas.upenn.edu	University of Pennsylvania
Jennifer	Wade	jennifer.wade@nau.edu	Northern Arizona University
Eric	Walter	eric.walter@pnnl.gov	Pacific Northwest National Laboratory
Hong	Wang	hong.wang@unt.edu	University of North Texas
Zhongyang	Wang	zhongyang@uchicago.edu	University of Chicago
Lei	Wang	lwang@bnl.gov	Brookhaven National Laboratory
Nancy	Washton	nancy.washton@pnnl.gov	Pacific Northwest National Laboratory
Juliane	Weber	weberj@ornl.gov	Oak Ridge National Laboratory
Claire	White	whitece@princeton.edu	Princeton University
Karen	Winey	winey@seas.upenn.edu	University of Pennsylvania
Chris	Wolverton	c-wolverton@northwestern.edu	Northwestern University
Dianne	Xiao	djxiao@uw.edu	University of Washington
Claire	Xiong	clairexiong@boisestate.edu	Boise State University
Ting	Xu	txuucb@gmail.com	University of California, Berkeley
Jie	Yao	yaojie@berkeley.edu	Lawrence Berkeley National Laboratory/ University of California, Berkeley
Guihua	Yu	ghyu@austin.utexas.edu	University of Texas, Austin
Andriy	Zakutayev	andriy.zakutayev@nrel.gov	National Renewable Energy Laboratory
Michael	Zdilla	mzdilla@temple.edu	Temple University
Xueli	Zheng	xuelizh8@slac.stanford.edu	SLAC National Accelerator Laboratory
Jeramy	Zimmerman	jdzimmer@mines.edu	Colorado School of Mines
Hans-Conrad	zur Loye	zurloye@mailbox.sc.edu	University of South Carolina